METEOR-Berichte 11-2

Climate- biogeochemistry interactions in the tropical ocean of the SE-American oxygen minimum zone

Cruise No. 77, Leg 1 - 4

October 22, 2008 – February 18, 2009
Talcahuano (Chile) - Callao (Peru) – Guayaquil (Ecuador) – Callao (Peru) – Colon (Panama)

Olaf Pfannkuche, Martin Frank, Ralph Schneider, Lothar Stramma

Editorial Assistance:
Senatskommission für Ozeanographie der Deutschen Forschungsgemeinschaft
MARUM – Zentrum für Marine Umweltwissenschaften der Universität Bremen

Leitstelle Deutsche Forschungsschiffe
Institut für Meereskunde der Universität Hamburg

2011

Table of Contents **Page**

Table of Contents Part 1 (M77/1) Page

Table of Contents Part 2(M77/2) **Page**

Table of Contents Part 3 (M77/3)

Table of Contents Part 4 (M77/4) **Page**

Abstract

Meteor cruise M77 comprised of four legs to investigate the water column and sediments of the oxygen minimum zone (OMZ) in the coastal upwelling areas off Peru and to a lesser extend off Ecuador (Fig 1.). The research was carried out in the context Sonderforschungsbereich 754 at the University of Kiel, "Climate – Biogeochemistry Interactions in the Tropical Ocean" funded by the German Research Council (DFG).

Oceanic oxygen levels are controlled by the interplay of physics and biology. Circulation and mixing transport oxygen into the ocean interior from the near-surface where it is produced by photosynthesis and exchanged with the atmosphere. Oxygen consumption occurs throughout the ocean and is fuelled by organic matter sinking out of surface waters into the depths. Both the supply and consumption of oxygen are sensitive to climate change in ways that are not fully understood. Major changes to marine sources and sinks of important nutrient elements such as nitrogen, phosphorus and iron occur when oceanic oxygen concentrations decrease below threshold levels. On crossing the threshold, radically different microbial and chemical processes start to operate. Oxygen levels can therefore be viewed as a "switch" or "tipping point" for nutrient cycling. The Oxygen Minimum Zones (OMZs) of the tropics are the key regions of low oxygen in today's ocean. The effects of oxygen-dependent nutrient cycling in these relatively small regions are carried into the rest of the ocean by the circulation. Hence "small" OMZs can impact nutrient budgets, biological productivity and CO_2-fixation of the global ocean. Paleo-records from the late Permian and Cretaceous give evidence for periods of dramatically reduced oceanic oxygen levels that had major consequences for marine ecosystems (including mass extinctions). Major low oxygen events, including Cretaceous Ocean Anoxic Events, were associated with warmer climates and higher atmospheric CO_2 levels. Recent modelling results suggest that oceanic oxygen levels will decrease significantly over the next decades in response to high atmospheric CO_2, climate change, and altered ocean circulation. Hence the future ocean may experience major shifts in nutrient cycling triggered by expansion and intensification of tropical OMZs. There are numerous feedbacks between oxygen levels, nutrient cycling and biological productivity. Positive biogeochemical feedbacks would accelerate climate-initiated oxygen depletion and the spreading of the oxygen minimum zones. Such changes would have profound global consequences for the future ocean, as they have had in the past. However, our existing knowledge is insufficient to understand past interactions or to adequately assess the potential for future change.

The SFB 754 addresses what we consider to be a newly recognised 'tipping point' of the global climate-biogeochemistry system. Specifically, the following key questions will be addressed: How does subsurface dissolved oxygen in the tropical ocean respond to changes in ocean circulation and ventilation? What are the sensitivities and feedbacks linking low oxygen levels and key nutrient source and sink mechanisms? What are the magnitudes, timescales and controlling factors of past, present and likely future variations in oceanic oxygen and nutrient levels? The overall goal is to improve understanding of the coupling of tropical climate variability and circulation with the ocean's oxygen and nutrient balance, to quantitatively evaluate the nature of oxygen-sensitive tipping points, as well as to assess consequences for the Ocean's future.

To address these questions we study interactions, tracers, mechanisms and thresholds operating in the present-day tropical ocean as well as examine new records of past changes. The SFB will link experimental studies with the development of improved models of redox-sensitive processes involving multiple bio-reactive elements: the biogeochemical models will be integrated with state-of-the-art models of climate change and ocean circulation. Addressing the SFB goals requires multi-disciplinary study. The SFB builds upon wide-ranging expertise available in Kiel, including chemical and physical oceanography, sediment biogeochemistry, marine ecology, molecular microbiology, paleoceanography, geology, as well as climate and biogeochemical modelling.

Zusammenfassung

Die Meteor Reise M77 umfasste vier Fahrtabschnitte auf denen Untersuchungen in der Wassersäule und an Sedimenten im süd-östlichen tropischen Pazifik durchgeführt wurden. Das Thema war die Untersuchung der Sauerstoffminimumzone (OMZ) im Bereich des Küstenauftriebsgebiets vor Peru und zu einem geringeren Anteil vor Ecuador (Abb. 1). Die Untersuchungen fanden im Rahmen an der Universität Kiel eingerichteten und von der Deutschen Forschungsgemeinschaft (DFG) geförderten Sonderforschungsbereichs 754 „Klima – biogeochemische Wechselwirkungen im tropischen Ozean“ statt.

Die Sauerstoffbedingungen im Ozean werden durch das Zusammenwirken von physikalischen, biologischen und geochemischen Prozessen kontrolliert. Sauerstoffquellen sind die Atmosphäre und Photosynthese. Zirkulation und Durchmischung transportieren Sauerstoff aus dem oberflächennahen Bereich in große Tiefen. Gleichzeitig wird ein Teil des Sauerstoffs im gesamten Ozean durch den Abbau organischer Substanz wieder aufgezehrt. Beide Prozesse reagieren sensibel auf klimatische Veränderungen im Ozean. Die Kernregionen mit stark reduziertem Sauerstoffgehalt sind heute auf die Sauerstoffminimum-Zonen (SMZ) in den Tropen beschränkt. Änderungen in diesen regionalen SMZ können sich durch die Ozeanzirkulation aber auch auf den globalen marinen Nährstoffhaushalt auswirken. Auf diese Weise kontrolliert die Sauerstoffverteilung im Ozean die Verfügbarkeit von Nährstoffen wie Stickstoff, Phosphor oder Eisen und kann deshalb beim Unterschreiten bestimmter Schwellenwerte radikal wirkende, mikrobiologische und chemische Prozesse in der Wassersäule und in den Ozeansedimenten in Gang setzen. Daher können derartige Schwellenwerte als „Schaltpunkte“ für die Nährstoffverteilung im Ozean betrachtet werden. Klimatisch erzeugte Änderungen in der Ausdehnung von SMZ können wiederum starke biogeochemische Reaktionen durch Effekte auf die biologische Produktion und die CO2 Aufnahme aus der Atmosphäre und damit auch wieder auf das Klima hervorrufen.

Aus der geologischen Vergangenheit sind Zeitabschnitte mit dramatisch reduziertem Sauerstoffgehalt im Ozean bekannt. Dies hatte extreme Auswirkungen auf die damaligen marinen Ökosysteme bis hin zu Massenaussterben. Derartige anoxische Ereignisse, z.B. im Perm oder in der Kreidezeit, traten bei sehr warmem Klima und sehr hohen CO2 Gehalten in der Atmosphäre auf. Simulationen mit Klimamodellen weisen auf eine Abnahme der Sauerstoffgehalte bei zunehmender Erwärmung und weiterem Anstieg der atmosphärischen CO2 Gehalte in den nächsten Dekaden hin. Der zukünftige Ozean könnte deshalb starke biogeochemische Veränderungen mit positiven und negativen Rückkoppelungseffekten auf

das Klima erfahren, erzeugt durch Wechselwirkungen zwischen Sauerstoffgehalt, Nährstoffhaushalt, biologischer Produktivität und Stofftransport aus Sedimenten. Die Intensität und Konsequenzen solcher Rückkoppelungseffekte sowie die auslösenden „Schaltpunkte“ sind aber weder für die Vergangenheit noch für den heutigen Ozean wirklich bekannt. Die Vorhersage von globalen Konsequenzen für das Klima durch weiter abnehmende Sauerstoffgehalte ist deshalb noch nicht möglich.

Der SFB soll helfen, die O2-Schwellenwerte und damit die „Schaltpunkte“ für radikale Änderungen im Wechselspiel von Klima und Biogeochemie des tropischen Ozeans besser zu definieren. Hierzu sollen folgende Kernfragen beantwortet werden: Wie reagieren die tropischen SMZ auf Änderungen in der Ozeanzirkulation und Ventilation des tiefen Ozeans? Wie reagieren Senken und Quellen von Nährstoffen auf Veränderungen im Sauerstoffgehalt? Was sind die Größenordnungen, Zeitskalen, und wichtigsten Kontrollmechanismen von früheren, heutigen und zukünftigen Veränderungen im ozeanischen Sauerstoff- und Nährstoffhaushalt? Durch den SFB wird ein besseres Verständnis über die Koppelung zwischen Klimavariabilität, O2-Gehalt und Biogeochemie im tropischen Ozean erwartet. Dies soll eine genauere Vorhersage von zukünftigen biogeochemischen Veränderungen im Ozean und den damit verbundenen klimatischen Konsequenzen erlauben. Der SFB verbindet die Untersuchung von klimatisch-biogeochemischen Wechselwirkungen und O2-Schwellenwerten im heutigen Ozean mit solchen die in der Vergangenheit gewirkt haben. Es sollen Experimente mit Tracern durchgeführt, biochemisches Planktonverhalten untersucht, sowie gekoppelte Klimasimulationen (Atmosphäre-Ozeanogra-phie-Biogeochemie) gerechnet und mit Messungen der heutigen Sauerstoff- und Nährstoffbedingungen verglichen werden. Diese sollen durch die Einbeziehung von Rekonstruktionen zur Variabilität von SMZs unter anderen klimatischen Randbedingungen (Holozän und Kreide) eine umfassende Synthese zu den vielfältigen Aspekten der Klima-Biogeochemischen Wechselwirkungen im tropischen Ozean ermöglichen. Hierfür arbeiten Forschungsgebiete wie chemische und physikalische Ozeanographie, marine Ökologie, molekulare Biologie, Biogeochemie der Sedimente, Paläozeanographie und Geologie sowie Klima- und biogeochemische Modellierung eng zusammenarbeiten.

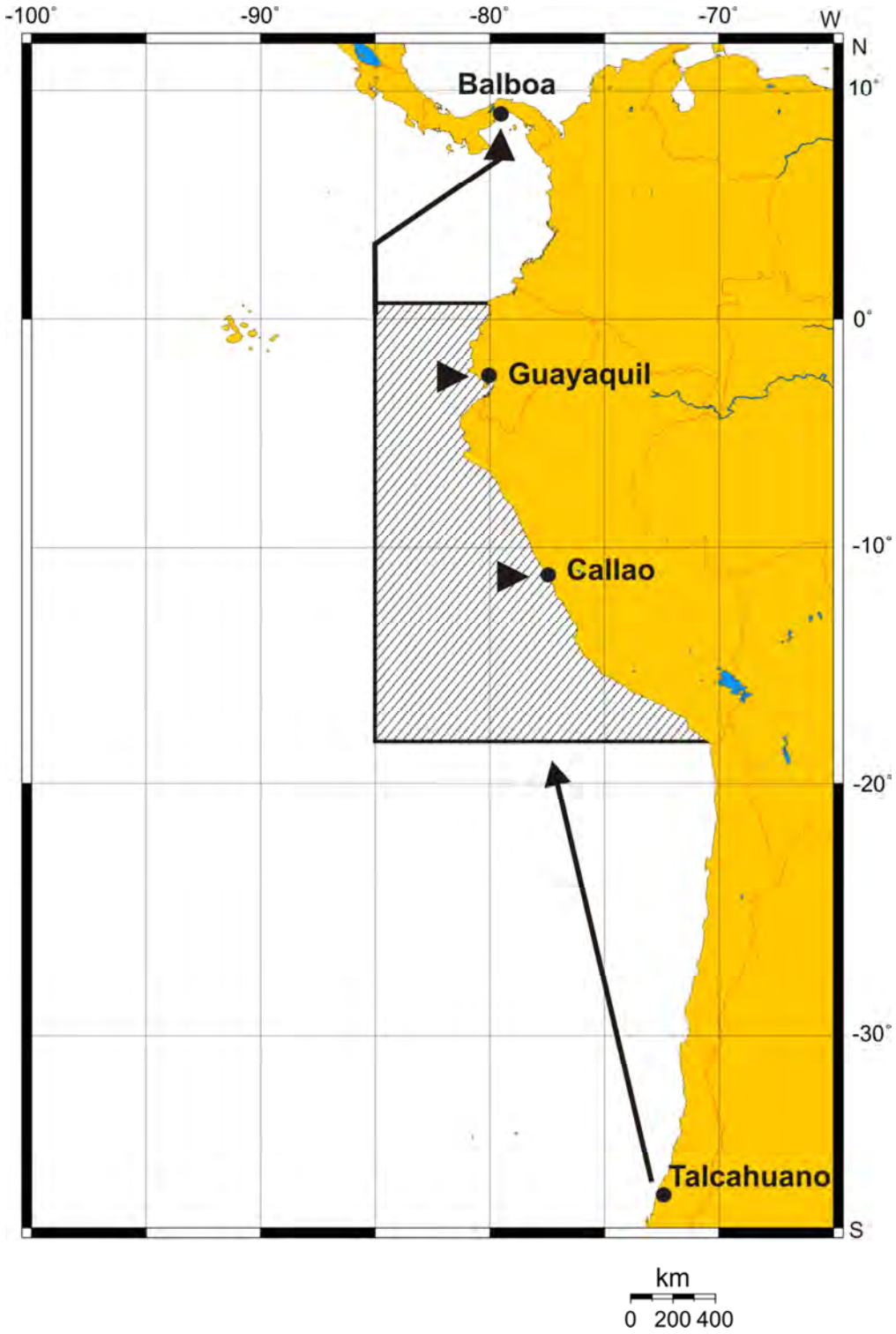

Fig. 1 Working area (shaded) and harbors of METEOR cruise M77

Research Objectives

The main goal of METEOR **Leg M77-1** was the investigation of the sediment and sediment bordering water body ("benthic boundary layer" in the Peruvian oxygen minimum zone. Investigations comprised the *in situ* measurements of turnover and fluxes of nitrogen

compounds, nutrients, trace metals, phosphate and iron across the sediment-water interface at variable oxygen concentrations of the bottom water on the shelf and upper continental slope, typically in a depths gradient from about 100m to 1200m. In parallel to these measurements of the natural environment, the effects of variable oxygen availability (thresholds) in the bottom water on N-speciation and release of nutrients were determined by additional in situ experiments. Further major activities comprised biological investigations of benthic bacterial and foraminiferal communities, the geochemistry of OMZ sediments as well as paleoceanographic and paleoclimatologic studies. Primary goal was to determine and quantify the effect of different oxygen/redox regimes on the speciation and in situ magnitude of nitrogen fluxes (N_2, NO_3^-, NO_2^-, NH_4^+) Fe^{2+}, PO_4^{3-}, O_2, and SO_4^{2-} across the sediment water interface underlying an extended oxygen minimum zone.

The objective of METEOR **Leg M77-2** were paleoceanographic studies for the reconstruction of past atmosphere and ocean climate interactions that could have controlled the behavior of one of the strongest oxygen minimum zone (OMZ) in the tropical ocean.. In the eastern tropical South Pacific, variations in OMZ conditions are not only sensitive to El Niño Southern Oscillation events, but also to longer-term climate variability. Climate-related changes in surface and sub-surface circulation regimes, including variations in preformed oxygen and nutrient conditions, as well as changes in local upwelling intensity and export production need to be considered when deciphering past fluctuations of OMZ conditions. Overall, the combined system of the Peru Coastal Current, the westward wind drift, and the subsurface Peru-Chile Counter Current maintain the upwelling along the coast. Also the varying supply of well or poorly oxygenated subsurface water masses may play a key role for shaping the extent and intensity of the Peruvian OMZ. The upper boundary of the OMZ is determined by maximum mixed-layer depth, while the lower boundary is regulated by eastward flowing equatorial undercurrents. M77-2 retrieved new sample material from the water column and Holocene to Last Glacial sediments from the shelf and upper slope to enable a comparison of past variations in the oxygen minimum conditions with changes in local or remote ocean and atmospheric circulation regimes as well as with past fluctuations in the biochemical processes associated with very high productivity and strong oxygen minimum conditions.

METEOR **leg M77-3** focused on the detailed investigation of the influence of the hydrographic, geochemical and isotopic structure of the water masses and their variability, on the oxygen content in the Peruvian coastal upwelling area with its pronounced oxygen minimum zone (OMZ). These investigations were the basis for a biological research program on the relationship between pelagic community structure and nutrient composition and utilization with particular emphasis on the nitrogen cycle. Three zonal sections covering the oxygen gradients from the upwelling centres near the coast to the open ocean were surveyed at 10°S, 12°S, 16°S, complemented by one section perpendicular to the coast line at 17°S, south of the main areas of coastal upwelling. Together with the meridional section at 85°W, as well as 3 zonal sections at 3°S, 6°S and 14°S that were covered by M77/4, a well-resolved and detailed picture of the water mass and oxygen distribution, their supply paths and their relationship to the pelagic community structure, as well as the distribution and cycling of

nutrients in the eastern equatorial Pacific upwelling areas was obtained. In addition, a detailed survey of the shelf waters south of Lima was carried out to study the variability of the system that partly led to sulphidic conditions in the water column.

METEOR **leg M77/4** had two main subjects. The first was to conduct a detailed survey of the present day distribution of the water masses and the strength of the oxygen minimum zone in the southeastern Pacific. This was mainly carried out to detect changes in comparison to earlier surveys. The second main subject was the investigation of geochemical components in the water column. For the investigation of circulation, water mass mixing and the influence of biological productivity, samples for the analysis of neodymium, silicon and nitrogen isotopes, as well as a number of natural radionuclides were sampled. Their distribution in the water column can be seen as 'stock-taking' under today's circulation and ventilation conditions and can be used in paleo-oceanographic investigations. M77-4 focused on the open ocean area where oxygen richer water is supplied to the OMZ and was closely linked to the activities of leg M77-3, where these investigations were made on the near-shelf areas and was complemented by additional biogeochemical measurements. The goal of the hydrographic measurements was to derive the present day distribution of the water mass and oxygen distribution in the oxygen minimum zone (OMZ) of the southeastern Pacific and resolve the oxygen differences in comparison with older data sets in the supply paths to the OMZ. On leg M77-4 a meridional section at 85°50'W as well as 3 zonal sections at 3°35'S, 6°S and 14°S were measured. Together with the measurements of the other 3 cruise legs this will lead to a well resolved distribution of the water masses and the oxygen status near and within the upwelling areas in the eastern equatorial Pacific at the time of the cruise.

Acknowledgements

The scientific parties aboard METEOR cruise M77 gratefully acknowledge the trustful cooperation and efficient technical support of Captain Baschek and Jacobi and their crew which layed the foundations to a very successful voyage. We like to thank the Auswärtiges Amt (Federal Foreign Ministry) in Berlin and the German embassies in the visited countries who helped to clear the necessary local regulations and working permits. Finally we acknowledge the logistical and administrative support of the Leitstelle Meteor, the shipping company Laeisz and Mr. Bohn (Lehnkering Projects & Logistics).

METEOR-Berichte 11-2

Climate- biogeochemistry interactions in the tropical ocean of the SE-American oxygen minimum zone

PART 1

Cruise No. 77, Leg 1

October 22, 2008 – November 21, 2008
Talcahuano (Chile) – Callao (Peru)

O. Pfannkuche, C. dos Santos Ferreira, P. Croot, S. Sommer, R. Camilli, A. Noffke, B. Domeyer, C. Hensen, F. Scholz, M. Dibbern, N. Glock, R. Ebbinghaus, T. Mosch, B. Bannert, J. Mallon, J. Hommer, T. Treude, M. Graco, E. Enriquez, D. Nürnberg, T. Böschen, S. Voigt, A. Bahr, C. Karas, T. Truscheit

Table of Contents Part 1 (M77/1) **Page**

1.1 Participants

Name	Discipline	Institution
Pfannkuche, Olaf, Dr.	Chief Scientist/Biogeochemistry	IFM-GEOMAR
Bahr, André	Paleoceanography	IFM-GEOMAR
Bannert, Bernhard	Video Technician	IFM-GEOMAR
Boeschen, Tebke	Paleoceanography	IFM-GEOMAR
Camilli, Richard, Dr.	Biogeochemistry	WHOI
Cherednichenko, Sergiy	Electronic Engineering	IFM-GEOMAR
Croot, Peter, Dr.	Marine Chemistry	IFM-GEOMAR
Dibbern, Meike	Geochemistry	IFM-GEOMAR
Domeyer, Bettina	Geochemistry	IFM-GEOMAR
dos Santos Ferreira, Christian	Hydroacoustics	IFM-GEOMAR
Ebbinghaus, Renate	Geochemistry	IFM-GEOMAR
Enriquez, Edgardo	Benthos Biology	IMARPE
Glock, Nicolaas	Geochemistry	IFM-GEOMAR
Graco, Michelle	Biogeochemistry	IMARPE
Hensen, Christian, Dr.	Geochemistry	IFM-GEOMAR
Hommer, Julia	Microbiology	IFM-GEOMAR
Karas, Cyrus	Paleoceanography	IFM-GEOMAR
Kriwanek, Sonja	Biogeochemistry	IFM-GEOMAR
Liebetrau, Volker, Dr.	Geochemistry	IFM-GEOMAR
Mallon, Jürgen	Paleoceanography	IFM-GEOMAR
Mosch, Thomas	Biogeochemistry	IFM-GEOMAR
Nürnberg, Dirk, Dr.	Paleoceanography	IFM-GEOMAR
Petersen, Asmus	Gear Technology	IFM-GEOMAR
Pfannkuche. Björn	IT-Engineering (Stud.)	IFM-GEOMAR
Queisser, Wolfgang	Gear Technology	IFM-GEOMAR
Scholz, Florian	Geochemistry	IFM-GEOMAR
Sommer, Stefan, Dr.	Biogeochemistry	IFM-GEOMAR
Truscheit, Torsten	Meteorology	DWD
Türk, Matthias	Electronic Engineering	IFM-GEOMAR
Voigt, Silke	Paleoceanography	IFM-GEOMAR

DWD	Deutscher Wetterdienst
IFM-GEOMAR	Leibniz-Institut für Meereswissenschaften an der Universität Kiel
IMARPE	Instituto del Mar del Peru
WHOI	Woods Hole Oceanographic Institution, USA

1.2 Research Program

The major objective of M77-1 was the investigation of the sediment and sediment bordering water body ("benthic boundary layer" in the Peruvian oxygen minimum zone. Investigations comprised the in situ measurements of turnover and fluxes of nitrogen compounds, nutrients, trace metals, phosphate and iron across the sediment-water interface at variable oxygen concentrations of the bottom water on the shelf and upper continental slope, typically in a depths gradient from about 100m to 1200m. In parallel to these measurements of the natural environment, the effects of variable oxygen availability (thresholds) in the bottom water on N-speciation and release of nutrients were determined by additional in situ experiments. Further major activities of leg 1 comprised biological investigations of benthic bacterial and foraminiferal communities, the geochemistry of OMZ sediments as well as paleoceanographic and paleoclimatologic studies. Primary goal was to determine and quantify the effect of different oxygen/redox regimes on the speciation and in situ magnitude of nitrogen fluxes (N_2, NO_3^-, NO_2^-, NH_4^+) Fe^{2+}, PO_4^{3-}, O_2, and SO_4^{2-} across the sediment water interface underlying an extended oxygen minimum zone. Key issues were:

- Determination of natural fluxes of nitrogen species, trace metals as well as sulfate, oxygen, iron and phosphate across the sediment water interface at selected shelf to upper slope transects across the oxygen minimum zone under different ambient oxygen conditions using state of the art benthic observatories (lander technology).
- Regional estimates of the sink function of the benthic boundary layer for fixed N.

Biogeochemical investigations on M77-1 comprised water column sediment and sediment pore water sampling to analyze key chemical species, whose chemical behavior and distribution are altered via oxygen mediated redox changes, most notably the key nutrients (fixed) nitrogen, phosphate, and iron. Specifically, we aimed to track the fate of dissolved iron and phosphate in the water column, to quantify the release of dissolved iron and phosphate from sediments, and to improve our understanding of their coupling to carbon, nitrogen, sulphur, and manganese cycles. The major goal of the biogeochemistry/geochemistry groups was to determine and quantify the effect of bottom water oxygenation on the magnitude of O_2, N (N_2, NO_3^-, NO_2^-, NH_4^+), Fe^{2+}, PO_4^{3-}, Si, and SO_4^{2-} fluxes across the sediment water interface underlying an extended oxygen minimum zone.

Investigations of the water column and sediments were conducted at a number of stations along transects across the oxygen minimum zone covering a depth range of 80 –1200m. Station work of M77-1 was exclusively performed in the Peruvian EEZ (Fig. 1.1). Five shelf to slope transects (transect A, C, D, E, F) and one single station (area B) were investigated. Investigations were performed without deviations from the planned activities. The concentration of activities particularly the deployment of landers to transect C enabled us to study the temporal and spatial variability of processes in the benthic boundary layer in a better resolution. New instrument such as the in situ mass spectrometer and the 3D-microelectrode profiler for sediments were used successfully for the first time and will broaden our instrumental capacity for biogeochemical BBL observations for the future.

Major gear employments were:

- Seafloor imaging with swath bathymetry and PARASOUND surveys,
- Water column surveys with CTD/Rosette water sampler,
- Ocean floor imaging with Ocean Floor Observation System transects (OFOS),
- Sediment sampling with gravity corer,
- Sediment sampling with TV-multi corer,
- Lander deployments for in situ flux measurements and experiments in benthic chambers (BIGO lander)
- Lander deployments with a novel sediment x/y/z-micro-electrode profiler.

1.3 Narrative

Wednesday, 22-10-08: Due to a delay in the ship yard inspections the M77-1 scientific party which arrived on the 20-10-08 could board METEOR only after a stay in a hotel on the morning of the 22-10-08. Until 15:00h we loaded our equipment from five containers on the pier. Four Containers were taken onboard and were unloaded by the scientists. It was also planned to refuel the ship on the same day and to leave the port lately the next morning but due to the weather situation the bunker vessel coming from Valparaiso was rescheduled for the afternoon of the 23-10-08.

Thursday, 23-10-08: We left the shipyard in the morning at 08.12h and anchored in the Bay of Talcahuano to await the bunker vessel which arrived at 16:00h. After refuelling followed by custom and immigration clearance we finally left Talcahuano roadstead at 23:30h with a delay of two days. We steamed north along the Chilenian coast heading to our first area of investigation at 18°S in the Peruvian EEZ.

Friday, 24-10-08: We continued our progress along the Chilenian coast which was supported by tailwinds and currents.

Saturday, 25-10-08: We further advanced to the north.

Sunday, 26-10-08: Our voyage to the first station continued.

Monday, 27-10-08: We continued our passage to the first working station. We passed into the Peruvian EEZ at 18:35h and reached our first station in 17°50´S/072°05´W at 21:30h where we started station work with a CTD/RO cast at 2000m water depth (Stat. 386).

Tuesday, 28-10-08: During the night until noon we surveyed an upslope transect (Transect A, Fig. 1.1) with multi-beam EM120 /EM710 and Parasound from 2000m to about 130m water depth with CTD/casts near the 1000m, 800m, 500m, 300m, and 200m depth contour (Stat. 387-95). In the afternoon we took 3 multi-corer samples in down slope direction at the 300m- and 500m-Stations (Stat. 396-398). In the later evening an OFOS transect at 120m water depth was carried out (Stat. 399).

Wednesday, 29-10-08: We continued our OFOS investigations around the 300m and 500m depth lines during the night (Stat. 400-01). We then steamed to the 2000m-contour for another CTD/RO cast (Stat. 402). Our activities were then centered again at the 300m-Station where we took two multi-corer samples and deployed a BIGO-T lander (Stat. 403-05). The afternoon and evening was dedicated to further multi-corer sampling at the 500m-, 700m- and 1000m-Stations (Stat. 406-410).

Thursday, 30-10-08: Multi-coring was continued at 2000m during the night followed by another CTD/RO cast (Stat. 411-412). During the day we performed gravity corer sampling along the depth transect from 2100m to 300m at five sites (Stat. 413-418) with variable success gaining core lengths between 6m and less than 1m. In the evening we retrieved the BIGO-T lander (Stat. 419) and left transect A in northern direction to 15° 11,4´S/075° 34,8´W.

Friday, 31-10-08: We reached the 15°N-Station (**Site B,** Fig. 1.1) in the afternoon and took a series of samples at the 500m contour comprising of two multi-corer, one gravity corer and

one CTD/RO cast (Stat. 420-23). Afterwards we left for 11°S to investigate a new depth transect. It was originally planned to investigate a transect in the vicinity of 12°S but the course of the 5miles coastal zone which limited our research area expanded too far out due to some islands. In consequence we could not investigate water depths beyond 150m. Therefore we shifted our area of investigation to 11°S where we could sample a water depth up to 80m outside the restricted five miles zone.

Saturday, 01-11-08: We arrived at our first station in 11´S/078°30´W at 21:00h (Transect C, Fig. 1.1) and started station work with a CTD/RO cast at 950m water depth (Stat. 424). This was followed by an upslope transect with multi-beam EM120 /EM710 and PARASOUND from Station 424 to about 85m water depth on the shelf interrupted by CTD/RO casts near the 700m, 800m, 500m, 300m, 200m, 150m and 85m depth contour (Stat. 425-36).

Sunday, 02-11-08: The multi-beam/PARASOUND- and CTD-survey line ended at 11:00h. Afterwards we turned 180° and steamed back down slope on another multi-beam/PARASOUND survey line slightly shifted to the South (Stat. 437). This transect was extended to water deeper than 1200m. At the end point of this track line we took a CTD/RO (Stat. 438) afterwards we drove another multi-beam/PARASOUND survey line slightly shifted to the North back up slope to 950m depth (Stat. 439) where we took a multi-corer sample (Stat. 440).

Monday, 03-11-08: During the night we made three CTD/RO casts with the in situ mass spectrophotometer built into the supporting frame of the rosette to measure di-nitrogen content in the benthic boundary layer water (Stat. 441-444). In the morning we shifted position to the 950m-station and took multi-corer samples (Stat. 445-448). We continued the multi-corer series upslope at 325m depth (Stat. 449-50). Afterwards we deployed a BIGO-Lander (Stat. 451). We then continued our up slope passage to the shallowest station in 85m to make a CTD/ RO cast (Stat. 452). After the release of the first rosette water bottle the command unit of the CTD failed and the station had to be abandoned. Afterwards we drove our first OFOS-survey line down slope heading 270°W (Stat 453).

Tuesday, 04-11-08: We continued with another OFOS starting at 200m during the night (Stat. 454). Unfortunately we had to abandon the station since the flash of the digital photo camera failed. Therefore we changed to multi-corer sampling and took three samples by 475m (Stat. 455-57) and two samples by 730m (Stat. 458-59) as well as a further sample by 1200m (Stat, 460). In the afternoon we enlarged our multi-beam survey to the West and drove a transect down slope to the 2000m depth contour (Stat. 461). With this survey transect C was extended to more than 40nm covering a depth range from 85m to 2000m. A multi-corer sample at 2000m followed (Stat. 462). Afterwards we steamed back up slope to retrieve the BIGO Lander deployed the day before at 325m (Stat. 464). During the evening we changed gear to OFOS and started with a survey line at 325m (Stat. 465).

Wednesday, 05-11-08: During the night we continued with OFOS surveys at 400m and 600m (Stat. 466-67). The morning started with a CTD/RO cast at 150m (Stat. 468) followed by two multi-corer casts (Stat. 469-70). The afternoon was dedicated again to multi-corer sampling at 325m (Stat. 471-73). The BIGO Lander and the PROFI Lander were deployed in the evening at 725m (Stat. 474-475). Afterwards we started with a CTD/RO survey with the in situ mass-spectrometer attached to the gear at 400m (Stat. 476).

Thursday, 06-11-08: During the night we continued with CTD/RO surveys at 300m, 200m, and 100m (Stat. 477-79). The morning started with another CTD/RO cast at 300m (Stat. 480) followed by two multi-corer casts at 370m (Stat. 481-82). Afterwards we steamed down slope for three multi-corer casts at 725m (Stat. 483-85). We then retrieved the PROFI lander (Stat. 486) which was moored in a distance of three cables. We changed position again to 600m and took two more multi-corer samples (Stat. 487-88). Afterwards we returned to 725m to retrieve the BIGO Lander (Stat. 489). During the evening we changed to OFOS and started with a survey line at 500m (Stat. 490).

Friday, 07-11-08: During the night we continued the OFOS survey in down slope direction with survey tracks at 700m and 1000m (Stat. 491-92). In the morning we shifted from coaxial cable to wire to perform a series of gravity corer casts which started in deep water at 2020m (Stat. 493-94) and was continued up slope at 1200m (Stat. 495-96) and at 925m (Stat. 497). During the evening until early morning next day we undertook CTD/RO casts at 150m, 250m, 500m and 1000m (Stat. 498-501).

Saturday, 08-11-08: We continued our gravity corer sampling in the early morning until the evening starting again at 925m (Stat. 502) afterwards we worked up slope at 700m, 500m, 300m and 150m (Stat.503-12). In the evening we started a multi-beam/PARASOUND survey to enlarge the mapping of our investigation area to North and South of the 11°S-transect line (Sta. 513).

Sunday, 09-11-08: We continued the multi-beam/PARASOUND survey (Stat. 513) during the night until mid morning. We then steamed to the 600m contour where we deployed a BIGO-T lander (Stat. 514) which was followed by a CTD/Ro cast two cables north of the lander position (Stat. 515). A series of multiple corers was taken up slope between 600m and 195m (Stat. 516-522).

Monday, 10-11-08: During the night we drove a series of OFOS transects at 480m, 340m and 200m (Stat. 523-526). This was followed during the day by the deployment of a BIGO lander by 395m (Stat. 526) and a lander with a micro electrode profiles (PROFI) by 990m (Stat. 527). Afterwards we retrieved the BIGO-T- lander deployed the day before (Stat. 528). We then left transect C and steamed about 40nm to the North to start a new transect line.

Tuesday, 11-11-08: During the night and morning we mapped the new **transect line D** (Fig. 1.1.) between 1100m and 150m driving three multi-beam/PARASOUND transects both in up slope and down slope direction (Stat. 529-531). At the shallowest part we made a CTD/RO cast and took two multi-corer samples (Stat. 532-34). We then steamed back to transect C to retrieve the BIGO lander and Profiler deployed the day before (Stat. 535-36).

Wednesday, 12-11-08: We continued with OFOS-surveys at transect C during the night at 300m, 200m, and 100m (Stat. 537-39). We continued with multi-corer sampling in the shallowest region at 80m (Stat. 540-43). Afterwards we steamed to the 300m contour to deploy another BIGO-T lander (Stat. 544). We then moved further down slope and made three CTD/RO casts at 500m and 1000m (Stat. 545-47). In the evening we deployed a BIGO lander and took a multi-corer sample at 1000m (Stat. 548-49).

Thursday, 13-11-08: We returned to transect D and drove a series of OFOS transects during the night at 140m, 320m, and 700m (Stat.550-552). This was followed during the morning by two multi-corer samples and two CTD/RO casts at 300m (Stat 553-56). During the afternoon we steamed back to transect C to retrieve the BIGO T and PROFI lander (Stat. 558-559).

Friday, 14-11-08: During the night three multiple-corer samples were taken around 450m (Stat. 559-561) followed by two OFOS survey lines around 300m and 500m (Stat. 562-63). During the day we continued with multi-corer sampling at 550m and 650m (Stat. 564-65). In the evening we deployed a BIGO-T lander by 300m and a PROFI lander by 765m (Stat. 566-67). We then drove up slope and deployed a BIGO lander by 85m (Stat. 568) followed by a CTD/RO cast at 185m (Stat. 569).

Saturday, 15-11-08: During the night we added a further multi-beam/PARASOUND transect line enlarging our mapped area of transect C (Sta. 570). We continued with OFOS surveys at 635m and 400m (Stat. 571-72). During the day we worked around the 300m contour where we took two multi-corer samples (Stat. 573-74), made a CTD/RO cast (Stat. 575) and retrieved the BIGO-T lander (Stat. 576). Afterwards we steamed to the shallowest position and retrieved the BIGO lander (Stat. 577).

Sunday, 16-11-08: The whole night was dedicated again to OFOS surveys at 200m, 500m, and 600m depth (Stat. 578-80). Afterwards we switched to multi-corer sampling during the morning (Stat. 581-84). During the afternoon we retrieved the PROFI lander (Stat. 585) and deployed a BIGO-T lander at 316m depth (Stat. 586). Two multi-corer casts were performed at 200m Stat. (Stat. 587-588). Afterwards we changed position to a new transect line (**transect E,** Fig. 1.1) where we continued multi-corer sampling by 500m (Stat. 589-90)

Monday, 17-11-08: Two OFOS surveys were driven at transect E during the night at 720m and 960m (Stat. 591-92). A series of five CTD/RO casts between 900m and 500m followed (Stat. 593-97). We returned to transect C to retrieve the BIGO-T lander (Stat. 598). Afterwards we steamed back to transect E and took two more CTD/RO samples (Stat. 599-600) and made four multi-corer casts on the mid slope (Stat. 601-04). Afterwards we left transect E and steamed south to 12°32´S to start a new transect line (**transect F**, Fig. 1.1).

Tuesday, 18-11-08: We started station work at transect F with two multi-beam/PARASOUND profiles in up slope and down slope direction (Stat. 605-606). During the day we took two multi-corer samples by 580m (Stat. 607-608), a CTD/RO cast by 300m (Stat. 609) and two more multi-corer casts by 400m (Stat. 610-611). An OFOS survey followed at 620m (Stat. 612).

Wednesday, 19-11-08: An additional multi-beam/PARASOUND profile was driven during the night to enlarge the sea floor mapping of transect F (Stat. 613). During the day we took a series of multi-corer samples and CTD/RO casts along the transect line between 250m and 1085m (Stat. 614-23).

Thursday 20-11-08: During the night and morning we drove four OFOS transects at 700m, 440m, 250m, and 160m (Stat. 624-27). Afterwards we continued with CTD/RO casts at 200m, 400m, 600m, 800m, and 1000m (Stat. 628-32). With Station 632 we finished station work of M77-1 in the afternoon.

Friday 21-11-08: During the night we steamed towards Callao where we docked in the morning around 08:00h. With the departure of the scientific crew in the afternoon METEOR cruise 77 leg 1 ended.

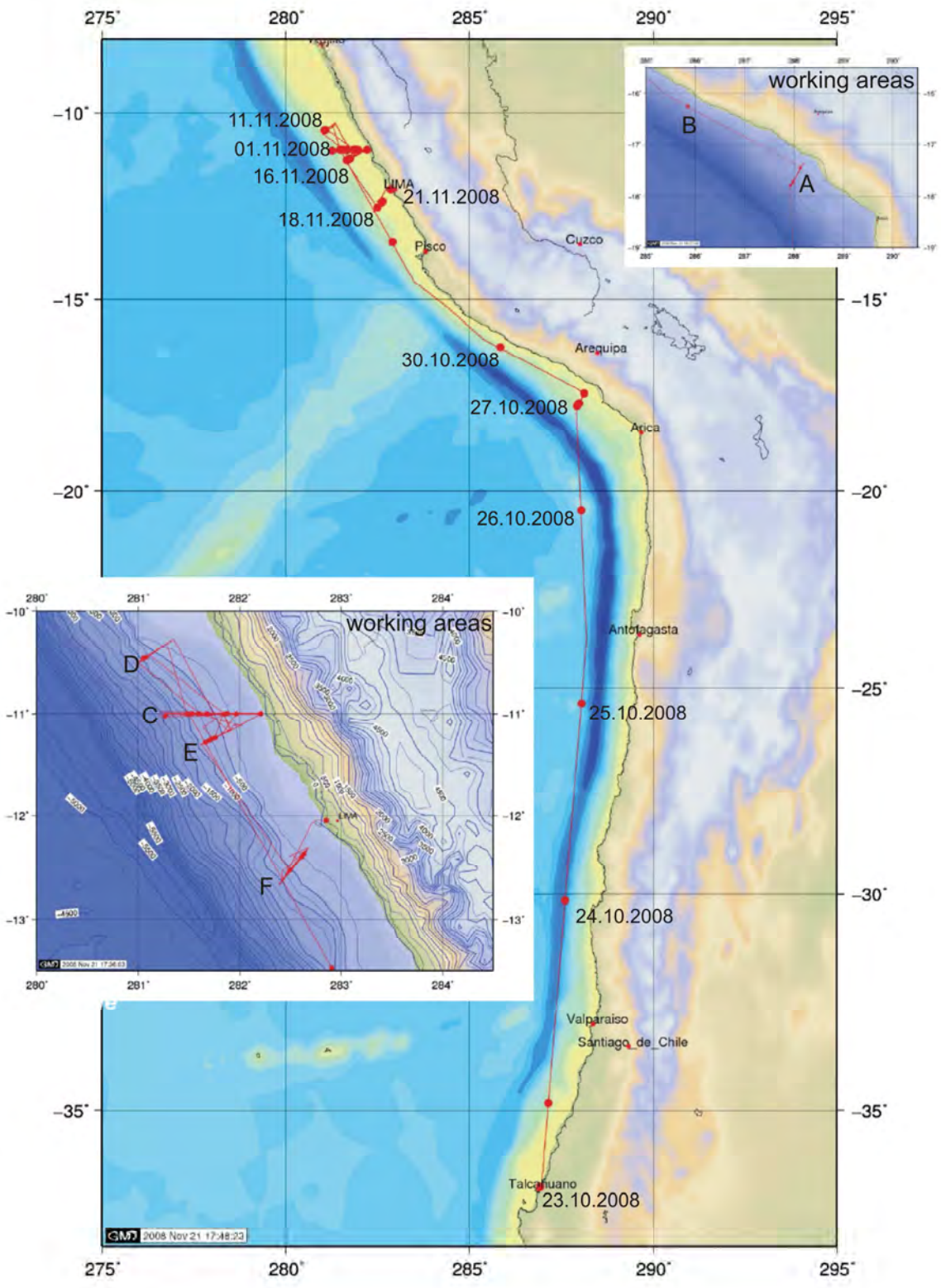

Fig. 1.1: Cruise track and working areas of cruise M77 leg consisting of five shelf to upper slope transects (transect lines A, C, D, E, F) and one single Station (B). A focus of our activities was centered at transect C

1.4. Preliminary Results

1.4.1 Multi-beam surveys

(C. dos Santos Ferreira)

Multi-beam surveys were made using the echo-sounders available at RV METEOR, both systems from KONGSBERG MARITIME (fomerly SIMRAD). The first was an EM120, a deep-water multi-beam operating at 12 kHz, and with 191 beams. This system is designed for mapping the full ocean depth and its best performance is between 600 meters and 12.000 meters water depth. The second was an EM710, 1-by-1-degree broadband multi-beam echo-sounder operating between 70 kHz and 100 kHz band. It has 400 beams, and its maximum water depth limit is at 1500-2000 meters according to the manufacturer. However, its best performance was obtained from 600-500 meters to shallow waters.

The EM120 echo-sounder was operating 24 hrs per day during the whole cruise, while the EM710 was switched on only at our main working areas, and when the depth was less than 1000 meters. In the surveys we identified in the data from the EM710 several spikes due to interferences caused by the PARASOUND system. For the EM120 there was no external interferences, but "internal ones", since the central beams showed clearly at water depths lower than 300 meters a "rail", probably created by the high intensity sound emissions at these beams and its interactions with the seafloor. The cruise maps were produced from the main working areas (transects A, C, D, E, F; Fig. 1.1) only using the data from the EM120 echo-sounder. The choice was based on the fact that the EM120 data was nearly "spikes free" (demanding a smaller amount of time for post processing). And this factor was important, since maps were needed as fast as possible for planning the next instrument deployments (MUC, Gravity Corer, OFOS, Landers and CTD).

The ship´s processing software Neptune proved to be unstable and slow to analyze data sets with more than 1 GB of multi-beam data. And since all the working area maps ended up larger than 2 Gb, the use of Neptune was simply skipped during the whole cruise.

For the fast post processing made on cruise, the multi-beam data were analyzed using MB System 5.1.1 (Caress and Chayes, 2001) included in the operational system Poseidon Linux 3.1 (Ferreira et. al, 2006). Since the amount of data was bigger than 2Gb, MB System was the only option capable to handle it, and to produce good maps in a short time (20-30 minutes). No filters or cleaning were applied at this time, and the grid size resolution was set between 30-40 meters.

1.4.2 Trace metal speciation and trace redox species measurements

(P. Croot)

1.4.2.1 Objectives

This work is a key part of project B5 in SFB754 which aims to combine water column and porewater sampling in the Oxygen Minimum Zone (OMZ) of the Eastern Tropical Pacific (Peru Upwelling) in order to improve our understanding of benthic-pelagic coupling in the present day ocean. This work examines key chemical species, most notably the key nutrients iron and phosphate, whose chemical behaviour and distribution are altered via oxygen mediated redox changes, in both the water column and sediment pore waters. During M77-1 the focus was on the Peruvian shelf and the direct benthic-water column interaction. Phosphate and iron are key nutrients/compounds controlling primary production in the surface ocean and their availability is largely subject to redox-dependent changes in the environment. Hence, the quantification of inventories and fluxes and the study of the dynamical response to variations of major environmental conditions are key to the understanding of climate induced biogeochemical variations and their feedbacks. In SFB 754 our work is focused on quantifying the source and sink fluxes for redox driven processes affecting soluble and colloidal Fe and Mn species in the water column in order to allow direct assessment of their overall contribution to the biogeochemical cycling of phosphate. This is supplemented by investigations of Mo and Cd distributions as these can provide important information on the role of sub-oxic and anoxic processes with particular relevance to paleo-tracers of past anoxia, or deep water nutrient conditions (Cd-phosphate).

It has recently been demonstrated that extensive parts of the Eastern Pacific upwelling systems are iron limited and that terrigenous sediments deposited on the continental shelf are the major iron source for these regions (Bruland et al. 2005; Hong and Kester 1986) predominantly as Fe(II) originating from the sediments in contact with OMZ waters. However it is currently unknown how far this signal persists out into the open ocean and this is important for understanding the supply of iron from the Peruvian shelf to the open ocean waters of the Tropical South Eastern Pacific and its potential role in controlling primary productivity (Bruland et al. 2005). An important consideration here also in assessing this iron supply is the lifetime of the Fe(II) in the OMZ waters and in the absence of O_2 the most important oxidant is H_2O_2. Currently there has only been a single published report on H_2O_2 in Peruvian waters (Zika et al. 1985) and the present work was designed to improve our knowledge and understanding or processes influencing the distribution of H_2O_2 and Fe(II) in the Eastern Tropical Pacific and Peruvian shelf waters.

Iodine is potentially a key element for climate change as iodine emissions from the ocean strongly influence the formation of new aerosol particles with impacts on cloud formation and radiative balances. The source and mechanism of iodine emissions from the ocean is poorly understood, as are other more fundamental aspects of iodine biogeochemistry in seawater such as the cycling between the major iodine species; Iodate and iodide. In the proposed work we investigated the biogeochemistry of iodine in the poorly studied waters of the Peruvian OMZ.

Central to this work are investigations into the threshold level for dissolved O_2 at which iodate was reduced to iodide in waters below the euphotic zone.

1.4.2.2 Methods

Fe(II) and H_2O_2 Measurements: For this cruise we developed using a single chemi-luminescence flow injection analyzer a reagent injection method to simultaneously measure both Fe(II) and H_2O_2 from a single sample in near real time. This method was based on previously published methods for H_2O_2 (Yuan and Shiller 1999) and Fe(II) (Croot and Laan 2002). Seawater samples were obtained using Niskin bottles on a standard CTD rosette. Samples were drawn into 100ml low density brown polyethylene bottles which were impervious to light. Samples were analyzed within 1-2 hours of collection where possible and were not filtered.

Iodide and Iodate Measurements: Sea water samples (unfiltered) were obtained using Niskin bottles on the standard CTD rosette from all depths. Samples were drawn into 60 or 250ml Teflon bottles and stored in the dark until analysis. Samples for iodide were analyzed by cathodic stripping square wave voltammetry (Luther et al. 1988), using a μAutolab III (Ecochemie) combined with a VA663 electrode (Metrohm), within 3-4 hours of collection. Iodate was measured by reduction to I^- via ascorbic acid and analysis by voltammetry.

Atmospheric Optical Thickness (AOT) Measurements: Discrete AOT measurements were made using a MICROTOPS II kindly loaned by the NASA/Goddard Space Flight Centre as part of the AERONET Maritime Aerosol Network program (http://aeronet.gsfc.nasa.gov/new_web/maritime_aerosol_network.html) (Smirnov et al. 2009). The MICROTOPS II is a hand held instrument that is well characterised for AOT measurements (Ichoku et al. 2002) and is capable of being used on moving platform such as a ship at sea (Porter et al. 2001).

1.4.2.3 Results (Shipboard)

High concentrations of Fe(II) were encountered in the bottom waters of all of the shelf stations occupied (Fig 1.2). indicating the strong flux of Fe(II) originating from the sediments. A more reduced Fe(II) signal was also seen in the OMZ waters of the open ocean. H_2O_2 concentrations were relatively low throughout the surveyed region despite the strong sunlight and this is believed to be due to a combination of slow production and fast decay. Apparent high H_2O_2 concentrations were detected in the presence of high Fe(II) levels but this appears to be more an analytical interference in the H_2O_2 assay from the oxidation of the Fe(II) in the detector leading to the formation of H_2O_2 *in situ.* Further work was carried out at sea to ascertain if this effect was able to be corrected for and the results adjusted accordingly to determine the true H_2O_2 concentration in the presence of significant Fe(II).

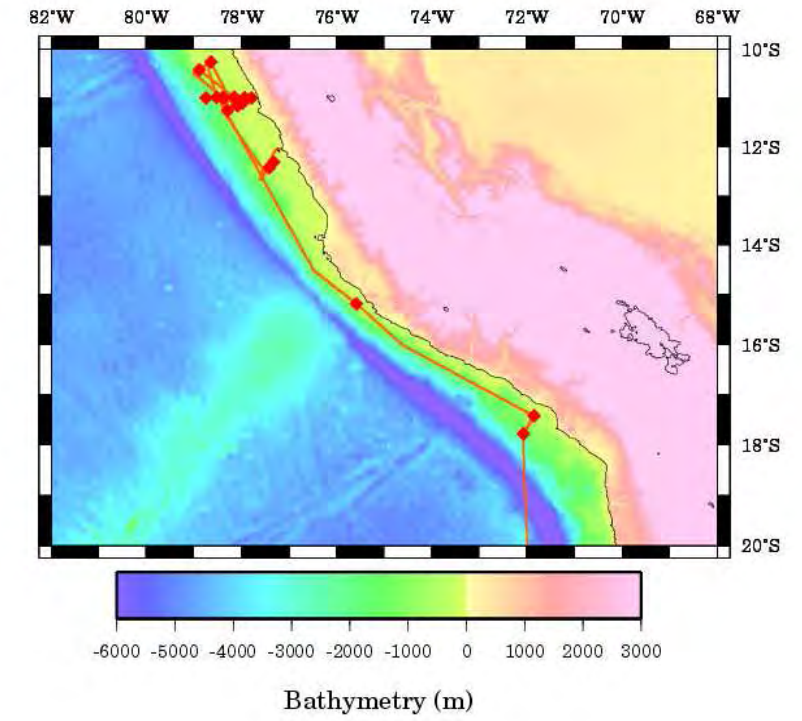

Fig. 1.2: Location of stations sampled for short lived redox species during M77-1.

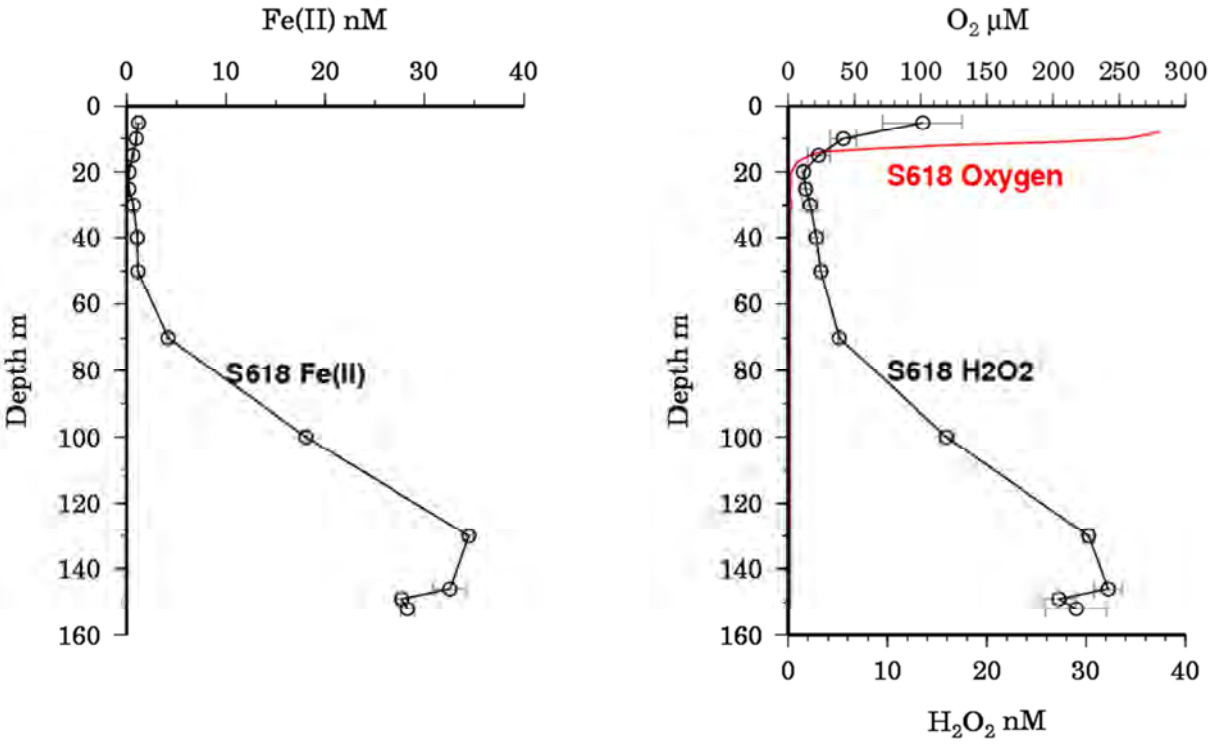

Fig. 1.3: (left) Fe(II) and (right) O2 and H2O2 at S618 on the Peruvian shelf.

Iodide concentrations were high along the productive shelf regions with a distinct difference seen between onshore and offshore waters of the Peruvian shelf with extremely high iodide levels in the shelf waters. In all regions sampled, the OMZ was clearly demarcated as a zone of high iodide with an inverse relationship between O_2 and I^-. The threshold O_2 level

for iodate reduction was apparently around 10 µM with lower levels of O_2 seeing sharp increases in the iodide concentrations. Interestingly there was some indication that close to the sediments total iodine may be enriched in the water column and this signal transported offshore in the core of the OMZ, suggesting a possible sedimentary source for iodide.

The preliminary Microtops data indicated moderately high AOT over the course track most of the time suggesting biogenic particle formation as there was apparently little dust encountered during the cruise as might be expected for this remote region. The collected AOT data is already available on the MAN webpage.

1.4.3 Nitrogen fluxes across the benthic boundary layer under different oxygen conditions

(S. Sommer, O. Pfannkuche, R. Camilli)

1.4.3.1 Objectives

Our major objective within subproject B6 of the SFB 754 is to determine and to quantify the effect of different oxygen/redox regimes on the speciation and in situ magnitude of nitrogen fluxes (N_2, NO_3^-, NO_2^-, NH_4^+), Fe_2^+, PO_4^{3-}, O_2, and SO_4^{2-} across the sediment water interface underlying an extended oxygen m inimum zone (OMZ). A further goal was to achieve a regional estimate of the sink function of the benthic boundary layer for fixed N based on in situ fluxes and pore water geochemistry in correlation with bathymetry, PARASOUND and image data from OFOS deployments, (see report by Mosch & Bannert).

1.4.3.2 Methods

Our investigations focused predominantly on a transect C (Fig. 1.1) covering a depth range of ~80m to ~1200m. At transect C the core of the oxygen minimum zone intercepts with the continental margin at water depths of about 50m down to 400m. Sediments in the core of the OMZ were densely covered by sulfide oxidizing bacterial mats (Beggiatoa/Thioploca). As soon as oxygen levels increased below 400m abundant macro – megafauna was observed.

In-situ investigations

Benthic chamber lander, BIGO and BIGO-T

Several deployments of BIGO and BIGO-T lander (Biogeochemical Observatory) which are equipped with 2 and 1 benthic flux chamber respectively, were conducted within the core of the OMZ (BIGO 3, BIGO 5, BIGO-T 3, BIGO-T 4) as well as at the lower boundary (BIGO 2, BIGO-T 2) and at water depths down to about 1000m (BIGO 4) to investigate nutrient, Fe, Mn, and P fluxes along this natural oxygen gradient. BIGO-T additionally to the flux chamber carried the under water membrane inlet mass spectrometer TETHYS, which was operated in cooperation with R. Camilli (WHOI), The TETHYS instrument (Fig 1.5) can quantitatively identify a wide range of hydrocarbons but also other volatiles such as N_2, Ar, O_2, CO_2 etc. During the deployment of BIGO-T 1 and BIGO-T 5 we measured temporal changes of predominantly N_2, Ar and other gases inside the benthic chambers.

The functional principle of the BIGO-type lander has been described by Pfannkuche & Linke (2003) and Sommer et al. (2006, 2008,2009). In brief BIGO and BIGO-T retrieve water samples from the enclosed chamber water at predefined time intervals. At the end of the flux measurement the incubated sediments are kept inside the chamber for further on-board sub-sampling. Geochemical measurements in the sediments included the following parameters: O_2, SO_4^{2-}, HS^-, NO_3^-, NO_2^-, NH_4^+, PO_4^{3-},Fe_2^+, Si, Br^-, I^-, trace metals, total alkalinity, the determination of physical properties of the sediment as well as the sediment C/N ratio, content of plant pigments and meiofauna. Geochemical parameters that were measured in the bottom/chamber water include O_2, N_2, Ar, N-compounds, PO_4^{3-}, Si, SO_4^{2-}, trace metals, and physical parameters (temperature, density, salinity). From the chamber water concentration gradients of the above listed parameters the respective interfacial fluxes are calculated and compared with fluxes derived from pore water profiles (cooperation with C. Hensen, P. Croot, SFB 754, B5).

Transecting profiler (O_2 micro-gradients)

In addition to the chamber lander a novel transecting profiler which allows to measure oxygen micro-gradients across the sediment water interface was deployed at the lower boundary of the OMZ mounted to a lander (Fig. 1.4). The profiling unit consists of a lower and upper glass fibre frame, which are connected by four glass fibre poles. The upper frame extends about 50 cm towards the front defining an area across which sensors can be moved in mm increments along the x- and the y-axis. Along the vertical z-axis, the sensors can be moved at freely selectable increments. Commercially available oxygen micro-sensors (tip diameters: ~ 100 µm. Unisense, DK) were used to measure in-situ oxygen concentration profiles. The sensors were connected to individual miniaturized amplifier units which were jointly developed with Unisense, DK.

Fig. 1.4: Transecting profiler to conduct 3-dimensional micro-scale measurements of oxygen, sulfide and ph in sediments. Profiler is mounted within a lander.

Water column investigations

Geochemical investigations were further conducted in the water column with particular focus on the benthic boundary layer. Major parameter studied were temperature, salinity, O_2, N_2, and Ar. In addition to conventional water sampling these gases were further measured on high spatial resolution using TETHY mounted on the frame of the CTD/Rosette, Fig. 1.5.

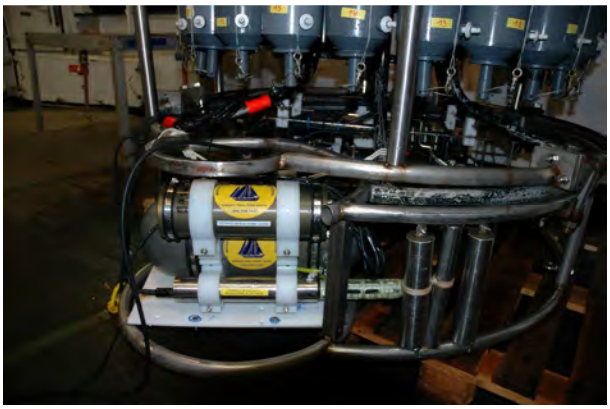

Fig. 1.5: TETHYS instrument (WHOI, R. Camilli) mounted on the frame of the CTD/water sampling rosette.

Geochemical analyses

Analyses of the above listed parameter were partly performed onboard in close collaboration with the subproject B5/A7 (C. Hensen, K. Wallmann, A. Noffke, L. Bohlen).

Ex situ N_2/Ar measurements

The in situ N_2/Ar measurements in the water column using TETHYS were complemented by additional ex situ N_2/Ar measurements using an onboard membrane inlet mass spectrometer (GAM 200, InProcessInstruments, Bremen). N_2 emission from the sediment (indicative for denitrification and anammox) was also measured using the water samples retrieved during the lander deployments. Membrane-inlet mass spectrometry (MIMS) starts to become a widely used method for the determination of dissolved gas concentrations in natural waters (e.g. Kana et al. 1994, Hartnett & Seitzinger 2003, Laursen & Seitzinger 2002, Guéguen & Tortell 2008). N_2/Ar ratios are calculated from the quadrupole instrument signal (ion currents detected via an electron multiplier) and are calibrated using air-equilibrated water standards. The sample standards and water samples are kept at a constant temperature to minimize instabilities due to temperature fluctuations. Nitrogen, argon and oxygen solubilities at different temperatures and salinities are calculated from Hamme & Emmerson (2004) and Garcia & Gordon (1992).

1.4.3.3 Results (Shipboard)

Benthic fluxes - Benthic chamber lander BIGO, BIGO-T

A total of ten chamber lander deployments were conducted (nine at transect C) in water depths of 85m (BIGO 5) to 1015m (BIGO 4). A typical oxygen data set retrieved from a lander deployment is shown in Fig. 1.6.

The lander deployments allows us to calculate the N-fluxes (beside the other parameters listed above) to determine the overall sink function for reactive nitrogen of the sediments at transect C. These data will be combined with the N_2/Ar data measured in the water column. In collaboration with subproject B5/A7 (C. Hensen, K. Wallmann) we further envisage to extrapolate these N-fluxes for a wider geographical area of the Peruvian continental margin using pore water geochemistry, as well as seafloor image data in combination with bathymetry and backscatter that was obtained at several sites north and south of transect C (see also Chapter 1.4.5).

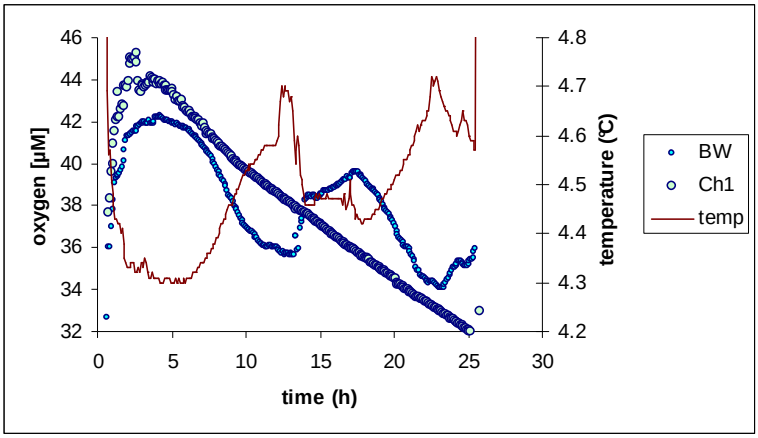

Fig. 1.6: Concentration of oxygen over time in the benthic chamber 1 (CH 1) and in the bottom water (BW) measured using Aanderaa optodes during deployment of BIGO 4. Changes of temperature during the deployment are indicated.

Micro-electrode Profiler

Profiler deployments were conducted in water depths of 727 and 1000 m. We retrieved 26 and 36 profiles respectively, which were measured along a horizontal transect of about 40 cm length. Figure 1.7 shows oxygen micro-gradients obtained from the 1000m station.

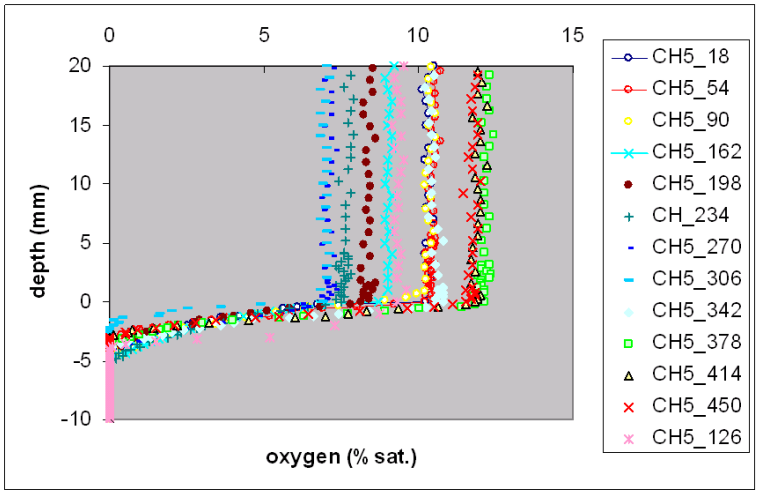

Fig. 1.7: Oxygen micro-profiles across the sediment water interface measured during the deployment of Profiler 2 (1000 m).

Water column investigations/TETHYS

Preliminary saturation normalized N_2/Ar ratios at seven stations along transect C indicated N_2 release in water depths shallower than 500 m, which are associated with low oxygen conditions, Fig.1.8. The saturation normalized N_2/Ar ratio represents the molar N_2/Ar ratio measured in a water sample divided by the ratio at equilibrium for a given temperature and salinity. This ratio indicates the relative excursion from solubility equilibrium with the atmosphere. However this parameterization bears uncertainties since it does for example not account for the "history" that an oceanic water mass undergoes since its last contact with the atmosphere.

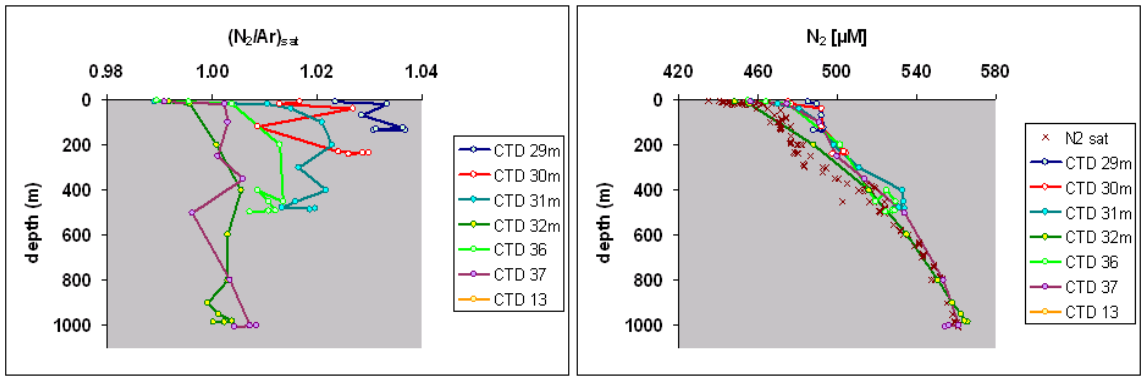

Fig. 1.8: Left panel: saturation normalized N_2/Ar ratio [$(N_2/Ar)_{sat}$ = $(N_2/Ar)_{molar\ ratio}/(N_2/Ar)_{sat.\ equilibrium\ ratio}$] at 7 stations along transect C; Right panel: N_2 concentration profiles at the same sites as shown in the left panel in comparison to the saturated N_2 concentration calculated to the respective temperature and salinity.

1.4 Preliminary Results

1.4.4 Pore Water Geochemistry

(A. Noffke, B. Domeyer, C. Hensen, F. Scholz, M. Dibbern, N. Glock, R. Ebbinghaus)

1.4.4.1 Objectives

Pore water composition of surface sediments was investigated in order to characterize and quantify sediment diagenetic processes below the oxygen-deficient waters offshore Peru. One aim of this cruise was to contribute to our understanding of the benthic-pelagic coupling in the ocean by examining key geochemical species, whose chemical behaviour and distribution are altered via changes in redox potential. It is well known that essential nutrients like phosphate and iron are preferentially released from sediments under anoxic conditions. However, the magnitude of this recycling flux, the relative importance of key control parameters, and the coupling to carbon and sulphur cycles are largely unconstrained. In order to overcome this lack of knowledge we performed geochemical analyses of pore water from surface sediments that were retrieved by multicorer, gravity corer lander deployments.

1.4.4.2 Methods

After retrieval all cores were immediately transferred into a cooling lab (4°C) and processed within 1-2 hours. Supernatant bottom water of the multicorer-cores was sampled and filtered for subsequent analyses. Two multicorer-cores were always processed in parallel in order to obtain sufficient amounts of pore water for onboard and subsequent, shore-based analyses. For all measurements and sub-samples of redox-sensitive parameters (e.g. Fe, nutrients) one core was cut in a glove bag using argon gas as protection atmosphere at maximum resolution of 1 cm; pore water separation was performed using a cooled centrifuge. Subsequently, the pore water samples were filtered (0.2 nm cellulose-acetate filters) under argon atmosphere. A second core was cut without protection gas at the same depth resolution and pore water was extracted by pressure filtration at up to 2.5 bar. Additional MUC-cores from the same

deployment were sampled by use of Rhizons at lower depth resolution. These samples were stored for subsequent, shore-based analyses of specific isotope systems. Gravity cores were cut lengthwise after recovery. On the working halves sample intervals of about 25 cm were taken for pressure filtration. Syringe samples for detection of volatile hydrocarbon gases were taken on deck from every cut segment surface. Samples of 5 ml of sediment were transferred into 20 ml septum vials containing 6 ml of a concentrated NaCl-solution.

Each sample depth for pore water squeezing was additionally sampled for (1) the calculation of sediment density and (2) for determination of redox-sensitive elements. Porosity sub-samples were filled into pre-weighed plastic vials and redox-samples were kept in specific gas-tight containers under argon atmosphere for subsequent analyses in the home laboratory. For pressure filtration Teflon- and PE-squeezers were used. The squeezers were operated with argon at a pressure gradually increasing up to 2.5 bar MUC and 5 bar (GC), respectively. Depending on the porosity and compressibility of the sediments, up to 30 ml of pore water were received from each sample. The pore water was filtered through 0.2 µm cellulose acetate membrane filters.

Pore water analyses of the following parameters were carried out during both cruises: ferrous iron, nitrate, nitrite, ammonia, phosphate, silicate, alkalinity, hydrogen sulfide, sulfate, bromide and chloride (Tab. 1.1). The analytical techniques used on board to determine the various dissolved constituents are listed in Table 1. Modifications of some methods were necessary for samples with high sulfide concentrations. Ferrous iron, phosphate, ammonium, hydrogen sulfide and silicate were measured photometrically using standard methods described by Grasshoff et al. (1997). Samples of the sediment pore water for total alkalinity measurements were analyzed by titration of 0.5-1 ml pore water according to Ivanenkov and Lyakhin (1978). Titration was finished until a stable pink color occurred. During titration the sample was degassed by continuously bubbling nitrogen to remove the generated CO_2 or H_2S. The acid was standardized using an IAPSO seawater solution. The method for hydrogen sulfide determination according to Grasshoff et al. (1997) has been adapted for pore water concentrations of S^{2-} up to mM amounts. For reliable and reproducible results, an aliquot of pore water was diluted with appropriate amounts of oxygen-free artificial seawater; the sulfide was fixed by immediate addition of zinc acetate gelatine solution immediately after pore-water recovery. After dilution, the sulfide concentration in the sample should be less than 50 µmol/l. For the analysis of iron concentrations sub-samples of 1 ml were taken within the glove bag and immediately complexed with 20 µl of Ferrozin and afterwards determined photometrically.

Tab. 1.1: Techniques used for pore water analyses.

Parameter	Method	Detection limit	analytical error (accuracy)
Fe^{2+}	Photometer	1 µmol/l	5 µmol/l
HS^-	Photometer	1 µmol/l	3 µmol/l
NH_4^+	Photometer	2 µmol/l	5 µmol/l
PO_4^{3-}	Photometer	1 µmol/l	5 µmol/l
SiO_4^{4-}	Photometer	1 µmol/l	5 µmol/l
Cl^-	ion chromatography		10 mmol/l
Br^-	ion chromatography		20 µmol/l
SO_4^{2-}	ion chromatography		0.2 mmol/l
NO_3^-, NO_2^-	ion chromatography		5 µmol/l
Alkalinity	Titration		0.1 meq/l

We used a Metrohm ion-chromatograph equipped with a conventional anion-exchange column and carbonate-bicarbonate solution as an eluent. While chloride, bromide, and sulphate could be measured with the same column, for nitrate measurements a different column had to be mounted. The IAPSO seawater standard was used for calibration. Acidified sub-samples (35µl suprapure HCl + 3 ml sample) were prepared for ICP analyses of major ions (K, Li, B, Mg, Ca, Sr, Mn, Br, and I) and trace elements. DIC, $\delta^{18}O$ and $\delta^{13}C$ of CO_2 will be determined on selected sub-samples in the shore-based laboratories.

1.4.4.3 Results (Shipboard)

In total, we processed samples from 23 MUC, 3 GC, and 7 benthic lander deployments. An overview of the coring locations is presented in Tab. 1.1 and Fig.1.1 (Übersichtskarte).

Along 11°S, the majority of 11 MUC, 2 GC, and 7 lander deployments were sampled and analysed. Overall, we observed considerable differences in mineralization patterns which can be attributed to strong variabilities with respect to the input of degradable (organic) material and the dynamic sedimentary environment. The most important factors are water depth and distance from the coast as these dominantly control the export flux from primary production and terrigeneous material, redistribution by downslope transport and winnowing by strong bottom currents, and small scale variations controlled by seafloor topography.

Below, selected pore water profiles from 3 stations at 80, 500 and 1000 m water depth are shown to illustrate differences in mineralization intensity and related benthic fluxes (Fig. 1). Phosphate and ammonia are released into pore water by organic matter breakdown, whereas the sub-seafloor increase of silica indicates the dissolution of diatom tests. The profiles reflect the decrease of organic matter input with increasing water depth. High subsurface peaks of dissolved iron at 500 and particularly at 80 m water depth further indicate the complete lack of oxygen and the instantaneous use of metal oxides for organic matter mineralization right below the sediment-water interface. The zone of Fe-release is shifted further downward as soon as oxygen becomes available at greater water depths (1000 m).

Although Fig. 1.9 indicates a clear water-depth dependence of mineralization processes and benthic reflux, a closer look to intermediate depths (Figs. 1.5-1.7) reveals that this relation is not that simple. In comparison to station 455 at 500 m water depth, the subsurface increase of

dissolved iron is lower at 300 to 400 m water depth and phosphate remobilization exhibits a strong variability. Particularly at station 449 at 300 m water depth sediments are extremely soft and densely populated with bacterial mats. Pore water profiles of alkalinity and ammonia strongly indicate intense anoxic mineralization accompanied by the enrichment of free H2S below 25 cm sediment depth. Low iron concentrations at this station may thus be explained by sulfate reduction occurring already at shallow subsurface depths so that most iron would immediately be precipitated in form of Fe-sulfides. Another reason for this observation could of course be that there is a strong regional and lateral variation in the supply of terrigeneous Fe-(hydr)-oxides. Specific questions like this one will only be answered after careful examination of the solid phase composition of the sediments.

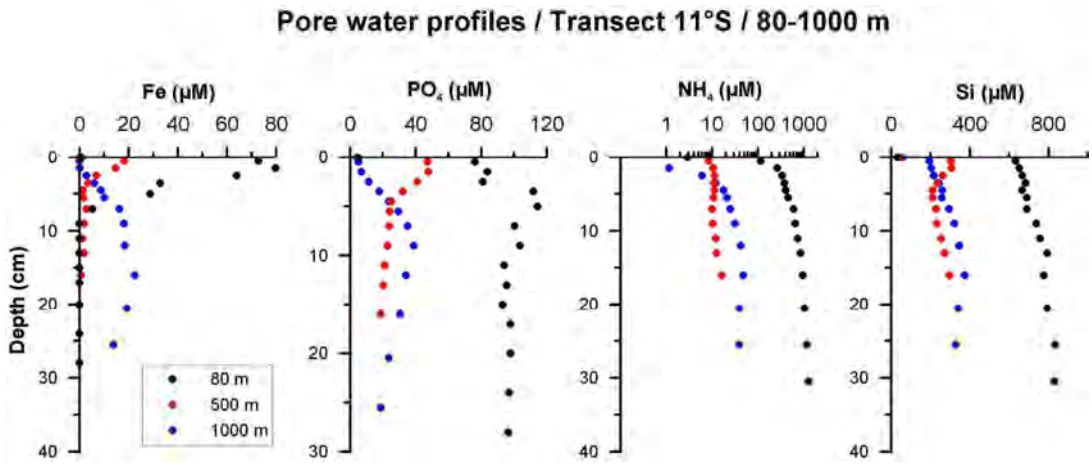

Fig. 1.9: Selected pore water profiles of iron, phosphate, ammonia and silicon at stations 543 (MUC 52, 80m), 455 (MUC 21, 500m), and 549 (MUC 53, 1000m) along the 11°S-transect.

As outlined above, one major goal of this cruise was to determine the benthic mobilization of dissolved iron and phosphate under oxygen limitation in the bottom water and to analyse the interplay of potential control factors. As a preliminary result, we estimated the diffuse benthic fluxes of iron and phosphate using the concentration gradients between the uppermost sediment layers and the bottom water. Since water depth may serve as a substitute parameter for export production and, hence organic matter input, the results are plotted vs. water depth in Figure 1.10 However, the large scatter in data clearly suggests that the depositional environment is highly complex and mineralization processes in the sediments cannot be approximated by such a simple relationship. The only obvious result that can be deduced from this plot is that iron and phosphate fluxes considerably decrease below 700m water depth where oxygen levels increase above 10 µM. Subsequent investigations on the solid phase will help to decipher the complex relationship early diagenetic processes and environmental control factors in this highly dynamic sedimentary system.

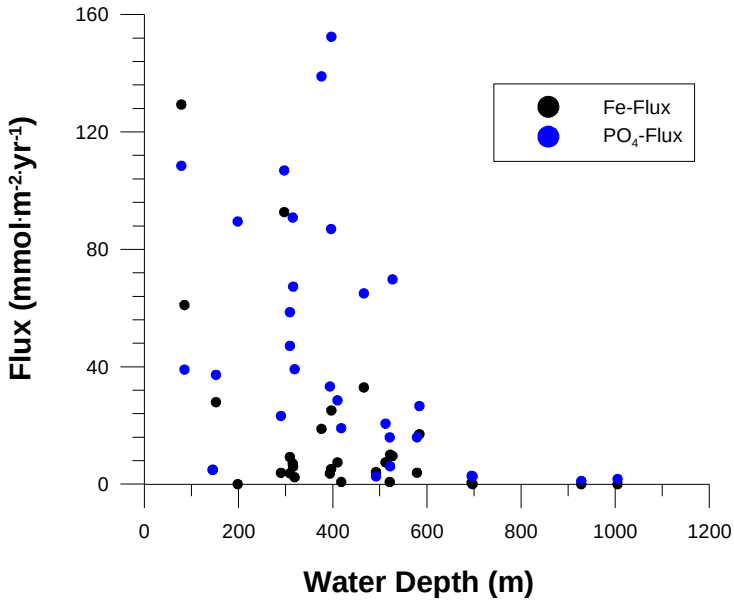

Fig. 1.10: Benthic flux of iron and phosphate across the sediment-water interface vs. water depth for all working areas.

Tab. 1.2: List of core locations.

Station No.	**Latitude (S)**	**Longitude (W)**	*Water Depth*	***Recovery***
397 - MUC2	17°26,02'	71°51,40'	297.3 m	28 cm, concretions
406 - MUC6	17°28,00'	71°52,40'	492 m	26 cm
418 – GC6	17°25,98'	71°51,82'	339.2 m	313 cm, concretions at 10 and 75 cm
412 – MUC13	15°11,38'	75°34,82'	522 m	16 cm, bioturbated, shell layers
445 – MUC15	10°59,997'	78°30,022'	928 m	20 cm
449 – MUC19	11°0,01'	78°09,97'	319 m	50 cm, black sediment sulfidic
455 – MUC21	11°00,00'	78°19,23'	466 m	20 cm, black
459 – MUC25	11°00,03'	78°25,60'	697 m	30 cm
464 – BIGO1	11°00,00'	78°09,92'	315 m	16 cm
470 – MUC29	11°00,02'	77°56,60'	145 m	50 cm
474 – BIGO2	11°0,01'	78°25,55'	695 m	14 cm
481 – MUC33	11°0,00'	78°14,19'	376 m	40 cm
487 – MUC39	11°00,00'	78°23,17'	579 m	12 cm
505 – GC16	11°0,004'	78°25,652'	699 m	430 cm
511 – GC22	11°0,05'	77°56,61'	146 m	330 cm
516 – MUC40	11°	78°20'	512 m	13 cm, phosphorites
519 – MUC43	11°0,01'	78°16,29'	410 m	22 cm
526 – BIGO3	11°0,022'	78°15,27'	397 m	12 cm
535 – BIGOT3	10°59,85'	78°15,38'	396.4 m	13 cm
543 – MUC52	10°59,99'	77°47,4'	78.4 m	34 cm
549 – MUC53	10°59,807'	78°31,266'	1005 m	28 cm
553 – MUC 54	10°26,38'	78°54,7'	521 m	31 cm, phosphorites
564 – MUC59	11°14,5'	78°15,7'	527 m	36 cm
566 – BIGOT4	11°	78°9,13'	309 m	18 cm
568 – BIGO5	11°0,02'	77°47,72'	85 m	16 cm
573 – MUC 61	11°9,9'	78°5,5'	309 m	45 cm
584 – MUC66	11°7'	77°59,3'	198 m	39 cm
586 – BIGOT5	11°	78°9,4'	316 m	17 cm
601 – MUC71	11°12,5'	78°10,8'	394 m	22 cm
607 – MUC75	12°32,5'	77°30,5'	584 m	16 cm, phosphorites
610 – MUC77	12°29,5'	77°27'	418 m	24 cm, phosphorites
614 – MUC79	12°25,6'	77°24,8'	290 m	40 cm, phosphorites
619 – MUC83	12°18,6'	77°19,1'	152 m	26 cm, , phosphorite

1.4.5 Ocean Floor Observation (OFOS)

(T. Mosch, B. Bannert)

1.4.5.1 Objectives

Ocean floor observation and imaging was performed to identify benthic habitats which can be related to different biogeochemical provinces across the continental margin. With a very detailed video mapping on one main transect a distinct faunal and lithological zonation can be resolved and might be related to benthic fluxes. Furthermore some other transects were mapped and classified in the same way and might be used for the extrapolation of benthic nutrient fluxes for a wider geographical area of the Peruvian margin.

1.4.5.2 Methods

The OFOS used during this cruise is a video sled and consists of a stainless steel frame, Fig. 1.11 It carries the video telemetry, 1 video camera, 2 Xenon lights (Oktopus), a still camera with flash light (Benthos) and a storage CTD (RBR: salinity, temperature, O_2 via 2 Aanderaa optodes, turbidity). A small weight is carried about 1.5 m below the sled as a reference point for the winch driver and scale for the images taken during the tow of the instrument. Furthermore 2 laser pointers were deployed to project two reference points 50 cm apart from each other on the seafloor for latter image analysis. A third laser projection provides information about the distance between still camera and the sea floor. During each deployment pictures were automatically triggered every 1 min, which means that with a towing speed of 0.5 to 1 knot every 10 to 15 m one picture was taken. Position of the OFOS in comparison to the ship position was recorded using the Posidonia system.

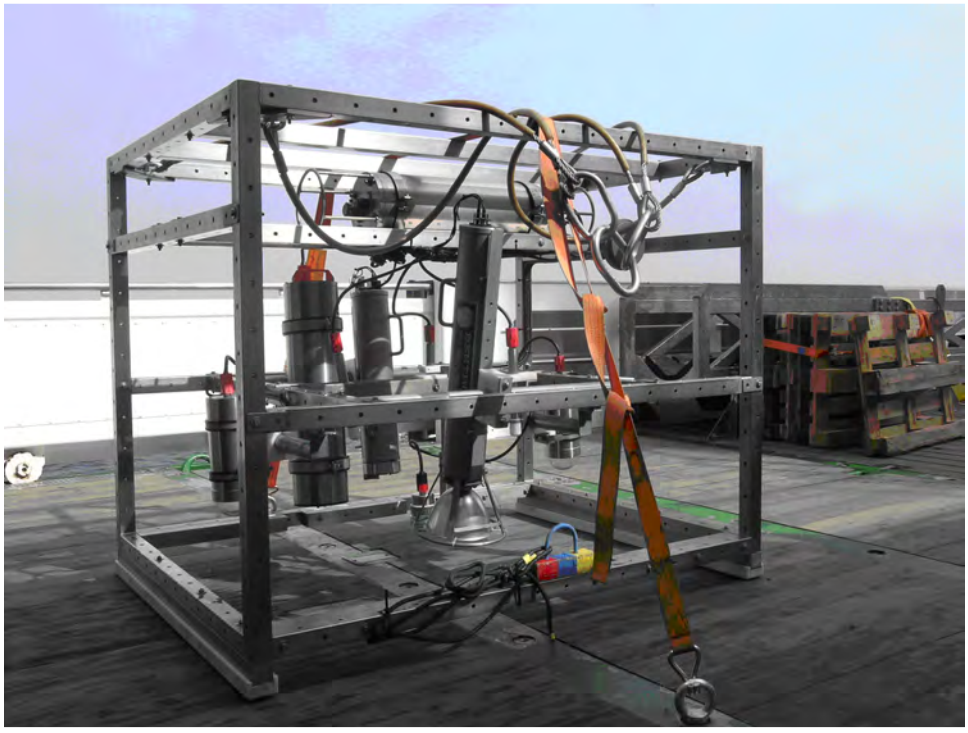

Fig. 1.11: Ocean Floor Observation System (OFOS)

During the cruise 34 OFOS-tracks were conducted (Tab. 1.3), whereof 14 were on the main transect at 11°S. A total of more than 4000 still images of the seafloor (about 1300 at the 11°S-transect) were yielded. With a overall time of 68 hours at bottom a total track length of approximate 89 km (this is 48 nautical miles) could be covered. At the 11°S-transect a depth range from 80 m up to 1050 m water depth was explored.

Tab. 1.3: Station list OFOS-tracks

Stat. Nr.	OFOS Nr.	Date	Time (UTC)	Latitude (S)	Longitude (W)	WD (m)	Posi-donia	Remarks/Recovery
399	1	08/10/29	1:40	17°23.95	71°50.56	145		at bottom
399	1	08/10/29	2:30	17°24.20	71°50.06	145		off bottom
400	2	08/10/29	3:27	17°25.74	71°51.70	294		at bottom
400	2	08/10/29	4:47	17°26.18	71°51.11	291		off bottom
401	3	08/10/29	5:39	17°27.67	71°52.87	494		at bottom
401	3	08/10/29	7:07	17°28.25	71°52.01	490		off bottom
453	4	08/11/04	3:43	11°	77°47.97	83		at bottom
453	4	08/11/04	4:48	11°	77°48.43	92		off bottom
454	5	08/11/04	6:20	11°	78°01.04	192		at bottom
454	5	08/11/04	7:46	11°	78°01.92	202		off bottom
465	6	08/11/05	4:39	11°	78°09.45	309		at bottom
465	6	08/11/05	5:41	11°	78°10.04	317		off bottom
466	7	08/11/05	6:50	11°	78°14.88	386		at bottom
466	7	08/11/05	9:17	11°	78°16.01	407		off bottom
467	8	08/11/05	10:41	11°	78°23.03	575		at bottom
467	8	08/11/05	12:43	11°	78°24.51	637		off bottom
490	9	08/11/07	1:00	11°	78°19.98	485	x	at bottom
490	9	08/11/07	6:12	11°	78°23.01	577		off bottom
491	10	08/11/07	7:38	11°	78°24.35	627		at bottom
491	10	08/11/07	10:14	11°	78°26.52	755		off bottom
492	11	08/11/07	11:48	11°	78°31.04	990		at bottom
492	11	08/11/07	12:22	11°	78°31.57	1022		off bottom
523	12	08/11/10	7:25	11°	78°20.00	482	x	at bottom
523	12	08/11/10	8:55	11°	78°18.90	461		off bottom
524	13	08/11/10	10:26	11°	78°11.49	340	x	at bottom
524	13	08/11/10	11:27	11°	78°10.61	329		off bottom
525	14	08/11/10	12:55	11°	78°02.50	206	x	at bottom
525	14	08/11/10	13:11	11°	78°02.29	200		off bottom
537	15	08/11/12	5:30	11°	78°10.77	332	x	at bottom
537	15	08/11/12	6:51	11°	78°09.83	317		off bottom
538	16	08/11/12	8:11	11°	78°02.35	202	x	at bottom
538	16	08/11/12	8:56	11°	78°01.83	196		off bottom
539	17	08/11/12	10:37	11°	77°49.48	103	x	at bottom
539	17	08/11/12	11:35	11°	77°48.65	89		off bottom
550	18	08/11/13	6:12	10°18.60	78°43.11	142	x	at bottom
550	18	08/11/13	7:10	10°18.25	78°42.43	142		off bottom
551	19	08/11/13	8:56	10°25.60	78°53.20	326	x	at bottom
551	19	08/11/13	9:57	10°25.19	78°52.61	269		off bottom

Stat. Nr.	OFOS Nr.	Date	Time (UTC)	Latitude (S)	Longitude (W)	WD (m)	Posi-donia	Remarks/Recovery
552	20	08/11/13	11:11	10°27.44	78°55.97	717	x	at bottom
552	20	08/11/13	12:30	10°26.83	78°55.00	593		off bottom
562	21	08/11/14	8:55	11°10.01	78°06.98	330	x	at bottom
562	21	08/11/14	10:14	11°09.54	78°06.20	313		off bottom
563	22	08/11/14	12:09	11°14.95	78°16.51	551	x	at bottom
563	22	08/11/14	13:06	11°14.53	78°15.77	530		off bottom
571	23	08/11/15	10:48	11°16.20	78°18.73	634	x	at bottom
571	23	08/11/15	13:02	11°15.18	78°16.91	564		off bottom
572	24	08/11/15	14:33	11°12.78	78°11.45	403	x	at bottom
572	24	08/11/15	15:04	11°12.61	78°11.10	398		off bottom
578	25	08/11/16	2:56	11°07.02	77°59.35	197	x	at bottom
578	25	08/11/16	4:20	11°06.54	77°58.32	184		off bottom
579	26	08/11/16	6:37	11°14.47	78°14.86	501	x	at bottom
579	26	08/11/16	8:02	11°14.05	78°13.96	473		off bottom
580	27	08/11/16	9:41	11°16.75	78°19.75	682	x	at bottom
580	27	08/11/16	11:01	11°16.17	78°18.67	633		off bottom
591	28	08/11/17	5:38	11°17,07	78°20.50	719	x	at bottom
591	28	08/11/17	6:48	11°16.75	78°19.75	682		off bottom
592	29	08/11/17	8:11	11°18.44	78°23.31	970	x	at bottom
592	29	08/11/17	9:07	11°18.14	78°22.64	891		off bottom
612	30	08/11/18	23:03	12°33.20	77°30.62	622	x	at bottom
612	30	08/11/18	1:48	12°31.28	77°29.15	487		off bottom
624	31	08/11/20	5:21	12°34.32	77°31.25	704	x	at bottom
624	31	08/11/20	7:17	12°33.10	77°30.52	613		off bottom
625	32	08/11/20	8:30	12°30.41	77°28.50	445	x	at bottom
625	32	08/11/20	9:38	12°29.69	77°27.94	421		off bottom
626	33	08/11/20	10:55	12°24.30	77°23.80	255	x	at bottom
626	33	08/11/20	12:00	12°23.74	77°23.27	235		off bottom
627	34	08/11/20	13:00	12°19.14	77°19.61	158	x	at bottom
627	34	08/11/20	14:08	12°18.52	77°19.12	150		off bottom

1.4.5.3 Results (Shipboard)

In the shallower parts underlying the OMZ (O_2 < 1 µM) large aggregations of bacterial mats, presumably *Beggiatoa* and *Thioploca*, occur with variable coverage (Fig. 1.12). At 200 m depth the seafloor is nearly completely covered with bacterial mats whereas by 400 m only singular patches of bacterial mats are visible. The part of the transect which is outside the core of the OMZ (between 450 m and 750 m water depth) was already completely mapped. The pictures show a great diversity of megafauna. Associated with a slight increase of the bottom-water oxygen concentration (O_2 >1 µM, ~ 500 m) distinct zones of gastropods, poriferans followed by pennatulaceans (O_2 ~ 1.6 µM, ~ 550 m), holothurians, and asteroids (O_2 ~ 2.4 µM, ~ 590 m) were recorded. At these depths foraminiferal sands as well as patches of hard substrates occurred. Phosphorites were sampled at depths of approximately 516 m. Between 600 and 650 m extremely abundant ophiuroids formed a distinct environment (Fig. 1.12). Decapod crustaceans (Anomura) appeared at oxygen concentrations of about 5 µM (~ 670 m). Beyond 1000 meters the number of megafauna organisms clearly decreases.

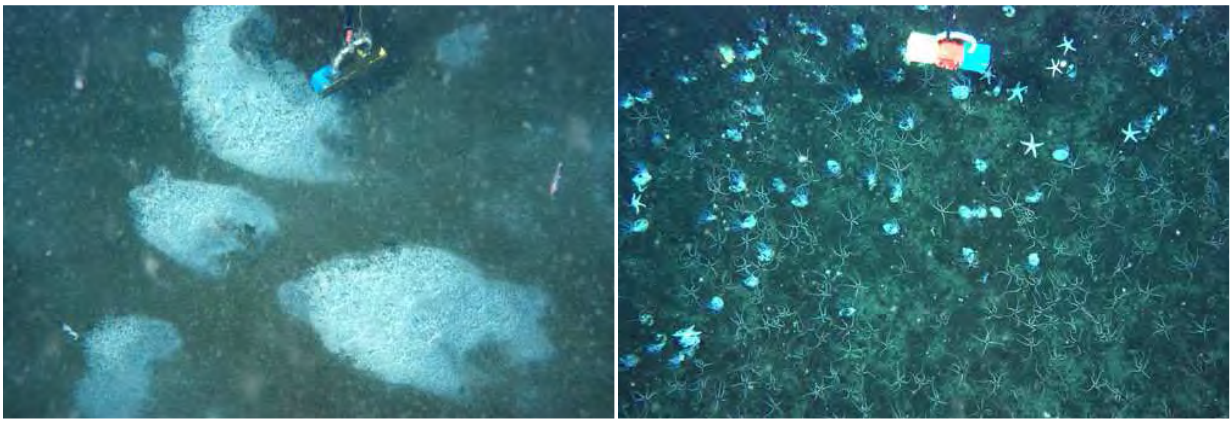

Fig. 1.12: Extended bacterial mats, presumably *Beggiatoa*, in a water depth of 150 m within the oxygen minimum zone (left side); brittle stars and holothurians at 650 m water depth (right side)

1.4.6 Benthic foraminifera

(J. Mallon)

1.4.6.1 Objectives

The focus of this study is the investigation of benthic foraminiferal assemblages due to bottom water oxygenation and eventually to find species associations which could be use as quantitative proxies for oxygen. During the 1st leg of M77 the main area was the Peruvian oxygen minimum zone (OMZ) between 17°S and 11°S with special focus of the transect C (11°S) were previous studies based on 4 multi-corer stations taken during a strong ENSO (El Nino) phenomenon has been done (LEVIN et al. 2002, PEREZ, M. E., in prep.). Two of these stations were visited during this leg so that comparisons between ENSO and non-ENSO conditions with all influences affecting benthic foraminiferal assemblages can be determined. The water depths of the taken samples are listed in Tab. 1.4, they cover an interval of 79 m down to 1004 m depth.

1.4.6.2 Methods

The samples were taken with a multi-corer equipped with up to 7 tubes of 10 cm in diameter and a video camera. Subsequent oxygen microprofiling in vertical steps of 0.25 mm to 0.5 mm gave quantitative information about the oxygen penetration depth in the sediment's pore water and was a prerequisit for calculating the following slicing steps; latter range between 2 mm to 10mm thickness until 5cm sediment depth. A few cores couldn't be measured because of resuspension of sediment. Finally each sample were stained with Ethanol+Rose Bengal and put into cooling container for transportation at 4°C. The stained and splitted samples are going to be picked for taxonomical identification and eventually evaluation of proxies for recent and past bottom water oxygen concentration.

Tab. 1.4: Locations for foraminifera sampling.

Station No.	Gear No.	Date 2008	Position at bottom		Water depth [m]
			Lat. [°S]	Long. °W]	
403	MUC 4	29.10.	17°26,01'	71°51,41'	298
406	MUC 6	29.10.	17°28,00'	71°52,40'	492
410	MUC 10	30.10.	17°38,385'	71°58,233'	918
421	MUC 13	31.10.	15°11,38'	75°34,82'	522
449	MUC 19	03.11.	11°0,01'	78°09,97'	319
456	MUC 22	04.11.	11°00,013'	78°19,234'	465
459	MUC 25	04.11.	11°00,03'	78°25,60'	697
470	MUC 29	05.11.	11°00,02'	77°56,60'	145
473	MUC 32	05.11.	11°0,01'	78°9,94'	317
482	MUC 34	06.11.	11°0,01'	78°14,17'	375
487	MUC 38	06.11.	11°	78°23,17'	579
516	MUC 40	09.11.	11°	78°20'	511
540	MUC 49	12.11.	11°0,01'	77°47,40'	79
549	MUC 53	13.11.	10°59,807'	78°31,266'	1004
553	MUC 54	13.11.	10°26,38'	78°54,7'	521
582	MUC 64	16.11.	11°9,69'	78°4,88'	291
583	MUC 65	16.11.	11°6,86'	78°3,06'	248
616	MUC 81	19.11.	12°22,69'	77°29,05'	302
619	MUC 83	19.11.	12°18,6'	77°19,1'	152
622	MUC 85	20.11.	12°32,757'	77°34,757'	823

1.4.7 Nitrogen fixation coupled to sulfate reduction in sediments of the OMZ

(J. Hommer, T. Treude)

1.4.7.1 Objectives

Aim of this study was to investigate a possible linkage between nitrogen and sulfur cycling in sediments of the OMZ through the activity of sulfate-reducing bacteria that fix nitrogen. Previous studies in coastal habitats indicate that nitrogen fixation by sulfate reducers represent an important percentage of the total benthic nitrogen fixation rate (Bertics et al., submitted). Factors inhibiting nitrogen fixation are high concentrations of oxygen and ammonia, wherefore we propose that surface sediments within the OMZ could be suitable habitats to find the two processes connected.

1.4.7.2 Methods

Sediment samples for nitrogen fixation, sulfate reduction, microbial diversity and abundance were taken from chambers of the lander system BIGO (Sommer et al. 2008) along a depth transect: (a) inside the OMZ, (b) at the lower boundary of the OMZ, and (c) beneath OMZ (Tab. 1.5). On board, nitrogen-fixation and sulfate-reduction samples were incubated according to the acetylene reduction (Capone 1993) and ^{35}S-sulfate-injection method (Jørgensen 1978), respectively. Samples for RNA/DNA analyzes were frozen (-20ºC).

Samples for fluorescence in situ hybridization were conserved after standard protocols (Amann et al. 1990). All samples will be analyzed in the home laboratory.

Tab. 1.5: Sediment sampling overview.

Station Ship#	Gear#	Date 2008	Time (UTC)	Device	Latitude (°S)	Longitude (°W)	WD (m)	Remarks/Recovery
464	BIGO1	04.11.08	03:37	BIGO	11°00,00’	78°09,92’	315	Inside OMZ
489	BIGO2	06.11.08	23:40	BIGO	11°00,29’	78°25,71’	695	Beneath OMZ
535	BIGO3	12.11.08	00:10	BIGO	11°00,00’	78°15,27’	396	Lower boundary of OMZ
577	BIGO5	16.11.08	01:20	BIGO	11°59,56’	77°47,73’	81	Inside OMZ, no nitrogen fixation measured

1.4.8 Geochemical reconstruction of past redox-conditions (Multi-corer and Rosette with Conductivity-Temperature-Depth-^Senso)

(N. Glock)

1.4.8.1 Objectives

Sampling sediment for the extraction of foraminifera to measure the TE/Ca ratios for several redox sensitive elements (TE = Mn, Fe, V, U, etc.). Sampling sediment, seawater and pore water for the measurement of the redox-sensitive trace-metal ratios (Re/Mo, U/Mo, Cd/Mo, Mn/Fe, etc.) and the isotope-ratios of redox-sensitive elements ($\delta^{98/95}$Mo, δ^{56}Fe, ^{234}U/^{238}U).

1.4.8.2 Methods

MULTI-CORER samples for the extraction of Foraminifera were mainly collected at the C-transect. MULTI-CORER-sediment-cores from several well chosen stations were completely deep-frozen without sample-preparation as archive. MULTI-CORER sediment-samples for the measurement of redox sensitive element- and isotope-ratios were collected in cooporation with the pore-water group und prepared in a glove-bag to exclude oxygen-contamination. Pore-water samples from the MULTI-CORER were collected with rhizones under oxygen-exclusion. Water-column and bottom-water samples were collected from the CTD-ROSETTE and the BIGO-LANDER without further sample preparation.

1.4.8.3 Results (Shipboard)

No shipboard-measurements were done.

Tab. 1.6:

Station M77-1	Date 2009	Time (UTC)	Device	Latitude (°N)	Longitude (°W)	WD (m)	Remarks/Recovery
397/MUC-02	28.10.	22:10	MUC	17°26.02	71°51.40	297	Whole archive-core
481/MUC-33	06.11.	13:53	MUC	11°00.00	78°14.19	376	Whole archive-core
487/MUC-38	06.11.	20:24	MUC	11°00.00	78°23.17	579	Whole archive-core
540/MUC-49	12.11.	12:11	MUC	11°00.01	77°47.40	78	Whole archive-core
553/MUC-54	13.11.	13:24	MUC	10°26.38	78°54.70	522	Whole archive-core
573/MUC-61	15.11.	16:22	MUC	11°09.90	78°05.50	309	Whole archive-core
584/MUC-66	16.11.	15:52	MUC	11°07.00	77°59.30	198	Whole archive-core
614/MUC-79	19.11.	14:37	MUC	12°25.60	77°24.80	290	Whole archive-core
619/MUC-83	19.11.	21:30	MUC	12°18.60	77°19.10	152	Whole archive-core
421/MUC-13	31.10.	21:37	MUC	15°11.38	75°34.82	519	Sediment
445/MUC-15	03.11.	12:23	MUC	10°59.98	78°30.022	928	Sediment, Porewater
449/MUC-19	03.11.	19:28	MUC	11°00.01	78°09.97	315	Sediment, Porewater
455/MUC-21	04.11.	11:30	MUC	11°00.00	78°19.23	465	Sediment, Porewater
470/MUC-29	05.11.	17:08	MUC	11°00.02	77°56.60	143	Sediment, Porewater
519/MUC-43	10.11.	01:45	MUC	11°00.01	78°16.29	410	Sediment, Porewater
565-/MUC-60	14.11.	16:20	MUC	11°08.00	78°21.40	640	Sediment
406/MUC-06	29.10.	21:19	MUC	17°28.00	71°52.40	492	Porewater
424/CTD-RO-09	02.11.	02:04	CTD-RO	11°00.041	78°30.027	928	
463/CTD-RO-22	04.11.	22:24	CTD-RO	11°00.008	78°44.864	2000	
468/CTD-RO-23	05.11.	15:50	CTD-RO	11°00.047	77°56.645	146	
532/CTD-RO-34	11.11.	19:11	CTD-RO	10°15.94	78°38.67	143	
545/CTD-RO-35	12.11.	18:07	CTD-RO	10°59.983	78°20.468	497	
464/BIGO-01	05.11.	03:37	BIGO	10°59.79	78°10.01	318	Bottom-Water
489/BIGO-02	06.11.	23:40	BIGO	11°00.01	78°25.55	693	Bottom-Water
535/BIGO-03	12.11.	00:10	BIGO	10°59.85	78°15.38	396	Bottom-Water
557/BIGO-T-03	13.11.	22:10	BIGO-T	11°00.00	78°09.15	306	Bottom-Water
558/BIGO-04	14.11.	00:56	BIGO	10°59.85	78°31.04	1016	Bottom-Water

1.4.9 Report M77-1 IMARPE

(M. Graco, E. Enríquez, C. Hensen)

During M77-1 in collaboration with SFB-754 researchers from IFM-GEOMAR, IMARPE team was focus in many different aspects, in order to understand more about the benthos, BIOLOGY and BIOGEOCHEMISTRY of the Peruvian OMZ.

The intensive work was doing along 11˚S across the continental shelf, from the coast (85 m) into the open and deep ocean (> 1000 m) (Fig. 1.13).

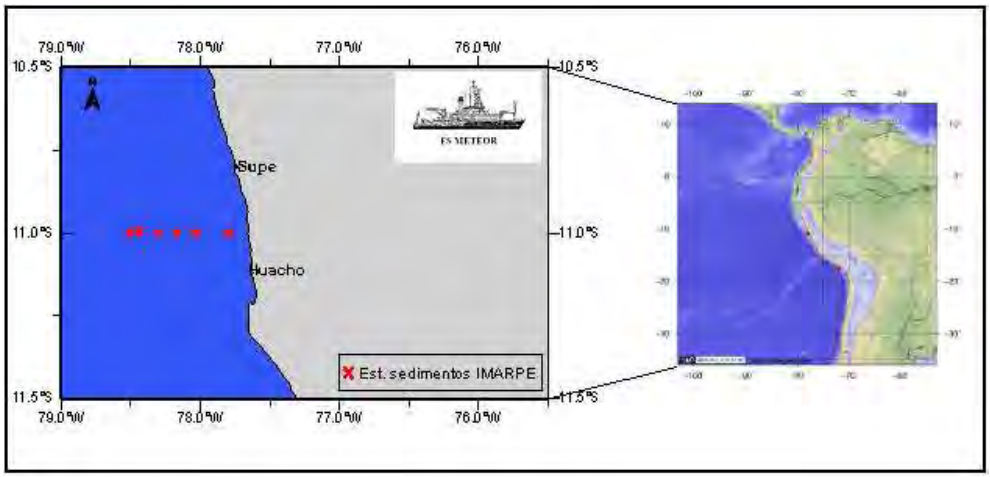

Fig. 1.13: Map with the sampling stations of IMARPE along the 11ºS transect.

This transect was characterized by a continental shelf under the influence of different oxygen conditions.

During the cruise the oxycline position (50 µMol/Kg) in the water column was at 10 m depth onshore and approximately at 50 m offshore. The upper boundary of the OMZ (< 25 µMol/Kg) was very shallow at 50 m depth and broad (up to 800 m), with an intense core of 2 µMol/Kg of oxygen in contact with the benthic system in the nearshore stations (Fig. 1.14).

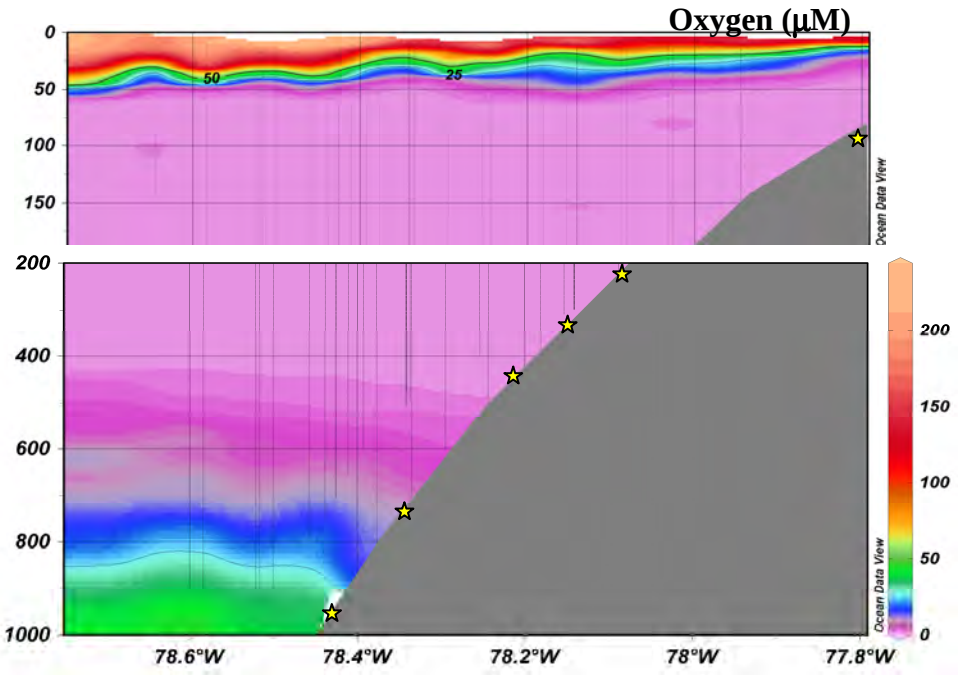

Fig. 1.14: Dissolved oxygen (µMol/ Kg) vertical distribution and OMZ structure off 11ºS.

Specific objectives and preliminary results

To identify the composition and abundance of the benthic communities, particularly the macrofauna and the distribution of bacteria biomass across different oxygen and organic matter conditions.

On the shelf and upper slope off Huacho (11°S), three cores (one core of each drop) were sampled for quantitative community analysis and immediately sliced up into a vertical profile (0-1 cm; 1-2 cm; 2-5 cm and 5-10 cm depth), sieved (0,5 cm mesh), preserved with formalin (10%) and stored until to be processed in the Benthic Laboratory at IMARPE. Samples for bacteria and for the biogeochemical characterization were obtained in the first 10 cm of the sediment and they were freezing until to be processed. This data will contribute to study the mineralogy and organic characterization of the benthos at each depth and station (Fig. 1.15).

The main objective was a detailed study of the communities of organisms that live in shallow sites (approx. 50-100m) on the upper boundary of OMZ with deeper upper slope areas (approx. 1000m), which are thought to differ remarkably in faunal composition and community structure. This approach is founded on the assumption that communities are affected by different oxygen and organic matter contents.

At the deeper station (around 1000m depth) a particular faunal community could be distinguished. The fauna is dominated by small polychaetes of the families Hesionidae, Owewnidae, Capitellidae, Terebellidae, Spionidae, Maldanidae, Paraonidae and Nereidae, crustaceans such as amphipods of the families Gammaridae, Ampeliscidae and Phoxocephalidae, isopodos and cumaceans and ophiuroids and nemerteans were identified as well.

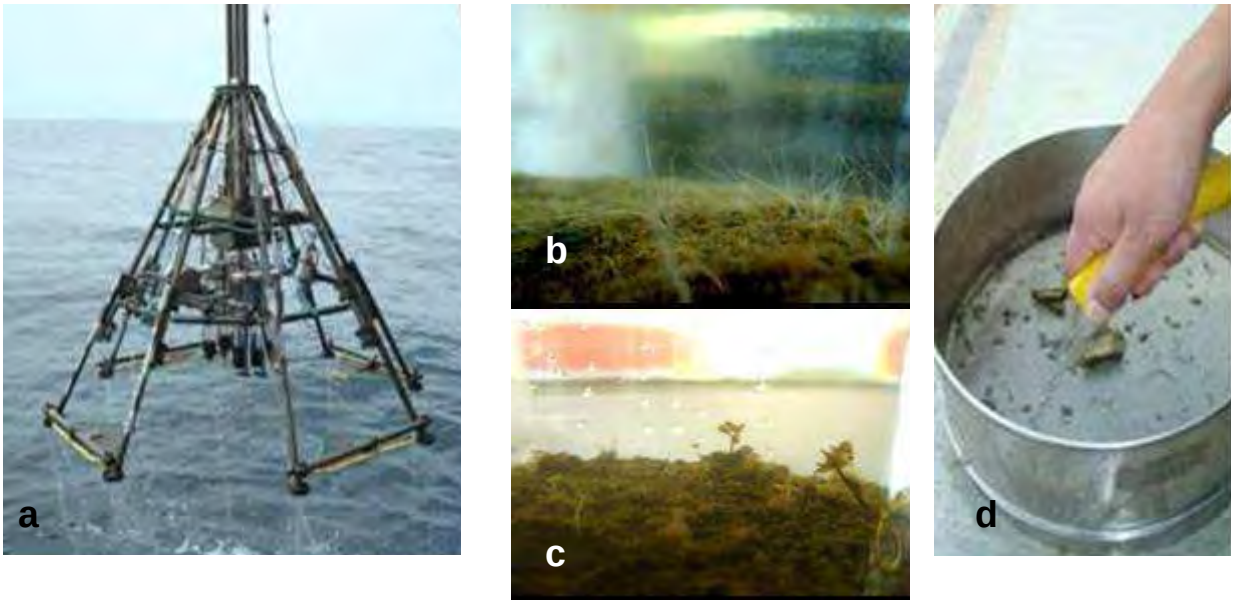

Fig. 1.14 a: Mullticore with sediments samples. b Filaments of giant bacteria, c. Terebellidae Polychaetes. d. Sieving macrofauna samples.

To determine nutrient exchange between the water column and the sediments and respiration rates across the continental shelf under different oxygen conditions.

We performed onboard the METEOR incubations of sediment in order to perform the experiments. We obtained at each station sediment-water samples with the Multi-corer. In a cold room (10º C), we subsampled in small cores (3.5 cm* 20 cm) and perform incubations (0, 1, 3, 6, 12, 24 hs). Net rates of sediment-water exchange of dissolved nutrients (NH4+, NO3-, NO2-, PO_4^2, Si_2O_3) were measured by triplicate. A magnetic stirrer gently mixed the overlying water in order to avoid the stratification in the system. The nutrient samples were measured on board by the porewater group of the IFM-GEOMAR. Our initial results indicate significant differences across the continental shelf. Under very reduced onshore conditions, where important bacterial mats occurs under low oxygen conditions, nitrate is practically depleted in the water column, low consumption rates occurs and high nitrite concentrations are characteristics (Fig. 1.15). At intermediate depths nitrate overlying the sediments are very high and they coexist with low oxygen conditions and explain the maximum rates of nitrate consumption that probably determine a massive nitrogen gas lost. At deeper depths where the oxygen increases (> 30 µMol/Kg), the recycling of nitrate decreases as is expected under a more oxygenated environment and also decrease the nitrite accumulation.

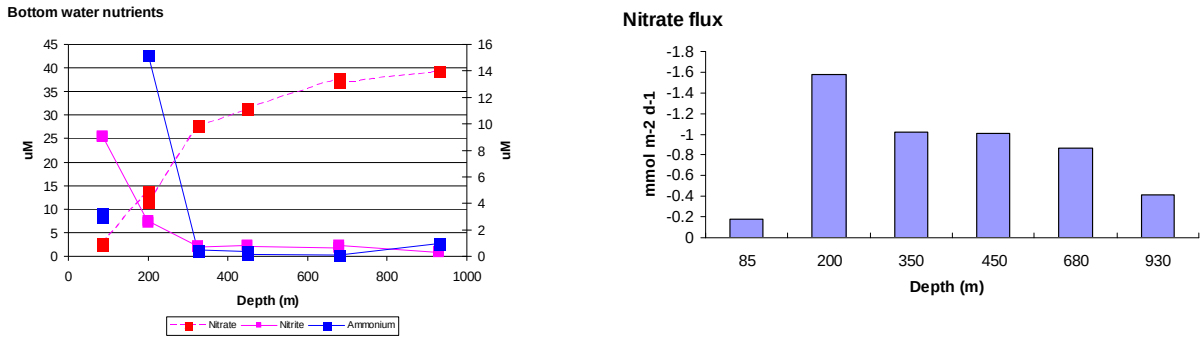

Fig. 1.15: Right panel. Bottom water concentrations of nutrients (nitrate, nitrite, ammonium at different experimental stations. Left panel. Nitrate fluxes across the sediment-water interface at different stations along an oxygen gradient (see Fig. 1.13).

1.4.10 Geological Sampling and Paleoceanography

(D. Nürnberg, T. Böschen, S. Voigt, A. Bahr, C. Karas)

1.4.10.1 Objectives

The overarching goal of the paleoceanographic studies (SFB754 Subproject A6: Centennial to millennial scale climate change and low-latitude oxygen minimum conditions, R. Schneider, C. Dullo, D. Nürnberg) is to reconstruct past atmosphere and ocean climate interactions over the last ~20.000 years that could have controlled the behaviour of the strongest oxygen minimum zone (OMZ) in the tropical ocean by changing physical and biochemical boundary conditions in the tropical ocean (e.g., changes in denitrification, upwelling, marine productivity, thermocline depth, intermediate water circulation, insolation, continental aridity and dust flux, as well as trade-wind strength). These results will put the magnitudes of modern OMZ changes (seasonal or interannual to decadal) into the context of a long-lasting history under natural climate forcing.

The paleoceanographic goals are orientated to the three major topics: How have past surface and subsurface ocean biogeochemical conditions changed with respect to temperature (salinity), thermocline structure, and productivity along N-S and E-W gradients inside and outside the tropical OMZ? What was the phasing (leads and lags) between past climate change and biogeochemical variability in the surface and subsurface ocean as well as in the atmosphere? How have remote rapid climate changes during the Holocene and the last deglacial period controlled the development of low oxygen conditions in the ETSP?

The paleoceanographic part of RV METEOR SFB-754 cruise M77-1 comprised a paleoclimate-oriented sampling programme of both the water column and uppermost sediment layers (Fig. 1.1, location map). Plankton and water samples will be used to improve calibration of paleohydrographic and paleo-oxygen proxies. After extensive sediment acoustic surveying along 5 transects perpendicular to the coastline, high-quality sediment cores were recovered from above, within, and below the OMZ between 10° and 18°S. A single core was additionally recovered at ~15°S. They will provide the archive to reconstruct physical and chemical variability of the surface ocean at centennial to millennial time scales together with

past OMZ changes over the last ~20.000 years. Up to now, long, continuous and high sedimentation-rate Holocene records are rare from this region (e.g., RV SONNE cruises SO-78 and SO-147, ODP Legs 112, 201, 202), because active tectonics as well as winnowing effects associated with strong coastal currents and sea-level transgression onto the shelf distorted continuous accumulation of soft sediments.

1.4.10.2 Methods

The following methods were applied: Detailed sediment acoustic surveys across the shelf and upper slope were performed by EM120 swath bathymetry and PARASOUND echosounding devices. The information was used to locate coring positions within the small-scale, undistorted, depositional centres of Holocene and deglacial muds.

Sediment surfaces were sampled with the multi-corer (MUC, max. 50 cm length, 7 tubes, partly TV-guided), while high-resolution Holocene to glacial sediment sequences were recovered by gravity corer (GC, max. 12 m length). The seven MUC tubes were sampled in 1 cm intervals for organic and inorganic geochemistry, sedimentological, biomarker and foraminiferal analysis. Organic geochemistry samples were deep frozen at -20 °C; all other samples were stored at 4 °C. After retrieval of the gravity cores, the liner were cut into 1 m segments which were first logged and subsequently cut open into an archive and a working half. The archive half was color scanned and used for sedimentological description; the working half mostly sampled every 5 cm with three series of 10 ml syringes (org. and inorg. geochemistry, foraminifers). Core catcher samples were stored separately in plastic bags.

Geophysical core logging techniques allowed to gather high-resolution sediment-physical data series, which were used to correlate sediment records and to establish a preliminary stratigraphic framework. The core liner were first logged with the MULTI-SENSOR CORE LOGGER (MSCL/016; designed and built by GEOTEK, Haslemere, UK), which provides the magnetic susceptibility (basically reflecting the amount of magnetizable minerals). The archive half of the core was visually described and scanned each centimeter with a color photo spectrometer (MINOLTA CM 508D), which provides the light reflectance of the sediment and was used to support the sedimentological description.

1.4.10.3 Preliminary Results of Sediment Sampling (Shipboard)

In total, 40 MUC were retrieved along transects A, B, C, D, E, and F perpendicular to the coastline, and 21 GC were recovered along transects A, B and C (Fig. 1 in Appendix, see also station list). Lithological descriptions and core logging data of each sampling station can be found in the Appendix. Gravity coring resulted in the total recovery of 66.5 m of sediment. Core length was from 0.6 m to a maximum of 5.75 m, with an average of ~3.1 m. The southernmost Transect A at ~17-18°S covers a depth range from ~300 m to ~2170 m. At working area B at ~15°S, a MUC and a GC were recovered from 520 m. Transect C at 11°S comprised 5 MUC and 16 GC from ~140 m to ~2000 m water depth. The northernmost working area D at 10.5°S consists of a MUC and a GC from ~500 m water depth. At 10.5°S, Transect E with only MUC covers a depth range from ~200 m to ~900 m. On Transect F at ~12-13°S, five MUC from ~150 m to ~1100 m water depth were recovered.

The appearance of sediments in the area offshore Peru is strongly influenced by their position relative to the OMZ. Dominant lithologies in the surveyed areas are grayish to olive-green silty clays with few or partly abundant foraminifera (Transect A and B) and brown silty clays to silts (Transect C and F). A soupy fluff layer is developed at all sampling sites. Brownish colors rapidly fade away downcore. In general, calcitic foraminifera were present in all sediments, although their appearance varied from foraminiferal sands to silty clays, which contained only few individuals. Bioturbated as well as laminated sediments were found; laminated sediments are prone to occur within the OMZ (most pronounced at Station 417 on Transect A) and laminations disappear below the OMZ. Laminated sediments often showed erosional discordances. Bioturbation occurred below, within and above the OMZ. Bioturbated sediments showed burrows as well as burrowed erosional surfaces.

Further lithologies found in the sediments are dark gray silts to fine sands. These layers are assumed to be ashes as they form distinct beds of 1 to 30 cm thickness with sharp bottom and top contacts. Another lithotype found comprises light gray clays of 2 to 5 mm thickness, also forming distinct layers, potential formation sites of phosphorite crusts.

Pure foraminiferal sands occur at Site 553 (Transect D) and Site 564 (Transect C) at the sediment surface. Both stations are at ~520 m water depth, which is the approximate upper boundary of the Antarctic Intermediate Water (AAIW). Within the according downcore records (GC stations 506 and 507 along Transect C) from ~520 m water depth, distinct beds of foraminiferal sand occur repeatedly in the successions, pointing to a dynamic evolution of the AAIW. These 5 to 10 cm thick foraminiferal layers consist entirely of sand-sized biogenic compounds and are free of clay and silt components. Often, phosphorite nodules and crusts occur on top of these sandy layers. Phosphorite nodules of varying size (0.5 to 10 cm) were also found elsewhere in the sediments.

In general, the sedimentation processes at the continental slope offshore Peru are affected by strong currents and bottom currents. In many cores, sedimentation was interrupted by slumps, turbidites or erosional processes. Distal turbidites were indicated through graded bedding among foraminifera-yielding silts between 700 m and 1000 m. It is speculated that both the AAIW and the Peru Undercurrent, which goes down to 400 m water depth, might have influenced the depositional environment of the Peru continental margin. Furthermore, the steep slope geometry apparently has a strong influence on the sedimentation pattern. Undisturbed sedimentary successions were only observed in shallow water depths (100 to 300 m) and at water depths greater than 2000 m.

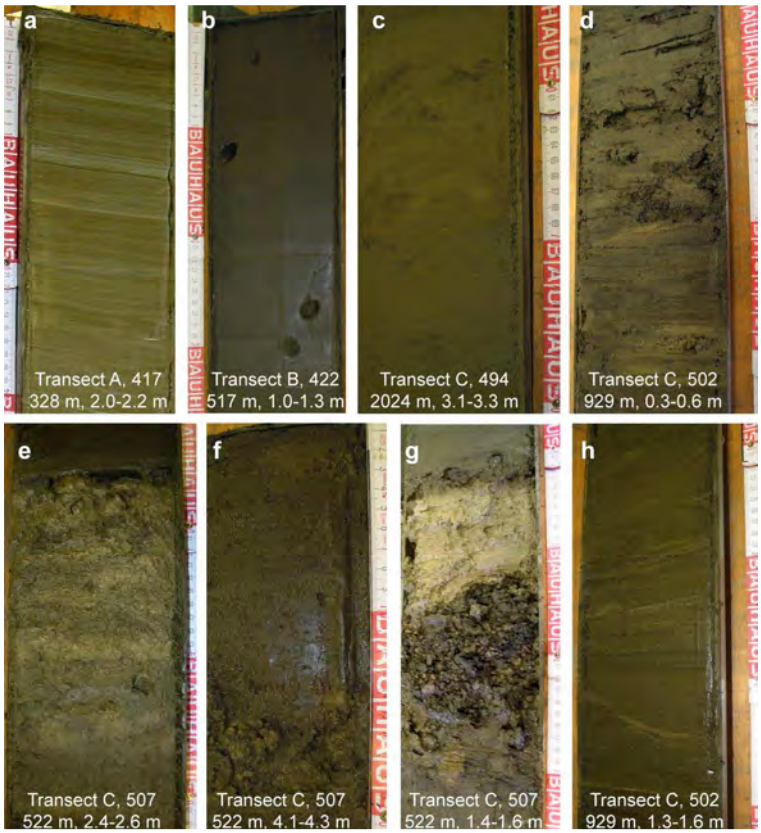

Fig.1.16: Typical lithologies along the continental slope off Peru, a) laminated silty clay, b) open burrows in bioturbated silty clay, c) bioturbated silty clay, d-h) sediments strongly influenced by current activity, sediment bypass and redeposition, d) bioturbated silty clay with irregular occurring phosphorite nodules, e) coarsenig-upward succession of foraminifera with phosphorite layer and sharp contact on top indicating increasing current strength and condensation, f) silty clay with enrichment of foraminifera by bypass of fine-grained sediments, g) channel deposits of a proximal turbidite: succession of foraminifera-yielding silty clay, rounded phosphorite pebbels, foraminiferal sand and phosphorite nodules deposited on an amalgamated surface, h) distal lower fan deposits comprising of thin-bedded graded layers of foraminifera.

1.5 Weather conditions during M 77/1

(Th. Truscheit)

In the night from October 23rd 2008 to 24th R/V METEOR left the port of Talcahuano/Chile for the leg M 77/1. The first working area was located approxiametely 1100 miles northward.

The synoptic situation in these days looked as follows:

A low with a pressure of 1011 hPa in its centre was analysed over the north of Argentina. While decreasing it moved north eastward and was expected on a position east of Uruguay at the following day. At the same time a high pressure system of 1035 hPa was analysed at a position 31°S 95°W. A wedge of this high reached with a pressure of 1020 hPa to the southern coast line of Chile. At the same time another high pressure system was approaching. It was expected to be on a position approximately 38°S 113°W on October 26th 2008. Over that a shallow low of 1014 hPa was located over the northern coast line of Chile. This constellation caused south to south westerly winds of 6 to 7 Beaufort and a swell of up to 3 meters in the beginnig of the transit to the first working area. Only some days later nearby “area 1” (first working area) the synoptic situation ahanged completely. An approaching sub tropical high was responsible for the now predominated south easterly trade-wind of 4 Beaufort, rarly 5 Beaufort. An inversion was responsible for the prevailing scattered cloud conditions most of the time. During the next days the swell decreasead only unessential. This swell was caused by low pressure systems which moved eastward south of 50°S.

On the whole the weather conditions were stable until the end of this leg. Only at the end of week 46 the influence of trade wind decreased temporary and for a very short time the the now southerly wind decreased to less than 1 m/s. As well the swell decreased to a maximum of 1.5 meters in these days.

However a new approaching subtropical high was responsible once more for the increasing trade winds at the end of this week end. Until the end of this expedition no significant changes of weather conditions could be observed. R/V METEOR reached the port of Callao/Peru on November 21st 2008.

1.6. Tab. 1.7: Station list

Stat.	Gear No.	Date	Position		Time	Depth	Position at bottom		Time	Depth	Position off bottom		Time	Depth
No.		2008	Lat. [°S]	Long. [°W]	[UTC]	[m]	Lat. [°S]	Long. [°W]	[UTC]	[m]	Lat. [°S]	Long. [°W]	[UTC]	[m]
386	CTD/RO 1	28.10.	17°50'	72°05,2'	01:44	2270								
387	MB/PS 1	28.10.	17°49'	72°52'	04:11	2270								
388	CTD/RO 2	28.10.	17°38,80'	71°58,78'	07:04	962								
389	MB/PS 2	28.10.	17°39,12'	71°58,89'	08:23	960								
390	CTD/RO 3	28.10.	17°34,15'	71°56,15'	09:35	790								
391	MB/PS 3	28.10.	17°34,31'	71°56,05'	10:37	793								
392	CTD/RO 4	28.10.	17°27,816'	71°52,590'	12:12	498								
393	MB/PS 4	28.10.	17°27,60'	71°52,48'	13:18	130								
394	MB/PS 5	28.10.	17°22,528'	71°48,463'	14:45	800								
395	CTD/RO 5	28.10.	17°26,071'	71°51,210'	19:26	284								
396	MUC 1	28.10.	17°26,01'	71°51,40'	21:05	299	17°26,01'	71°51,40'	21:18	296				
397	MUC 2	28.10.	17°26,02'	71°51,40'	22:10	300	17°26,02'	71°51,40'	22:21	297.3				
398	MUC 3	28.10.	17°28,049'	71°52,44'	23:13	496	17°28,011'	71°52,40'	23:28	496				
399	OFOS 1	29.10.	17°23,97'	71°50,54'	00:58	145	17°23,953'	71°50,533'	01:09	145	17°24,20'	71°50,06'	02:30	145
400	OFOS 2	29.10.	17°25,739'	71°51,724'	03:15	295	17°25,74'	71°51,70'	03:27	294	17°26,18'	71°51,11'	04:47	291
401	OFOS 3	29.10.	17°27,71'	71°52,84'	05:27	494	17°27,67'	71°52,87'	05:39	494	17°28,25'	71°52,01'	07:07	490
402	CTD/RO 6	29.10.	17°46,659'	72°03,133'	09:33	195								
403	MUC 4	29.10.	17°26,00'	71°51,41'	14:40	296	17°26,01'	71°51,41'	15:08	298				
404	MUC 5	29.10.	17°26,01'	71°51,40'	15:40	295.5	17°26,00'	71°51,41'	15:53	295				
405	BIGO-T 1	29.10.	17°26,037'	71°51,417'	20:05	298	17°26,01'	71°51,39'	20:20	303				
406	MUC 6	29.10.	17°28,01'	71°52,40'	21:19	492	17°28,00'	71°52,40'	0.9	492				
407	MUC 7	29.10.	17°34,37'	71°56,00'	22:56	788	17°34,385'	71°55,992	23:28	787				
408	MUC 8	30.10.	17°34,377'	71°56,007'	00:19	790	17°34,38'	71°55,99'	00:44	789.3				
409	MUC 9	30.10.	17°38,36'	71°58,25'	02:08	920	17°38,388'	71°58,242'	0.108	918				
410	MUC 10	30.10.	17°38,404'	71°58,232'	03:20	917	17°38,385'	71°58,233'	03:46	918				
411	MUC 11	30.10.	17°47,158'	72°44,7'	05:29	2167	17°47,083'	72°44,17'	06:22	2166				

Stat.	Gear No.	Date	Position		Time	Depth	Position at bottom		Time	Depth	Position off bottom		Time	Depth
No.		2008	Lat. [°S]	Long. [°W]	[UTC]	[m]	Lat. [°S]	Long. [°W]	[UTC]	[m]	Lat. [°S]	Long. [°W]	[UTC]	[m]
412	CTD/RO 7	30.10.	17°47,047'	72°04,413'	07:38	2166								
413	GC 1	30.10.	17°47,100'	72°04,443'	12:03	2166	17°47,078'	72°04,423'	12:49	2168				
414	GC 2	30.10.	17°38,606'	71°58,382'	15:51	928	17°38,606'	71°58,382'	15:51	00:00				
415	GC 3	30.10.	17°34,395'	71°56,198'	18:46	800	17°34,391'	71°56,199'	18:48	792.7				
416	GC 4	30.10.	17°28,135'	71°52,621'	20:30	505	17°28,135'	71°52,621'	20:30	504.6				
417	GC 5	30.10.	17°26,027'	71°51,761'	21:51	300	17°26,026'	71°51,718'	21:52	328.7				
418	GC 6	30.10.	17°25,97'	71°51,81'	22:39	338.2	17°25,98'	71°51,82'	22:51	339.2				
419	BIGO-T 1 recovery	30.10.	17°25,81'	71°51,59'	23:21	292.5								
420	MUC 12	31.10.	15°11,355'	75°34,885'	20:47	516	15°11,40'	71°34,83'	21:00	524				
421	MUC 13	31.10.	15°,11,39'	75°34,81'	21:37	519	15°11,38'	75°34,82'	21:43	522				
422	GC 7	31.10.	15°11,398'	75°34,87'	22:40	517	15°11,42'	75°34,86'	22:56					
423	CTD/RO 8	31.10.	15°11,44'	75°34,86'	23:38	530.5								
424	CTD/RO 9	02.11.	11°0,041'	78°30,027'	02:04	928								
425	MB/PS 6	02.11.	10°59,99'	78°29,90'	03:23	937								
426	CTD/RO 10	02.11.	10°59,95'	78°25,497'	04:31	693								
427	MB/PS 7	02.11.	11°0,02'	78°25,48'	05:26	629								
428	CTD/RO 11	02.11.	11°0,108'	78°20,519'	06:58	499								
429	MB/PS 8	02.11.	11°0,09'	78°20,48'	07:41	497								
430	CTD/RO 12	02.11.	10°59,99'	78°8,48'	09:56	292.2								
431	MB/PS 9	02.11.	11°0,049'	78°8,489'	10:28	300								
432	CTD/RO 13	02.11.	10°59,98'	78°1,94'	11:50	198								
433	MB/PS 10	02.11.	11°0,00'	78°1,95'	12:19	202								
434	CTD/RO 14	02.11.	11°0,07'	77°56,69'	13:27	142								
435	MB/PS 11	02.11.	11°0,03'	77°56,50'	13:57	150								
436	CTD/RO 15	02.11.	11°0,03'	77°47,48'	15:41	85.9								
437	MB/PS 12	02.11.	11°0,011'	77°48,62'	16:22	100								
438	CTD/RO 16	03.11.	11°0,688'	78°35,025'	00:59	1261								

Stat.	Gear No.	Date	Position		Time	Depth	Position at bottom		Time	Depth	Position off bottom		Time	Depth
No.		2008	Lat. [°S]	Long. [°W]	[UTC]	[m]	Lat. [°S]	Long. [°W]	[UTC]	[m]	Lat. [°S]	Long. [°W]	[UTC]	[m]
439	MB/PS 13	03.11.	11°0,780'	78°35,065'	02:22	1270								
440	MUC 14	03.11.	10°39,96'	78°30,05'	03:44	928	11°0,01'	10°39,05'	03:44	928				
441	CTD/RO 17	03.11.	11°0,00'	78°27,44'	05:23	797								
442	CTD/RO 18	03.11.	11°0,00'	78°26,290'	07:00	746								
443	CTD/RO 19	03.11.	11°0,00'	78°25,550'	08:26	695								
444	CTD/RO 20	03.11.	11°0,00'	78°24,65'	09:55	645								
445	MUC 15	03.11.	10°59,98'	78°30,02'	12:23	928	10°59,997'	78°30,022'	12:52	928				
446	MUC 16	03.11.	11°0,44'	78°30,06'	13:50	932	11°0,02'	78°30,06'	14:17	932				
447	MUC 17	03.11.	10°59,99'	78°30,48'	15:05	928	11°0,03'	78°30,03'	15:30	935				
448	MUC 18	03.11.	10°59,97'	78°30,04'	16:16	926	10°59,97'	78°30,05'	16:36	928				
449	MUC 19	03.11.	11°0,00'	78°09,97'	19:28	315	11°0,01'	78°09,97'	19:41	319				
450	MUC 20	03.11.	10°59,98'	78°10,04'	20:25	319	10°59,99'	78°10,00'	20:35	315				
451	BIGO 1	03.11.	11°00,00'	78°09,84'	23:28	319	11°00,00'	78°09,92'	23:41	315				
452	CTD/RO 21	04.11.	11°00,04'	77°98,18'	02:26	90.9								
453	OFOS 4	04.11.	11°00,00'	77°47,97'	03:11	90	11°00,00'	77°47,97'	03:17	83	11°00,00'	77°48,43'	04:48	92
454	OFOS 5	04.11.	11°00,00'	78°01,00'	06:12	189	11°00,00'	78°01,04'	06:20	192	11°00,00'	78°01,92'	07:46	202
455	MUC 21	04.11.	11°00,01'	78°19,24'	11:30	465	11°00,00'	78°19,23'	11:48	466				
456	MUC 22	04.11.	11°00,01'	78°19,23'	12:30	465	11°00,013'	78°19,234'	12:50	465				
457	MUC 23	04.11.	11°,00,05'	78°19,26'	13:19	467	11°00,02'	78°19,24'	13:32	467				
458	MUC 24	04.11.	11°00,12'	78°25,59'	14:43	698	11°00,05'	78°25,64'	15:01	700.5				
459	MUC 25	04.11.	11°00,02'	78°25,6'	15:40	698	11°00,03'	78°25,60'	16:00	697				
460	MUC 26	04.11.	11°00,01'	78°35,16'	17:24	1245	11°00,01'	78°35,11'	17:56	1242				
461	MB/PS 14	04.11.	11°00,03'	78°35,3'	18:36	1259								
462	MUC 27	04.11.	10°59,999'	78°44,7'	20:17	2020	10°59,97'	78°44,76'	21:05	2025				
463	CTD/RO 22	04.11.	11°00,008'	78°44,864'	22:24	#####								
464	Lander	05.11.	10°59,79'	78°10,01'	03:37	318.1								
465	OFOS 6	05.11.	11°00,093'	78°09,452'	04:27	310	11°00,094'	78°9,450'	04:39	309	10°59,983'	78°10,042'	05:41	317
466	OFOS 7	05.11.	11°00,005'	78°14,785'	06:31	385	10°59,966'	78°14,883'	06:50	386	10°59,990'	78°16,012'	09:17	407

Stat.	Gear No.	Date	Position		Time	Depth	Position at bottom		Time	Depth	Position off bottom		Time	Depth
No.		2008	Lat. [°S]	Long. [°W]	[UTC]	[m]	Lat. [°S]	Long. [°W]	[UTC]	[m]	Lat. [°S]	Long. [°W]	[UTC]	[m]
467	OFOS 8	05.11.	10°59,986'	78°22,989'	10:22	575	10°59,966'	78°23,027'	10:41	575	10°59,990'	78°24,511'	12:43	673
468	CTD/RO 23	05.11.	11°00,047'	77°56,645	15:50	145.5								
469	MUC 28	05.11.	11°00,06'	77°56,6'	16:28	145	11°00,03'	77°56,58'	16:37	145				
470	MUC 29	05.11.	11°00,00'	77°56,61'	17:08	143	11°00,02'	77°56,60'	17:16	145				
471	MUC 30	05.11.	11°00,007'	78°9,938'	18:47	316.5	11°0,00'	78°9,924'	18:59	320				
472	MUC 31	05.11.	11°00,02'	78°9,96'	19:35	320	11°00,01'	78°9,96'	19:46	318				
473	MUC 32	05.11.	11°0,03'	78°9,95'	20:25	316	11°0,01'	78°9,94'	20:35	317				
474	BIGO 2	05.11.	11°0,01'	78°25,48'	22:35	693	11°0,01'	78°25,55'	23:03	695				
475	PROFI 1	05.11.	11°0,01'	78°25,91'	01:25	723	11°0,02'	78°25,98'	01:56	727				
476	CTD/RO 24	06.11.	11°0,1'	78°15,20'	03:52	391.7								
477	CTD/RO 25	06.11.	11°0,02'	78°8,457'	05:51	302								
478	CTD/RO 26	06.11.	10°59,997'	78°1,572'	0.319	198								
479	CTD/RO 27	06.11.	11°	77°49,22'	09:46	92								
480	CTD/RO 28	06.11.	11°00,003'	78°08,415'	12:18	297.2								
481	MUC 33	06.11.	11°0,01'	78°14,15'	13:53	376	11°0,00'	78°14,19'	14:04	376				
482	MUC 34	06.11.	11°0,02'	78°14,17'	14:51	375	11°0,01'	78°14,17'	14:51	375				
483	MUC 35	06.11.	10°59,71'	78°25,98'	16:20	723	10°59,78'	78°25,78'	16:48	721				
484	MUC 36	06.11.	10°59,74'	78°25,98'	17:32	720	10°59,74'	78°25,96'	17:52	722				
485	MUC 37	06.11.	10°59,75'	78°25,98'	18:31	721	10°59,74'	78°25,96'	18:51	720				
486	PROFI 2	06.11.	10°59,76'	78°26'	19:30	721.3								
487	MUC 38	06.11.	11°00,00'	78°23,17'	20:27	579	11°00,00'	78°23,17'	20:42	579				
488	MUC 39	06.11.	11°00,02'	78°23,18'	21:27	580	11°00,02'	78°23,17'	21:45	579				
489	BIGO 2	06.11.	11°00,29'	78°25,71'	23:40									
490	OFOS 9	07.11.	11°	78°19,9'	00:40	483	10°59,98'	78°19,98'	01:00	485	10°59,97'	78°23,01'	06:12	577
491	OFOS 10	07.11.	11°	78°24,35'	07:11	628	10°59,97'	78°24,35'	07:38	627	10°59,99'	78°21,521'	10:14	755
492	OFOS 11	07.11.	11°	78°31,015'	11:21	988	10°59,99'	78°31,04'	11:48	990	11°	78°31,57	12:22	1022
493	GC 8	07.11.	10°59,97'	78°44,79'	14:44	2020	11°00,01'	78°44,81'	15:06	2025				
494	GC 9	07.11.	11°0,025'	78°44,80'	16:25	2020	11°0,01'	78°44,81'	16:42	2024				

Stat.	Gear No.	Date	Position		Time	Depth	Position at bottom		Time	Depth	Position off bottom		Time	Depth
No.		2008	Lat. [°S]	Long. [°W]	[UTC]	[m]	Lat. [°S]	Long. [°W]	[UTC]	[m]	Lat. [°S]	Long. [°W]	[UTC]	[m]
495	GC 10	07.11.	10°59,96'	78°34,44'	18:35	1195	11°0,01'	78°34,39'	19:00	1194				
496	GC 11	07.11.	11°0,01'	78°34,39'	20:02	1192	11°0,01'	78°34,38'	20:25	1197				
497	GC 12	07.11.	11°0,01'	78°30,05'	20:54	932.5	11°0,01'	78°30,05'	21:58	930				
498	CTD/RO 29	08.11.	11°0,030'	77°55,997'	01:54	138.8								
499	CTD/RO 30	08.11.	11°0,02'	78°5,29'	03:49	249								
500	CTD/RO 31	08.11.	11°0,01'	78°20,21'	05:46	487.6								
501	CTD/RO 32	08.11.	11°	78°31'	08:52	988								
502	GC 13	08.11.	11°0,01'	78°30,05'	11:09	929	11°	78°30,05'	11:29	930				
503	GC 14	08.11.	11°	78°25,65'	12:49	698.4	11°	78°25,65'	13:01	697.5				
504	GC 15	08.11.	11°0,01'	78°25,67'	13:43	699.2	11°0,01'	78°25,65'	14:02	700				
505	GC 16	08.11.	11°0,01'	78°25,66'	14:38	700.6	11°0,004'	78°25,652'	14:55	698.9				
506	GC 17	08.11.	11°	78°21,14'	16:04	520	11°	78°21,13'	16:14	522.7				
507	GC 18	08.11.	11°0,03'	78°21,13'	17:03	520	11°0,01'	78°21,13'	17:13	522.2				
508	GC 19	08.11.	11°0,03'	78°14,19'	18:29	376	11°0,03'	78°14,19'	18:35	379				
509	GC 20	08.11.	11°0,03'	78°17,18'	0.806	379	11°0,04'	78°14,17'	0.81	397				
510	GC 21	08.11.	11°0,02'	78°13,31'	20:06	365.7	11°0,023'	78°13,314'	20:16	365	11°0,024'	78°13,317'	20:18	365
511	GC 22	08.11.	11°0,05'	77°56,61'	22:19	144	11°0,05'	77°56,61'	22:23	146				
512	GC 23	08.11.	11°0,05'	77°56,61'	22:48	143.5	11°0,05'	77°56,61'	22:55	144				
513	MB/PS 15	08.11.	10°99,74'	77°92,44'	23:55	138.9								
514	BIGO-T 2	09.11.	10°59,99'	78°23,54'	17:46	592	11°0,002'	78°23,548'	18:15	594.2				
515	CTD/RO 33	09.11.	10°59,813'	78°23,547'	19:08	595.6								
516	MUC 40	09.11.	10°59'	78°21'	20:43	513	11°	78°20'	21:29	511.6				
517	MUC 41	09.11.	11°0,1'	78°20,92'	22:23	510	11°	78°20,91'	22:54	511				
518	MUC 42	10.11.	11°0,01'	78°16,3'	01:03	411.6	11°0,01'	78°16,3'	01:16	412				
519	MUC 43	10.11.	11°0,01'	78°16,28'	01:54	410	11°0,01'	78°16,29'	02:04	410				
520	MUC 44	10.11.	11°0,02'	78°1,87'	03:53	196	11°0,01'	78°1,87'	04:00	195				
521	MUC 45	10.11.	11°	78°1,86'	04:27	195	11°0,01'	78°1,86'	04:35	195				
522	MUC 46	10.11.	11°0,02'	78°1,88'	05:03	198	11°0,02'	78°1,88'	05:10	195				

Stat.	Gear No.	Date	Position		Time	Depth	Position at bottom		Time	Depth	Position off bottom		Time	Depth
No.		2008	Lat. [°S]	Long. [°W]	[UTC]	[m]	Lat. [°S]	Long. [°W]	[UTC]	[m]	Lat. [°S]	Long. [°W]	[UTC]	[m]
523	OFOS 12	10.11.	11°	78°20'	07:05	481	11°	78°20'	07:25	482	11°	78°18,9'	08:55	461
524	OFOS 13	10.11.	11°	78°11,5'	10:10	340	11°	78°11,485'	10:26	340	11°	78°10,61'	11:27	329
525	OFOS 14	10.11.	11°	78°2,5'	12:40	202	11°	78°2,5'	12:55	206	11°	78°2,29'	13:11	200
526	BIGO 3	10.11.	11°	78°15,27'	18:32	395.9	11°0,022'	78°15,27'	18:47	397.3				
527	PROFI 2	10.11.	11°	78°30,98'	0.881	990.4	11°	78°30,981'	0.911	999.8				
528	BIGO-T 2	10.11.	10°59,81'	78°23,62'	23:29	594								
529	MB/PS 15	11.11.	10°30,07'	79°0,12'	04:03	1091								
530	MB/PS 16	11.11.	10°15,90'	78°38,98'	08:30	143								
531	MB/PS 17	11.11.	10°29,84'	79°0,49'	12:42	1100								
532	CTD/RO 34	11.11.	10°15,94'	78°38,67'	17:25	143								
533	MUC 47	11.11.	10°16'	78°38,9'	18:30	140	10°16'	78°38,9'	18:35	142.5				
534	MUC 48	11.11.	10°15,9'	78°38,8'	19:11	140	10°15,8'	78°38,8'	19:18	140				
535	BIGO 3	12.11.	10°59,85'	78°15,38'	00:10	396.4								
536	PROFI 2	12.11.	10°59,95'	78°31,1'	02:40	1061								
537	OFOS 15	12.11.	11°	78°10,76'	05:15	332	11°	78°10,77'	05:30	332	11°	78°9,83'	06:51	317
538	OFOS 16	12.11.	11°	78°2,36'	08:00	202	11°	78°02,35'	08:11	202	11°	78°1,83'	08:56	196
539	OFOS 17	12.11.	11°	77°49,48'	10:30	103	11°	77°49,48'	10:37	103	11°	78°48,65'	11:35	89
540	MUC 49	12.11.	11°0,01'	77°47,41'	12:11	78	11°0,01'	77°47,40'	12:16	79				
541	MUC 50	12.11.	10°59,99'	77°47,4'	12:36	78	11°	77°47,4'	12:40	78				
542	MUC 51	12.11.	11°	77°47,4'	13:02	78	11°0,01'	77°47,4'	13:05	79				
543	MUC 52	12.11.	10°59,99'	77°47,4'	13:27	77	10°59,99'	77°47,4'	13:30	78.4				
544	BIGO-T	12.11.	11°	78°9,12'	16:11	303								
545	CTD/RO 35	12.11.	10°59,983'	78°20,468'	18:07	497								
546	CTD/RO 36	12.11.	11°0.024'	78°22,444'	19:02	499.4								
547	CTD/RO 37	12.11.	10°59,98'	78°31,26'	21:15	1010								
548	BIGO 4	12.11.	10°59,97'	78°31,27'	23:32	1018	10°59,99'	78°31,25'	00:13	1015				
549	MUC 53	13.11.	10°59,81'	78°31,26'	01:14	1008	10°59,807'	78°31,266'	01:43	#####				
550	OFOS 18	13.11.	10°18,6'	78°43,1'	06:05	141	10°18,6'	78°43,11'	06:12	142	10°18,25'	78°42,43	07:10	142

Stat.	Gear No.	Date	Position		Time	Depth	Position at bottom		Time	Depth	Position off bottom		Time	Depth
No.		2008	Lat. [°S]	Long. [°W]	[UTC]	[m]	Lat. [°S]	Long. [°W]	[UTC]	[m]	Lat. [°S]	Long. [°W]	[UTC]	[m]
551	OFOS 19	13.11.	10°25,57'	78°53,29'	08:40	322	10°25,6'	78°53,2'	08:56	326	10°25,19'	78°52,61'	09:57	269
552	OFOS 20	13.11.	10°27,45'	78°55,96'	10:46	715	10°27,44'	78°55,97'	11:11	717	10°26,83'	78°55'	12:30	593
553	MUC 54	13.11.	10°26,38'	78°54,7'	13:24	522	10°26,38'	78°54,7'	13:41	521				
554	MUC 55	13.11.	10°26,38'	78°54,74'	14:16	522	10°26,37'	78°54,74'	14:31	518				
555	CTD/RO 38	13.11.	10°25,49'	78°53,29'	15:18	318								
556	CTD/RO 39	13.11.	10°25,547'	78°53,247'	15:43	314.9								
557	BIGO-T 3	13.11.	11°	78°09,15'	22:10	306								
558	BIGO 4	14.11.	10°59,85'	78°31,4'	00:56	1016								
559	MUC 56	14.11.	11°0,02'	78°18,02'	03:24	446	11°0,03'	78°17,97'	03:36	444				
560	MUC 57	14.11.	11°0,04'	78°17,98'	04:05	445	11°0,01'	78°17,97'	04:17	445				
561	MUC 58	14.11.	11°0,01'	78°17,94'	04:45	445	11°0,02'	78°17,96'	04:58	445				
562	OFOS 21	14.11.	11°10'	78°06,97'	07:00	327	11°10,02'	78°06,99'	09:12	331	11°09,54'	78°06,2'	10:14	313
563	OFOS 22	14.11.	11°14,96'	78°16,53'	11:47	550	11°14,95'	78°16,51'	12:09	551	11°14,63'	78°15,77'	13:06	530
564	MUC 59	14.11.	11°14,6'	78°15,8'	14:39	526	11°14,5'	78°15,7'	14:55	527				
565	MUC 60	14.11.	11°7,99'	78°21,41'	16:20	650	11°8'	78°21,4'	16:39	640				
566	BIGO-T 4	14.11.	11°	78°9,12'	19:05	306	11°	78°9,13'	19:17	309				
567	PROFI 3	14.11.	10°59,99'	78°26,58'	21:22	765	11°	78°26,52'	21:55	765.0				
568	BIGO 5	15.11.	11°	77°47,72'	02:05	82	11°0,02'	77°47,72'	02:14	85				
569	CTD/RO 40	15.11.	11°6,491'	77°58,201'	03:59	184.5								
570	MB/PS 18	15.11.	11°6'	77°58'	04:50	188								
571	OFOS 23	15.11.	11°16,18'	78°18,72'	10:25	635	11°16,2'	78°18,73'	10:48	634.0	11°15,183'	78°16,91'	13:02	564
572	OFOS 24	15.11.	11°12,76'	78°11,51'	14:15	407	11°12,78'	78°11,45'	14:33	403	11°12,61'	78°11,1'	15:04	398
573	MUC 61	15.11.	11°9,8'	78°5,5'	16:22	304	11°9,9'	78°5,5'	16:32	309				
574	MUC 62	15.11.	11°10,02'	78°5,54'	17:05	305	11°1'	78°5,53'	17:13	303				
575	CTD/RO 41	15.11.	10°59,77'	78°9,19'	20:06	303.9								
576	BIGO-T 4 Re.	15.11.	10°59,96'	78°09,26'	21:30	314								
577	BIGO 5	16.11.	10°59,82'	77°47,72'	01:04									

Stat.	Gear No.	Date	Position		Time	Depth	Position at bottom		Time	Depth	Position off bottom		Time	Depth
No.		2008	Lat. [°S]	Long. [°W]	[UTC]	[m]	Lat. [°S]	Long. [°W]	[UTC]	[m]	Lat. [°S]	Long. [°W]	[UTC]	[m]
578	OFOS 25	16.11.	11°7,01'	77°59,4'	02:46	205	11°7,02'	77°59,35'	02:56	197	11°06,54'	77°58,32'	04:20	184
579	OFOS 26	16.11.	11°14,47'	78°14,86'	06:20	502	11°14,47'	78°14,86'	06:37	501	11°14,05'	78°13,96'	08:02	473
580	OFOS 27	16.11.	11°16,75'	78°19,75'	09:13	680	11°16,75'	78°19,75'	09:41	682	11°16,17'	78°18,67'	11:01	633
581	MUC 63	16.11.	11°11,2'	78°8,15'	12:48	352	11°11,2'	78°8,12'	12:57	351				
582	MUC 64	16.11.	11°9,7'	78°4,93'	13:51	299	11°9,69'	78°4,88'	14:01	291				
583	MUC 65	16.11.	11°6,856'	78°3,11'	14:51	250	11°6,86'	78°3,06'	15:00	248				
584	MUC 66	16.11.	11°7'	77°59,3'	15:52	200	11°7'	77°59,3'	16:00	198				
585	PROFI 3	16.11.	10°59,91'	78°26,62'	19:30	765								
586	BIGO-T 5	16.11.	10°59,99'	78°9,4'	22:05	315	11°	78°9,4'	22:19	316				
587	MUC 67	16.11.	11°0,01'	78°1,87'	23:17	205	11°	78°1,85'	23:34	203				
588	MUC 68	17.11.	11°	78°1,86	00:01	198	11°0,01'	78°1,86	00:08	204				
589	MUC 69	17.11.	11°14,27'	78°14,66'	02:37	495	11°14,29'	78°14,62'	02:51	494				
590	MUC 70	17.11.	11°15,1'	78°16,42'	03:45	547	11°15,13'	78°16,44'	04:00	548				
591	OFOS 28	17.11.	11°17,09'	78°20,51'	05:15	720	11°17,07'	78°20,5'	05:38	719	11°16,75'	78°19,75'	06:48	682
592	OFOS 29	17.11.	11°18,44'	78°23,25'	07:39	965	11°18,44'	78°23,31'	08:11	970	11°18,14'	78°22,64'	09:07	891
593	CTD/RO 42	17.11.	11°18,115'	78°22,587'	09:43	887								
594	CTD/RO 43	17.11.	11°17,734'	78°21,587'	10:49	791								
595	CTD/RO 44	17.11.	11°16,87'	78°20,118'	11:46	693								
596	CTD/RO 45	17.11.	11°15,643'	78°17,666'	12:55	597								
597	CTD/RO 46	17.11.	11°14,211'	78°14,605'	14:07	491								
598	BIGO-T 5	17.11.	11°00,34'	78°09,14'	11:35	313.5								
599	CTD/RO 47	17.11.	11°9,689'	78°4,918'	18:04	293								
600	CTD/RO 48	17.11.	11°12,474'	78°10,865'	19:52	394								
601	MUC 71	17.11.	11°12,5'	78°10,8'	21:14	394	11°12,5'	78°10,8'	21:29	394				
602	MUC 72	17.11.	11°16,04'	78°18,38'	22:39	618	11°16,05'	78°18,35'	22:54	620				
603	MUC 73	17.11.	11°17,53'	78°21,53'	23:46	794	11°17,54'	78°21,52'	00:08	793				
604	MUC 74	18.11.	11°17,96'	78°22,42'	00:52	878	11°17,97'	78°22,42'	01:14	878				
605	MB/PS 19	18.11.	12°31,8'	77°29,93'	09:55	535								

Stat.	Gear No.	Date	Position		Time	Depth	Position at bottom		Time	Depth	Position off bottom		Time	Depth
No.		2008	Lat. [°S]	Long. [°W]	[UTC]	[m]	Lat. [°S]	Long. [°W]	[UTC]	[m]	Lat. [°S]	Long. [°W]	[UTC]	[m]
606	MB/PS 20	18.11.	12°19,5'	77°19,93'	12:40	170								
607	MUC 75	18.11.	12°32,5'	77°30,5'	16:29	583	12°32,5'	77°30,5'	16:45	584				
608	MUC 76	18.11.	12°32,55'	77°30,47'	17:02	584	12°32,53'	77°30,49'	17:36	584				
609	CTD/RO 49	18.11.	12°25,81'	77°24,9'	19:06	294								
610	MUC 77	18.11.	12°29,5'	77°27'	20:40	418	12°29,5'	77°27'	20:51	418				
611	MUC 78	18.11.	12:29,47'	77°27,96'	21:18	417	12°29,45'	77°27,95'	21:46	418				
612	OFOS 30	18.11.	12°33,07'	77°30,64	22:39	620	12°33,2'	77°30,62'	23:03	622	12°31,28'	77°29,15'	01:48	487
613	MB/PS 21	19.11.	12°32,12'	77°30,14'	02:30	558								
614	MUC 79	19.11.	12°25,6'	77°24,8'	14:37	290	12°25,6'	77°24,8'	14:43	290				
615	MUC 80	19.11.	12°25,58'	77°24,86'	15:13	290	12°25,56'	77°24,83'	15:21	289				
616	MUC 81	19.11.	12°22,69'	77°29,06'	18:46	302	12°22,69'	77°29,05'	18:55	302				
617	MUC 82	19.11.	12°22,69'	77°29,05'	19:21	302	12°22,71'	77°29,05'	19:30	303				
618	CTD/RO 50	19.11.	12°18,628'	77°19,157'	20:59	149								
619	MUC 83	19.11.	12°18,6'	77°19,2'	21:30	151	12°18,6'	77°19,1'	21:37	152				
620	MUC 84	19.11.	12°18,62'	77°19,2'	22:08	150	12°18,62'	77°19,2'	22:13	150				
621	MUC 85	20.11.	12°32,75'	77°34,75'	00:25	820	12°32,757'	77°34,757'	00:56	823.1				
622	MUC 86	20.11.	12°32,74'	77°34,73'	01:35	819	12°32,75'	77°34,74'	01:57	819				
623	MUC 87	20.11.	12°38,16'	77°34,58'	03:03	1085	12°38,18'	77°34,59'	03:32	1085				
624	OFOS 31	20.11.	12°34,31'	77°31,25'	04:54	702	12°34,32'	77°31,25'	05:21	704	12°33,1'	77°30,52'	07:17	613
625	OFOS 32	20.11.	12°30,4'	77°28,49'	08:11	444	12°30,41'	77°28,5'	08:30	445	12°29,69'	77°27,94'	09:38	421
626	OFOS 33	20.11.	12°24,31'	77°23,82'	10:45	255	12°24,3'	77°23,8'	10:55	255	12°23,74'	77°23,27'	12:00	235
627	OFOS 34	20.11.	12°19,11'	77°19,59'	12:52	159	12°19,14'	77°19,61'	13:00	158	12°18,52	77°19,12'	14:08	150
628	CTD/RO 51	20.11.	12°21,599'	77°21,644'	14:53	190.2								
629	CTD/RO 52	20.11.	12°28,8'	77°27,45'	16:27	392.7								
630	CTD/RO 53	20.11.	12°32,304'	77°30,627'	17:53	575								
631	CTD/RO 54	20.11.	12°34,468'	77°32,176'	19:03	798								
632	CTD/RO 55	20.11.	12°36,351'	77°33,543'	20:23	993.8								

1.7 Acknowledgements

The scientific party aboard R/V METEOR during leg M77-1 gratefully acknowledges the good cooperation and efficient technical assistance of Captain W. Baschek, his officers and crew who significantly contributed to the scientific success of this cruise. The cruise was funded by the DFG through the Collaborative Research Project (SFB) 754 at the University Kiel and IFM-GEOMAR.

1.8 References

Amann, R.I., Krumholz, L., Stahl, D.A., 1990, Fluorescent-oligonucleotide probing of whole cells for determinative, phylogenetic, environmental studies in microbiology. Bacteriol:, J. 172, 762-770

Bertics, V.J., Sohm, J.A., Chow, C.-E.T., Treude, T., Capone, D.G., Fuhrman, J.A., Ziebis, W. (submitted) Burrowing deeper into benthic nitrogen fixation, PNAS

Bruland, K. W., Rue E. L., Smith, G. J., Ditullio, G. R.., 2005, Iron, macronutrients and diatom blooms in the Peru upwelling regime: brown and blue waters of Peru. Marine Chemistry 93**:** 81-103.

Capone, D.G., 1993, In: Handbook of Methods in Aquatic Microbial Ecology, eds Kemp PF, Sherr BF, Sherr EB, Coles JJ (CRC Press LLC, Boca Raton), 621-631.

Caress, D.W., Chayes, D.N., Improved Management of Large Swath Mapping Datasets in MB-System Version 5, Abstract OS11B-0373. Eos Trans. Fall Meet. Suppl., 2001, 82(47).

Croot, P. L., Laan P., 2002, Continuous shipboard determination of Fe(II) in Polar waters using flow injection analysis with chemiluminescence detection. Analytica Chimica Acta 466**:** 261-273.

Ferreira dos S., C., Velasco, G., Vaz B. dos S., Albergone, E. H., Hellebrandt, D., Poseidon Linux – uma distribuição Linux voltada para público acadêmico e científico. Panamjas, 1(2): III-VI. ISSN 1809-9009. http://www.panamjas.org/ Arquivos/PANAMJAS 1(2)_III-VII.pdf

Garcia, H.E., Gordon, L., 1992, Oxygen solubility in seawater: Better fitting equations. Limnol Oceanogr, 37, 1307-1312.

Grasshoff, K., Ehrhardt, M., Kremling, K. ,1997, Methods of seawater analysis. Verlag Chemie.

Guéguen, C., Tortell, P.D., 2008, High-resolution measurement of Southern Ocean CO_2 and O_2/Ar by membrane inlet mass spectrometry. Mar Chem, 108, 184-194.

Hamme, R.C., Emerson, S.R. ,2004, The solubility of neon, nitrogen and argon in distilled water and seawater. Deep-Sea Res I, 51: 1517-1528.

Hartnett, H.E., Seitzinger, S.P., 2003, High-resolution nitrogen gas profiles in sediment porewaters using a new membrane probe for membrane-inlet mass spectrometry. Mar Chem, 83, 23-30.

Hong, H., Kester D.R.. 1986, Redox state of iron in offshore waters of Peru. Limnology and Oceanography 31**:** 512-524.

Ichoku, C. and others. 2002, Analysis of the performance characteristics of the five-channel Microtops II Sun photometer for measuring aerosol optical thickness and precipitable water vapor. Journal of Geophysical Research 107**:** 4179, doi:4110.1029/2001JD001302.

Ivanenkov, V.N., Lyakhin, Y.I., 1978, Determination of total alkalinity in seawater. In: Bordovsky, O.K., Ivanenkov, V.N. (Eds.), Methods of Hydrochemical Investigations in the Ocean. Nauka Publ. House, pp. 110–114, in Russian.

Jørgensen, B.B.,1978, A comparison of methods for the quantification of bacterial sulphate reduction in coastal marine sediments: I. Measurements with radiotracer techniques. Geomicrobiol J, 1, 11-27

Kana, T.M., Darkangelo, C., Hunt, M.D., Oldham, J.B., Bennett, G.E., Cornwell, J.C., 1994, A membrane inlet mass spectrometer for rapid high precision determination of N_2, O_2, and Ar in environmental water samples. Anal Chem, 66, 4166– 4170.

Laursen, A.E., Seitzinger, S.P., 2002, The role of denitrification in nitrogen removal and carbon mineralization in Mid-Atlantic Bight sediments. Cont Shelf Res, 22, 1397– 1416.

Levin, L., D., Gutierrez, A., Rathburn, C., Neira, J., Sellanes, P., Munoz, V., Gallardo, Salamanca, M:, 2002, Benthic processes on the Peru margin: a transect across the oxygen minimum zone during the 1997–98 El Nino, Progress in Oceanography, V. 53, 1–27.

Luther, G. W.,Swartz, C.B., Ullman,W.J.. 1988. Direct determination of Iodide in Seawater by Cathodic Stripping Square Wave Voltammetry. Analytical Chemistry **60:** 1721-1724.

Perez, M. E., unpubl., Living benthic foraminiferal distributions across the Peru margin oxygen minimum zone, Marine Micropaleontology.

Pfannkuche, O., Linke, P., 2003, GEOMAR landers as long-term deep sea observatories. Sea Technology, 44, 50-55.

Porter, J. N.,. Miller, M., Pietras, C., Motell, C., 2001, Ship-Based Sun Photometer Measurements Using Microtops Sun Photometers. Journal of Atmospheric and Oceanic Technology 18**:** 765-774.

Smirnov, A. and others. 2009, Maritime Aerosol Network (MAN) as a component of AERONET. Journal of Geophysical Research (in press).

Sommer, S., Linke ,P., Pfannkuche, O. and 6 others,2009, Seabed methane emissions and the habitat of frenulate tubeworms on the Captain Arutyunov mud volcano (Gulf of Cadiz) Mar Ecol Prog Ser., Doi:10.3354/meps07956.

Sommer, S., Pfannkuche, O., Linke, P. and 7 others,2006, Efficiency of the benthic filter: Biological control of the emission of dissolved methane from sediments containing shallow gas hydrates at Hydrate Ridge. Global Biogeochem Cycles 20, GB 2019,14pp

Sommer, S., Türk, M., Kriwanek, S., Pfannkuche, O., 2008, Gas exchange system for extended in situ benthic chamber flux measurements under controlled oxygen conditions: First application Sea bed methane emission measurements at Captain Arutyunov mud volcano. Limnol Oceanogr: Methods, 6, 23-33.

Yuan, J., Shiller, A.M., 1999, Determination of Subnanomolar Levels of Hydrogen Peroxide in Seawater by Reagent-Injection Chemiluminescence Detection. Analytical Chemistry **71:** 1975-1980.

Zika, R. G., Saltzman, E.S., Cooper, W.J., 1985, Hydrogen Peroxide concentrations in the Peru Upwelling area. Marine Chemistry **17:** 265-275.

METEOR-Berichte 11-2

Climate- biogeochemistry interactions in the tropical ocean of the SE-American oxygen minimum zone

PART 2

Cruise No. 77, Leg 2

November 24, 2008 – December 22, 2008
Callao (Peru) – Guayaquil (Ecuador)

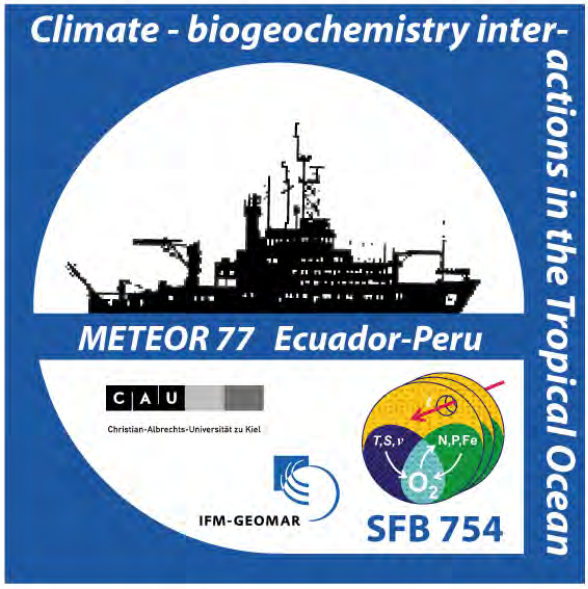

R. Schneider, T. Blanz, F. Block, L. Bohlen, P. Carillo, M. Dibbern, R. Duttmann, C. Ehlert, C. Ferreira, D. Gutierrez, C. Icaza, H. Kawohl, L. Klostermann, S. Kriwanek, G. Leduc, P. Martinez, J. Mallon, E. Mollier-Vogel, T. Mosch, W.-T. Ochsenhirt, A. Petersen, B. Pfannkuche, S. Sommer, H. Sonnabend, P. Tapia, N. Tepe, R. Thomas, M. Türk, K. Wallmann, B. Willie, P. Winterstaller

Table of Contents Part 2 (M77/2) Page

1.1 Participants

Name	Discipline	Institution
Schneider, Ralph, Prof.	Marine Geology	IfG
Blanz, Thomas, Dr.	Organic Geochemistry	IfG
Block, Frederike, stud.	Marine Geology	IfG
Carillo, Paulina	Sedimentology	INOCAR
Bohlen, Lisa	Geochemistry	IFM-GEOMAR
Dibbern, Meike	Technician	IFM-GEOMAR
Duttmann, Rainer, Prof.	Mapping, GIS	IfGeography
Ehlert, Claudia	Isotope Geochemistry	IFM-GEOMAR
Ferreira, Christian	Hydroacoustic Mapping	IFM-GEOMAR
Gutierrez, Dimitri	Marine Geology	IMARPE
Icaza-Galarza, Caroline	Water chemistry	INOCAR
Kawohl, Helmut	Piston coring	Fa. Kawohl
Klostermann, Lars, stud.	Paleoceanography	IFM-GEOMAR
Kriwanek, Sonja	Marine Technology	IFm-GEOMAR
Leduc, Guillaume, Dr.	Paleoceanography	IfG
Martinez, Philippe, Dr.	Isotope Geochemistry	EPOC
Mallon, Jürgen	Micropaleontology	IFM-GEOMAR
Mollier-Vogel, Elfi	Paleoceanography	IfG
Mosch, Thomas	Geochemistry	IFM-GEOMAR
Ochsenhirt, Wolf-Thilo	Meteorology	DWD
Petersen, Asmus	Marine Technology	IFM-GEOMAR
Pfannkuche, Jörn	Marine Technology	IFM-GEOMAR
Sommer, Stefan, Dr.	Geochemistry	IFM-GEOMAR
Sonnabend, Hartmut	Meteorology	DWD
Tapia, Pedro, Dr.	Micropaleontology	IMARPE
Tepe, Nathalie, stud.	Marine Geology	IfG
Thomas, Rüdiger, Eng.	Marine Geology	IfG
Türk, Matthias	Marine Technology	IFM-GEOMAR
Wallmann, Klaus, Prof.	Geochemistry	IFM-GEOMAR
Willie, Bianca,	Mapping, GIS	IfGeography

DWD	Deutscher Wetterdienst
IfG	Institut für Geowissenschaften
IfGeography	Geographisches Institut,
IfM-GEOMAR	Leibniz Labor für Altersbestimmung und Isotopenforschung
IMARPE	Instituto de Mar del Perú
INOCAR	Instituto Oceanógrafico de la Armada del Ecuador
EPOC	Environnements et Paléoenvironnements OCéaniques,
Fa. Kawohl	Marinetechnik Kawohl,

1.2 Research Program

The main goal of Leg M77-2 were paleoceanographic studies for the reconstruction of past atmosphere and ocean climate interactions that could have controlled the behaviour of one of the strongest oxygen minimum zone (OMZ) in the tropical ocean by changing physical and biochemical boundary conditions. In the eastern tropical South Pacific, variations in OMZ conditions are not only sensitive to El Niño Southern Oscillation events, but also to longer-term climate variability. Climate-related changes in surface and sub-surface circulation regimes, including variations in preformed oxygen and nutrient conditions, as well as changes in local upwelling intensity and export production need to be considered when deciphering past fluctuations of OMZ conditions. Overall, the combined system of the Peru Coastal Current, the westward wind drift, and the subsurface Peru-Chile Counter Current maintain the upwelling along the coast. Also the varying supply of well or poorly oxygenated subsurface water masses may play a key role for shaping the extent and intensity of the Peruvian OMZ. The upper boundary of the OMZ is determined by maximum mixed-layer depth, while the lower boundary is regulated by eastward flowing equatorial undercurrents. Under modern conditions the oxygen content along the Peruvian margin ranges from saturated values at the surface to values less than 100 mmol/kg or even less than 10 mmol/kg below 50 meters depth. On average, the Peruvian OMZ is located between 30-70 m and 300-400 m water depth. Leg M77-2 aimed to retrieve new sample material from the water column and Holocene to Last Glacial sediments from the shelf and upper slope to enable a comparison of past variations in the oxygen minimum conditions with changes in local or remote ocean and atmospheric circulation regimes as well as with past fluctuations in the biochemical processes associated with very high productivity and strong oxygen minimum conditions. With this new material, centennial to millennial-scale paleoceanographic studies are planned in the eastern tropical South Pacific from the northern rim of the OMZ at the equator into the central zone off Callao. Herefore past changes in marine productivity and denitrification, upwelling intensity and thermocline depth, intermediate water circulation, insolation, continental aridity and dust flux, as well as trade-wind strength will be estimated. These results should help to relate magnitudes of modern OMZ changes (seasonal or interannual to decadal) with the longer history of OMZ conditions under natural climate forcing.

The paleoceanographic goals were orientated to the three major topics:

1. How have past surface and deeper Pacif-ic ocean biogeochemical conditions varied with respect to temperature (salinity), thermocline structure, and productivity along N-S and E-W gradients inside and outside the tropical OMZ? 2. What was the phasing (leads and lags) between global climate change and biogeochemical variability in the eastern tropical Pacific and associated atmospheric processes? 3. How have remote rapid climate changes during the Holocene and the last Glacial period influenced the development of low oxygen conditions in the eastern tropical Pacific?

The second major goal of Leg M77-2 was the detailed investigation of the benthic biogeochemical processes leading to the exchange of material and fluid fluxes across the bottom water – sediment interface. For this purpose we continued the scientific targets and working programme on the 2 transects perpendicular to the Peruvian coast at 10° and 12° S, that were in the focus of leg M77-1 beforehand.

1.3 Narrative of the Cruise

(R. Schneider)

The detailed schedule of ship operations during Leg M77-2 is given in the station list in the Annex with the cruise track presented here in figure 2.1. Leg M77-2 started at Callao, Lima, 24th November, 2008 after exchange of part of the crew members from CAU Kiel and IFM-GEOMAR and taking onboard 4 scientific observers from Ecuador and Peru. After bunkering overnight outside the harbour, RV METEOR headed southward on Tuesday 25th to about 15°05´ S for hydro-acoustic surveys under the southern centre of the OMZ. The hydro-acoustic survey executed lasted until the 26th in the morning and aimed to map the distribution of Holocene and Last Glacial sediment packages on the outer shelf. Using crossing profiles with the PARASOUND system we identified the centre of sediment accumulation between 250 and 350 m water depth for geological sampling with a multicorer and the Fa Kawohl 15 m long piston corer. Two 13 to 15 m long laminated sediment cores were retrieved, completed by multicorer samples with undisturbed sediment surfaces, and water samples from rosette and CTD hauls. After this southernmost geological sampling station was finished the same day at in the evening, we performed multibeam and PARASOUND surveying before starting the second sampling station at about 12°05´ S off Callao at 210 m water depth. The sampling program at 12°05´ S started November, 27th in the late afternoon and was accomplished at midnight. This station yielded again 2 sediment cores, 13 to 15 m in length, associated with surface sediment and water samples. The rest of the first week was dedicated to finish the bottom lander program at 11°S started already during Leg M77-1. The 3 days program from November, 28th early morning to November, 30th in the evening comprised the launching and retrieval of the different lander systems with three 6 to 10 hours lasting multibeam and echosounder surveys in between. The 24h launching times of the lander systems were used for OFOS video surveys, multicorer surface sediment and CTD/rosette water column sampling. The night from November, 30th to December, 1st was used for geological sampling at 11°05´ S. Here the piston corer deployment failed due to a bended core barrel. The next four days were preferentially used to identify and sample undisturbed and thicker sequences of Last Glacial to Holocene sediments in the northern part of the Peruvian OMZ on transects across the outer shelf and upper slope at 10°45´ S, 09°10´ S, and 08°00´ S. After retrieval of the last lander system on the 11° S transect, the geological sampling program restarted with a hydro-acoustic survey December, 1st in the night at 10°53´ S and went on until December, 2nd early in the morning. It was finished by a hydro-acoustic survey towards 9° S until December, 3rd at noon. Afterwards, geological sampling took place at 2 stations on a transect at 09°17´ S until December, 4th early in the morning, followed by a hydro-acoustic survey and one geological sampling station at 09°03´ S / 79°37´ W. The piston corer was empty due to wash out of the sandy sediment and thus sampling was finished December 4th at midnight on this transect. December, 5th and 6th, were dedicated to the second benthic biogeochemical sampling transect at 08° S, deploying the lander systems and using deployment intervals for water column and surface sediment sampling as well as for OFOS benthic faunal communities and hydro-acoustic surveys at this latitude. December, 7th, was used for performing two geological sampling stations at the 08° S transect and retrieval of the last lander deployed during this cruise. Similar to the southernmost transects, the depositional centres between 11° and 8° were found between 200 and 600 m water depth. At shallower depths no soft sediments of sufficient

thickness were found. At water depths below 1500 m mainly turbidites and slumps were found and thus piston coring was restricted to shallower sites on the outer shelf and upper slope. Here, several 11 to 18 m long sediment cores were retrieved, representing depositional settings from below, within, and at the upper limit of the northern part of the OMZ, with sediments from the OMZ showing distinct mm-scale laminae.

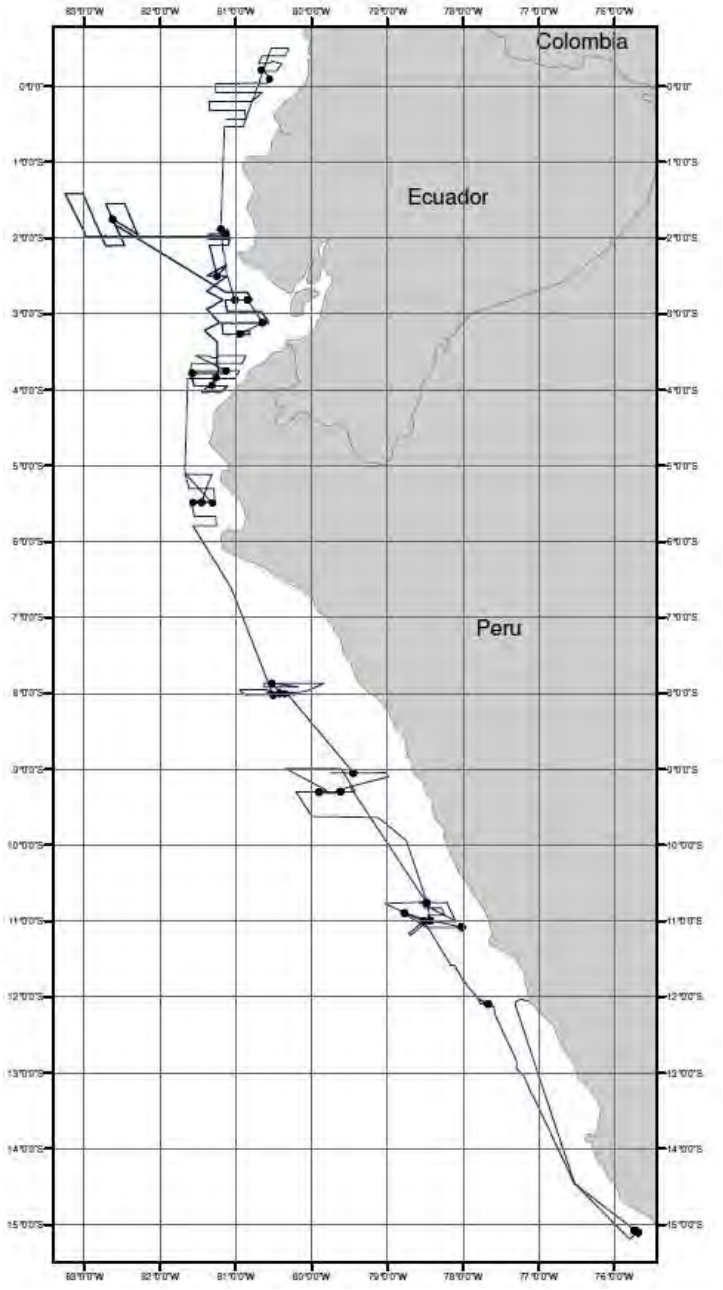

Fig. 2.1: M77-2 cruise track with geological sampling stations

During December, 8th and half of December, 9th we concentrated on extensive hydro-acoustic mapping to search for appropriate coring sites at the narrow shelf and very steep slope between 5°40´ S and 5°10´ S. Geological sampling was then performed at a depth transect at 5°30´S with three stations, deploying CTD, rosette, multicorer and piston corer several times

until the morning of December, 10th. The remaining December, 10th as well as December, 11th and 12th were used for hydro-acoustic surveying, three geological stations plus one deep-water CTD deployment beneath the northernmost rim of the modern OMZ at about 3°50´ S. No laminated sediment sections were found at this latitude on the shelf and outer slope, indicating that the northern limit of the Peruvian upwelling area did not experience oxygen free conditions over the last 20.000 years. The last week of leg M77-2 continued with extensive hydro-acoustic mapping off Ecuador and along the southeastern flank of the Carnegie Ridge west of the deep-sea trench to search for coring sites of Last Glacial to Holocene sediments of several meters in thickness which should serve as archives of past hydrographic and land climate changes in the tropical realm outside the OMZ and coastal upwelling. After 16h of extensive zick-zack hydro-acoustic survey across the upper continental slope until the evening of December 13th to find the deposition centre of the Holocene mud wedge of the Guayas River, a geological sampling station was performed at 2°30´S in the outer Gulf of Guayaquil at 1670 m water depth. No undisturbed, 10 m thick Holocene sediment sequences could be found anymore at these latitudes in shallower water depths. As we had no permit for sampling within the 12 nm of Ecuadorian waters, we could not survey the interior of the Gulf of Guayaquil immediately, but received the permit two days later with the help of the Ecuadorian observers onboard. Therefore we proceeded northward to sample a depth transect 1°55´ S off central Ecuador for reconstruction of past changes in the area of the eastern tropical Pacific surface and subsurface water masses independent from changes in the Humboldt Current during December, 14th. December 15th and 16th were used to survey the Carnegie Ridge at about 01°45´ S and 82°50´ W and to sample the open ocean water column and calcareous sediments not influenced by terrigenous supply and trench turbidites at 2080 water depth. With the permit for the Ecuadorian waters inside the 12 nm zone we could survey and sample the shelf sediments from December 17th early morning to December, 18th early morning. Holocene sediments several meter in thickness could be retrieved at two stations in water depths of about 340 and 430 m while the shelf was void of Holocene hemipelagic muds. Here only surface sediments and water samples could be taken at two stations for studying the river outflow on the sediment composition and paleoceanographic proxies in use. December 19th was needed to reach and survey the northernmost sampling transect just north of the equator for water samples and sediment cores that document hydrographic conditions in the North Equatorial current systems in the eastern tropical Pacific. Unfortunately the PARASOUND system did operate sufficiently during this final part of the survey program and we could sample only one station at 1315 m water depth with the piston corer while a second trial at 290 m failed. With the lack of a fully operating PARASOUND system we stopped the working program December, 20th noon and headed back to the port of Guayaquil, that was reached December, 22nd. The very successful cruise ended with the acquisition of more than 4000 nm of hydro-acoustic mapping and echosounder data, 27 geological piston and multicorer stations, 28 Rosette water sampler stations, and 33 CTD casts along the margins of Peru and Ecuador as well as with 7 stations of in-situ biogeochemical measurements of the benthic boundary layer with different lander systems, 7 OFOS video surveys for benthic communities across the limits of the OMZ, and 27 plankton net hauls in the upwelling off Peru.

1.4 Preliminary Results

1.4.1 Multibeam and Sediment Echosounder Surveys

(C. Ferreira, N. Tepe, P. Wintersteller)

The multibeam mapping surveys during Leg M77-2 were made with the two SIMRAD systems permanently installed on the RV Meteor. Routinely used during all surveys was the EM120 (with 191 beams) designed for best performance at water depths starting at 600 meters until 12.000 meters. The second system used was the EM710 (with 400 beams) designed to operate from 800 meters to shallow waters. The EM120 system was operating 24hrs during the whole cruise, while the EM710 was normally switched on only at water depths shallower than 1000 m. However, due to hardware defects and overheating the EM 170 was operating with only 256 beams and was available only during the first half of M77-2. Therefore the EM120 was operated the whole cruise acquiring multibeam data from deep waters at about 3000 m on the slope and Carnegie Ridge up to 60 meters, the shallowest depth surveyed in the Gulf of Guayaquil.

To reduce interference of the sediment echosounder PARASOUND system with the shallow water EM710 system, we had to reduce the gain of the PARASOUND system from 140mV (maximum) to 100 mV, and the opening angle of the EM710 beams to 80-90°. For the EM120 there were no external interferences, but internal ones, since the central beams showed clearly a “rail”, at water depths lower then 300 meters. The acquired data from the EM710 has a very good spatial resolution, however, it will need extensive post-processing after the cruise before establishing sophisticated maps. The examples given in the cruise report are only using the data from the EM120. During the cruise the pre-processing of the multibeam data was using MB System 5.1.1, included in the operational system Poseidon Linux 3.1. (see example in Fig. XX)Since the data amount was high, MB System was the only option capable to handle this amount of data, and produce reliable maps in a short time for identification of coring locations. The multibeam maps were produced for each coring and biogeochemical sampling transect, based the raw data from the EM120 system. No filtering or cleaning techniques were applied and the grid-size was between 30-40 meters for depths down to 2000 m, and about 50-70 for deeper surveys. At the end of the cruise final storage of the multibeam data was on two external hard discs. The amount of data for the EM120 was 21.3 Gb, and 33.1 Gb for the EM710.

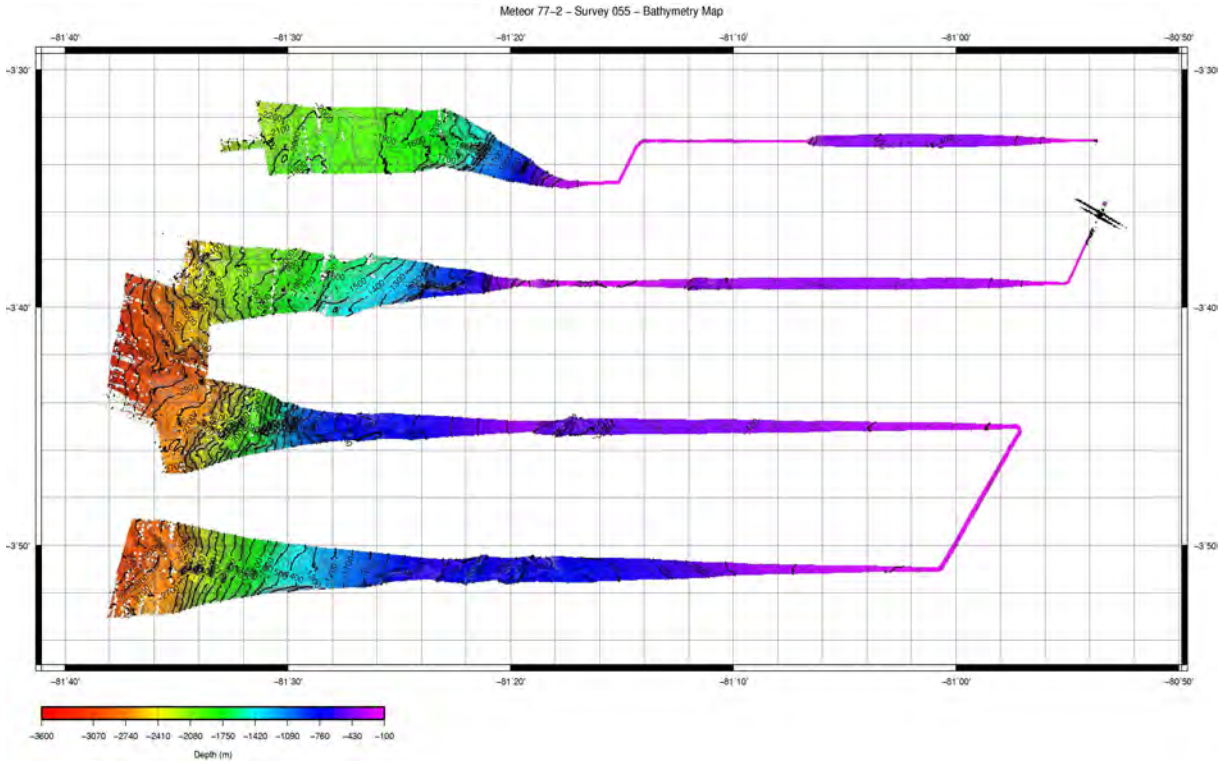

Fig. 2.2: EM 120 survey at 03°50´S for bathymetry mapping and searching for Last Glacial to Holocene sediment depositonal centres.

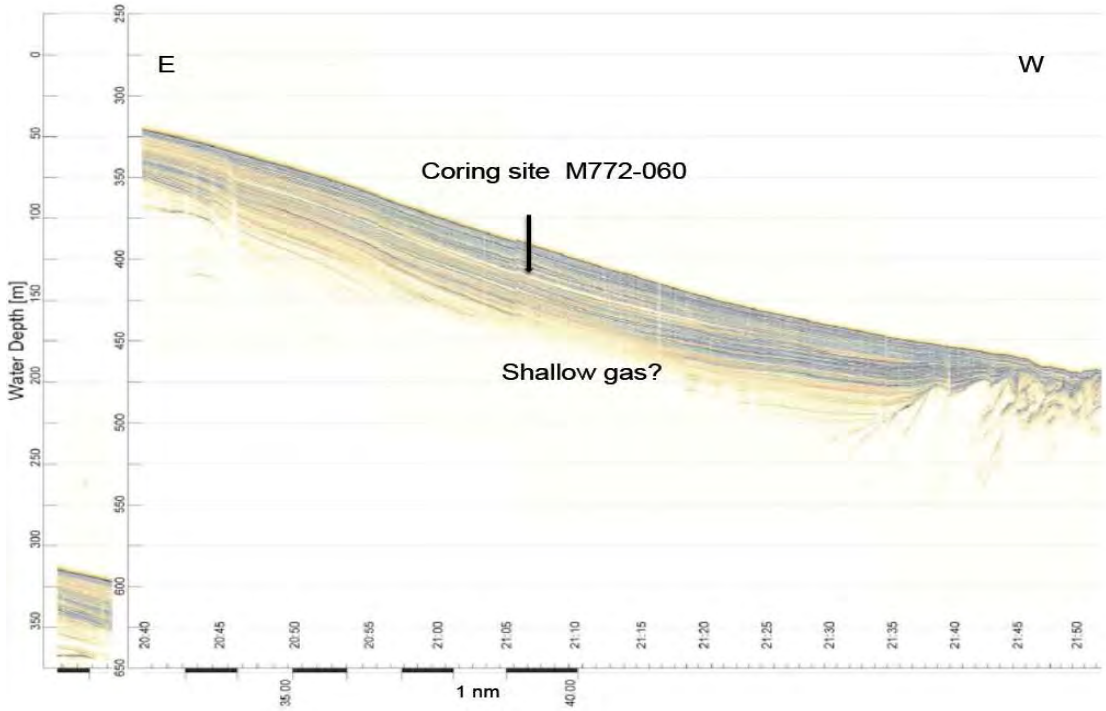

Fig. 2.3: PARASOUND profile at 03°45´ S as an example for enhanced thickness of Late Glacial to Holocene sediments at the shelf break off northern Peru.

The sediment echosounder system PARASOUND was operated by the scientific crew continuously during the ship navigation to ensure fulltime observation and high-resolution information on the uppermost 50 m of sediment structures during the entire cruise. The primary frequency of 18 kHz (PHF) and a second adjustable 18.5-28 kHz signal are generating a parametric secondary frequency of desired 4 kHz (SLF). The primary frequency is used to release the parametric effect and is able to work as well as a narrow beam sediment echosounder. The secondary frequency develops through nonlinear acoustic interaction of the primary waves at high signal amplitudes. This takes place only in the emission cone of the high frequency primary signals which is limited to an aperture angle of only 4° for the PARASOUND DS3. We worked with both single mode and quasi-equidistant transmission mode. In the single pulse mode, the PARASOUND System sends out one pulse and waits until receiving signal. In greater deaths below about 1500m to get a higher resolution of the SLF-signal we switched to the quasi-equidistant transmission mode. The quasi-equidistant transmission mode allows the user to fix a desired-time interval between the sending of pulses. Depending on the water depth the PARASOUND automatically calculates the actual resulting time interval between the pulses and continues with pulsing when no sediment data is received. The main task of the watch-keeper was to adjust the reception window as well as system operating and quality control. The PARASOUND system worked well throughout the survey schedule except for some hardware-problems the last three days of the cruise. After error-analyses done by the scientific technical service aboard (WTD), it turned out that the High-Voltage-Power-Module (HVPM) was not charging correctly so we could not reach a useful transmission voltage. The result was a decreasing S/N (signal to noise) ratio, especially on the SLF-signal. Due to a defect spare HVPM it was not possible to solve the problem. After further repair trials the original HVPM was working again, S/N ratio could be improved but the signal was far from "perfect" as the weeks before the damage. Because of this problem the three days of searching for coring sites were not successful. The entire set of PARASOUND data was stored directly in PS3-format as well as I raw-data-format. For all surveys, PARASOUND sections were plotted with SeNT with a vertical scale of several hundred meters to eliminate most of the changes in window depth. The plots (see example in Fig.2.5) were all saved as PDF-files and used during already during the cruise to identify geological sampling stations.

1.4.2 Water Column Sampling

1.4.2.1 CTD and Rosette

(L. Klostermann, C. Santos Ferreira)

The CTD (Conductivity-Temperature-Depth) based on a pumping system with integrated sensors, that measure conductivity, temperature, density, oxygen and salinity to define different water masses. The CTD used was model SBE 9plus from Seabird connected to a rosette with 24 bottles (also from Seabird, model SBE 32) to collect water samples from defined water masses and from different depths. The CTD's deployments were conducted using a deck unit (again from Seabird, SBE 11plus V2) connect to a PC for real-time acquisition, for both, downcast and upcast, and for firing the bottles at the choosed depths.

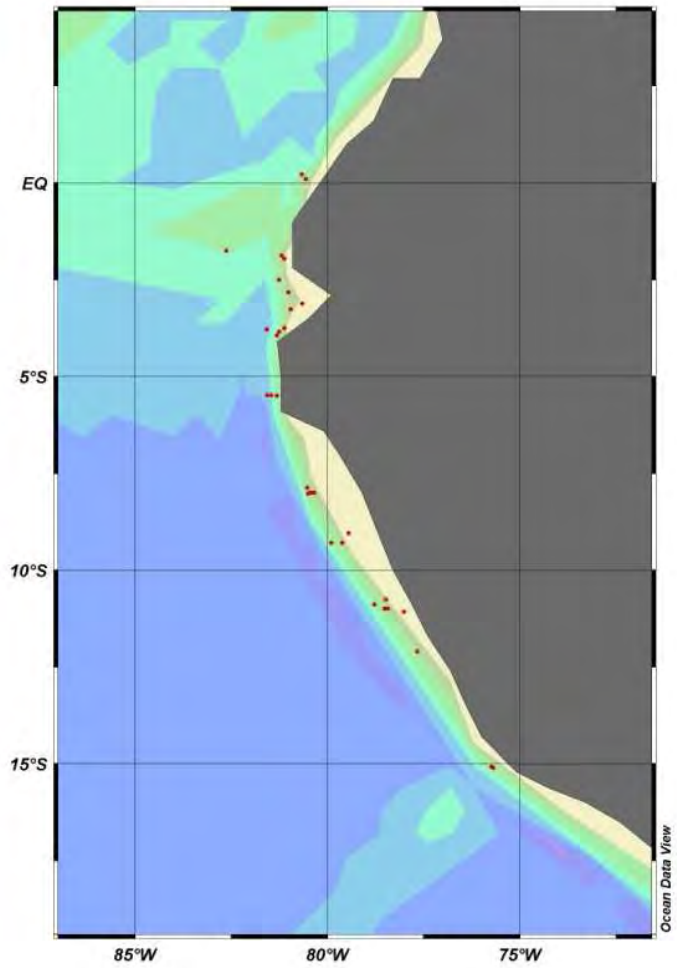

Fig. 2.4: Distribution of the CTD stations (red dots) between 15 and 1° S along the margins of Peru and Ecuador.

The stations were along the cost of Peru and Ecuador, between 15 and 1° S (Fig.2.4). The major objective of the CTD-measurement during this cruise was to get a short overview of the distribution of the oxygen minimum zone (OMZ) in the water column between 5 and 2600m (Fig.2.5). The water was collected through the whole water column for the measurement of stable isotopes ($\delta^{18}O$, $\delta^{13}C$ (DIC) and $\delta^{88/86}Sr$), and the water below the OMZ was collected for the measurement of trace metals. Water close to the surface was collected for analyses of nano- and phytoplankton (D. Gutierrez, P. Tapia) and for TEX86 (T. Blanz). S. Sommer collected the water close to the bottom to measure the dissolved oxygen to calibrate the oxygen sensor from the CTD and to measure the dissoved gases to compare it with the measured data of the lander.

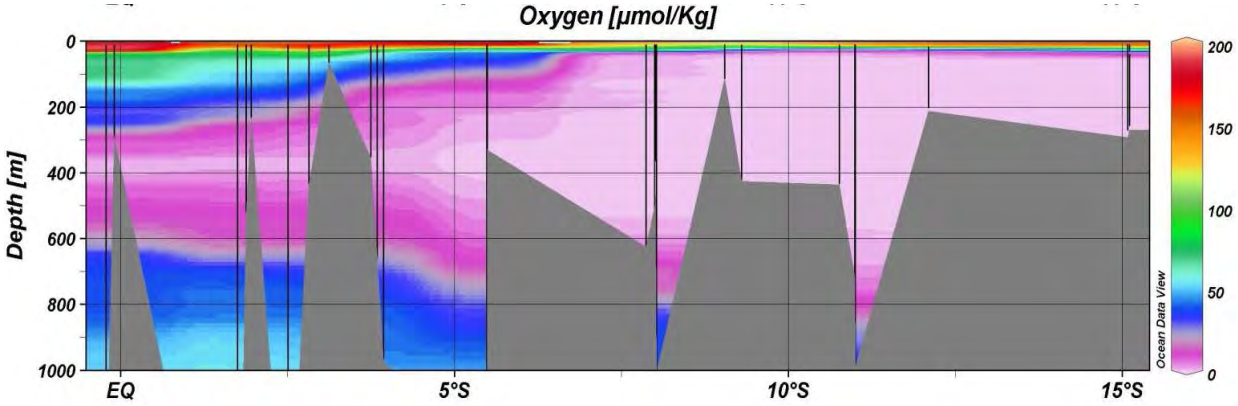

Fig. 2.5: The profile of the OMZ (purple area) along the cost of Peru and Ecuador, its size decreasing to the north.

The collected and produced Data from the CTD Deck unit was converted with „Sea-Bird Electronics (SBE) Data Processing, Version 7.18“ and is plotted with „Ocean Data View (ODV), Version 3.3.2“. The potential temperature, salinity and oxygen were plotted against the depth to characterize the different water masses and to show the variation of the OMZ (Fig. 2.6 and 2.7).

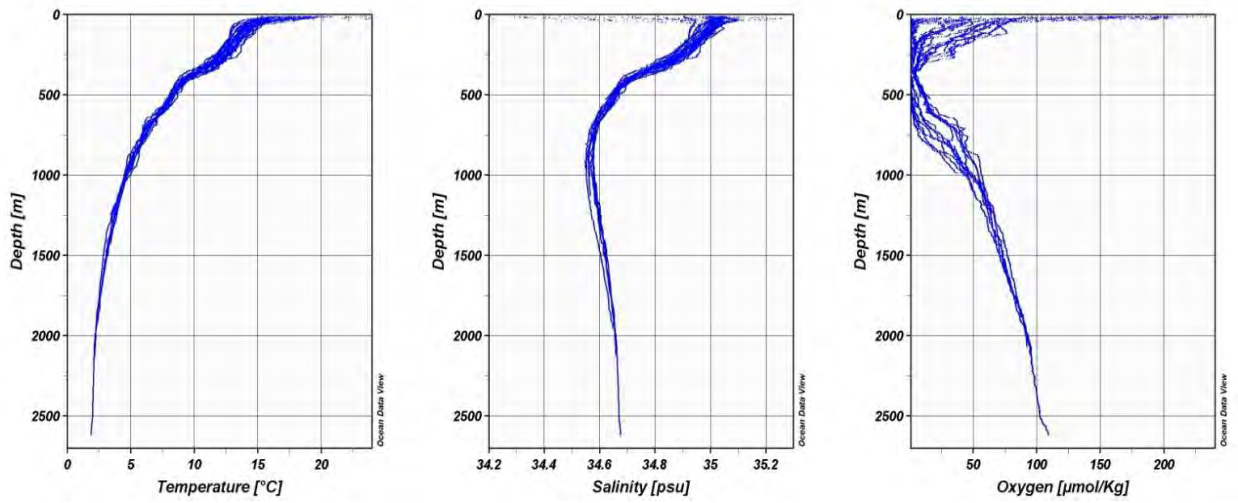

Fig. 2.6: Temperature, salinity and oxygen plotted against the depth, all stations.

During the Meteor-cruise 77-2 we sampled water at varying water depth intervals from water depth ranging between 63 and 2628 m (Tab. 2.1). Once the water sampler was on deck, the water was collected with a tube and was filled in 115 ml glas bottles for the measurement of stable isotopes ($\delta^{18}O$, $\delta^{13}C$ (DIC)). These samples were poisened with 0.2 ml saturated mercuric chloride ($HgCl_2$) and were colsed with a rubby cap, crimped with an aluminium cap and got fixed with Parafilm. The samples for the measurement of $\delta^{88/86}Sr$ were filled in 20 ml PE bottles and were fixed with concentrated HCl (closed with a plastic cap and Parafilm). The sampled water for the measurement of trace metals were filled in 200 ml PE bottles (closed with a plastic cap and Parafilm). The volume of the samples for the analyse of nano- and phytoplankton was 300 ml, for TEX86 it was 1 l and for the gases it was 12 ml.

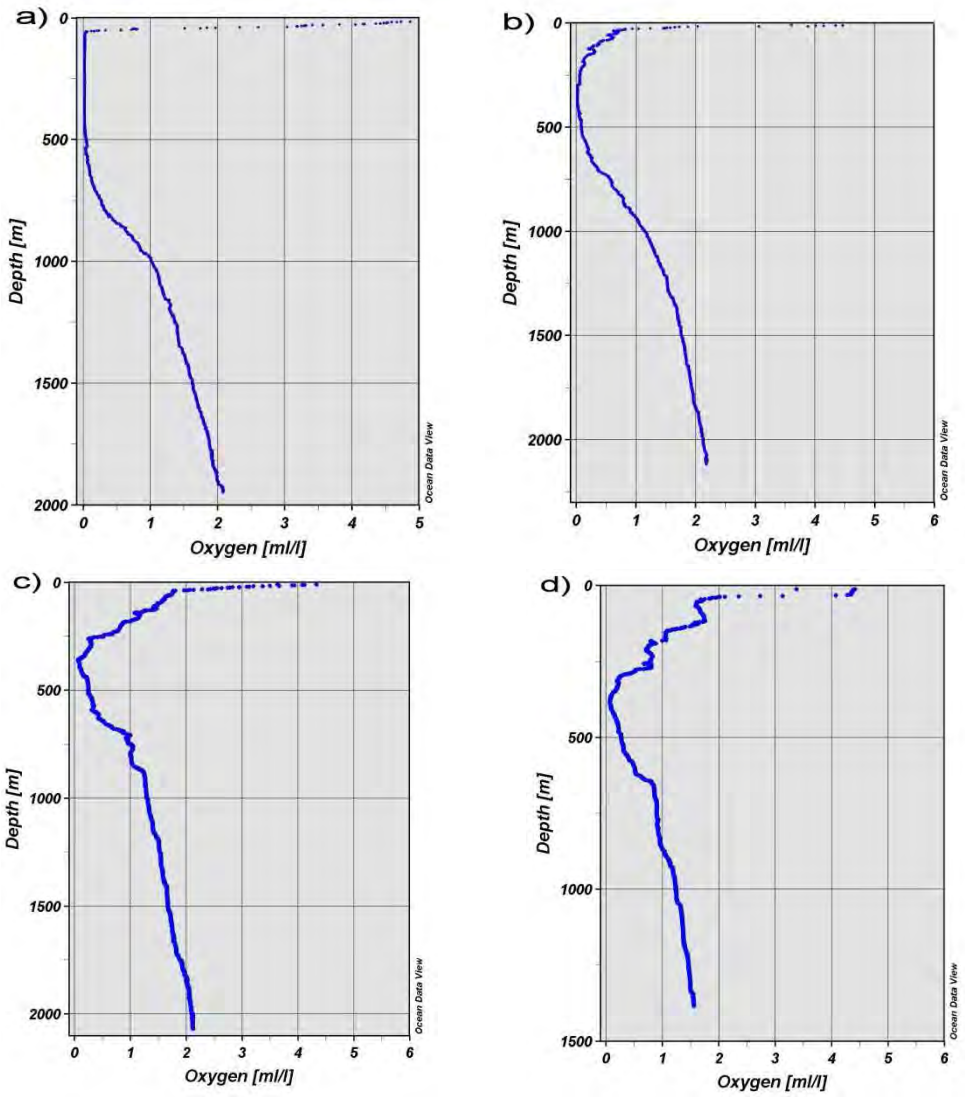

Fig. 2.7: Vertical depths profiles of oxygen concentration levels showing the extent of the OMZ from south to north off Peru and Ecuador
a) Station M772-022, Lat 10°53.65'S, Lon 78°46.33' W;
b) Station M772-053, Lat 5°29.02'S, Lon 81°34.00'W ;
c) Station M772-067, Lat 1°45.14'S, Lon 82°37.48'W ;
d) Station M772-075, Lat 0°12.70'N, Lon 80°39.77'W .

Tab. 2.1: Rosette sampling stations, M77-2.

No.	Date	Coordinates		Depth	Sampling depth (m)
		Lat. (°N)	Long. (°E)	(m)	
2	26.11.2008	15°4.77'S	75°43.97'W	293	296, 60, cabl e problems
3	26.11.2008	15°6.21'S	75°41.28'W	270	265, cable pr oblems
5	27.11.2008	12°5.66'S	77°40.07'W	213	200, 190, 180, 150, 120, 100, 80, 55, 45, 35, 30, 25, 20, 15, 10
8	28.11.2008	11°0.01'S	78°30.91'W	990	990, 900, 800, 700, 635, 556, 455, 300, 200, 100, 40, 30, 20, 10, 5
20	30.11.2008	10°59.75'S	78°25.92'W	716	719, 700, 650, 600, 500, 400, 300, 200, 100, 75, 50, 30, 20, 15, 10, 5
22	01.12.2008	10°53.65'S	78°46.33'W	1957	1970, 1500, 1000, 900, 800, 700, 600, 500, 400, 300, 200, 150, 100, 75, 50, 40, 30, 25, 20, 15, 10, 5
24	01.12.2008	11°5.01'S	78°0.91'W	209	200, 150, 100, 75, 50, 40, 30, 25, 20, 15, 10, 5
26	02.12.2008	10°45.69'S	78°28.54'W	437	435, 300, 200, 150, 100, 75, cable problems
28	03.12.2008	9°18.11'S	79°53.97'W	1137	1135, 1000, 900, 800, 700, 600, 500, 400, 300, 200, 150, 100, 75, 50, 40, 30, 25, 20, 15, 10, 5
29	03.12.2008	9°17.70'S	79°37.11'W	426	no samples
31	04.12.2008	9°02.97'S	79°26.88'W	114	100, 75, 50, 40, 30, 25, 2 0, 15, 10, 5
33	05.12.2008	8°00.03'S	80°25.27'W	503	500, 400, 300, 200, 150, 100, 75, 50, 30, 20, 10, 5
34	05.12.2008	8°00.05'S	80°27.63'W	717	718, 715
36	05.12.2008	8°00.04'S	80°23.46'W	417	420, 300, 200, 150, 100, 7 5, 50, 30, 20
45	07.12.2008	8°00.34'S	80°20.85'W	366	365, 200, 150, 100, 75, 50, 40, 30, 25, 20, 15, 10, 5
47	07.12.2008	7°52.01'S	80°31.36'w	626	no samples
50	08.12.2008	8°01.55'S	80°30.19'W	1007	1000, 900, 800, 700, 600, 500, 400, 300, 200, 150, 100, 75, 50, 40, 30, 25, 20, 15, 10, 5
52	09.12.2008	5°29.01'S	81°27.00'W	1255	1252, 1000, 900, 800, 700, 600, 500, 400, 300, 200, 150, 100, 75, 50, 40, 30, 25, 20, 15, 10, 5
53	09.12.2008	5°29.02'S	81°34.00'W	2594	no samples
54	10.12.2008	5°29.61'S	81°18.41'W	329	330, 200, 150, 100, 75, 50, 40, 30, 25, 20, 15, 10, 5
56	11.12.2008	3°45.00'S	81°07.47'W	355	356, 200, 150, 100, 75, 50, 40, 35, 30, 25, 20, 15, 10, 5
57	12.12.2008	3°47.01'S	81°34.36'W	2628	2628, 200, 1500, 1000, 900, 800, 700, 600, 500, 400, 300, 200, 150, 100, 75, 50, 40, 30, 25, 20, 15, 10, 5
59	12.12.2008	3°56.51'S	81°18.81'W	974	978, 900, 800, 700, 600, 500, 400, 300, 200, 150, 100, 75, 50, 40, 30, 20, 15, 10, 5
60	12.12.2008	3°50.51'S	81°15.41'W	658	no samples
62	14.12.2008	2°30.59'S	81°14.99'W	1685	1690, 1000, 900, 800, 700, 600, 500, 400, 300, 200, 150, 100, 75, 50, 40, 30, 25, 20, 15, 10, 5
64	14.12.2008	1°52.92'S	81°11.70'w	521	525, 400, 370, 300, 200, 150, 100, 75, 50, 30, 20, 10, 5
65	14.12.2008	1°57.29'S	81°07.54'W	227	no samples
67	16.12.2008	1°45.14'S	82°37.48'W	2075	2091, 1500, 1000, 900, 800, 700, 600, 500, cable problems
69	17.12.2008	3°15.79'S	80°57.25'W	369	370, 367, 320, 200, 150, 100, 75, 50, 30, 20, 10, 5
70	17.12.2008	3°07.18'S	80°39.11'W	60	63, 60, 50, 40, 30, 20, 10, 5
72	18.12.2008	2°49.37'S	81°00.72'W	437	435, 300, 200, 150, 100, 75, 50, 40, 30, 25, 20, 15, 10, 5
75	19.12.2008	0°12.70'N	80°39.77'W	1387	1387, 1377, 1100, 900, 800, 700, 600, 500, 400, 300, 200, 150, 100, 75, 50, 30, 20, 10, 5
76	19.12.2008	0°05.44'N	80°33.39'W	291	5

1.4.2.2. Plankton net Tows

(P. Tapia, D. Gutierrez)

One objective of the Peruvian scientists onboard during Leg M77-2, was the collection of plankton and surface sediment samples from the Peruvian margin to better understand biogenic proxies (e.g. diatoms, forams, fish scales) in the sedimentary record. In order to achieve this goal, one major activity was to take a systematic collection of phytoplankton with a simple portable plankton net device made of 10 µm mesh Nytal® fabric. One or two vertical plankton net deployments in the upper 30-m of water column were taken at each geological sampling station. A total of 27 plankton net samples was taken from 15º S to the equator (0º 12.7'N), covering a large latitudinal gradient (Tab. 2.2), and water masses from coastal upwelling, into subtropical and tropical surface water masses (Fig. 2.8).

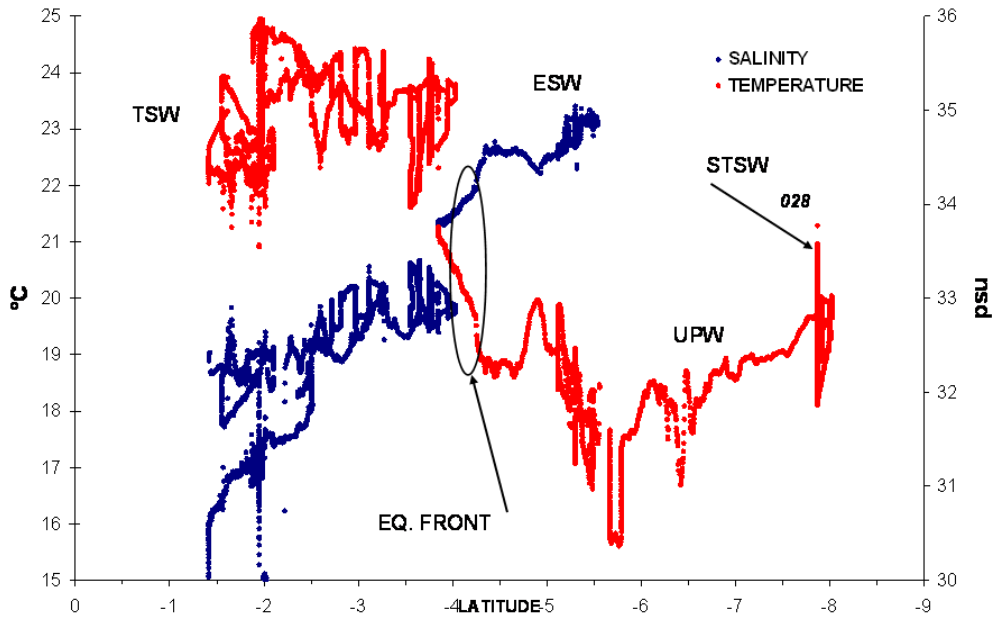

Fig. 2.8: Surface water masses distribution during the northward track of leg M77-2. according the shipboard thermosalinograph data. Data excursions at distinct latitudes correspond to onshore/off-shore transects. All stations located south of 5° S, indicate upwelling waters (UPW), except station M77-2-028 that has subtropical waters (STSW). North of 5º S tropical surface waters (TSW) prevailed. The equatorial front was observed around 4°S.

Tab. 2.2: Handnet stations of METEOR cruise M77-2, collected by IMARPE

Station Nº	Date	Time (UTC)	Latitude	Longitude	Water Depth (m)	Tows
M772-003-1	11/26/2008	17:00	15°06.21'S	75°41.28`W	271	2
M772-005-	11/27/2008	23:45	12°05.66'S	77°40.07`W	214	1
M772-014-	11/29/2008	13:45	11°00.02'S	78°31.16'W	1004	2
M772-016-	11/29/2008	21:35	10°59.80'S	78°05.91'W	259	1
M772-020-	11/30/2008	15:30	10°59.76'S	78°25.92'W	717	1
M772-024-	12/1/2008	14:20	11°05.01'S	78°00.91'W	207	1
M772-026-	12/1/2008	2:30	10º45.13'S	78º28.43'W	424	1
M772-028-	12/3/2008	19:40	09°18.11'S	79°53.97'W	1141	1
M772-029-	12/3/2008	23:35	09°17.70'S	79°37.11'W	426	2
M772-031-	12/4/2008	16:20	09°02.97'S	79°26.88'W	114	1
M772-045-	12/7/2008	1:45	08°00.34'S	80°20.85'W	365	2
M772-047-	12/7/2008	15:30	07°52.01'S	80°31.36'W	627	2
M772-050-	12/8/2008	1:00	08°01.55'S	80°30.19'W	1244	2
M772-052-	12/9/2008	12:00	05°29.00'S	81°27.00'W	1251	1
M772-053-	12/9/2008	23:30	05°29.02'S	81°43.00'W	2589	2
M772-054-	12/10/2008	4:45	05°29.61'S	81°18.41'W	329	2
M772-056-	12/11/2008	20:30	03°44.99'S	81°07.47'W	355	2
M772-059-	12/12/2008	18:00	03°56.48'S	81°18.83'W	973	2
M772-060-	12/12/2008	23:15	03°50.51'S	81°15.50'W	661	2
M772-062-	12/14/2008	1:45	02°30.50'S	81°14.97'W	1671	2
M772-064-	12/14/2008	18:00	01°52.93'S	81°11.70'W	524	2
M772-067-	12/16/2008	14:20	01°45.65'S	82°37.43'W	2082	2
M772-069-	12/17/2008	20:30	03°15.82'S	80°57.29'W	372	2
M772-070-	12/17/2008	23:30	03°07.16'S	80°39.13'W	60	2
M772-072-	12/18/2008	6:32	02°49.37'S	81°00.75'W	437	2
M772-075-	12/19/2008	18:20	00°12.70'N	80°39.77'W	1381	2
M772-076-	12/19/2008	22:15	00°05.44'N	80°33.40'W	288	2

1.4.3 Sediment Sampling

1.4.3.1 Lander Operation and Ocean Floor Observation (OFOS)

(S. Sommer, T. Mosch, S. Kriwanek, A. Petersen, B. Pfannkuche, M. Türk)

Major goal was to determine and to quantify the effect of different oxygen/redox regimes on the speciation and in situ magnitude of nitrogen fluxes (N_2, NO_3^-, NO_2^-, NH_4^+), Fe_2^+, PO_4^{3-}, O_2, and SO_4^{2-} across the sediment water interface at the Peruvian continental margin underlying an extended oxygen minimum zone. Further goal was to achieve a regional estimate of the sink function of the benthic boundary layer for fixed N based on in situ fluxes and pore water geochemistry in correlation with bathymetry, para sound and image data from camera sledge deployments, OFOS.

Current estimates of mass transfer rates of total nitrogen indicate that sources (riverine- and atmospheric input, bacterial and anthropogenic N-fixation; 287 Tg N yr^{-1}; Tg = 1012g) and sinks (burial in sediments, denitrification; 482 Tg N yr^{-1}) are out of balance implying a large deficit of 195 Tg N yr^{-1} (Codispoti et al. 2001). Despite novel pathways of nitrogen turnover have been discovered (cf. Hulth et al. 2005, Brandes et al. 2007) it is still elusive whether the present day estimates of fixed N input needs an upward revision or whether the oceanic N cycle is far from steady state (Codispoti 2001). In comparison to the water column our knowledge about sedimentary nitrogen metabolism in continental margin sedimentary environments is scant. Rate estimates of single processes of the sedimentary nitrogen metabolism are based on diagenetic models of pore water gradients and models of benthic solute exchange (Middelburg et al. 1996) rather then on direct measurements (cf. Devol 1991). For the Santa Barbara Basin, Sigman et al. (2003) suggested that the loss of nitrate in the sediments is 3-times larger than in the overlying water column.

To carry out in situ flux measurements different types of benthic landers were deployed (see below). A total of 6 lander deployments were conducted during M77-2 (Table XX). BIGO 6, BIGO T6 and Profiler 4 were deployed to fill gaps on a transect at 11° S spanning a depth range of 80 to ~1300 m. This transect was the major working area for lander deployments also during leg M77-1 before. BIGO 8, BIGO T7 and Profiler 5 were deployed at a northern station at 8° S. All lander deployments were successful and allowed determination of benthic fluxes. Furthermore detailed visual investigations of the seafloor were conducted to resolve specific features, e.g., fauna, microbial mats, sediment facies, which can be related to benthic nutrient, and N_2/Ar as well as oxygen fluxes.

Tab. 2.3: Station list M77-2 for Lander and OFOS Surveys

M77_2_005-2	CTD_3	27.11.2008	12°5.66´S	77°40.07´W	18:18	2 13	
M77_2_008-01	CTD_4	28.11.2008	11°0.01´S	78°30.91´W	14:40	1000	
M77_2 699	CTD_11	05.12.2008	8°0.026´S	80°25.268´W	00:24	5 02	
M77_2 701	CTD_12	05.12.2008	8°0.05´S	80°27.63´W	02:01	732	
M77_2_69_4	CTD_29	17.12.2008	3°15.816´S	80°57.286´W	19:3 0	372	
M77_2_70_3	CTD_30	17.12.2008	3°7.16´S	80°39.13´W	23:16	60	
M77_2_75_4	CTD_33	19.12.2008	0°12.698´N	80°39.776´W	16:3 5	1387	
M77_2 653	BIGO_6	28.11.2008	11°0.009´S	78°30.94´W	13:02	990	deployment
M77_2 655	Profiler_4	28.11.2008	11°0.00´S	78°27.28´W	18: 28	797	deployment
M77_2 656	BIGO T_6	28.11.2008	11°0.011´S	78°5.856´W	22:2 6	254	deployment
M77_2 659	BIGO_6	29.11.2008	10°59.82´S	78°31.07´W	13:03	990	recovery
M77_2 661	Profiler_4	29.11.2008	10°59.75´S	78°27.39´W	18 :13	796	recovery
M77_2 662	BIGO T_6	29.11.2008	10°59.80´S	78°05.91´W	22:0 2	259	recovery
M77_2 664	BIGO_7 Cal	30.11.2008	10°59.75´S	78°25.92´W	1 3:18	718	calibration
M77_2 666	BIGO_7	30.11.2008	10°59.75´S	78°25.93´W	18:30	716	deployment
M77_2 678	BIGO_7	01.12.2008	10°59.47´S	78°26.10´W	17:18	7 16	recovery
M77_2 705	BIGO_8 Cal	05.12.2008	8°0.011´S	80°25.785´W	13 :41	530	calibration
M77_2 707	BIGO 8	05.12.2008	8°0.049´S	80°23.459´W	19:15	4 18	deployment
M77_2 708	BIGO_T_7	05.12.2008	8°0.048´S	80°23.582´W	21: 25	420	deployment
M77_2 712	Profiler_5	06.12.2008	8°0.012´S	80°27.581´W	14 :32	699	deployment
M77_2 714	BIGO_T_7	06.12.2008	7°59.73´S	80°23.80´W	19:24	426	recovery
M77_2 725	BIGO_8	07.12.2008	7°59.96´S	80°23.64´W	19:36	42 2	recovery
M77_2 726	Profiler_5	07.12.2008	7°59.79´S	80°27.77´W	20: 36	679	recovery
M77_2 651	OFOS_35	28.11.2008	11°35.01´S	78°06.52´W	04:30	469	at bottom
M77_2 651	OFOS_35	28.11.2008	11°35.01´S	78°09.45´W	08:45	559	off bottom
M77_2 657	OFOS_36	29.11.2008	10°45.01´S	78°13.00´W	00:54	251	at bottom
M77_2 657	OFOS_36	29.11.2008	10°45.02´S	78°12.28´W	02:04	242	off bottom
M77_2 663	OFOS_37	30.11.2008	10°45.01´S	78°34.54´W	01:58	657	at bottom
M77_2 663	OFOS_37	30.11.2008	10°45.02´S	78°31.77´W	05:30	494	off bottom
M77_2 703	OFOS_38	05.12.2008	8°0.03´S	80°26.45´W	05:33	56 8	at bottom
M77_2 703	OFOS_38	05.12.2008	8°0.00´S	80°23.86´W	08:44	43 0	off bottom
M77_2 704	OFOS_39	05.12.2008	8°0.01´S	80°18.01´W	10:26	28 4	at bottom
M77_2 704	OFOS_39	05.12.2008	8°0.01´S	80°17.00´W	11:54	25 5	off bottom
M77_2 709	OFOS_40	05.12.2008	8°0.00´S	80°19.57´W	22:59	34 0	at bottom
M77_2 709	OFOS_40	06.12.2008	8°0.00´S	80°18.00´W	01:16	28 4	off bottom
M77_2 710	OFOS_41	06.12.2008	8°0.01´S	80°28.40´W	03:43	83 1	at bottom
M77_2 710	OFOS_41	06.12.2008	8°0.01´S	80°26.37´W	06:38	56 4	off bottom

Benthic chamber lander, BIGO & BIGO T

BIGO and BIGO T represent benthic chamber lander, which were equipped with 2 and 1 benthic flux chamber respectively. The functional principle of this lander type was described by Pfannkuche & Linke (2003) and Sommer et al. (2006, 2008). BIGO and BIGO T retrieve water samples from the bottom contact water as well as sediments. Geochemical measurements in the sediments include the following parameters: O_2, SO_4^{2-}, HS^-, NO_3^-, NO_2^-, NH_4^+, PO_4^{3-},Fe_2^+, Si, Br^-, I^-, trace metals, total alkalinity, the determination of physical properties of the sediment as well as the sediment C/N ratio, content of plant pigments and

meiofauna. Geochemical parameters that will be measured in the bottom water include O_2, N_2, Ar, N-compounds, PO_4^{3-}, Si, SO_4^{2-}, trace metals, and physical parameters (temperature, density, salinity).

Profiler

A novel prototype of profiler for micro-sensor measurements was deployed successfully at 11°S and 8° S in water depths of 797 and 699 m respectively, Fig. 2.9.The profiling unit consists of lower and upper glass fibre frames, which are connected by four glass fibre poles. The upper frame extends about 50 cm towards the front defining an area across which sensors can be moved in mm increments along the x and the y-axis. Along the vertical z-axis, the sensors can be moved at freely selectable increments. The rear part of the profiler houses four battery packs, the data logging- and the control unit steering the movements of the micro sensors. For the deployment the profiling unit was mounted into a lander.

Fig. 2.9: Novel prototype of a profiler to conduct micro-scale spatial measurements of oxygen, sulfide and ph in sediments. Profiler is mounted within a benthic lander.

Commercially available oxygen micro sensors (tip diameters: ~ 100 µm. Unisense, DK) were used to measure in-situ oxygen concentration profiles, Figure 2. The sensors (A) were connected to miniaturized amplifier units (C) which were jointly developed with UNISENSE, DK. The connecting steel tube (B) was filled will silicone oil, pressure compensation of the sensor was allowed by the transparent flexible tubing shown in Fig. 2.10.

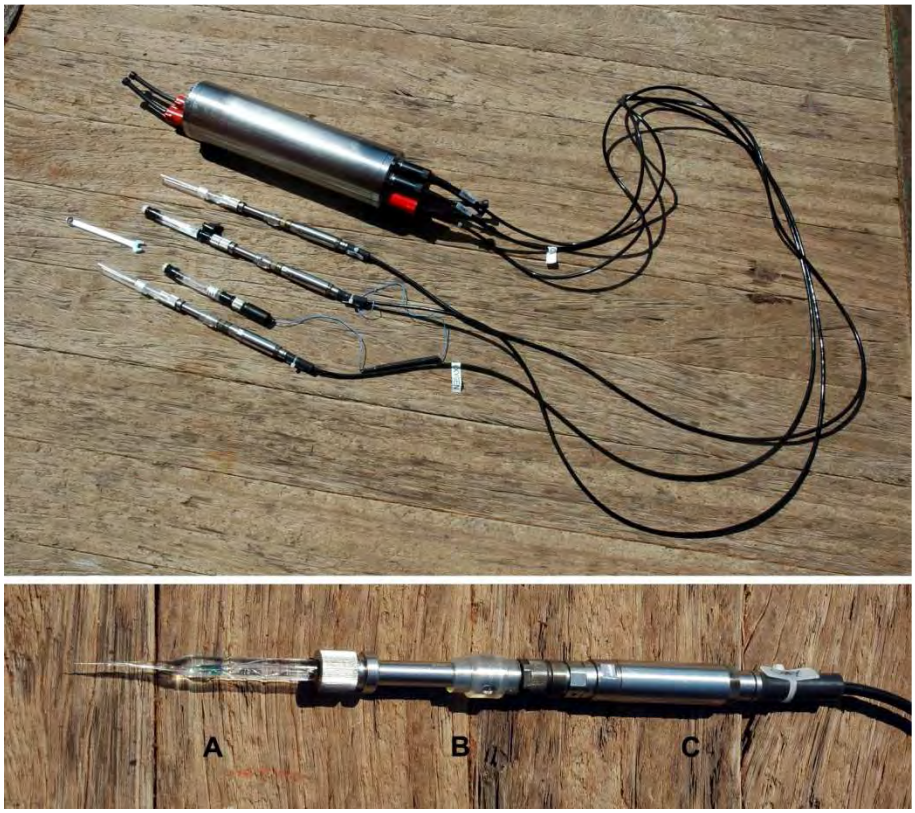

Fig. 2.10: upper panel, in situ micro-sensors connected to the data logging unit; lower panel, detail of in situ O_2 micro-sensor (A) connected to the amplifier (C) via an oil filled steel tube (B).

Ocean Floor Observation System, OFOS

The OFOS used during this cruise is a video sled and consists of a stainless steel frame, Fig. 1.1.It carries the video telemetry, 1 video camera, 2 Xenon lights (OKTOPUS), a still camera with flash light (Benthos) and a storage CTD (RBR: salinity, temperature, O_2 via 2 AANDERAA optodes, turbidity). A small weight is carried about 1.5 m below the sled as a reference point for the winch driver and scale for the images taken during the tow of the instrument. Furthermore 2 laser pointers were deployed to project two reference points 50 cm apart from each other on the seafloor for latter image analysis. A third laser projection provides information about the distance between still camera and the sea floor. During each deployment pictures were taken every 1 min. Position of the OFOS in comparison to the ship position was recorded using the POSIDONIA system.

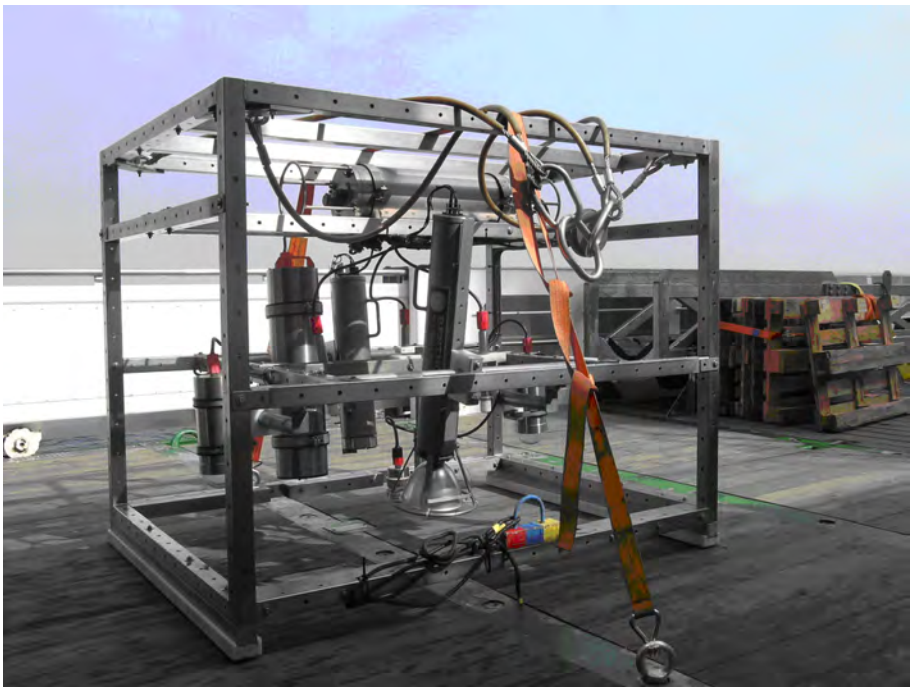

Fig. 2.11: Ocean floor observation system (OFOS)

Preliminary Results

Benthic chamber lander BIGO, BIGO T

All lander deployments were successful, however during BIGO T 7 and BIGO 8 (chamber 2) the chambers did not retrieve sediments due to coarse sediments blocking the shutter which drives underneath the chamber. Based on these deployments in situ fluxes of N_2/Ar, O_2 (cf. Fig. 2.12. 2.13) as well as nitrogen species, phosphate and silicate will be determined.

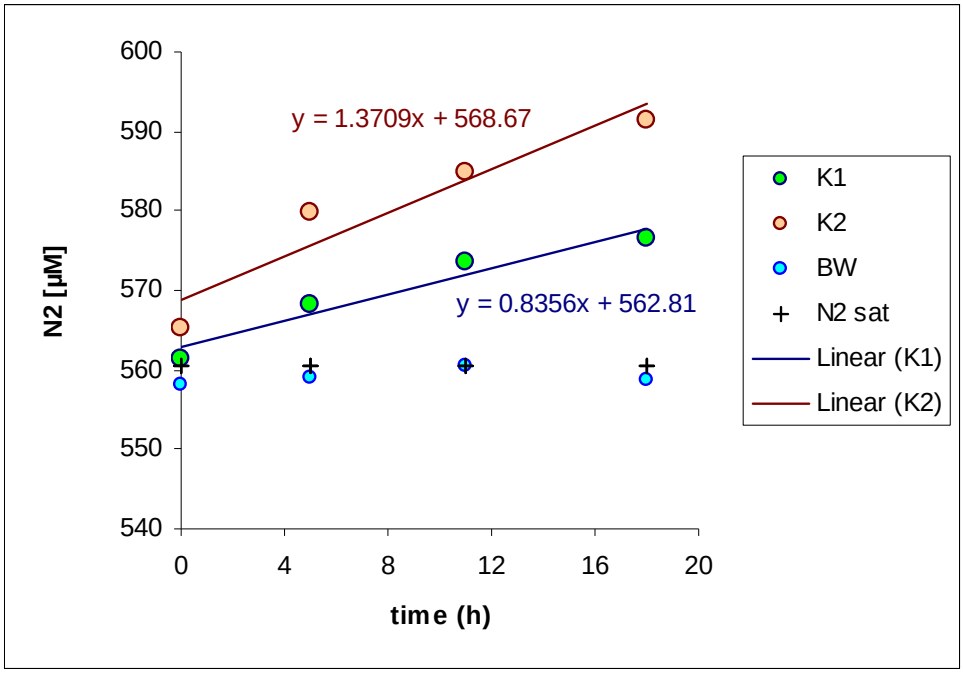

Fig. 2.12: Concentration of di-nitrogen over time in the benthic chamber 1 and 2 (K1, K2) and in the bottom water (BW) in comparison the saturated N_2 content for the respective temperature and salinity (N2 sat).

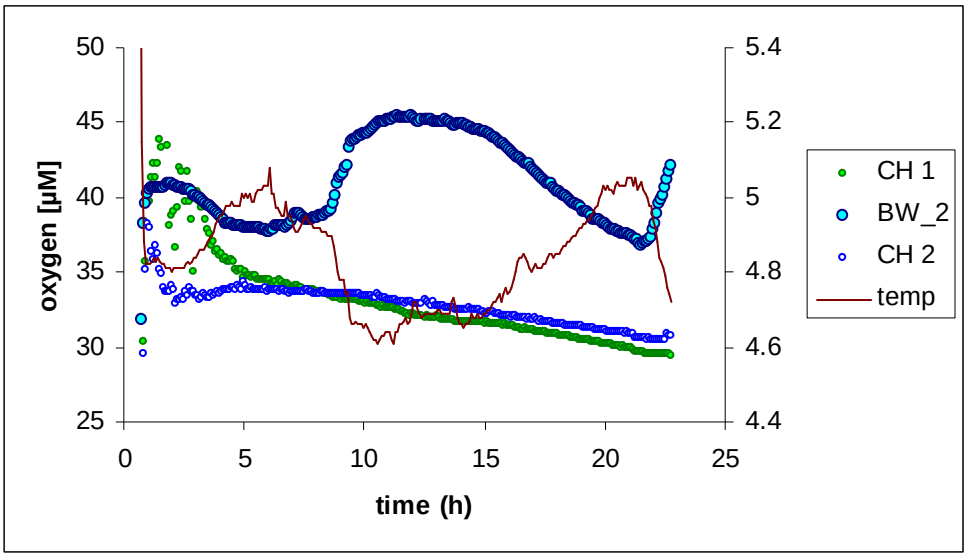

Fig. 2.13: Concentration of oxygen over time in the benthic chamber 1 and 2 (CH 1, CH 2) and in the bottom water (BW_2) measured using Aanderaa optodes. Changes of temperature during the deployment are indicated.

Profiler

The profiler deployments at the 11° S transect and the 8° S station were successful. During both deployments two oxygen micro sensors conducted 22 profiles along the x-axis at increments of 40 mm. At about 800 m depth at the 11° S transect the oxygen penetrated ~ 2.2 to 4.4 mm deep into the sediment, Fig. 2.14.The oxygen concentration within the overlying water body varied between 9 and 15 µM. Further profiler measurements were conducted during M77-1 at the 11° S transect at 1000, 800 and 780 m water depths and will contribute to understand the oxygen dynamics at the lower fringe of the oxygen minimum zone.

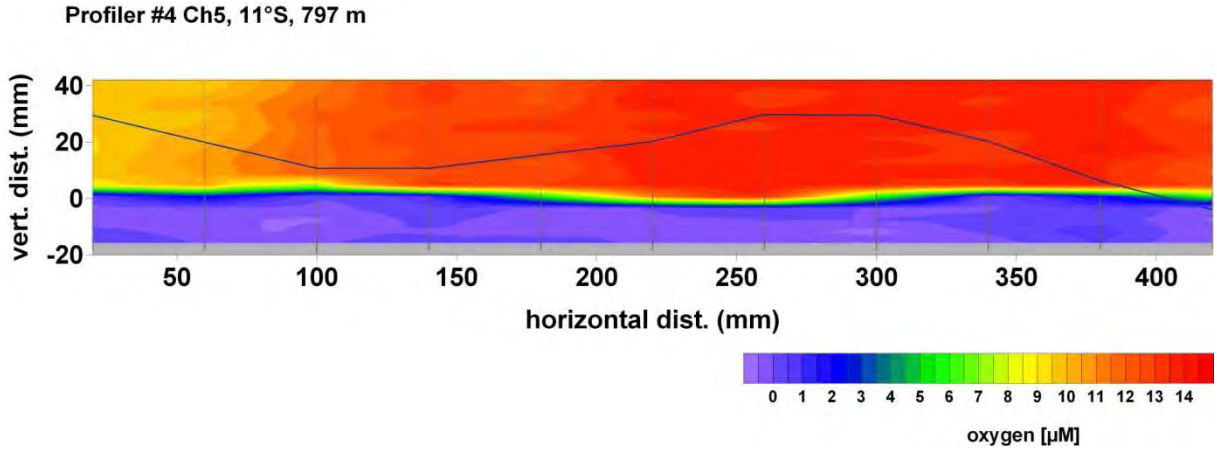

Fig. 2.14: Oxygen distribution in the sediment and the overlying water body. Contour plot is based on 11 micro-profiles, their positions are indicated by thin lines.

Ocean Floor Observation

Seven tracks were conducted in several regions along the continental margin of Peru (see Tab. 2.3). Distinct faunal and lithological features on the seafloor were resolved which might be related to benthic fluxes. Key organisms include extended bacterial mats, Fig. 2.15, and dense accumulations of Ophiuroidea.

Fig. 2.15: Extended bacterial mats, presumably *Beggiatoa*, in a water depth of 150 m within the oxygen minimum zone.

1.4.3.2 Pore Water Geochemistry

(K. Wallmann, L. Bohlen, M. Dibbern, C. Ehlert)

The initial results presented in this report address the biogeochemical turnover in surface sediments and the fluxes of dissolved nutrients and other species across the sediment-water interface (SWI) under contrasting oxygen conditions. Samples were taken with the multi-corer (MUC), piston corer (PC), the benthic chamber (BIGO), and the CTD and are listed in Tab.2.4.

Tab. 2.4: List of stations sampled for geochemical analysis during M77-2. Temperatures, salinities and oxygen concentrations at the seafloor were taken from CTD measurements in ambient bottom waters.

Station M772-	Date 2008	Gear	Lat. S	Long. E	Water depth (m)	T (°C)	Sal.	O_2 (µM)
002-4	26.11.	MUC	15°04.75'S	75°44.00'E	290	12.3	34. 9	1.0
002-6	26.11.	PC	15°04.75'S	75°44.00'E	285	12.3	34.9	1.0
003-2	26.11.	PC	15°06.21'S	75°41.28'E	271	12.2	34.9	1.1
005-1	27.11.	PC	12°05.64'S	77°39.91'E	209	12.5	34.9	1.1
005-4	27.11.	MUC	12°05.66'S	77°40.07'E	213	12.5	34. 9	1.1
013	29.11.	BIGO	10°59.82'S	78°31.05'E	978	4.8	34.6	36.5
016	29.11.	BIGO-T	10°59.80'S	78°05.91'E	259	11.7	34 .9	1.1
022-3	01.12.	MUC	10°53.22'S	78°46.38'E	1933	2.3	34. 6	93.0
025	01.12.	BIGO	10°59.47'S	78°26.10'E	716	6.4	34.6	6.4
026-3	02.12.	MUC	10°45.13'S	78°28.43'E	424	9.1	34.7	1.1
028-2	03.12.	MUC	09°17.69'S	79°53.86'E	1107	4.3	34. 6	52.6
029-4	04.12.	MUC	09°17.70'S	79°37.11'E	433	9.0	34.7	1.2

Station M772-	Date 2008	Gear	Lat. S	Long. E	Water depth (m)	T (°C)	Sal.	O_2 (µM)
031-2	04.12.	MUC	09°02.97'S	79°26.88'E	114	13.4	35. 0	1.1
044	06.12.	BIGO-T	07°59.73'S	80°23.80'E	426	9.0	34. 7	1.2
045-2	06.12.	MUC	07°59.99'S	80°20.51'E	359	10.2	34. 8	1.1
047-3	07.12.	MUC	07°52.01'S	80°31.36'E	625	7.2	34.6	3.2
049	07.12.	BIGO	07°59.79'S	80°27.77'E	679	7.1	34.6	3.8
050-1	07.12.	MUC	08°01.04'S	80°30.13'E	1013	4.7	34. 6	44.1
052-3	09.12.	MUC	05°29.01'S	81°27.01'E	1252	3.5	34. 6	68.6
053-1	09.12.	MUC	05°28.94'S	81°34.03'E	2607	2.2	34. 7	97.1
054-2	10.12.	MUC	05°29.01'S	81°18.35'E	297	11.6	34. 9	2.8
056-2	11.12.	MUC	03°45.02'S	81°07.26'E	349	10.4	34. 8	4.2
059-2	12.12.	MUC	03°56.95'S	81°19.16'E	995	5.0	34.6	66.2
060-1	12.12.	MUC	03°51.09'S	81°15.49'E	701	6.1	34.6	33.5
062-2	13.12.	MUC	02°30.01'S	81°14.71'E	1678	2.7	34. 6	81.3
062-4	14.12.	CTD	02°30.50'S	81°14.97'E	1671	2.7	34. 6	81.2
064-2	14.12.	MUC	01°53.49'S	81°11.75'E	525	7.8	34.6	16.9
065-2	14.12.	MUC	01°57.01'S	81°07.23'E	206	13.3	34. 9	29.2
067-2	16.12.	MUC	01°45.14'S	82°37.47'E	2075	2.2	34. 7	95.7
069-1	17.12.	PC	03°16.00'S	80°56.86'E	338	11.4	34.8	5.9
069-2	17.12.	MUC	03°16.02'S	80°56.87'E	339	11.4	34. 8	5.9
071-1	18.12.	MUC	02°48.99'S	80°50.72'E	100	14.7	35. 0	54.3
072-1	18.12.	MUC	02°49.00'S	81°00.53'E	427	9.0	34.7	7.8

Short sediment cores retrieved with the multicorer were transferred into the cold room immediately after retrieval. The cores were cut within a glove bag under argon atmosphere to prevent oxygenation of pore fluids and sediments. Within the glove bag, the cores were cut into 1 - 3 cm thick slices and the sediment segments were transferred into centrifugation tubes pre-flushed with argon gas. Further sub-samples were given into argon-flushed glass vials for later analysis of solid phase iron, sulfur and phosphorus speciation. Additional sub-samples were taken for the determination of physical sediment properties. Sediment-filled centrifugation tubes were closed tightly and the pore water was separated by centrifugation. After centrifugation, the tubes were again transferred into the glove bag and the supernatant was filtered through 0.2 µm membrane filters. Aliquots of the filtered pore water were given into plastic vials filled with ascorbic acid for later ferrous iron analysis. Subsequently, the glove bag was opened and the pore water samples were processed in the laboratory.

Additional bottom water samples and surface sediments were recovered with the bottom lander (BIGO). Glass syringes were used to take water samples at the seafloor from the

bottom waters enclosed by the benthic chamber. Aliquots from each syringe sample were analyzed in the on-board laboratory. Surface sediments retrieved by the benthic chamber were processed in the same way as described above for the multi-corer sediments.

Aliquots were taken from each pore water and bottom water sample for shore-based analysis. 2 ml of water were given into acid-cleaned plastic vials and acidified with supra-pure HNO_3 for ICP-OES analysis, 1.8 ml were given into plastic vials for ion-chromatograph, 1 ml was separated and stored in glass vials for isotope analysis, 2 ml of water were poisoned with $HgCl_2$ solution and stored in gas-tight glass vials for $\delta^{13}C$ analysis, and two more milliliters of sample were given into acid-cleaned plastic vials and acidified with supra-pure HNO_3 for ICP-OES analysis.

During the last two BIGO deployments (stations M772-044 and M772-059), water samples from the benthic chambers were given directly from the glass syringes into plastic vials containing 30 µl of concentrated HNO_3 (supra-pure) for later ICP-MS analysis immediately after retrieval of the BIGO to prevent any loss of iron caused by oxygen exposure during sample splitting and handling.

On-Board Chemical Analysis

Water samples were analyzed for dissolved silica (H_4SiO_4), phosphate (TPO_4), nitrite (NO_2^-), ammonium (NH_4), sulfide (TH_2S), and ferrous iron (Fe^{2+}) using standard photometric procedures. Total alkalinity (TA) was determined by titration with 0.02 M HCl and dissolved nitrate (NO_3^-) by ion chromatography. Nitrate values presented in this report do not include nitrite but represent the nitrate concentration, only, because nitrite has separated from nitrate on the ion chromatographic column. Selected samples were also analyzed for dissolved chloride, sulfate, and bromide using ion chromatography. Water samples retrieved with the CTD were analyzed for dissolved silica, phosphate, nitrite and nitrate, only.

Results

A selection of pore water profiles from sediment cores retrieved during piston corer and multicorer deployments are shown in Annex. Time series of dissolved species measured in the bottom water enclosed by the benthic chamber are presented in Fig. 2.16 – 2.19.

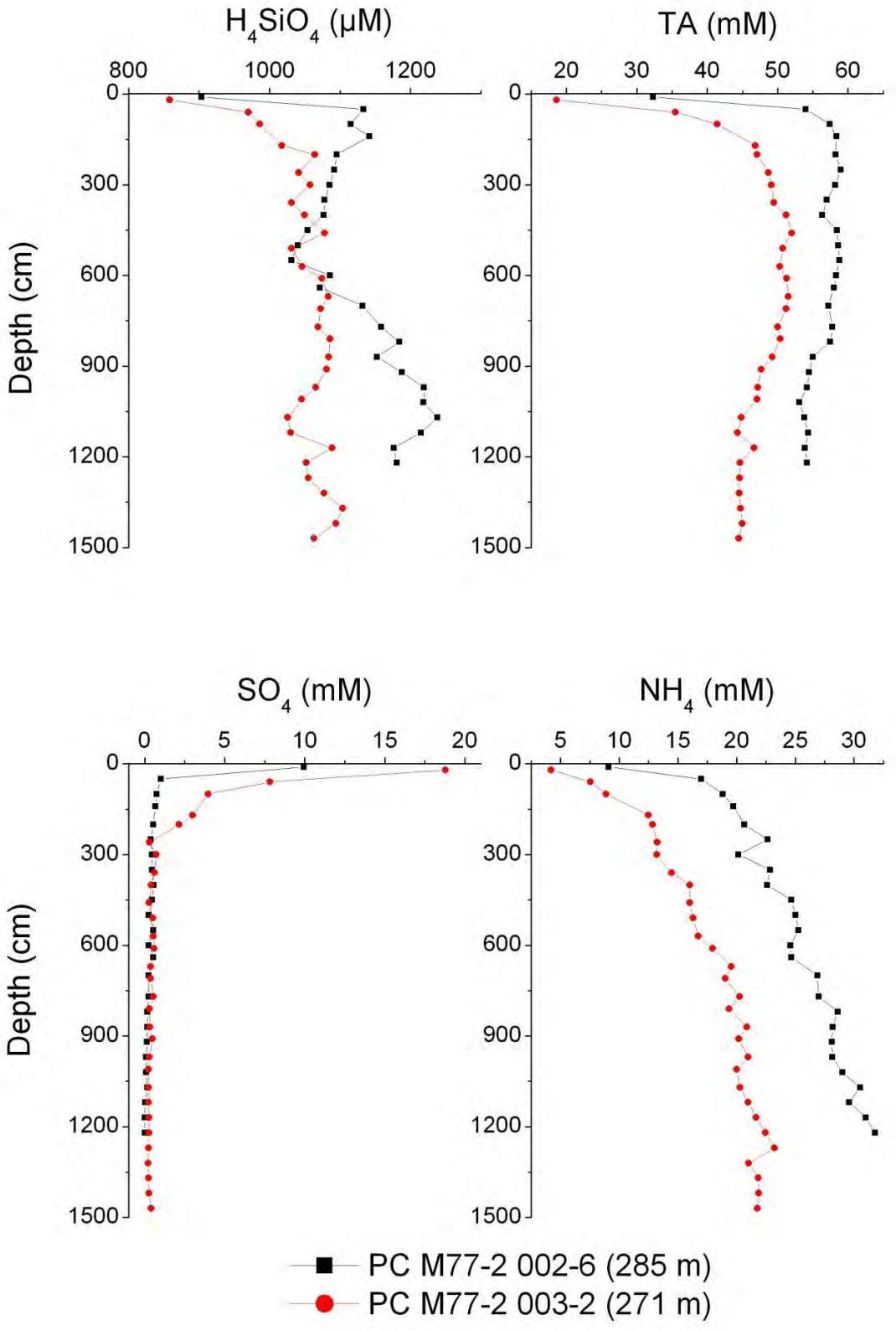

Fig. 2.16: Concentrations of dissolved silica, total alkalinity, ammonium, and sulfate in sediments retrieved with the piston corer.

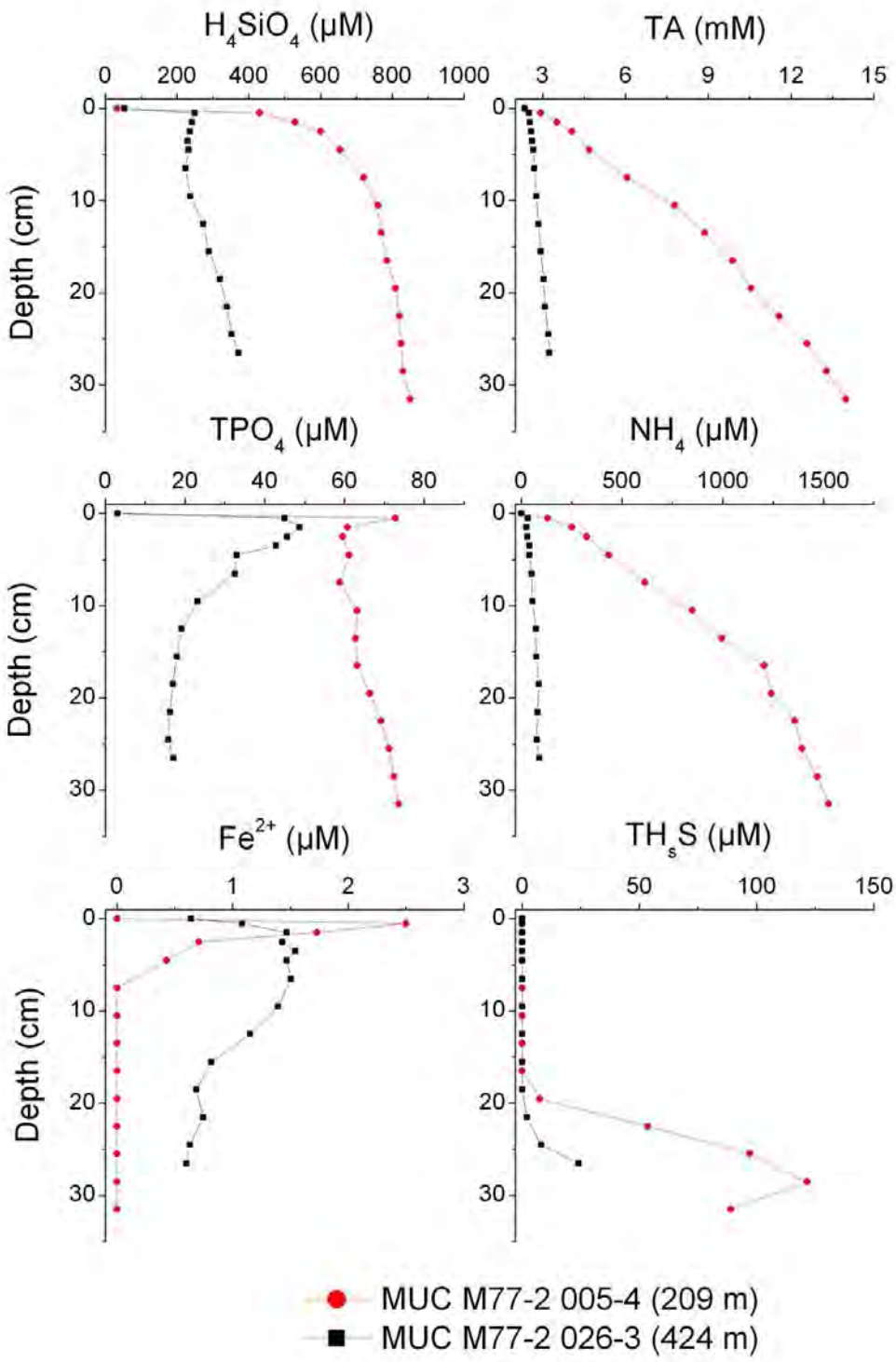

Fig. 2.17: Concentrations of dissolved silica, total alkalinity, phosphate, ammonium, ferrous iron, and sulfide in surface sediments retrieved with the multicorer.

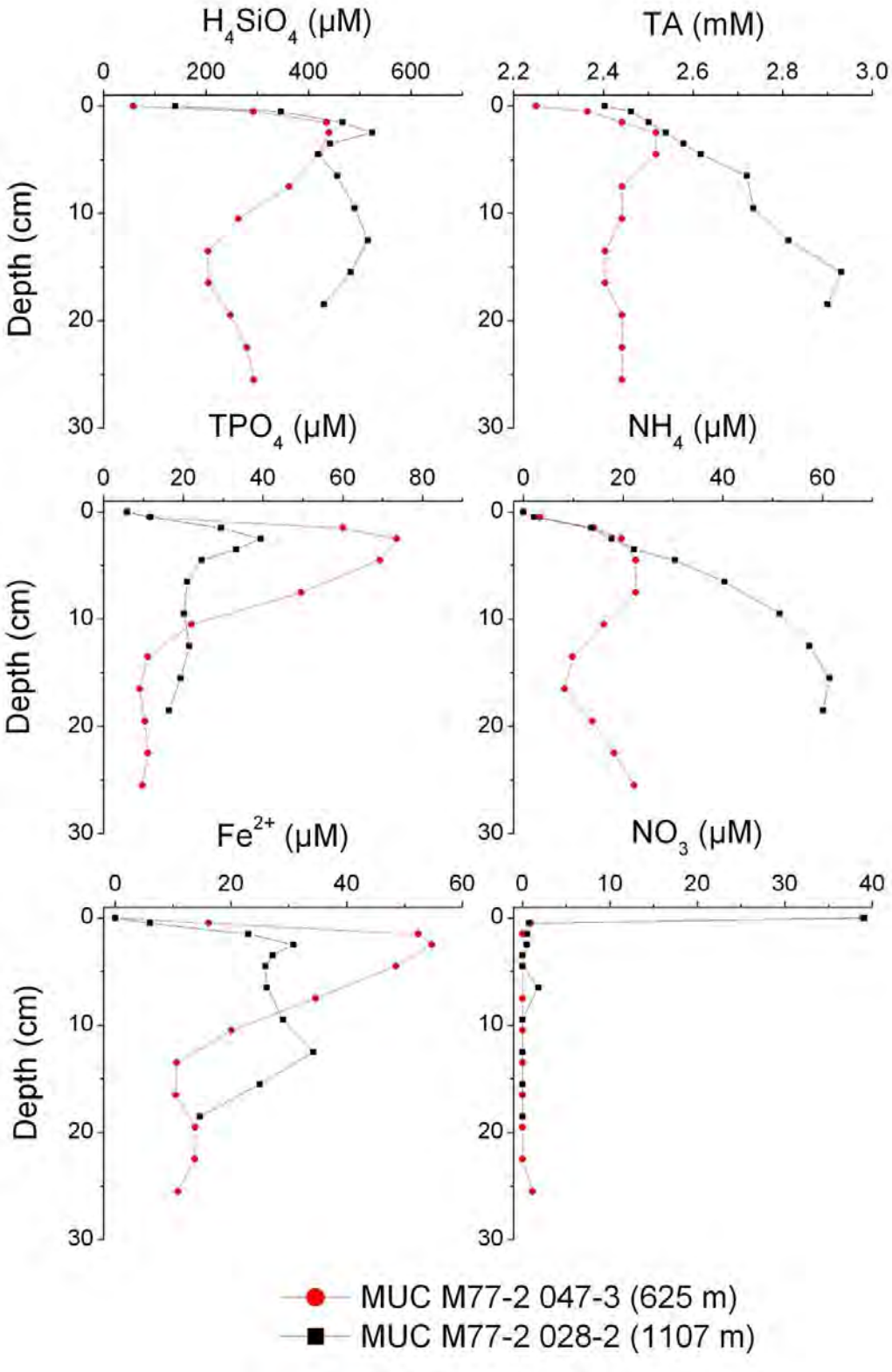

Fig. 2.18: Concentrations of dissolved silica, total alkalinity, phosphate, ammonium, ferrous iron, and nitrate in surface sediments retrieved with the multicorer.

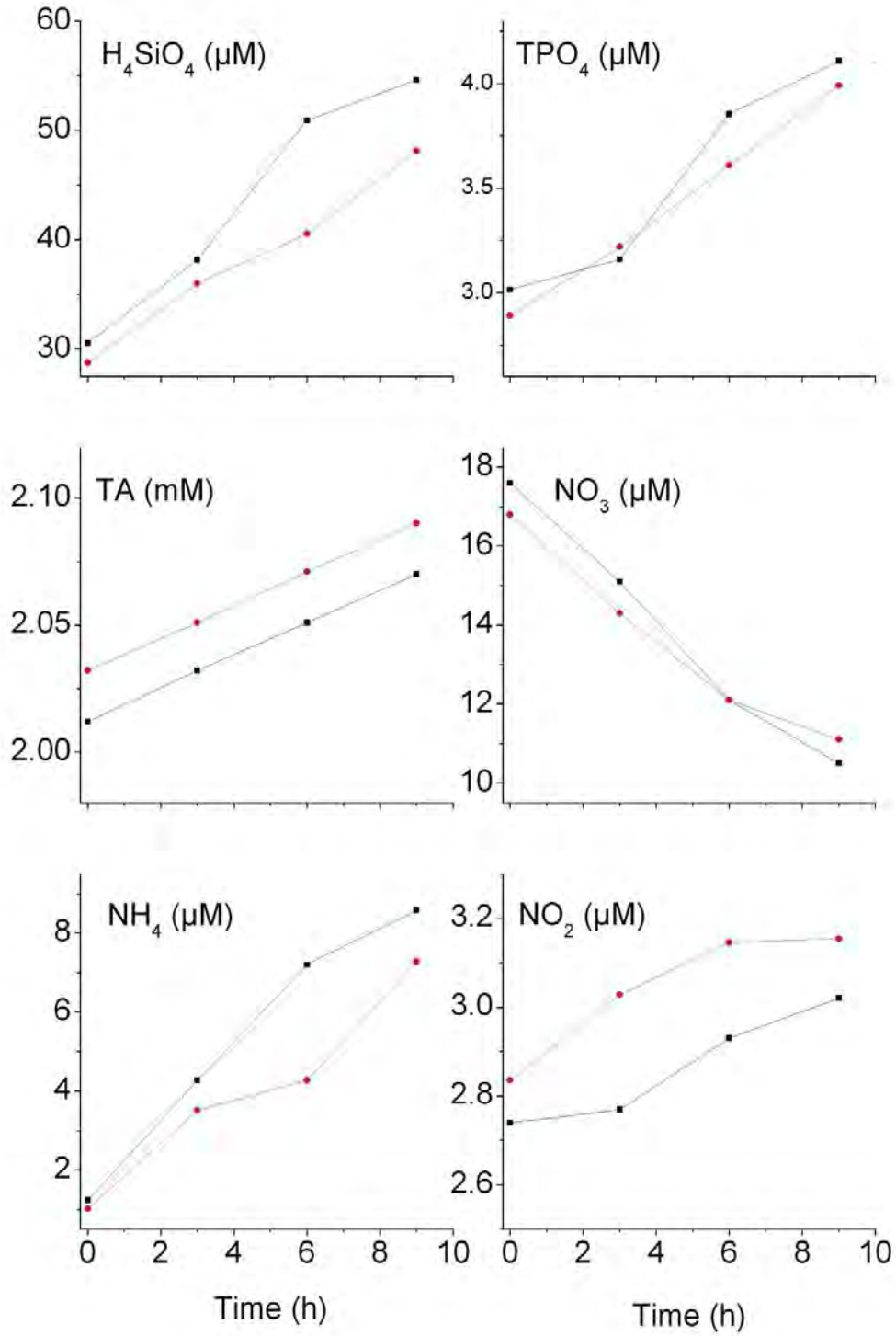

Fig. 2.19: Change in the composition of bottom water enclosed by the benthic chamber at station M772-016 (259 m water depth). After the first flux measurement (black squares) the chamber was flushed with ambient bottom water and a second incubation was performed (red dots) to control the reproducibility of the flux measurement. Please note that the concentrations still need to be corrected for dilution with Milli-Q water originating from the water-filled tubing connecting the glass syringes and the chamber.

1.4.4 Paleoceanography

(T. Blanz, F. Block, P. Carrillo, D. Gutierrez, C. Icaza, G. Leduc, P. Martinez, E. Mollier-Vogel, P. Tapia, N. Tepe, R. Thomas)

1.4.4.1 Piston Corer Sampling

During the M77-2 cruise 28 sediment cores were recovered using the Split-Piston-Corer developed and manufactured by Helmut Kawohl;Fig. 2.20). This device comprises one long piston corer (12.5 cm in diameter) and one gravity pilot corer (1 m length; 6 cm in diameter) used to release the piston corer and to retrieve the first undisturbed meter of sediment. Once the core was retrieved on the deck, the core liners were cut into 1 m segments, closed with caps at both ends and inscribed according to the scheme applied in the Geosciences Department, University Kiel.

Fig. 2.20: Scheme of the Split-Piston-Corer (Kawohl Marinetechnik

A total length of 317 meters of sediment was recovered. Commonly, the piston core recovery was very good with average recoveries of about 11 to 12 m of sediment (see Tab.2.5). All cores were cut along-core in two half pieces: one archive and one work-half. The sediments were described and photos were taken. For colour scanning, a Minolta CM-508i hand-held spectrophotometer was used to measure the percent reflectance values of sediment colour over the visible light range between 400 nm and 700 nm. The digital reflectance data of the spectrophotometer readings were routinely obtained from the surfaces of split archive halves immediately after the core opening to provide a continuous record of the sediment colour variation. From the work-half two parallel series of syringe samples (10 cc) were taken at intervals of 5 cm for selected cores. These samples were taken for the measurements and determination of stable isotopes on foraminifera and organic geochemistry. From five stations, three of them with duplicate coring, work-halves were sent to IMARPE after M77-3, and the corresponding archive halves to Kiel for finishing core logging with the XRF scanner. Due to time constraints, cores off Ecuador were only spliced and stored without description and color scanning. Core descriptions and color scanning were performed right after arrival of these cores in the core repository. The preliminary lithologic summary of the sediments retrieved with gravity corer is based on macroscopic visual description and color scanner data. Core descriptions are presented in the Annex to this report, representing the main lithologies, their color according to the MUNSELL soil color chart, and the sedimentary structure. Color scanner readings of the ratio 700nm/400nm (red/blue ratio) and L* of the core sediments are plotted for comparison at the same depth scale.

On the basis of the shipboard sedimentological description the recovered sediments can be grouped in two types: (1) mm to cm scale laminated or banded, clayey and silty-clayey, sediment cores were retrieved from 15°S to 9°S within the Oxygen Minimum Zone (OMZ) off Peru ; (2) Faintly banded to bioturbated, clayey to silty-clayey, sediment cores were retrieved from 15°S to 2°S below the OMZ off Peru. Fig. 2.21 display the distribution of laminated and bioturbated sediments with respect to the modern extent to oxygen minimum conditions as measured by CTD casts during M77-2 (see 1.4.2.1). Commonly, the sediments are clayey/silty mud and silty mud with variable amounts of foraminifera, which were retrieved in 9 latitudinal windows along the Peruvian and Ecuadorian margin at about 15°S, 12°S, 11°S, 9°S, 8°S, 5°S, 4°S, 2°S (Guayaquil area) and just north of the Equator (0°30´ N). Only the one sediment core from the southeastern flank of the Carnegie Ridge consistet mainly of carbonate ooze. The background colour of both laminated and non-laminated sediment cores is dominated by dark olive gray to olive gray. The dominant colour of the laminations varies from pale-yellow to yellow, and some rare greenish gray and light greenish gray laminae were also found. In addition, some fish remains and shell fragments were found in several cores from the shelf areas (see Annex).

Reflectance values given lightness L* are general lower than 40 %, which indicates that the contribution of calcareous remains (e.g., nannofossils and microfossils) is not dominant, due to a combination of high amounts of organic and terrigenous components. Lightness is controlled mainly by organic (autochtonous) and siliciclastic (allochtonous) input to the sediment. The lightness has been measured at a resolution of 2 cm on most of the cores, in

order to look for possible common sedimentary characteristics and hence to try to correlate the cores between each other. At 15 and 12°S, due to the presence of laminated intervals, a few unconformities (discordant layers, non-horizontal laminations), and because of the width of the lightness measurements (1 cm, i.e. integrating several mm-scale laminations), it is not possible to recognize common features shared between nearby sediment cores. On the other hand, there are some cores retrieved by different water depth in the same latitudinal window that share the same patterns of lightness, attesting that these cores record regional sedimentation characteristics. These results indicate that, as expected, shallow cores have higher sedimentation rates.

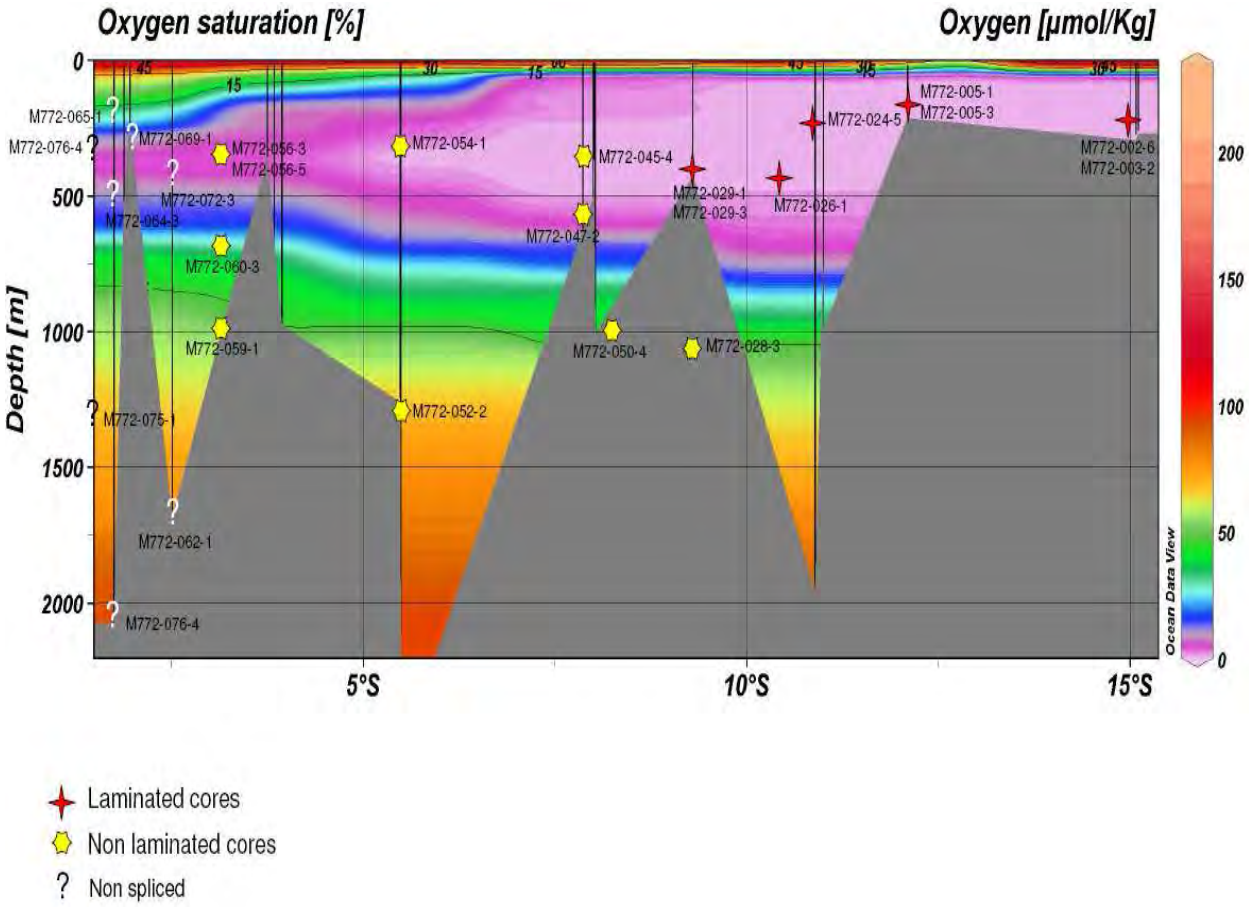

Fig. 2.21: Oxygen concentration in the water column off the Peruvian and Ecuadorian margins. Labels indicate the position of the piston cores retrieved during leg M77-2.

Tab. 2.5: Piston corer sampling during cruise 77-2. Core numbers with asterisks will be worked on In collaboration with IMARPE.

station No	Gears	Latitude	Longitude	Water Depth (m)	Recovery	Comments
M772-002-6	PC/15	15°04.75`S	75°44.00`W	285	1248 cm	see core description
M772-003-2*	PC/15	15°06.21'S	75°41.28`W	271	1497 cm	see core description
M772-005-1	PC/20	12°05.64'S	77°39.91`W	209	1474 cm	see core description
M772-005-3*	PC/20	12°05.66'S	77°40.07`W	214	1336 cm	see core description
M772-022-1	PC/15	10°53.22'S	78°46.38'W	1929	97 cm	B anana
M772-024-5	PC/15	11°05.01'S	78°00.91'W	210	1492 cm	see core description
M772-026-1	PC/15	10°45.13'S	78°28.43'W	425	1129 cm	see core description
M772-028-3	PC/15	09°17.69'S	79°53:86'W	1104	1096 cm	see core description
M772-029-1	PC/15	09°17.70'S	79°37.11'W	444	1490 cm	see core description
M772-029-3*	PC/15	09°17.70'S	79°37.11'W	433	1354 cm	see core description
M772-031-3	SL/5	09°02.97'S	79°26.88'W	114	-	tube em pty
M772-045-4	PC/15	07°59.99'S	80°20.51'W	359	1280 cm	see core description
M772-047-2	PC/15	07°52.01'S	80°31.36'W	626	1305 cm	see core description
M772-050-4	PC/20	08°01.01'S	80°30.10'W	1013	1776 cm	see core description
M772-052-2	PC/15	05°29.01'S	81°27.00'W	1249	1307 cm	see core description
M772-053-2	PC/15	05°29.02'S	81°43.00'W	2591	1239 cm	see core description
M772-054-1*	PC/15	05°29.00'S	81°18.35'W	299	1215 cm	see core description
M772-056-3	PC/20	03°44.99'S	81°07.25'W	350	1101 cm	see core description
M772-056-5*	PC/20	03°44.99'S	81°07.48'W	355	1061 cm	see core description
M772-059-1	PC/15	03°57.01'S	81°19.23'W	997	1359 cm	see core description
M772-060-3	PC/15	03°50.98'S	81°15.50'W	699	1426 cm	see core description
M772-062-1	PC/15	02°29.98'S	81°14.72'W	1675	1227 cm	see core description
M772-064-3	PC/15	01°53.49'S	81°11.76'W	523	1116 cm	see core description
M772-065-1	PC/10	01°57.01'S	81°07.23'W	204	424 cm	s ee core description
M772-067-4	PC/15	01°45.18'S	82°37.50'W	2080	1179 cm	see core description
M772-069-1	PC/15	03°16.00'S	80°56.86'W	338	780 cm	s ee core description
M772-072-3	PC/15	02°49.00'S	81°00.53'W	425	1283 cm	see core description
M772-075-1	PC/15	00°13.00'N	80°39.44'W	1316	1032 cm	see core description
M772-076-4	PC/15	00°05.45'N	80°33.40'W	291	396 cm	B anana

1.4.4.2 Multicorer Sediment Surface Sampling

The main tool for the recovery of undisturbed sediment surfaces was the multicorer device equipped with 8 tubes of 10 cm in diameter. The multicorer was used twice at each station, with a total of 31 stations (Tab. 2.6). Commonly, the core recovery was sufficient. Typically, 10 to 12 tubes with excellent quality of the bottom water-sediment interface and with a mean recovery of 36 cm of sediment could be retrieved with the 2 deployments. Sediment surface samples and downcore sediments from each tube were sliced into Petri dishes (8.5 cm diameter = ca. 56.7 cm^2 surface area), except for foraminiferal samples which were collected in plastic boxes (10.5 cm * 7 cm = ca. 73.5 cm^2 surface area).

Tab.2.6: Multicorer sampling during cruise 77-2. The recovery and the number of archive cores for each station (L = 10 cm, S = 6 cm diameter).

Station No	Latitude	Longitude	Water Depth (m)	Recovery	Comments
M772-002-2	15°04.75`S	75°44.00`W	283		overpenetration
M772-002-3	15°04.75`S	75°44.00`W	280		overpenetration
M772-002-4	15°04.75`S	75°44.00`W	290	average: 55 cm	Biom, Forams
M772-002-5	15°04.75`S	75°44.00`W	290	average: 46 cm	Trace, Corg, 1 frozen
M772-005-4	12°05.66'S	77°40.07`W	213		
M772-005-5	12°05.66'S	77°40.07`W	214	average: 46 cm	Biom, Corg, Forams, Trace, Tex86, 1 frozen
M772-022-2	10°53.22'S	78°46.38'W	1923	average: 10 cm	3 tubes only
M772-022-3	10°53.22'S	78°46.38'W	1933	average: 10 cm	
M772-024-2	11°05.01'S	78°00.91'W	209		overpenetration
M772-024-3	11°05.01'S	78°00.91'W	208	average: 53 cm	Biom, Corg, Forams, Trace, Tex86, 1 frozen
M772-024-4	11°05.01'S	78°00.91'W	210	average: 53 cm	
M772-026-2	10°45.13'S	78°28.43'W	425	average: 31 cm	Biom, Corg, Forams, Trace, Tex86
M772-026-3	10°45.13'S	78°28.43'W	424	average: 26 cm	
M772-028-1	09°17.69'S	79°53:86'W	1105	average: 28 cm	Biom, Corg, Trace, 1 frozen
M772-028-2	09°17.69'S	79°53:86'W	1107	average: 17 cm	Forams, Tex86, radionuclides
M772-029-4	09°17.70'S	79°37.11'W	433	average: 50 cm	Forams
M772-029-5	09°17.70'S	79°37.11'W	437	average: 54 cm	Biom, Trace, Corg
M772-031-1	09°02.97'S	79°26.88'W	114	average: 10 cm	Forams, 1 frozen
M772-031-2	09°02.97'S	79°26.88'W	114	average: 15 cm	Biom, Corg, Tex86, Trace
M772-045-1	08°00.00'S	80°20.40'W	356		overpenetration
M772-045-2	07°59.99'S	80°20.51'W	359	average: 50 cm	Tex86, Trace, 1 frozen
M772-045-3	07°59.99'S	80°20.51'W	359	average: 48 cm	Biom, Corg, Forams
M772-047-3	07°52.01'S	80°31.36'W	625	average: 29 cm	Forams, Corg, Trace
M772-047-4	07°52.01'S	80°31.36'W	626	average: 25 cm	Biom, Tex86, frozen tube
M772-050-1	08°01.04'S	80°30.13'W	1013	average: 35 cm	Biom, Forams, Corg, 1 frozen
M772-050-2	08°01.04'S	80°30.13'W	1012	average: 28 cm	Trace, Tex86, radionucl
M772-052-3	05°29.01'S	81°27.01'W	1252	average: 40 cm	Bio, Corg, Trace
M772-052-4	05°29.01'S	81°27.01'W	1255	average: 40 cm	Tex86, Forams, radionucl, 1frozen
M772-053-1	05°28.94'S	81°34.03'W	2607	average: 38 cm	Forams, Corg, Biom, Trace,Tex86, radionucl
M772-054-2	05°29.01'S	81°18.35'W	297	average: 52 cm	Bio, Trace
M772-054-3	05°29.01'S	81°18.35'W	307	average: 52 cm	Forams, Corg, Tex86
M772-056-1	03°45.01'S	81°07.29'W	350	average: 52 cm	Biom, Corg, Trace, 1 frozen

Station No	Latitude	Longitude	Water Depth (m)	Recovery	Comments
M772-056-2	03°45.02'S	81°07.26'W	349	average: 49 cm	Foram, Tex86
M772-059-2	03°56.95'S	81°19.16'W	995	average: 40 cm	Corg, Biom, Foram
M772-059-3	03°56.95'S	81°19.16'W	995	average: 38 cm	Trace, Tex86, radionucl., 1 frozen
M772-060-1	03°51.09'S	81°15.49'W	701	average: 42 cm	Biom, Corg, Foram
M772-060-2	03°51.01'S	81°15.49'W	699	average: 36 cm	Trace, Tex86
M772-062-2	02°30.01'S	81°14.71'W	1678	average: 47 cm	Bio, Corg, Foram
M772-062-3	02°30.01'S	81°14.71'W	1673	average: 46 cm	Trace, Tex86, radionucl, 1 frozen
M772-064-1	01°53.50'S	81°11.76'W	529	average: 50 cm	Biom, Trace, Forams, Corg
M772-064-2	01°53.49'S	81°11.75'W	525	average: 50 cm	Tex86, 1 frozen
M772-065-2	01°57.01'S	81°07.23'W	206	average: 25 cm	Biom, Corg,Tex86
M772-065-3	01°57.01'S	81°07.23'W	206	average: 26 cm	Forams, Trace,
M772-067-2	01°45.14'S	82°37.47'W	2075	average: 29 cm	Corg, Biom, Tex86
M772-067-3	01°45.15'S	82°37.47'W	2076	average: 29 cm	Trace, Foram, radionucl, 1 frozen
M772-069-2	03°16.02'S	80°56.87'W	339	average: 45 cm	Biom, Corg, Trace
M772-069-3	03°16.02'S	80°56.86'W	339	average: 43 cm	Tex86, Forams, 1 frozen
M772-070-1	03°07.01'S	80°38.79'W	59	average: 15 cm	Biom, Corg, Trace, Foram
M772-070-2	03°07.00'S	80°38.84'W	59	average: 16 cm	Tex86
M772-071-1	02°48.99'S	80°50.72'W	100	average: 28 cm	Corg, Biom, Trace, Tex86
M772-071-2	02°49.01'S	80°50.73'W	101	average: 29 cm	Foram, 1 frozen
M772-072-1	02°49.00'S	81°00.53'W	427	average: 38 cm	Biom, Tex86, Trace
M772-072-2	02°49.01'S	81°00.53'W	425	average: 36 cm	Foram, Corg, 1 frozen
M772-075-2	00°13.00'N	80°39.44'W	1314	average: 33 cm	Biom, Corg, Trace
M772-075-3	00°13.00'N	80°39.44'W	1313	average: 36 cm	Forams, radionucl, Tex86, 1 frozen
M772-076-2	00°05.45'N	80°33.40'W	290	average: 30 cm	Biom, Corg, Trace
M772-076-3	00°05.45'N	80°33.40'W	290	average: 32 cm	Forams

The general distribution of samples for paleoceanographic purposes send to Kiel for the different research targets was as follows:

2 large tubes for foraminifera
1 large tube for biomarkers
1 large tube for elementar analyses ($C_{org;}$ N_{org}, TC, TN)
1 large tube for trace element (e.g., metals)
1 large tube frozen as archive material
1 surface sample (0-1 cm) for TEX86, taken from one of the two tubes dedicated to foraminifera or from an extra tube when available.

Each core was sampled in 1 cm slices, except for the archive tubes. The biomarker samples were frozen immediately after collection at -20 ^{o}C. All other samples were kept at 4 ^{o}C. The archive cores were removed from the plastic tube after complete freezing and stored at -20 ° C in plastic bags.

The remaining filled tubes of the two deployments at each station were taken for geochemical and interstitial water studies (section 1.4.3.2), for inspection of laminae and sediment structures by IMARPE scientists (section 1.4.4.3), and for the study of living benthic foraminifera with respect to oxygen concentration levels downcore (section 1.4.4.4).

1.4.4.3 Multicorer Sediment Sampling by IMARPE

(P. Tapia, D. Gutierrez)

The IMARPE team also collected multicorer samples for documentation and proxy calibration studies. Off the Peruvian coast, generally about 2 to 3 multicorer tubes were collected at each station, with the main purposes as explained below:

Sediment core description. One of the tubes was subsampled with a 6-cm diameter PVC tube which was later sliced in two halves, described, photographed and color-scanned (Fig.2.22). Lithological descriptions were then assembled using the same tools as those applied for the piston cores (see Annex). After the documentation, both halfs were stored at cool room until the end of M77-3. Afterwards the multicore halfs will be X-rayed and kept as archive material for further studies. In the northern part of the cruise (< 4°S), surface sediments were also sieved on board, using a 0.5 mm mesh, in order to identify the living benthic bioturbating animals.

Proxy calibration samples. Other of the tubes was subsampled and sectioned at 0.5-cm (0 -2 cm) and at 1-cm resolution (> 2 cm). A set of these samples will be used for sorting of diatom valves, fish remains, foram tests and other biogenic remains (e.g. coccoliths) under different sedimentary and oxygenation settings. Another set of samples, only belonging to the top 2 – cm, will be used for work on organic matter palinofacies, bulk organic geochemical analyses, as elemental CNS and sedimentary chlorophyll-a contents.

High-resolution applications. In some selected stations (stations M772-05, M772-45 and M772-56) an additional multicore tube was subsampled with rectangular acrylic liners (Fig.2.22) that will be used for digital X-ray photography, thin-section preparations and XRF scanning. The same procedure will be applied for the archive PVC surface sediment cores associated with the piston cores that will be studied in collaboration with IMARPE. This will aid to reconstruct the modern sedimentological variability for the past few centuries to the present.

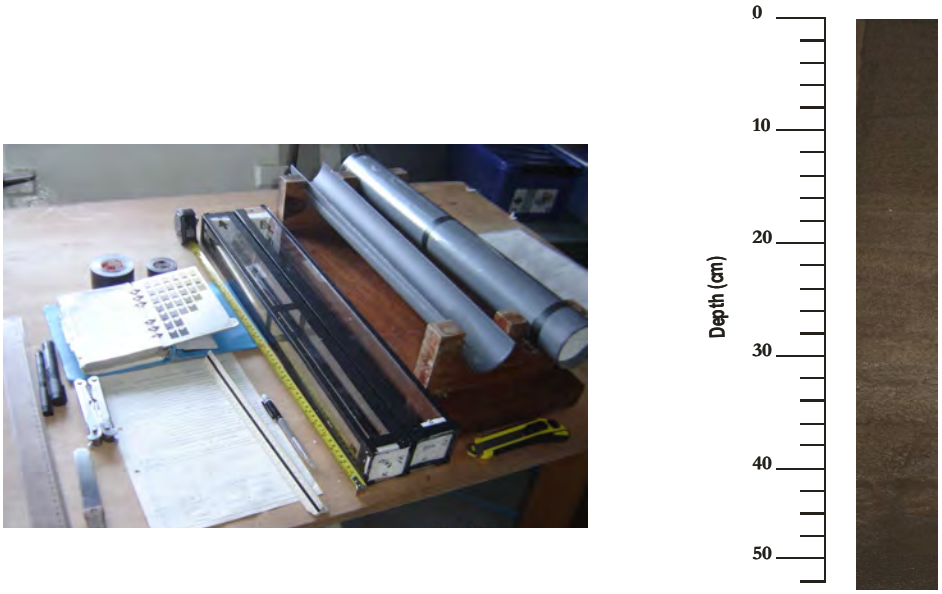

Fig. 2.22: Left: PVC and acrylic liners used for surface sediment core descriptions and archiving; Right: photography of the surface core M772-024-3.

1.4.4.4 Multicorer Sampling for Living Benthic Foraminifera

(J. Mallon)

In order to determine not only the lateral but also the vertical distribution of living benthic foraminifera in surface sediments with respect to bottom water oxygen content in the Peru oxygen minimum zone (OMZ) multicorer samples were taken at 15 stations between 10°26' S and 1°45' S (Tab. 2.7) along the margin off Peru and Equador. Together with the 21 multicorer samples gained during leg M77-2 they represent the area within the OMZ and also the transition zone to water masses with higher oxygen saturation.

The sediment cores have been profiled with polarized electrodes to determine oxygen penetration depth. Usually the penetration depth varies between 0.5 mm within OMZ and 4.5 mm outside. After profiling the sediment cores were sliced into intervals between 2 and 10 mm thickness depending on oxygen penetration depth. Then each subsample was treated with Rose Bengal for distinguishing living from dead foraminifera.

Depending on the oxygen content of bottom waters there should be distinct assemblages of benthic foraminifera which can be used to trace benthic indicator species for reconstructing past oxygen concentration levels and it's variability within the OMZ off Peru and Equador. The laboratory work of counting and more quantitative investigations of species composition by using statistical methods will be executed at the IFM-GEOMAR, Kiel, Germany.

Tab. 2.7: List of multicorer sampling for living benthic foraminifera.

Station	Latitude [°S]	Longitude [°W]
M772-005-4	12°5,66'	77°40,07'
M772-022-2	10°53,22'	78°46,38'
M772-024-4	11°5,01'	78°0,91'
M772-029-5	9°17,7'	79°17,7'
M772-028-1	9°17,69'	79°53,86'
M772-031-1	9°2,97'	79°26,88'
M772-045-2	7°59,99'	80°20,51'
M772-047-3	7°52,01'	80°31,36'
M772-052-3	5°29,1'	81°27'
M772-056-1	3°45,01'	81°7,27'
M772-064-2	1°53,49'	81°11,75'
M772-059-2	3°56,95'	81°19,16'
M772-060-2	3°50,99'	81°15,49'
M772-065-2	1°57,01'	81°7,23'
M772-067-2	1°45,14'	82°37,47'

1.5 Ship's Meteorological Station

(H. Sonnabend, W.T. Ochsenhirt)

RV METEOR left the harbour of Callao in the afternoon of 24.11.2008 to take fuel while lying in the roads at first. After having finished this action in the very early morning of the next day, METEOR set course for the first scientific station approximately 200 nautical miles south-southeast of Callao. All following stations were operated from this position step by step towards the coastal waters of Ecuador.

The general weather situation was defined by a large ridge of high pressure extending from the south pacific subtropical high towards the coastlines of northern Chile, Peru und Ecuador. Along the northeastern flank of this pressure system and flat lows east of the central range of the Andes, light to moderate trade winds varying between southeasterly and southwesterly directions predominated at first. However, a long termed south-southwesterly swell of about 3 m affected station work especially on 26.11. at times. While the swell dropped down to heights between 2 and 2,5 meters slowly within the next days, the trade wind remained light to moderate, apart from the night to 30.11. when the southeast wind freshened up to Bft. 5 for a while. Mainly fine weather with a lot of sunshine occurred throughout the whole first time, interrupted only by some cloudy days between 30.11. and 3.12. Especially over the coastal areas with upwelling water the visibility was reduced by haze occasionally. The temporarily increasing gradient between a flat low along the coastline of Peru and a ridge of high pressure which extended northward up to latitude of 10 degrees brought RV Meteor with southeast winds up to 5 Beaufort a comparatively lively interlude on 6.12. coastal effects in addition with a thermal gradient between the cool upwelling water and the warm interior let the southeast trade wind breeze up to 6 Beaufort near Punta Aguja in the northwest of Peru 2 days later in the afternoon. Meanwhile the water temperatures dropped down to 14,6 degrees

Celsius for a short period within the centre of the upwelling water at a latitude of 5,7 degrees south. Locally the visibility was reduced by haze over the areas of the cold water and the still existing swell from south-southwestlery directions with heights between 1,5 and 2 meters effected station work at times.

The strongest wind on this cruise was measured in the morning of 10.12. while RV Meteor passed the northwestern tip of Peru shortly before entering into the southern part of the Gulf of Guayaquil. Responsible for this event was an intensifying gradient between a flat low over the Gulf of Panama and the west coast of Columbia and the northernmost ridge of the subtropical high south of RV Meteors position. In addition with coastal effects the wind breezed up to forces of 6 – 7 Beaufort for some hours. Shortly after having entered the Gulf of Guayaquil the wind decreased rapidly and shifted to southwest. This trend – soft winds around the eastern most waypoints and fresh to strong breeze in the western parts - continued throughout the transect within the new working area. During the following station works in the area of the Gulf of Guayaquil the wind generally decreased to a soft to moderate breeze predominantly from south westerly directions associated with a flat swell of about 1 – 1,5 meters from the same direction. As this area lays out of the direct influence of the Humboldt Current, the temperatures of air and water rose up to nearly 24 degrees Celsius.

During the inclusive transit times two days lasting stay of RV Meteor in the working area above the Carnegie Ridge around 83 degrees West the mainly southerly trade wind freshened a little by reaching wind forces up to 5 Beaufort at times. In a distance of only 100 – 150 miles to the equator the temperatures of air and water dropped down to 21 – 22 degrees Celsius again.

Next the research in the Gulf of Guayaquil area was continued. The wind remained fresh from the southwest at first but weakened soon towards the eastern parts of the working area. But during the final station works in this region one more short interval with strong winds up to 6 Beaufort from south-southwest was measured in the night to 18.12. associated with a relative rough wind sea for a short time.

On the way to the last scheduled working area off the northwest coast of Ecuador the wind decreased to moderate wind forces soon. The final program in the vicinity of the equator could be carried out without problems at a soft southwesterly breeze. At this time the Intertropical Convergence Zone (ITCZ) extended from the northwest coast of Columbia westward between 4 and 6 degrees north, mainly without significant weather activities. However parts of the cloudiness from there spread along the whole coast of Ecuador at times. The temperatures of air and water rose to nearly 25 degrees Celsius, the maximum values of this cruise.

After having finished the last survey a few miles south of the equator, RV Meteor set course for Guayaquil directly at a moderate and later on soft southwesterly breeze.

To summarize, it can be said that this cruise was favoured by predominantly moderate trade winds associated with the corresponding sea state. It was mainly sunny and no precipitation was measured throughout the whole cruise.

1.6 Station List

The complete station list can be found on the PANGAEA website and on the IFM-GEOMAR data archive. In the electronic version of this report the station list can be found as annex.

Table 2.8: Station list of METEOR cruise M77/2

Station No	Date	Time (UTC)	Meteor station No	Gears	Latitude	Longitude	Water Depth (m)	Recovery
M772-001-1	25.11.08	09:39	M772/633	MB-PS	12°12.23'S	77°16.58'W	113	
M772-001-2	26.11.08	04:02	M772/634	MB-PS	15°10.98'S	75°47.65'W	990	
M772-002-1	26.11.08	09:18	M772/635-1/2	CTD/ROS	15°04.73`S	75°43.99`W	296	2 samples
M772-002-2	26.11.08	09:54	M772/635-3	MUC	15°04.75`S	75°44.00`W	283	
M772-002-3	26.11.08	10:28	M772/635-4	MUC	15°04.75`S	75°44.00`W	280	
M772-002-4	26.11.08	11:02	M772/635-5	MUC	15°04.75`S	75°44.00`W	290	average: 55 cm
M772-002-5	26.11.08	11:43	M772/635-6	MUC	15°04.75`S	75°44.00`W	290	average: 46 cm
M772-002-6	26.11.08	13:12	M772/635-7	PC/15	15°04.75 `S	75°44.00`W	285	1248 cm
M772-003-1	26.11.08	17:00	M772/635-8	HN	15°06.21'S	75°41.28`W		
M772-003-2	26.11.08	17:52	M772/636-1	PC/15	15°06.21 'S	75°41.28`W	271	1497 cm
M772-003-3	26.11.08	18:55	M772/637-1	CTD/ROS	15°06.20'S	75°41.28`W	260	1 sample
M772-004-1	26.11.08	19:12	M772/638	MB-PS	15°06.19'S	75°41.30'W	264	
M772-005-1	27.11.08	17:32	M772/639-1	PC/20	12°05.64 'S	77°39.91`W	209	1474 cm
M772-005-2	27.11.08	18:30	M772/640-1	CTD/ROS	12°05.66'S	77°40.07`W	211	15 samples
M772-005-3	27.11.08	21:14	M772/647-1	PC/20	12°05.66 'S	77°40.07`W	214	1336 cm
M772-005-4	27.11.08	23:29	M772/648-1	MUC	12°05.66'S	77°40.07`W	213	
M772-005-5	28.11.08	00:07	M772/649-1	MUC	12°05.66'S	77°40.07`W	214	average: 46 cm
M772-006	28.11.08	04:09	M772/651	OFOS	11°35.01'S	78 °06.52'W	469	
M772-007	28.11.08	13:00	M772/653	BIGO	11°00.00'S	78 °30.95'W	988	
M772-008	28.11.08	14:34	M772/654	CTD/ROS	11°00.01'S	78°30.91'W	987	16 samples
M772-009	28.11.08	18:29	M772/655	LANDER	11°00.01'S	78°27.29'W	796	
M772-010	28.11.08	22:24	M772/656	BIGO	11°00.01'S	78 °05.86'W	255	
M772-011	29.11.08	00:43	M772/657	OFOS	10°45.01'S	78 °13.00'W	251	
M772-012	29.11.08	02:39	M772/658	MB-PS	10°45.42'S	7 8°15.79'W	289	
M772-013	29.11.08	13:00	M772/659	LANDER	10°59.82'S	78°31.05'W	978	
M772-014	29.11.08	14:00	M772/660	MB-PS	11°00.02'S	7 8°31.16'W	1004	
M772-015	29.11.08	18:13	M772/661	LANDER	10°59.75'S	78°27.39'W	796	
M772-016	29.11.08	22:02	M772/662	LANDER	10°59.80'S	78°05.91'W	259	
M772-017	30.11.08	01:30	M772/663	OFOS	10°45.01'S	78 °34.54'W	656	
M772-018	30.11.08	06:21	M772/664	MB-PS	10°45.00 'S	78°32.54'W	523	
M772-019	30.11.08	13:16	M772/665	LANDER	10°59.75'S	78°25.93'W	718	
M772-020	30.11.08	15:34	M772/666	CTD/ROS	10°59.76'S	78°25.92'W	717	15 samples
M772-021	30.11.08	18:29	M772/667	LANDER	10°59.75'S	78°25.93'W	716	
M772-022-1	30.11.08	22:43	M772/668	PC/15	10°53.22'S	78°46.38'W	1929	97 cm
M772-022-2	01.12.08	00:53	M772/669	MUC	10°53.22'S	7 8°46.38'W	1923	average: 10 cm
M772-022-3	01.12.08	02:43	M772/670	MUC	10°53.22'S	7 8°46.38'W	1933	average: 10 cm
M772-022-4	01.12.08	04:05	M772/671	CTD/ROS	10°53.65'S	78°46.33'W	1972	21 samples
M772-023	01.12.08	06:15	M772/672	MB-PS	10°53.64'S	7 8°46.36'W	1951	
M772-024-1	01.12.08	13:44	M772/673	CTD/ROS	11°05.01'S	78°00.91'W	207	9 samples
M772-024-2	01.12.08	14:32	M772/674	MUC	11°05.01'S	7 8°00.91'W	209	
M772-024-3	01.12.08	15:36	M772/675	MUC	11°05.01'S	7 8°00.91'W	208	average: 53 cm
M772-024-4	01.12.08	16:13	M772/676	MUC	11°05.01'S	7 8°00.91'W	210	average: 53 cm

Station No	Date	Time (UTC)	Meteor station No	Gears	Latitude	Longitude	Water Depth (m)	Recovery
M772-025	01.12.08	17:18	M772/678	LANDER	10°59.47'S	78°26.10'W	716	
M772-026-1	01.12.08	22:59	M772/679	PC/15	10°45.13'S	78°28.43'W	425	1129 cm
M772-026-2	02.12.08	00:04	M772/680	MUC	10°45.13'S	7 8°28.43'W	425	average: 31 cm
M772-026-3	02.12.08	00:51	M772/681	MUC	10°45.13'S	7 8°28.43'W	424	average: 26 cm
M772-026-4	02.12.08	01:57	M772/682	CTD/ROS	10°45.69'S	78°28.53'W	436	6 samples
M772-027	02.12.08	02:49	M772/683	MB-PS	10°45.69'S	7 8°28.48'W	430	
M772-028-1	03.12.08	13:37	M772/684	MUC	09°17.69'S	7 9°53:86'W	1105	average: 28 cm
M772-028-2	03.12.08	15:03	M772/685	MUC	09°17.69'S	7 9°53:86'W	1107	average: 17 cm
M772-028-3	03.12.08	16:32	M772/686	PC/15	09°17.69'S	79°53:86'W	1104	1096 cm
M772-028-4	03.12.08	18:44	M772/687	CTD/ROS	09°18.11'S	79°53.97'W	1141	18 samples
M772-029-1	03.12.08	22:09	M772/688	PC/15	09°17.70'S	79°37.11'W	444	1490 cm
M772-029-2	03.12.08	23:45	M772/689	CTD/ROS	09°17.70'S	79°37.11'W	426	no samples
M772-029-3	04.12.08	02:09	M772/690	PC/15	09°17.70'S	79°37.11'W	433	1354 cm
M772-029-4	04.12.08	03:13	M772/691	MUC	09°17.70'S	7 9°37.11'W	433	average: 50 cm
M772-029-5	04.12.08	03:54	M772/692	MUC	09°17.70'S	7 9°37.11'W	437	average: 54 cm
M772-030	04.12.08	04:22	M772/693	MB-PS	09°17.38'S	7 9°36.78'W	429	
M772-031-1	04.12.08	14:06	M772/694	MUC	09°02.97'S	7 9°26.88'W	114	average: 10 cm
M772-031-2	04.12.08	14:44	M772/695	MUC	09°02.97'S	7 9°26.88'W	114	average: 15 cm
M772-031-3	04.12.08	15:34	M772/696	SL/5	09°02.97'S	79°26.88'W	114	-
M772-031-4	04.12.08	15:50	M772/697	CTD/ROS	09°02.97'S	79°26.88'W	114	10 samples
M772-032	04.12.08	23:40	M772/698	MB-PS	08°00.04'S	8 0°19.56'W	339	
M772-033	05.12.08	00:42	M772/699	CTD/ROS	08°00.03'S	80°25.22'W	500	13 samples
M772-034	05.12.08	02:28	M772/701	CTD/ROS	08°00.05'S	80°27.63'W	735	2 samples
M772-035	05.12.08	05:09	M772/703	OFOS	08.00.03'S	80°26.42'W	567	
M772-036	05.12.08	13:36	M772/705	LANDER	08°00.01'S	80°25.79'W	529	
M772-037	05.12.08	17:48	M772/706	CTD/ROS	08°00.04'S	80°23.46'W	417	9 samples
M772-038	05.12.08	19:10	M772/707	LANDER	08°00.05'S	80°23.46'W	417	
M772-039	05.12.08	21:22	M772/708	LANDER	08°00.05'S	80°23.58'W	421	
M772-040	05.12.08	22:45	M772/709	OFOS	07°59.99'S	80 °19.57'W	370	
M772-041	06.12.08	07:14	M772/711	MB-PS	07°59.95'S	8 0°27.49'W	671	
M772-042	06.12.08	14:22	M772/712	LANDER	08°00.01'S	80°27.58'W	703	
M772-043	06.12.08	15:35	M772/713	MB-PS	08°00.14'S	8 0°27.62'W	713	
M772-044	06.12.08	19:24	M772/714	LANDER	07°59.73'S	80°23.80'W	426	
M772-045-1	06.12.08	20:54	M772/715	MUC	08°00.00'S	8 0°20.40'W	356	
M772-045-2	06.12.08	21:47	M772/716	MUC	07°59.99'S	8 0°20.51'W	359	average: 50 cm
M772-045-3	06.12.08	22:24	M772/717	MUC	07°59.99'S	8 0°20.51'W	359	average: 48 cm
M772-045-4	06.12.08	23:18	M772/718	PC/15	07°59.99'S	80°20.51'W	359	1280 cm
M772-045-5	07.12.08	00:45	M772/719	CTD/ROS	08°00.34'S	80°20.85'W	365	13 samples
M772-046	07.12.08	01:53	M772/720	MB-PS	07°59.81'S	8 0°19.84'W	345	
M772-047-1	07.12.08	14:35	M772/721	CTD/ROS	07°52.01'S	80°31.36'W	627	no samples
M772-047-2	07.12.08	15:25	M772/722	PC/15	07°52.01'S	80°31.36'W	626	1305 cm
M772-047-3	07.12.08	17:02	M772/723	MUC	07°52.01'S	8 0°31.36'W	625	average: 29 cm
M772-047-4	07.12.08	17:53	M772/724	MUC	07°52.01'S	8 0°31.36'W	626	average: 25 cm
M772-048	07.12.08	19:36	M772/725	LANDER	07°59.96'S	80°23.64'W	422	
M772-049	07.12.08	20:36	M772/726	LANDER	07°59.79'S	80°27.77'W	679	
M772-050-1	07.12.08	21:30	M772/727	MUC	08°01.04'S	8 0°30.13'W	1013	average: 35 cm
M772-050-2	07.12.08	22:37	M772/728	MUC	08°01.04'S	8 0°30.13'W	1012	average: 28 cm
M772-050-3	07.12.08	23:45	M772/729	CTD/ROS	08°01.55'S	80°30.19'W	1244	20 samples
M772-050-4	08.12.08	01:46	M772/730	PC/20	08°01.01'S	80°30.10'W	1013	1776 cm
M772-051	08.12.08	03:15	M772/731	MB-PS	08°01.27'S	8 0°30.53'W	1022	
M772-052-1	09.12.08	10:41	M772/732	CTD/ROS	05°29.00'S	81°27.00'W	1251	21 samples
M772-052-2	09.12.08	12:16	M772/733	PC/15	05°29.01'S	81°27.00'W	1249	1307 cm
M772-052-3	09.12.08	14:02	M772/734	MUC	05°29.01'S	8 1°27.01'W	1252	average: 40 cm
M772-052-4	09.12.08	15:14	M772/735	MUC	05°29.01'S	8 1°27.01'W	1255	average: 40 cm
M772-053-1	09.12.08	17:08	M772/736	MUC	05°28.94'S	8 1°34.03'W	2607	average: 38 cm
M772-053-2	09.12.08	19:30	M772/737	PC/15	05°29.02'S	81°43.00'W	2591	1239 cm
M772-053-3	09.12.08	21:56	M772/738	CTD/ROS	05°29.02'S	81°43.00'W	2589	no samples

Station No	Date	Time (UTC)	Meteor station No	Gears	Latitude	Longitude	Water Depth (m)	Recovery
M772-054-2	10.12.08	02:33	M772/740	MUC	05°29.01'S	81°18.35'W	297	average: 52cm
M772-054-3	10.12.08	03:08	M772/741	MUC	05°29.01'S	81°18.35'W	307	average: 52cm
M772-054-4	10.12.08	03:58	M772/742	CTD/ROS	05°29.61'S	81°18.41'W	329	13 samples
M772-055	10.12.08	05:03	M772/743	MB-PS	05°29.48'S	81°18.87'W	2376	
M772-056-1	11.12.08	14:54	M772/744	MUC	03°45.01'S	81°07.29'W	350	average: 52 cm
M772-056-2	11.12.08	15:32	M772/745	MUC	03°45.02'S	81°07.26'W	349	average: 49 cm
M772-056-3	11.12.08	17:50	M772/746	PC/20	03°44.99'S	81°07.25'W	350	1101 cm
M772-056-4	11.12.08	19:48	M772/747	CTD/ROS	03°44.99'S	81°07.47'W	355	14 samples
M772-056-5	11.12.08	21:15	M772/748	PC/20	03°44.99'S	81°07.48'W	355	1061 cm
M772-057	12.12.08	02:00	M772/750	CTD/ROS	03°47.01'S	81°34.37'W	2625	27 samples
M772-058	12.12.08	05:30	M772/751	MB-PS	03°56.84'S	81°33.02'W	2237	
M772-059-1	12.12.08	13:08	M772/752	PC/15	03°57.01'S	81°19.23'W	997	1359 cm
M772-059-2	12.12.08	14:45	M772/753	MUC	03°56.95'S	81°19.16'W	995	average: 40 cm
M772-059-3	12.12.08	15:59	M772/754	MUC	03°56.95'S	81°19.16'W	995	average: 38 cm
M772-059-4	12.12.08	17:10	M772/755	CTD/ROS	03°56.48'S	81°18.83'W	973	19 samples
M772-060-1	12.12.08	19:14	M772/756	MUC	03°51.09'S	81°15.49'W	701	average: 42 cm
M772-060-2	12.12.08	20:06	M772/757	MUC	03°51.01'S	81°15.49'W	699	average: 36 cm
M772-060-3	12.12.08	21:10	M772/758	PC/15	03°50.98'S	81°15.50'W	699	1426 cm
M772-060-4	12.12.08	22:44	M772/759	CTD/ROS	03°50.51'S	81°15.50'W	661	no samples
M772-061	13.12.08	02:15	M772/760	MB-PS	03°21.97'S	81°15.02'W	1132	
M772-062-1	13.12.08	18:52	M772/761	PC/15	02°29.98'S	81°14.72'W	1675	1227 cm
M772-062-2	13.12.08	20:48	M772/762	MUC	02°30.01'S	81°14.71'W	1678	average: 47 cm
M772-062-3	13.12.08	22:23	M772/763	MUC	02°30.01'S	81°14.71'W	1673	average: 46 cm
M772-062-4	14.12.08	00:09	M772/764	CTD/ROS	02°30.50'S	81°14.97'W	1671	21 samples
M772-063	14.12.08	04:18	M772/765	MB-PS	02°05.57'S	81°20.89	1897	
M772-064-1	14.12.08	13:22	M772/766	MUC	01°53.50'S	81°11.76'W	529	average: 50 cm
M772-064-2	14.12.08	14:04	M772/767	MUC	01°53.49'S	81°11.75'W	525	average: 50 cm
M772-064-3	14.12.08	14:55	M772/768	PC/15	01°53.49'S	81°11.76'W	523	1116 cm
M772-064-4	14.12.08	17:04	M772/769	CTD/ROS	01°52.93'S	81°11.70'W	524	13 samples
M772-065-1	14.12.08	19:04	M772/770	PC/10	01°57.01'S	81°07.23'W	204	424 cm
M772-065-2	14.12.08	19:58	M772/771	MUC	01°57.01'S	81°07.23'W	206	average: 25 cm
M772-065-3	14.12.08	20:25	M772/772	MUC	01°57.01'S	81°07.23'W	206	average: 26 cm
M772-065-4	14.12.08	20:54	M772/773	CTD/ROS	01°57.21'S	81°07.63'W	235	no samples
M772-066	15.12.08	00:00	M772/774	MB-PS	01°57.02'S	82°58.97'W	2387	
M772-067-1	16.12.08	06:48	M772/775	CTD/ROS	01°45.18'S	82°37.56'W	2075	8 samples
M772-067-2	16.12.08	08:46	M772/776	MUC	01°45.14'S	82°37.47'W	2075	average: 29 cm
M772-067-3	16.12.08	10:31	M772/777	MUC	01°45.15'S	82°37.47'W	2076	average: 29 cm
M772-067-4	16.12.08	12:28	M772/778	PC/15	01°45.18'S	82°37.50'W	2080	1179 cm
M772-068	16.12.08	23:50	M772/779	MB-PS	02°49.93'S	81°08.19'W	754	
M772-069-1	17.12.08	17:10	M772/780	PC/15	03°16.00'S	80°56.86'W	338	780 cm
M772-069-2	17.12.08	18:12	M772/781	MUC	03°16.02'S	80°56.87'W	339	average: 45 cm
M772-069-3	17.12.08	18:50	M772/782	MUC	03°16.02'S	80°56.86'W	339	average: 43 cm
M772-069-4	17.12.08	19:32	M772/783	CTD/ROS	03°15.82'S	80°57.29'W	372	12 samples
M772-070-1	17.12.08	22:33	M772/784	MUC	03°07.01'S	80°38.79'W	59	average: 15 cm
M772-070-2	17.12.08	22:51	M772/785	MUC	03°07.00'S	80°38.84'W	59	average: 16 cm
M772-070-3	17.12.08	23:16	M772/786	CTD/ROS	03°07.16'S	80°39.13'W	60	8 samples
M772-071-1	18.12.08	02:13	M772/787	MUC	02°48.99'S	80°50.72'W	100	average: 28 cm
M772-071-2	18.12.08	02:34	M772/788	MUC	02°49.01'S	80°50.73'W	101	average: 29 cm
M772-072-1	18.12.08	03:58	M772/789	MUC	02°49.00'S	81°00.53'W	427	average: 38 cm
M772-072-2	18.12.08	04:35	M772/790	MUC	02°49.01'S	81°00.53'W	425	average: 36 cm
M772-072-3	18.12.08	05:26	M772/791	PC/15	02°49.00'S	81°00.53'W	425	1283 cm
M772-072-4	18.12.08	06:50	M772/792	CTD/ROS	02°49.37'S	81°00.75'W	437	12 samples
M772-073	18.12.08	19:44	M772/793	MB-PS	00°32.17'S	81°09.00'W	2567	
M772-074	19.12.08	03:14	M772/794	MB-PS	00°29.93'N	80°32.01'W	1950	
M772-075-1	19.12.08	12:29	M772/795	PC/15	00°13.00'N	80°39.44'W	1316	1032 cm
M772-075-2	19.12.08	14:07	M772/796	MUC	00°13.00'N	80°39.44'W	1314	average: 33 cm

Station No	Date	Time (UTC)	Meteor station No	Gears	Latitude	Longitude	Water Depth (m)	Recovery
M772-075-4	19.12.08	16:32	M772/798	CTD/ROS	00°12.70'N	80°39.77'W	1381	19 samples
M772-076-1	19.12.08	21:48	M772/799	CTD/ROS	00°05.44'N	80°33.40'W	288	2 samples
M772-076-2	19.12.08	22:27	M772/800	MUC	00°05.45'N	8 0°33.40'W	290	average: 30 cm
M772-076-3	19.12.08	22:57	M772/801	MUC	00°05.45'N	8 0°33.40'W	290	average: 32 cm
M772-076-4	19.12.08	23:36	M772/802	PC/15	00°05.45'N	80°33.40'W	291	396 cm
M772-077	20.12.08	02:18	M772/803	MB-PS	00°02.17'S	8 0°42.30'W	1191	

(Abrev.: MUC= Multicorer, SL= Gravity corer, PC= Pisten corer, CTD/ROS= CTD Rosette, HN= handnet)

1.7 Acknowledgements

The scientific party aboard R/V METEOR during leg M77-2 gratefully acknowledges the friendly cooperation and efficient technical assistance of Captain W. Baschek, his officers and crew who significantly contributed to the scientific success of this cruise. The cruise was funded by the DFG through the Collaborative Research Projekt (SFB) 754 at Kiel University and IFM-GEOMAR.

1.8 References

Brandes JA, Devol AH, Deutsch C, 2007, New developments in the marine nitrogen cycle. Chem Rev, 107, 577-589.

Codispoti LA, Brandes JA, Christensen JP, Devol AH, Naqvi SWA, Paerl HW, Yoshinari T, 2001, The oceanic fixed nitrogen and nitrous oxide budgets: Moving targets as we enter the Anthropocene? Sci Mar, 65, 85-105.

Devol AH, 1991, Direct measurement of nitrogen gas fluxes from continental shelf sediments. Nature, 349, 319-321.

Hulth S, Aller RC, Canfield DE, Dalsgaard T, Engström P, Gilbert F, Sundbäck K, Thamdrup B ,2005 , Nitrogen removal in marine environments: recent findings and future research challenges. Mar Chem, 94, 125-145.

Middelburg JJ, Soetaert K, Herman PMJ, Heip CHR ,1996, Denitrification in marine sediments: A model study. Glob Biogeochem Cycles, 10, 661-673.

Pfannkuche O, Linke P. 2003, GEOMAR landers as long-term deep sea observatories. Sea Technology, 44, 50-55.

Sigman et al., 2003, Distinguishing beteen water column and sedimentary denitrification in the santa Barbara Basin using the stable isotopes of nitrate. Geochem Geophys Geosys, 4, 1040, doi:10.1029/2002GC000384.

Sommer S, Pfannkuche O, Linke P, Luff R, Greinert J, Drews M, Gubsch S, Pieper M, Poser M, Viergutz T ,2006 ,Efficiency of the benthic filter: Biological control of the emission of dissolved methane from sediments containing shallow gas hydrates at Hydrate Ridge. Glob Biogeochem Cycl 20: doi: 10.1029/2004GB002389.

Sommer S, Türk M, Kriwanek S, Pfannkuche O , 2008, Gas exchange system for extended in situ benthic chamber flux measurements under controlled oxygen conditions: First application – Sea bed methane emission measurements at Captain Arutyunov mud volcano. Limnol Oceanog: Methods 6: 23-33.

Annexes

Core descriptions of piston corers

Core descriptions of IMARPE multicorers

Complete Station list M77-2

METEOR-Berichte 11-2

Climate-biogeochemistry interactions in the tropical ocean of the SE-American oxygen minimum zone

PART 3

Cruise No. 77, Leg 3

December 27, 2008 – January 24, 2009
Guayaquil (Ecuador) – Callao (Peru)

M. Frank, O. Baars, E. Behrens, S. Contreras, A. Dammshäuser, A. Ellrott, J. Franz, G. Friederich, P. Fritsche, P. Grasse, T. Großkopf, H. Hauss, T. Kalvelage, G. Klockgether, G. Krahmann, J. LaRoche, G. Lavik, V. Leon, R. Link, C. Löscher, N. Nunes, W. Ochsenhirt, A. Paulmier, C. Schlosser, H. Schunck, F. Schwarzkopf, U. Sommer, H. Sonnabend, R. Stumpf, M. Vogt

Table of Contents Part 3 (M77/3) Page

3.1 Participants

Name	Discipline	Institution
Frank, Martin, Prof.	Chief Scientist/Isotope Geochemistry	IFM-GEOMAR
Baars, Oliver	Trace Metals	IFM-GEOMAR
Behrens, Erik	CTD/ADCP Watch	IFM-GEOMAR
Contreras Quintana, Sergio H., Dr.	Nitrogen Loss	MPI-Bremen
Dammshäuser, Anna	Trace Metals	IFM-GEOMAR
Ellrott, Andreas	Nitrogen Loss	MPI-Bremen
Franz, Jasmin	POM/DOM/HPLC/Pelagic Communities	IFM-GEOMAR
Friederich, Gernot, Dr.	TCO_2/pCO_2	MBARI
Fritsche, Peter	Nutrients	IFM-GEOMAR
Grasse, Patricia	Nd-Si Isotopes	IFM-GEOMAR
Großkopf, Tobias	Nitrogen Fixation	IFM-GEOMAR
Hauss, Helena	Pelagic Communities	IFM-GEOMAR
Kalvelage, Tim	Nitrogen Loss	MPI-Bremen
Klockgether, Gabriele	O_2, nutrients	MPI-Bremen
Krahmann, Gerd, Dr.	CTD, Glider	IFM-GEOMAR
LaRoche, Julie, Prof.	Nitrogen Fixation	IFM-GEOMAR
Lavik, Gaute, Dr.	Nitrogen Loss	MPI-Bremen
Leon, Violeta	Biological Productivity, O_2	IMARPE
Link, Rudolf	CTD Technics	IFM-GEOMAR
Löscher, Carolin	Nitrogen Fixation	IFM-GEOMAR
Nunes, Nuno, Dr.	CTD Watch / ADCP Processing	IFM-GEOMAR
Ochsenhirt, Wolf-Thilo	Meteorologist	DWD
Paulmier, Aurelien	Nitrogen Loss	MPI-Bremen
Schlosser, Christian, Dr.	Trace Metals	IFM-GEOMAR
Schunck, Harald	Nitrogen Fixation	IFM-GEOMAR
Schwarzkopf, Franziska	CTD/Salinometer	IFM-GEOMAR
Sommer, Ulrich, Prof.	Pelagic Communities	IFM-GEOMAR
Sonnabend, Hartmut	Meteorologist	DWD
Stumpf, Roland	Nd-Si Isotopes	IFM-GEOMAR
Vogt, Martin	CTD Watch / ADCP Processing	IFM-GEOMAR

IFM-GEOMAR	Leibniz-Institut für Meereswissenschaften an der Universität Kiel
MPI Bremen	Max Planck Institut für Marine Mikrobiologie
MBARI	Monterey Bay Aquarium Research Institute
IMARPE	Instituto del Mar del Peru
DWD	Deutscher Wetterdienst, Geschäftsfeld Seeschiffahrt

3.2 Research Program

The third leg of M77 focused on the detailed investigation of the influence of the hydrographic, geochemical and isotopic structure of the water masses and their variability, on the oxygen content in the Peruvian coastal upwelling area with its pronounced oxygen minimum zone (OMZ). These investigations were the basis for a biological research program on the relationship between pelagic community structure and nutrient composition and utilization with particular emphasis on the nitrogen cycle. Three zonal sections covering the oxygen gradients from the upwelling centres near the coast to the open ocean were surveyed at 10°S, 12°S, 16°S, complemented by one section perpendicular to the coast line at 17°S, south of the main areas of coastal upwelling. Together with the meridional section at 85°W, as well as 3 zonal sections at 3°S, 6°S and 14°S that were covered by M77/4, a well-resolved and detailed picture of the water mass and oxygen distribution, their supply paths and their relationship to the pelagic community structure, as well as the distribution and cycling of nutrients in the eastern equatorial Pacific upwelling areas was obtained. In addition, a detailed survey of the shelf waters south of Lima was carried out to study the variability of the system that partly led to sulphidic conditions in the water column. These investigations, in particular the processes controlling the oxygen content, were carried out in the frame of the Kiel SFB 754: *Climate – Biogeochemistry Interactions in the Tropical Ocean*.

High temporal and spatial surveys of hydrography, oxygen and fluorescence (cholorophyll/turbidity) were acquired using ADCP/CTD and an autonomous underwater vehicle (Glider). The Glider survey focussed on detailed investigations of small scale features (filaments, eddies), which play a potentially important role in the communication between the shelf area and the open ocean.

A detailed sampling program of the water column for geochemical parameters was carried out. The main water sampling system consisted of 24 10 litre Niskin bottles attached to the CTD and rosette. Large volume water samples for the isotopic characterisation of neodymium (Nd) (20 litres) and silicon (Si) isotopes in the water masses of the coastal upwelling area and the Tropical Eastern Pacific and their mixing were taken. The extent of Si isotope fractionation induced by diatom productivity under different upwelling intensities will be determined and the influence of the Si signal advected with water masses on the dissolved Si isotope composition will be investigated. These data will be compared with the nitrogen isotope distribution of dissolved nitrate on the same samples and their controlling factors to distinguish effects of denitrification in the OMZ and biological utilisation in the surface waters. The information obtained from the biologically influenced Si and N isotope systems will be compared with the Nd isotope distribution. Nd behaves quasi-conservatively in the water column and its dissolved isotope composition is mainly controlled by water mass mixing. On the basis of these results all three isotope systems will be used as paleo proxies for the paleoceanographic reconstruction of water mass mixing and upwelling intensity within the SFB754 using the sediments recovered on the first two legs of M77.

The second focus of the geochemical work in the water column was the investigation of the origin and the mixing of trace metals and their biogeochemical cycling. Water samples were collected under trace metal clean conditions using GO-FLO bottles on the ship's own Kevlaer wire. Some of the trace metals, such as iron, are important biolimiting micronutrients that control nutrient utilisation in the nutrient replete surface waters of the High Nutrient Low Chlorophyll

(HNLC) areas off Peru. Their availability thus has a large impact on the marine bioproductivity and thus the strength and extent of the OMZ. This impact is linked to chemical speciation and residence time of the trace metals, and the role of colloidal and nanoparticles as carrier phases for example for phosphate and iron. The four transects covered the Fe-enriched near coastal high productivity areas and the Fe-depleted HNLC areas at a distance from the coast. In addition, the influence of the width of the shelf and thus the extent of mobilization and release of redox-sensitive metals such as Fe and Mn from the sediments was a goal of the sampling and measurements for the trace metal work, a part of which was also carried out during M77/1 and M77/4. The shelf is very narrow at the southernmost transect at 16°S and thus a small supply of redox-sensitive metals to the surface waters is expected, wheras the opposite is the case at the two northern transects. This work was supported by collecting large volume samples at 9 stations for Ra isotope measurements, which are released from the coastal sediments and can serve as a source tracer for dissolved trace metals. A further focus of the sampling and measurements of the trace metal work was the influence of the diurnal cycle of hydrogen peroxide on the dissolved Fe concentrations in the water column.

A large part of the cruise was dedicated to biological investigations of the nitrogen cycle, in particular nitrogen fixation and nitrogen loss. For these projects detailed, high resolution sampling of the water column was required, which was achieved by the operation of a Pump-CTD that allowed to sample waters down to a depth of 375 m at exactly the same water mass and to adjust to internal waves. A central scientific question with respect to nitrogen fixation is whether the OMZ and its effect on the overlying waters influence the community of N_2-fixing microorganisms (diazotrophs) and their activity and thus the overall input of new nitrogen into the ecosystem. The direct ([O_2]) and indirect (N/P) effects of O_2 on rates of N_2 fixation and the functional gene diversity of the diazotrophs was examined using a variety of approaches ranging from vertical profiles of N_2-fixation to nutrient addition bioassays. In addition, microcosm experiments and phytoplankton competition experiments enabled an assessment of pelagic community response. A metagenomic approach will be used to determine the extent to which phylogenetically-related diazotroph ecotypes are adapted to specific nutrient stoichiometry and O_2 concentrations.

In the Peruvian OMZ substantial loss of total nitrogen occurs, which has mainly been attributed to denitrification (reduction of nitrate to N_2 by heterotrophic bacteria). Recently it has been shown that the anammox process (the anaerobic oxidation of ammonium by nitrite to yield N2) rather than heterotrophic denitrification is mainly responsible for nitrogen loss in oxygen-deficient upwelling regions and anoxic basins. This does, however, require a supply of ammonium under oxygen-depleted conditions. The main objective during this cruise was to examine how aerobic and anaerobic processes including the involved microorganisms influence and control the nitrogen cycle with a particular focus on the oxygen-sensitivity of anammox and nitrification.

A further main goal of the biological projects was to analyse how phytoplankton and zooplankton respond to changes in the N:P supply ratio to surface waters. This work was carried out by a field sampling program using plankton nets and by on-board mesocosm experiments. Phytoplankton and zooplankton were sampled for analysis of their taxonomic and functional type composition and biomass stoichiometry (C:N:P). Composition and stoichiometry of the plankton will be related to the in-situ nutrient regime. In the on-board mesocosm experiments,

the response of phytoplankton and zooplankton (growth rate, composition, biomass stoichiometry) to experimentally manipulated N:P ratios was studied.

3.3 Narrative of the Cruise

Cruise M77/3 started in Guayaquil/Ecuador, where the scientists from the IFM-GEOMAR in Kiel and the MPI for Marine Microbiology in Bremen arrived in the early morning of the 26th December and were directly transferred to the ship. One additional scientist from the MBARI in Monterey, U.S.A. had already arrived on the 24th December and one scientist from the cooperative partner institute of IFM-GEOMAR in Peru, the IMARPE in Callao, also arrived on the 26th December. The air freight had arrived with the exception of a spectrometer and the containers were already on board so that unpacking and moving of equipment into the laboratories started immediately. Installation of the PUMP-CTD of the MPI in Bremen and its dedicated winch started under supervision of K. Wlost, a technician who had been flown in for this purpose from IOW in Warnemünde. Meteor left the pier in Guayaquil at 3:00 UTC on the 27th December to remain at anchor near the harbor for another 6 hours in order to finalize the installation and testing of the PUMP-CTD. At 8:00 UTC this work was finished successfully and the technician left Meteor with the customs boat.

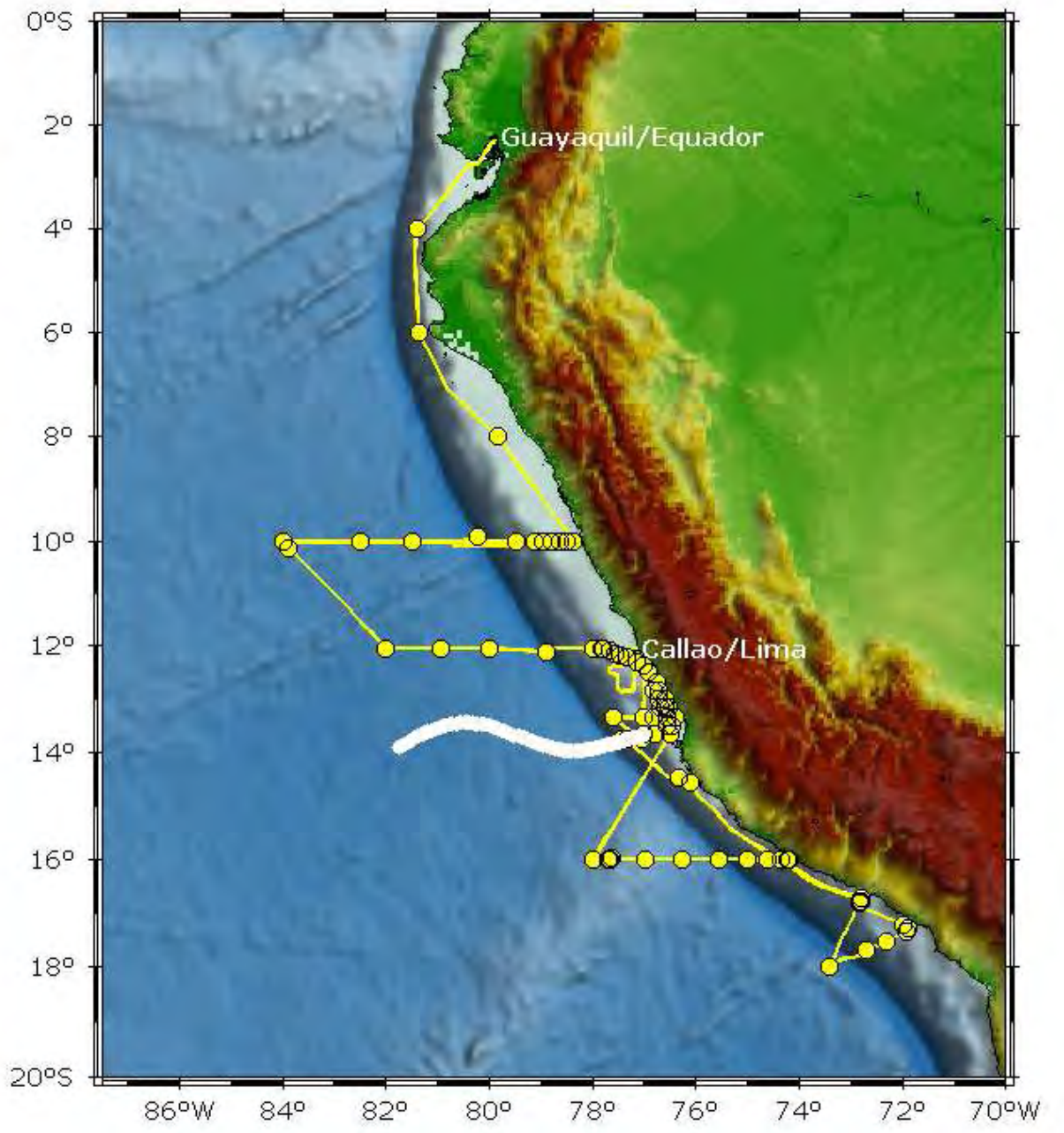

Fig. 3.1: Working area and cruise track of Meteor 77/3. The white line marks the pathway of the deployed glider

The ship then steamed towards the endpoint of the first planned section at 10°S, 78°23'W (Fig. 3.1). On the way the water column was sampled at 2 stations down to 1000m depth (4°S, 6°S) and at 8°S on the shelf (140 m depth). The first 6 CTD casts for the collection of water samples using the Niskin bottles on the CTD-rosette were deployed. Routine sampling in the upper 150 m was carried at a resolution of 10-20 m due the large gradients in biologically controlled parameters, whereas below 150 m depth samples were only taken every 100-200m. Due to partially damaged cables on the W2 and W3 winches, sampling was restricted to the uppermost 1800m of the water column, which was sufficient for essentially all goals of the

cruise. Routine sampling in the uppermost 150 m generally included samples for cholorphyll, POC/PON, POP, biogenic opal, DOC, DON, DOP, and dissolved CO_2. Calibration samples for oxygen content and salinity, and large volume samples for Nd and Si isotopes were also obtained from greater depths. At the station at 6°S the GO-FLO bottles on the ship's Kevlaer wire to guarantee trace metal clean sampling were tested and following the station at 8°S, the towed fish for trace metal clean sampling of surface waters was tested successfully.

The ship arrived at the endpoint of the first transect at 10°S, 78°23'W on the shelf (110 m water depth) at 7 a.m. on the 30th December. During the following almost 24 hours a detailed sampling of the water column was undertaken using CTD rosette, PUMP-CTD and GO-FLO, as well as in situ pumps and plankton nets for the particulate fraction. On this and the following PUMP-CTD stations, which lasted between 6 and 9 hours each, the microbiologists collected a large amount of water samples at a high depth resolution of up to 1 m to carry out incubation experiments with various ^{15}N-, ^{13}C, and ^{18}O-labeled substrates and in order to investigate the nitrogen cycle (nitrogen loss and nitrogen fixation). The in situ pumps were run for about 3 hours each from the wire on winch W3, whereby always 4 pumps were attached at different depths The 5 GO-FLO casts on that day served to collect trace metal clean samples to measure the diurnal cycle of the concentration of reduced Fe as a function of the availability of hydrogen peroxide. At this station the on board mesocosms of the plankton biologists were for the first time filled with 900 litres of surface water from the CTD rosette to conduct cultivation experiments with different N:P ratios.

On 31st December the section along 10°S was continued with 5 more stations at a 10 nm spacing down the continental slope (Fig. 3.1) using the CTD rosette and the PUMP-CTD until a water depth of 350 m was reached. Between 21:00 on 31st December and 13:40 on the 1st of January a detailed profile of the surface water parameters was taken with the ship's own CTD system and the 75 kHz ADCP in order to investigate the highly variable surface current system in this region. The section at 10°S was continued with further 5 stations at water depths between 1650 m and 6300 m at a spacing between 20 and 90 nm until the endpoint was reached at 84°W and a water depth of 4540 m at 1:00 on 4th January (Fig. 3.1). Altogether 11 stations were sampled on this section including 19 CTD casts, 4 PUMP-CTD casts, 9 GO-FLO casts, 6 in situ pumps, and 7 plankton nets. There were electric problems with the cables on winches 2 and 3, which required two 3 hour test stations on 3rd and 4th January, at the last one of which it was possible to shortly switch on the CTD for a few minutes on W2 and close several Niskin bottles for large volume samples for Nd and Si isotope analyses at depths greater than 1800 m.

After a 14 h transit the second section at 12°02'S started at 19:30 on January 5th at the outermost station at 82°W and a water depth of 4750m. The section was continued at 12°02'S with a spacing of 30 to 90 nm until 77°47'W was reached at a water depth of 350m (Fig. 3.1). Due to the minimum 5 nm distance from the coast, the section was continued from there to 12°22'S, 77°W with a closer spacing of stations of about 10 nm. The end point of the section at 90 m water depth was reached on 10th January at 3:20 in sight of the harbour of Callao, where the most extreme oxygen depletion accompanied by dissolved H_2S in the water column was found. At three stations (7th January: down to 2000m, 8th January down to 700m and 350m) profiles of large volume water samples (20 l each) were collected for Ra isotope analyses. Altogether 13 stations were sampled on this section including 25 CTD casts, 4 PUMP-CTD casts, 4 GO-FLO casts, 3 in situ pumps, and 5 plankton nets. For the second mesocosm

experiment of the plankton biologists 900 litres of surface water from the CTD rosette were provided on the 8th January. The GO-FLOs were used to collect samples for a second set of measurements of the diurnal cycle of reduced Fe/hydrogen peroxide on the 8th January. In addition, the towed fish was used to provide clean water for the incubation experiments of the microbiologists and one further test of the cable on winch 2 was conducted.

On the transit to the section at 16°S a glider was successfully deployed from the zodiac at 13°40'S, 77°W and was tested between 13:30 and 18:30 on the 10th January. The glider successfully operated in autonomous mode from deployment until it was picked up again by Meteor on the following 4th leg of M77.

Work on the third section at 16°S started at a water depth of 3400 m at 78°W on January 11th and continued until 17:00 on January 15th. The mesocosm experiments were filled with 900 litres of surface water from the CTD for the third set of experiments on 14th January. Similar to the previous two sections spacing of the stations on the shelf was smaller than in the open ocean and resulted in 16 stations in water depths between 6170 m and 110 m on this section (Fig. 1). 4 additional CTD casts and a plankton net on this transect were carried out to sample the water column and the plankton in a bloom of ciliates that the ship met on 11th January at 16°S, 77°40'W. At three stations (13th January: down to 1800 m, 14th January down to 700 m and 250 m) profiles of large volume water samples (20 l each) were collected for Ra isotope analyses. In total 19 CTD casts, 3 PUMP-CTD casts, 5 GO-FLO casts, 3 in situ pumps, and 10 plankton nets were operated on the 16°S section. Two more cable tests revealed that the relatively new cable on winch 2 was broken and therefore it was decided that the cable should be replaced by a new one in Callao in order to guarantee operations for the following 4th leg.

The ship then steamed south to the starting point of the fourth shorter section perpendicular to the coastline at 17°13.3'S, 72°W. On the transit three additional CTD casts and 2 plankton nets were operated to sample the narrow shelf to monitor the N-S variability of the hydrography on the shelf and top take samples for the water mass tracers and metals released from the sediments. Interesting patterns of low oxygen distribution and a deep chlorophyll maximum were detected at 16°49'S, 72°50'S and it was decided to revisit this station on the way back north after finalizing the section work. The section work started at 18:00 on 16th January and continued to the end point of the section at 18°S, 73°25'W at 19:00 on the 17th January. On this section 6 stations including 6 CTD casts, 1 PUMP-CTD, 3 plankton nets and 3 GO-FLO profiles were operated. The ship then steamed back to the coast in northeasterly direction to re-occupy the previously identified station on the shelf with the PUMP-CTD but it turned out that an intrusion of open Pacific waters had completely removed all previously observed patterns including the deep chlorophyll maximum. The ship then steamed north to investigate the deep chlorophyll maximum observed by the glider at ~14°N with 2 PUMP-CTD and 2 in situ pump stations at , which was carried out between 17:00 on 19th January and 23:00 on the 20th January. These casts were bracketed by a set of GO-FLO casts to collect samples for a third set of measurements of the diurnal cycle of reduced Fe/hydrogen peroxide.

The remaining ship time on the way back to Callao was used for a detailed survey of the shelf hydrography given that it was found highly variable on time scales as short as 48 hours at the station at 16°49'S and given that the most extreme sulphidic conditions had been found at the end of the 12°S section at a station south of Callao. From a position immediately north of the Paracas national reserve 13°30'S to 12°20'S large areas of the water column on the shelf

shallower than 150 m contained dissolved H_2S. A detailed mapping of the H_2S occurrence on the shelf was carried out by 15 shallow CTD stations and 2 last PUMP CTD stations between 10:00 on the 21st January and 18:00 on the 22nd January.

The ship reached the harbor of Callao on January 23rd in the afternoon (local time) and the cruise ended with the disembarking of the scientists between late afternoon and evening of the 24th of January. On 26th January the chief scientists of M77/3 and the following M77/4 and a number of the members of the science party of both legs participated in a joint seminar series at IMARPE in Callao (the partner institution of IFM-GEOMAR, Kiel), which was organized by IMARPE scientists on behalf of the cruises. At the same time several scientists of M77/3 were still busy organizing the shipment of frozen samples (-80°C and -20°C) with World Courier through harbor authorities, customs, and airport authorities, which lasted until the night of the 26th January.

3.4 Preliminary Results

3.4.1. Hydrographic Observations (CTD-O-Chl, ADCP, Glider)

(G. Krahmann, N. Nunes, M. Vogt)

Hydrographic measurements were collected using a variety of systems, including a CTD-watersampler system with dissolved oxygen and chlorophyll sensors, a Vesselmounted ADCP system, and an Autonomous Glider. The objective was to achieve a detailed picture of the currents prevailing in the research area and their origin and variability. A particular focus was the distribution and variability of the oxygen and chlorophyll content as a function of hydrography.

3.4.1.1 Tools

CTD-WATERSAMPLER data were collected to provide a detailed picture of the water mass distribution in the research area. The CTD system measured physical parameters such as temperature and salinity as well as dissolved oxygen and chlorophyll concentration. The system was equipped with 24 10-liter sample bottles for the collection of waters for calibration purposes and to provide water samples for various other groups.

VESSELMOUNTED ADCP systems were used to measure upper ocean currents while the vessel was underway or on station. Together with the water-mass information obtained from the CTD, spreading pathways of water masses and physical processes were investigated.

AUTONOMOUS GLIDERS augment hydrographic data collected from ship-based systems. A second platform from which measurements can be performed greatly enhances the potential for a detailed understanding of the observed data and delivers data in a resolution that cannot be achieved with ship-based observations of the water column. On this cruise a Glider system was for the first time used in conjunction with ship-borne techniques.

3.4.1.2 Methods

In total 111 CTD profiles were taken with the CTD-WATERSAMPLER. The CTD-system used was a Seabird (SBE) 9 plus owned by IFM-GEOMAR (SBE-5 with serial number 09p10108-0410), to which a pressure sensor was connected (s/n 61184). Two independent sets of temperature, conductivity, and oxygen sensors were used. T: s/n 4867 and 2120, C: s/n 2537 and 1494, O: s/n 0215 and 0992. A fluorescence (Chlorophyll A, no serial number) sensor was also attached to the

CTD. An altimeter was installed and reliably used for bottom approaches to within 5m of the sea floor. Because of problems with the ship's two coaxial cables (winches WP2 and WP3) routine CTD casts could only be operated from surface to 1800 m depth. Initially WP2 with a relatively new cable was used for deeper stations, but very intermittent and not reproducible shorts in the cable forced us to go to the backup winch WP3 with only 1800m of reliable cable. After leg M77/3 the apparently broken cable on WP2 was replaced (originally intended for the broken cable on WP3). For a few stations WP2 was used to lower the CTD to greater depths than 1800 m and the CTD system was only switched on to close the Niskin bottles. Except for the CTD's pressure sensor all sensors had calibrations from within the past two years. The two oxygen sensors were calibrated in June 2008 with a new type of calibration that is aimed at reducing the hysteresis between down- and up-casts. During the cruise it was found that the secondary sensor still had a hysteresis of more than 5 µmol/kg. Examining data from cruise leg M77/1 during which this sensor was first used showed that it had exhibited this problem from the beginning of M77/1. The Seabird bottle release unit used with the rosette worked properly until profile 73, when the release unit failed. The whole rosette and water sampling system was exchanged for the spare one while the reliably working CTD system was kept.

For calibration purposes water samples were taken from the Niskin bottles at most stations. Bottle salinities were determined with a Guildline Autosal salinometer (Kiel AS7), which was set up at the very beginning of the cruise. In general, the unit worked reliably but showed some drift during each of the measurement sessions. Through regular measurements of standard and substandard water (collected at one of the few deep CTD casts) a drift of up to 0.004 PSU will be corrected. The CTD values to be calibrated were chosen from the downcast profiles only in order to avoid hysteresis and rosette wake problems. Calibration of the CTD conductivity sensors was carried out for the 111 profiles using a total of 424 samples. Routinely the third of CTD-lab-value pairs with the largest deviations were tagged and removed from the calibration analysis. Control plots showed that these points were mostly located in the high gradient zone directly underneath the surface mixed layer. After correcting the conductivity with respect to temperature, pressure, and conductivity itself, the rms difference between the bottle samples and the CTD's primary sensor was 0.00030 mS/cm, corresponding to 0.0028 PSU in salinity.

Oxygen concentrations were determined from 299 bottle samples using the Winkler titration method. After correction for pressure and temperature, the rms difference between bottle data and sensor was 2.1 µmol/kg for the oxygen concentrations. The extremely low oxygen content prevailing in the research area posed a problem for the accuracy of the oxygen measurements. Our standard Winkler titration system was obviously limited in accuracy for samples that did not contain any oxygen whereas the titration system never showed values below 1 µmol/kg. A modified calibration may be needed in the case of very low oxygen waters in the future. Chlorophyll A samples were taken and analyzed from 376 bottles on board. At present the final calibration for Chlorophyll A content is not finalized.

A preliminary calibration of the two temperature sensors shows differences of about 0.0018°C, while the two conductivity sensors differ by about 0.0007 PSU. Since the second oxygen sensor was not working well, no comparison values were calculated. To obtain consistent values only the primary sensors will be used for the final calibration.

Sections of current velocities were obtained with a vesselmounted 75 kHz shipboard ADCP. A 38 kHz instrument was also used initially, but abandoned after the 10°S section due to

persistent malfunctions which could not be fixed with the engineers on board and with the help of the RDI Field Service. A replacement cable for the 38 kHz instrument was ordered, to ensure reliable operation of the ADCP during the following leg M77/4. Both instruments installed on the FS Meteor are RDI Ocean Surveyors.

Initially, a broadband setup for the 75 kHz instrument with 100 bins of 8 m each was used. Due to the occurrence of gaps in the data in the Oxygen Minimum Zone (OMZ) during the 10°S section and the poor quality of the 38 kHz data, the setting was changed to 50 Bins of 16 m size (narrow-band) at the beginning of the second transect. No gaps in the OMZ data were encountered any more after this change. During stations, heavy interferences were caused by the DopplerLog acoustics used by the bridge to assist in keeping precise position. During the night from January 6th to 7th the Ashtec GPS (ADUII) lost satellite contact and needed to be restarted, which caused gaps in the ship heading and position supplied to the ADCP. Shorter gaps in the navigational data from a few seconds to 5 minutes occurred more frequently, but weren't a problem in processing the data.

Two autonomous glider systems of IFM-GEOMAR (ifm02 and ifm05, manufacturer units #36 and #87) had been prepared for the cruise. Unit ifm02, equipped with long endurance Lithium batteries, was to be deployed at the beginning of the cruise while unit ifm05 was to be deployed after about two thirds of the cruise. Both units had CTD, oxygen, fluorescence, and turbidity sensors and were prepared deployment ready. Unit ifm02 had been prepared at IFM-GEOMAR, but had not undergone thorough testing due to insufficient time before shipment to FS Meteor. Unit ifm05 had been prepared by the manufacturer. During the preparations for the deployment of ifm02 it became clear that the unit's CTD sensor was not delivering data. Despite advice from the manufacturer and opening of the glider it was not possible to fix this problem, which led to the decision not to deploy the glider. Unit ifm05 was prepared for deployment as intended. Testing in the ship's pool on the main deck proved to be very helpful and showed that all sensors were working properly, that it was able to descend and ascend in the local surface water, i.e. it was properly ballasted, and it was able to communicate with the land station at IFM-GEOMAR via the Iridium satellite network. The deployment took place during the morning of January 10th 2009 at 13°40'S, 77°W. At wind force 4-5 and seas of about 2 m the glider was loaded into FS METEOR'S zodiac and together with three persons lowered into the water. At a safe distance the glider which had been started on deck, was lowered into the water by hand. During the initial dive a safety buoy with 30m of rope was attached to the glider. The glider managed to reach the target depth of 20 m and resurfaced 15 minutes later. A second successful 20 m dive without safety rope followed. Subsequently the dive depth was raised to 150 m and then 500 m. After the 150 m again contact could be made to the glider via radio communication and the initial data were downloaded. After the 500 m dive no contact could be established and we waited for the maximum time the glider should need for such a dive. This failed contact was despite the ship's location within 2 nautical miles of the expected surfacing location, a distance over which there is usually unproblematic contact. After the missed contact the colleagues at the station in Kiel were called and confirmed that the glider had surfaced as expected and was already on the next dive. The glider was recovered during leg M77/4.

3.4.1.3 Results (Shipboard)

The CTD data document the extent and variable thickness of the oxygen minimum zone that was a central goal of the cruise. The vertical extent of the oxygen minimum was highly variable. During strong upwelling, waters without observable oxygen were found at water depths of only 3m on the shelves. Away from the shelves, waters without measurable oxygen were generally found at depths below 30-100 m (Fig. 3.2). In addition, internal waves caused variations of the upper boundary of the OMZ by several 10s of meters within hours. Besides the usual chlorophyll maximum near the surface, a pronounced second maximum at depths of 80-150 m within the oxygen minimum was observed between 10°S and 14°S, which may have been caused by cyanobacteria.

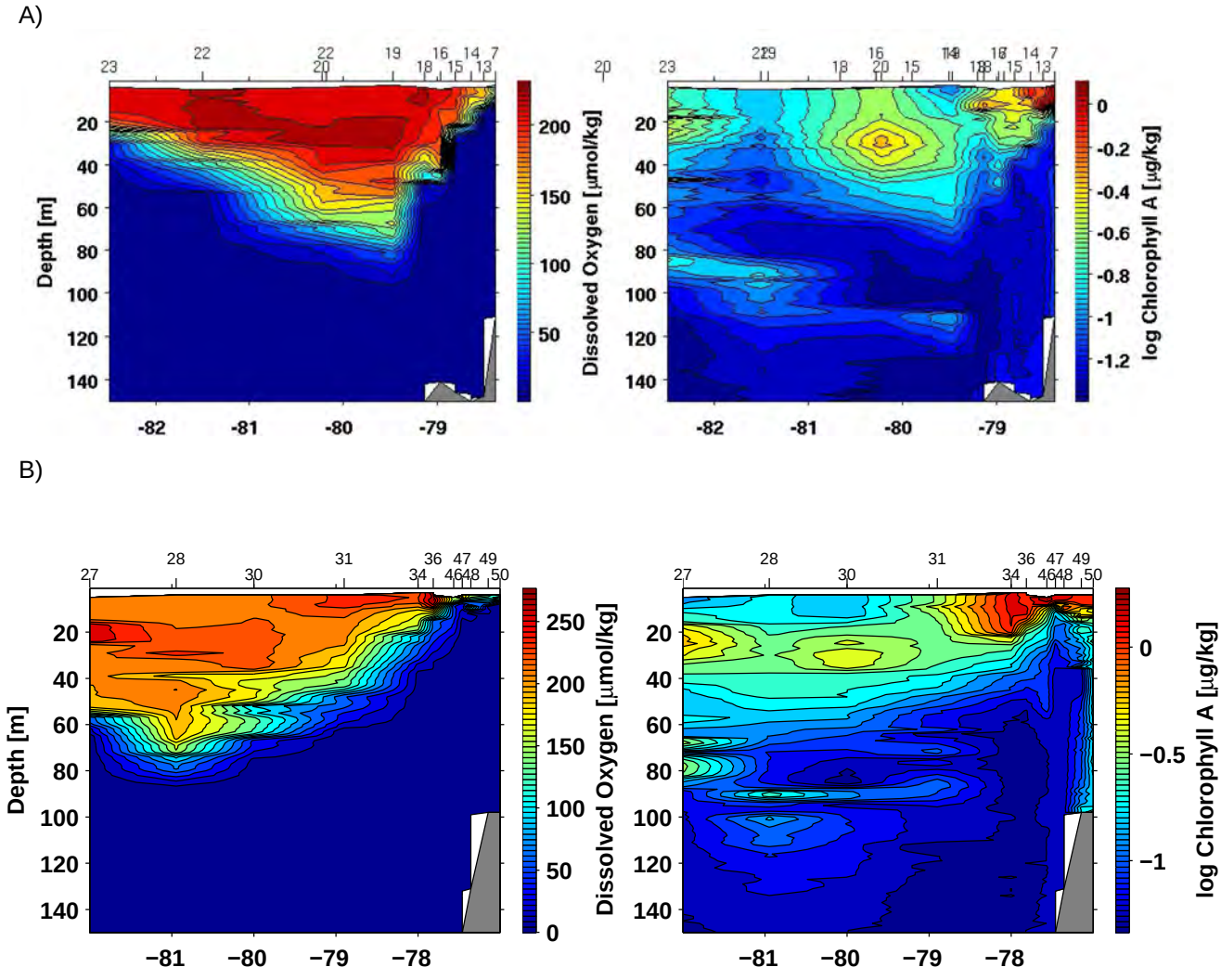

Fig. 3.2: Dissolved oxygen and chlorophyll contents observed by the CTD-O-Chl system on the section at A) 10°S, B) 12°S. The numbers on the x-a xes of all plots denote western longitude.

C)

D)

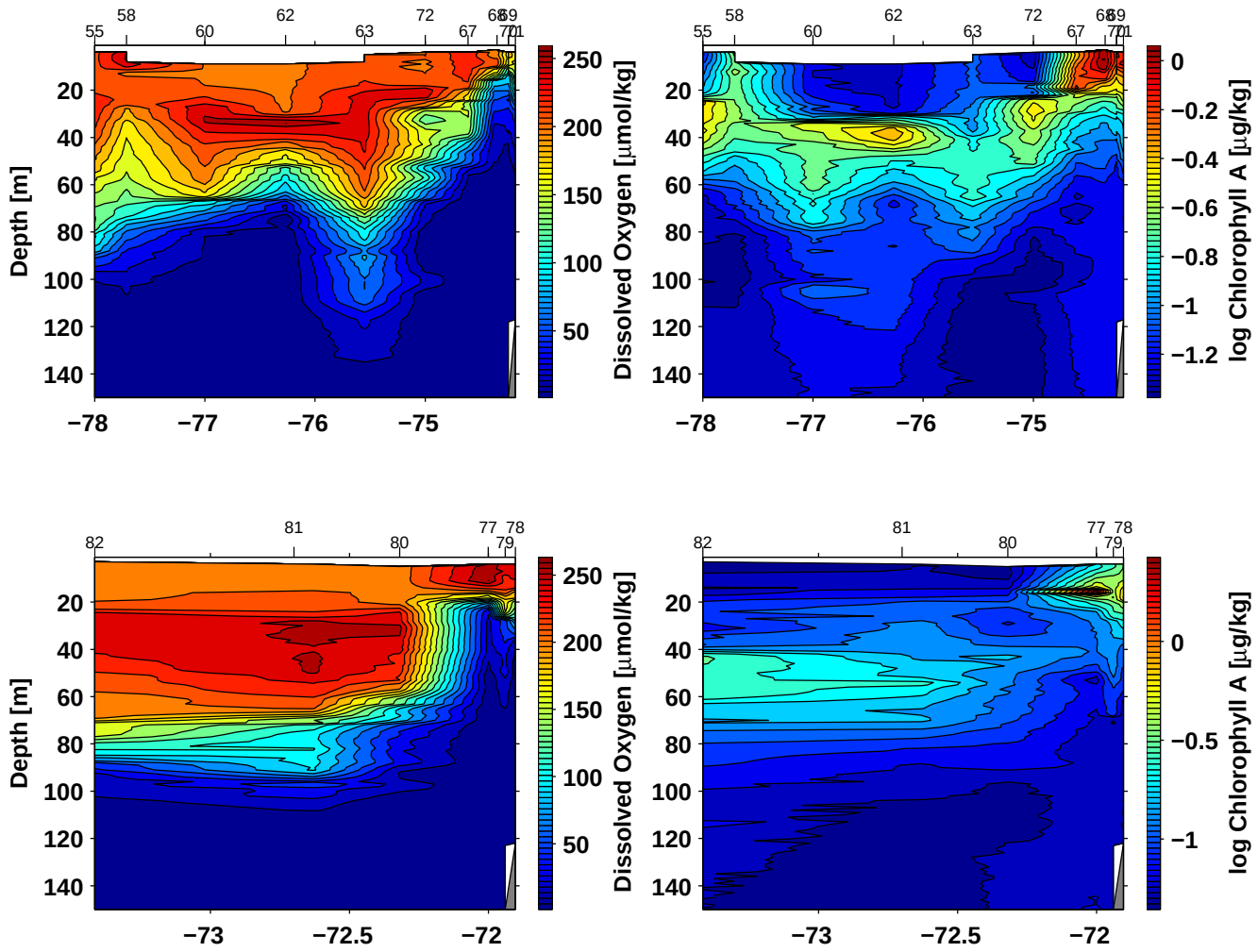

Fig. 3.2 (continued): Dissolved oxygen and chlorophyll contents observed by the CTD-O-Chl system on the section at C) 16°S, D) 17.13°S-18°S. The number s on the x-axes of all plots denote western longitude.

Fig. 3.3 shows the average current vectors between 50 and 100 m depth obtained with the 75 kHz ADCP (Fig. 3). These results indicate a high variability but the patterns are generally in good agreement with the current structure described by Karstensen et al. (2009).

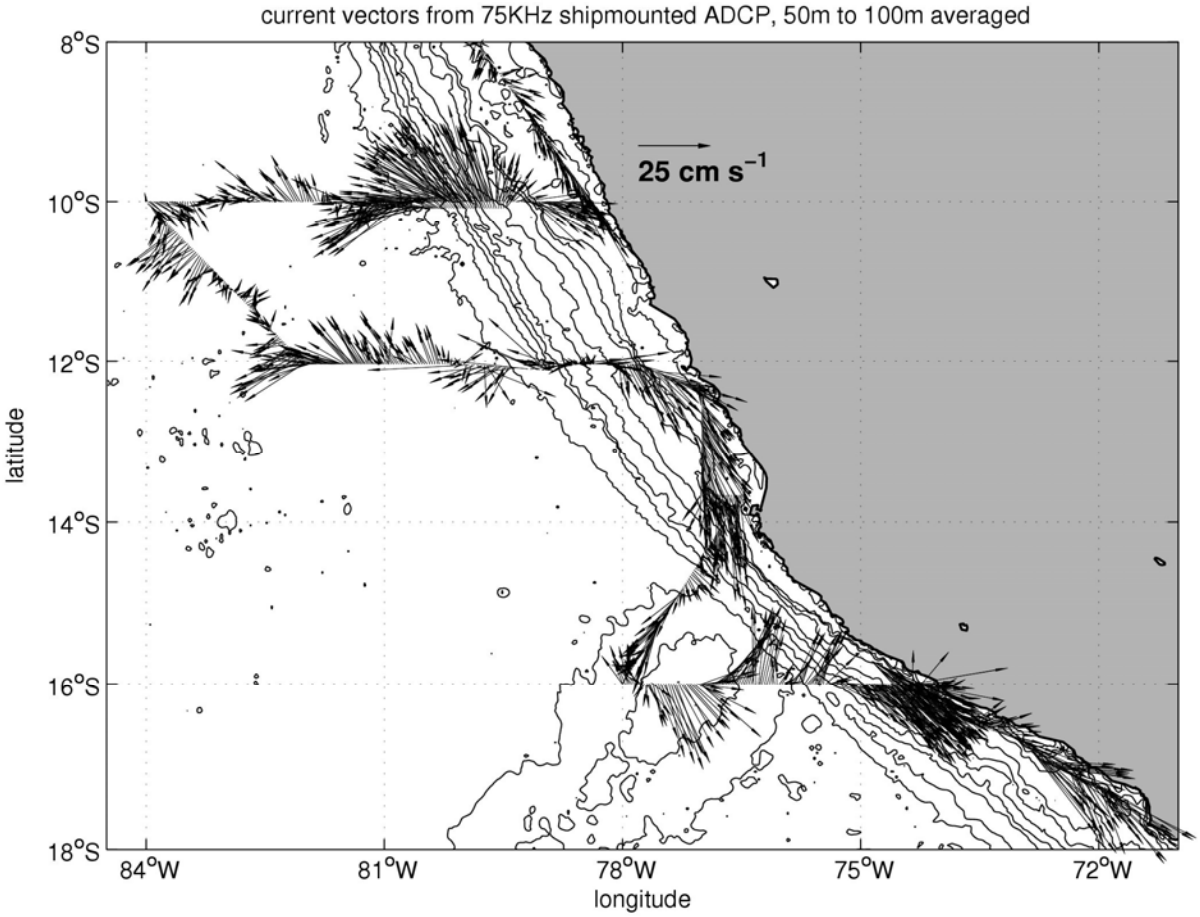

Fig. 3.3: Current vectors from 75 kHz ADCP averaged between 50m and 100m depth.

Four zonal sections were obtained with the 75 kHz ADCP. The sections at 12°S and 16°S are shown as examples. In the 12°S section the poleward Peru Chile Undercurrent (PCUC) at water depths from 0 to 300 m depth is clearly visible near the coast (e.g. Karstensen et al., 2009). A second poleward flow around 80°W occupies the entire water depth between the surface and 700 m, which is the Peru Chile Counter Current (PCCC). Northward flowing water masses are the Peru Coastal Current (PCoastalC) around 78.5°W and the much more pronounced Peru-Chile Current (PCC) around 81°W. The separation between polewards flowing PCUC near the coast and the PCCC separated by the equatorward flow of the PCoastalC are clearly more pronounced at the section at 16°S, which most likely is caused by the westward deflection of the currents north of 15°S.

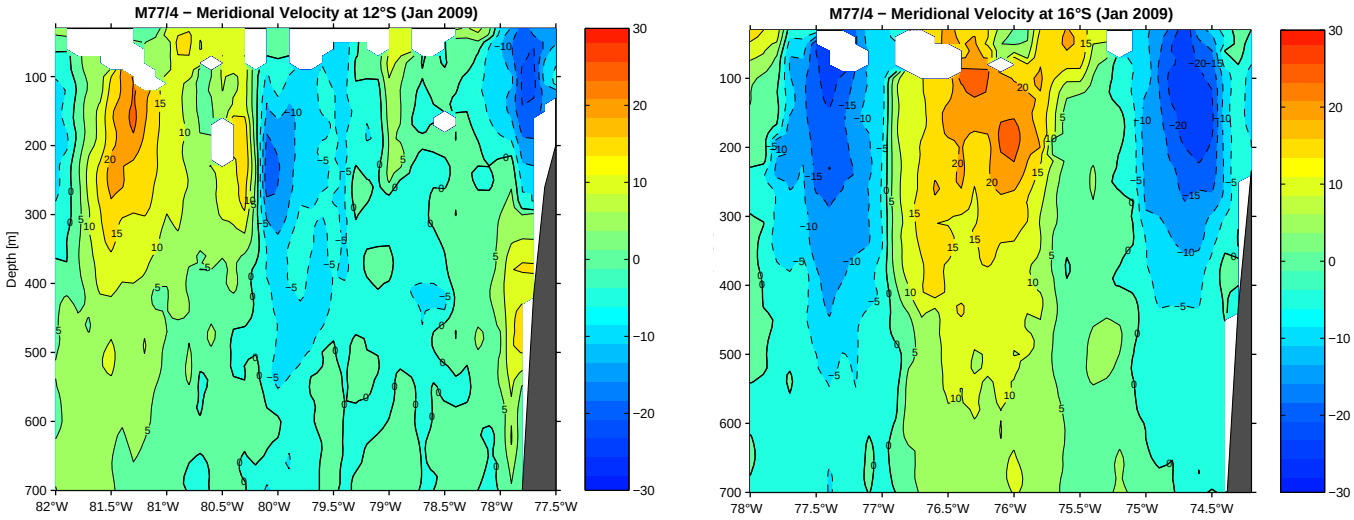

Fig. 3.4: Meriodional velocity in cm/s along 12°S and 16°S m easured by the 75 kHz Ocean Surveyor. Negative numbers and blue fields mark poleward flow and orange and red fields mark equatorward flow.

The glider data shown in Fig. 5 were received by the land station in Kiel during M77/3 and M77/4.

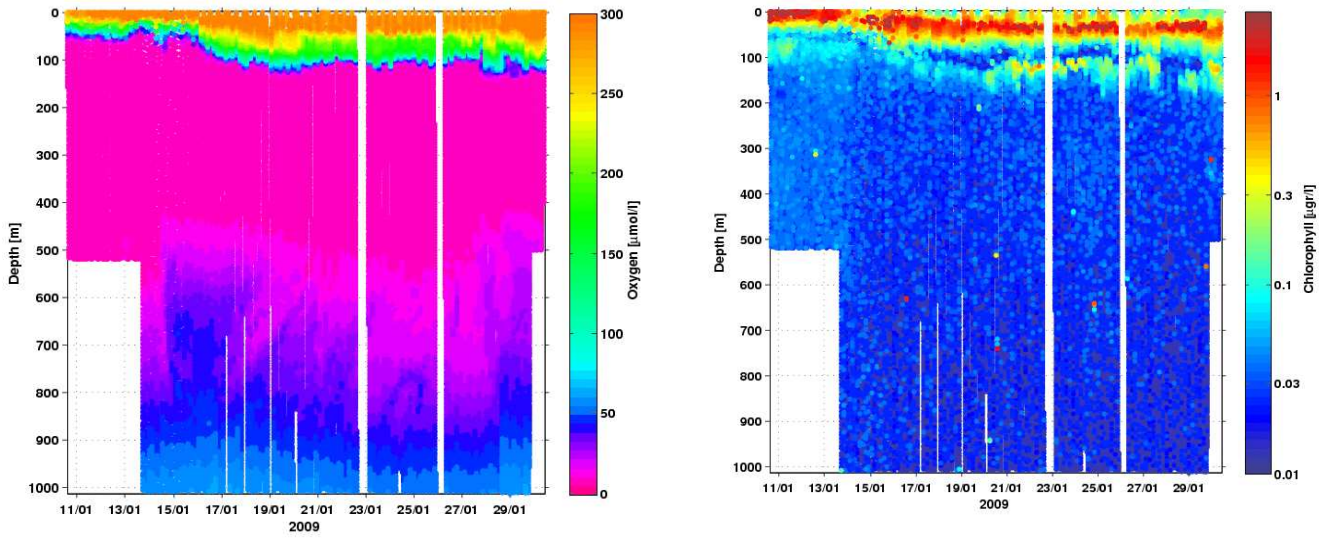

Fig. 3.5: Dissolved oxygen and chlorophyll concentration measurements obtained by the glider. Clearly visible is a different regime near the continental shelf break on the left of the graphs in comparison with the open ocean on the right side of the graphs. There is a remarkable secondary chlorophyll maximum at depths of 100-150 m depth within the oxygen minimum, possible caused by cyanobacteria.

3.4.2. Nitrogen Cycling in the Oxygen Minimum Zone off Peru

(G. Lavik,T. Kalvelage,S. Contreras,A. Paulmier,G. Klockgether,A. Ellrott)

3.4.2.1 Objectives

In many oceanic regions, growth of phytoplankton is nitrogen limited because fixation of N_2 cannot make up for the removal of fixed inorganic nitrogen (NH_4^+, NO_2, NO_3^-) by anaerobic microbial processes. Globally, 30-50% of the total nitrogen loss occurs in oxygen minimum zones (OMZs) and is commonly attributed to denitrification (reduction of nitrate to N_2 by heterotrophic bacteria). However, it has previously been shown that the anammox process (the anaerobic oxidation of ammonium by nitrite to yield N_2) rather than heterotrophic denitrification is mainly responsible for nitrogen loss in oxygen-deficient upwelling regions and anoxic basins. With insignificant remineralisation of organic matter due to heterotrophic dentrification to N_2 in these waters there has to be an alternative pathway providing NH_4^+ as a substrate for anammox. In a recent study of the OMZ off Peru, it has been shown that dissimilatory nitrate reduction to ammonium (DNRA) and microaerobic respiration are the main processes fuelling anammox bacteria. NO_2^- on the other hand might be provided by nitrate reduction to nitrite or aerobic ammonium oxidation (nitrification) at low but non-zero oxygen concentrations as has already been demonstrated for the Black Sea, where zones of active nitrifiers, as well as anammox bacteria overlap. The finding that anammox occurs at oxygen concentrations up to several µM is surprising and implies that the water masses affected by N-loss are larger than assumed so far. The main objective during this cruise was to examine how these aerobic and anaerobic processes are regulated and coupled - including the identification and quantification of the involved microorganisms - with a particular focus on the oxygen-sensitivity of anammox and nitrification. We carried out experiments to determine respiration rates and recycling of organic matter in the Peruvian OMZ.

3.4.2.2 Methods and First Results of the PUMP-CTD Operations

We used a combination of high-resolution nutrient measurements, various $^{15}N/^{13}C/^{18}O$ incubation experiments and DNA/RNA-based techniques, as well as microsensors to investigate the processes responsible for nitrate/nitrite reduction, ammonium oxidation, remineralisation of organic matter and to determine respiration rates in the OMZ off Peru. In addition, we performed $^{15}N/^{18}O$-incubation experiments and high-precision O_2-measurements to investigate the impact of molecular oxygen on anaerobic and aerobic processes at specific stations.

A Pump-CTD (PCTD) system (Fig. 3.6A-D) allowed us to continuously pump water from the water column directly into the ship's laboratory (Fig. 3.6E) where it was sub-sampled for nutrients (NH_4^+, NO_2^-, NO_3^-, PO_4^{3-}, Si) at 1-2m resolution and analysed for gaseous compounds (N_2, Ar, O_2: Fig. 6F) online by membrane inlet mass spectrometry (MIMS: Fig. 3.6G). The PCTD rosette was additionally equipped with fast responding microsensors for oxygen, pH and sulphide as well as a so-called STOX microsensor, which can detect oxygen concentrations down to 20-30 nM (Fig. 3.6C). The STOX microsensor was generously provided by Prof. Niels Peter Revsbech from Århus University.

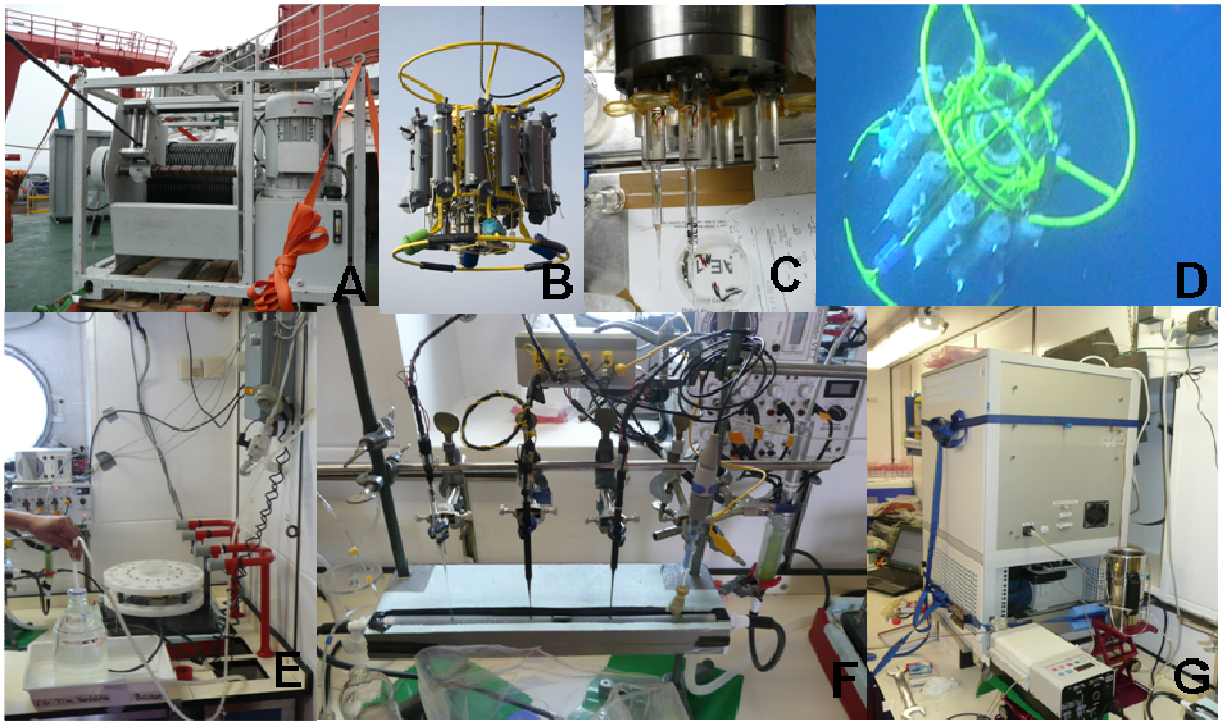

Fig. 3.6: Pump-CTD (PCTD) system. A) The PCTD uses a special cable with an integrated 6-mm wide pump hose that is operated with its own winch. The length of the pump hose cable allows PCTD operations down to 300 m water depth. B) Deployment of the PCTD over the side of the ship. C) Zoom in on the microsensors (2 O_2 normal microsensors, 1 STOX for ultra-low O_2, 1 for pH) of the pump-CTD. D) The pump-CTD in the water during the downcast. E) The auto-samplers for nutrient measurements. F) A pump rate of ~2.5 l/min allows electrochemical sensor measurements (O_2, H_2S, pH) in the water stream or sampling within 4 minutes after leaving the in-situ depth. G) the MIMS (membrane inlet mass spectrometry) for gaseous compound analysis (N_2, Ar, CH_4 O_2).

By the end of the cruise fifteen high resolution PCTD stations were carried out (Fig. 3.7A) with oxygen, nitrite and ammonium analyzed on board (e.g. Fig. 3.8). Complementary $H_2S/N_2O/N_2Ar$ measurements were performed at several stations (17, 19, 21, 22, 43, 59, 60, 62, 64, 65, 66, 67, 68, 69, 70, 71, 72, 73, 74, 75) associated with sulphidic events on the shelf close to the Peruvian coast (Fig. 3.7B).

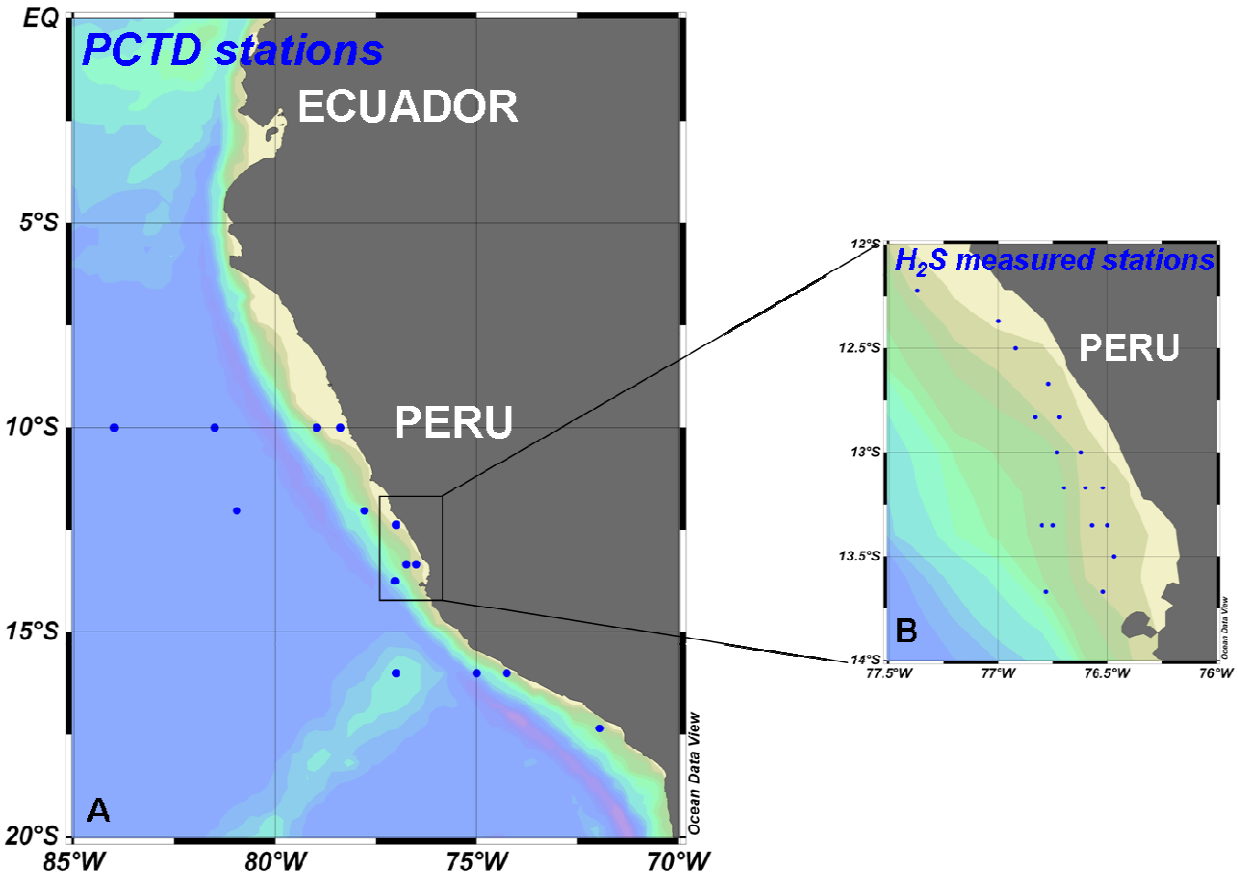

Fig. 3.7: A) Pump-CTD (PCTD) stations. B) Zoom on the area where sampling with emphasis on mapping of sulphide was carried out between Lima and the protected Paracas National reserve (small dots).

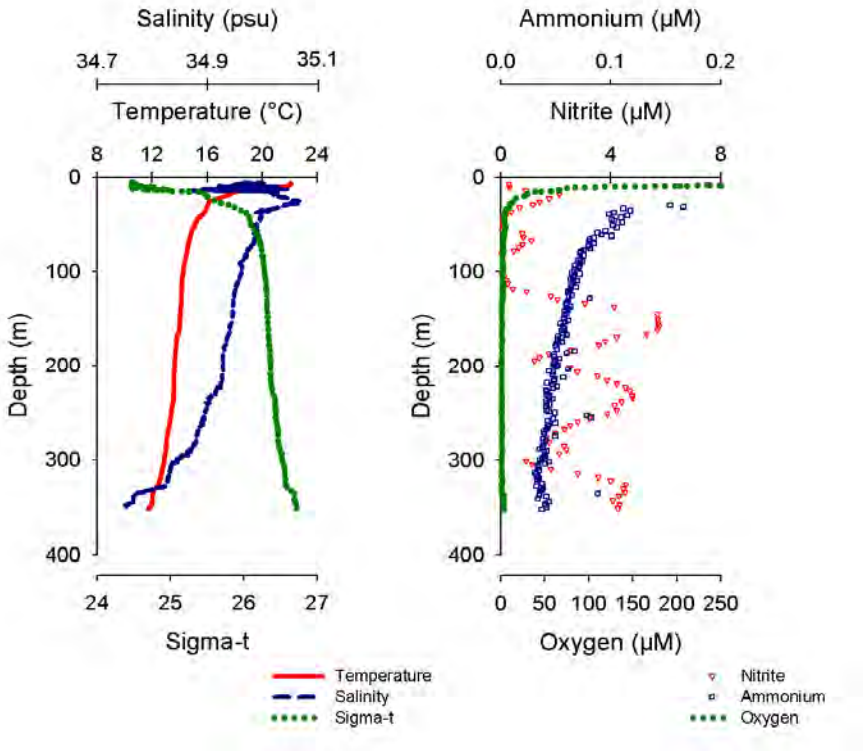

Fig.3.8: High resolution pump-CTD profiles (Station 13: 12°02.03' S/77°47.34' W). On the left panel the physical parameters (temperature, salinity, sigma for the density) from the classical CTD profile are displayed. On the right panel, oxygen content from the fast responding O_2-microsensors, as well as nitrite and ammonium content from the pump CTD are shown (all data are preliminary). The salinity maximum with low oxygen is associated with the poleward moving Peru-Chile undercurrent. Several nitrite maxima (>4 µM) are observable at this location, which might be water mass related or activity related. The uppermost nitrite maximum is at the base of the oxycline representing the uppermost extent of the OMZ at ~40m. For ammonium, no significant accumulation is observed, except at the base of the oxycline (~0.2 µM), probably related to the oxic remineralisation of organic matter.

3.4.2.3 Incubation Experiments

Water samples from the OMZ were collected from 3 to 6 discrete depths (max. ~375m) at those stations, where the Pump-CTD system was operated. After addition of ^{15}N-labeled substrates, as well as $^{18}O_2$, samples were incubated in 12 ml exetainers at in situ temperatures. All organisms in the sub-samples from each incubation experiment were killed after 0.3 (for $^{18}O_2$) 6, 12, 24 and 48 hours by adding 100 µl saturated mercuric chloride and were then stored at room temperature. The stable isotopic composition of the N_2 gas, as well as labelled products containing ^{18}O or ^{15}N (i.e. NH^{4+}, NO^{2-}, NO^{3-}, CO_2) will be analyzed by gas chromatography isotope ratio monitoring mass spectrometry at the Max Planck Institute for Marine Microbiology in Bremen (MPI Bremen). $^{18}O_2$ concentrations will be determined by MIMS.

To determine respiration rates in the various zones of the OMZ, ~2.5 L seawater samples collected at 2-3 depths at each pump-CTD station were incubated at in situ temperatures. The

decrease in oxygen over time was recorded using a STOX sensor, which is highly sensitive and allows the detection of O_2 concentration changes in the lower nM range.

At the same depths where incubation experiments were conducted (plus some intermediate as well as over- and underlying depths), up to 250ml of seawater were collected for 16S rRNA-targeted fluorescence *in situ* hybridization (FISH) and preserved with paraformaldehyde (1% final concentration) prior to filtration. At the same depths about two litres of water collected from each incubation depth were filtered to obtain particulate organic matter for DNA/RNA extraction. Filters (0.22 µm pore size) were stored at -80°C until further analysis at the MPI Bremen and will be used to identify and determine gene expression and the abundance of specific groups of microbes involved in nitrogen cycling, such as aerobic nitrifiers and anammox bacteria.

Furthermore, in order to directly link the identities of microbes to anammox, nitrification, nitrogen assimilation and remineralization activities on a cellular level, incubation experiments with ^{15}N- and/or ^{13}C- labelled substrates were conducted to determine bulk reaction rates, while at the same time samples for FISH-like analyses using the state-of-the-art nanoscale secondary ion mass spectrometry (nanoSIMS) at the MPI-Bremen were preserved. NanoSIMS analyses will facilitate to simultaneous determination of cellular activities and 16S rRNA identification on a single-cell basis. Using this novel technology, also the growth rates of marine anammox bacteria in the OMZ off Peru will be determined.

In addition, at each pump-CTD station samples to determine N_2/Ar, N_2O, DIC, POC/PON, O_2 (Winkler method) and $\delta^{18}O_2$ were taken. These parameters, as well as nutrients (all stations) were also sampled from the CTD-rosette stations at the same locations as the corresponding pump-CTD.

Tab. 3.1: Number of incubation depths, experiments, and sub sampling.

Station	INCUBATIONS		SUBSAMPLING									
No.	Depths (n°)	Experiments (n°)	DIC	N_2/Ar	N_2O	Nutrients	Amonium	Winkler	FISH/DNA	$\delta^{18}O$	POC/PON	Respiration rates
805-1	4	6	X	X	X	X	X	X	X	X		X
807-3	6	6	X	X	X	X	X	X	X	X		X
811-2	6	6	X	X	X	X	X	X	X	X		X
003-5	6	7	X	X	X	X	X	X	X	X		X
005-6	6	7	X	X	X	X	X	X	X	X		X
008-6	6	7	X	X	X	X	X	X	X	X		X
013-2	6	7	X	X	X	X	X	X	X	X	X	X
019-3	4	8	X	X	X	X	X	X	X	X	X	X
028-4	5	6	X	X	X	X	X	X	X	X	X	X
036-2	6	5	X	X	X	X	X	X	X	X	X	X
038-1	3	3	X	X	X	X	X	X	X	X	X	X
044-3	6	5	X	X	X	X	X	X	X	X	X	X
054-2	6	4	X	X	X	X	X	X	X	X	X	X
062-1	6	4	X	X	X	X	X	X	X	X	X	X
065-1	3	3	X	X	X	X	X	X	X	X	X	X
TOTAL	79	84										

3.4.2.4 Large Volume Filtration with In-situ Pumps

(G. Lavik,A Paulmier,C. Löscher)

Large volume water filtrations for chlorophyll, stable isotopic analyses and metagenome library were carried out at stations #807, #3, #8, #13, #28, #37, and #56 (Fig. 9).

Samples were generally taken from four depths at each station by four MCLANE WTS-LV Sampler (WTS 6-1-142LV) in-situ-pumps. During each pumpcast water was filtered on a GF/F and metagenomic filters (ø 150 mm) for 90 minutes with an average flow rate of ~6 L/min. Samples were stored at –80°C. In total, 20 GF/F and 20 metagenomic filters have been acquired, with a filtered seawater volume of between 60 and 700 L.

Fig 3.9: A) Deployment of one of the four In-situ Pumps B) Filters from four different standard depths. C) Highly charged GF/F filter from 45 m depth at station #13.

3.4.3. Nitrogen Fixation in the Peruvian Upwelling and the OMZ

(J. LaRoche,C. Löscher,T. Großkopf,H. Schunck)

3.4.3.1 Objectives

For the investigation of nitrogen fixation, DEPTH PROFILES were sampled for analysis of the composition of the microbial community in the euphotic zone, for the determination of absolute cell numbers, for the identification of key ecotypes, and in order to find genes involved in nitrogen fixation. In addition, samples for METAGENOMICS/METATRANSCRIPTOMICS were taken. The information obtained from these methods is by far more extensive than the analysis of single genes and provides a holistic picture of the composition of the microbial community and their activity at particular locations. In order to reveal the nutrients limiting phytoplankton and diazotrophic growth, and to compare nutrient uptake kinetics and measure nitrogen fixation rates, on deck incubation EXPERIMENTS were conducted.

3.4.3.2 Methods

Two liter samples were taken with the CTD rosette from the surface to 100 meter depth at a depth resolution of 10 meters. In addition samples from 150 and 200 m depth were taken and all samples were filtered through 0.22 µm Millipore DNA filters. The focus of these investigations was on the variability on the transects at 10° S and 16° S, which were sampled at high resolution by taking profiles from almost every CTD station. In parallel, 2 ml of seawater of each depth

where fixed with paraformaldehyde for later analysis in the flow cytometer. Chlorophyll-a samples from the euphotic zone (surface to 150m depth) where taken throughout the whole cruise. From each depth 500 – 2000 ml of seawater were filtered and the pigments were extracted with acetone. The fluorescence of the acetone extract was measured onboard and the chlorophyll-a concentration was calculated.

METAGENOMICS required sampling of at least 100 liters of seawater, which was achieved by deploying the in-situ pumps that filter several thousands of liters in two hours at depths of up to 2000 meters. For sampling of the surface waters the CTD-rosette was used. Surface water samples were prefiltered with a 10 µm filter to remove eukaryotes.

METATRANSCRIPTOMICS is restricted to a smaller amount of water as the crucial point is filtration time. Samples have to be filtered and frozen within less than half an hour to capture a gene expression profile that is representative of the environmental conditions prevailing at the time of sampling. Five to 7 liters were pumped with the Pump-CTD system from up to 365 meters depth directly into the laboratory on the ship within 6 minutes, where they were filtered and frozen within 20 minutes of sample collection.

Three types of EXPERIMENTS were conducted in triplicates during the cruise, which all consisted of on-deck incubations of seawater in seawater-cooled incubators that simulate a light attenuation at 15 m water depth. The typical incubation times were between 6 and 48 hours. At the end of each experiment samples for several parameters were taken, including carbon- and nitrogen content, chlorophyll-a content, DNA, flow cytometry, nanoSIMS, DIC, FRRf and label uptake (^{13}C bicarbonate or glucose and ^{15}N, N_2, NH_4^+, or NO_3^-).

3.4.3.3 Results (Shipboard)

DNA and flow cytometry samples were taken back to the home laboratory in frozen condition for further analysis. In total, 218 DNA and 218 flow cytometry samples were taken. Chlorophyll data revealed high biomass at the surface near the coast and deeper chlorophyll maxima further off the coast (Fig.3.10).

In total 9 METAGENOMICS profiles and 14 METATRANSCRIPTOMICS profiles were taken with up to seven depths per profile. Given that the analysis of each sample is very labour intensive, the sites of sampling where chosen for interesting events in the water column, such as deep chlorophyll maxima, sulfide enrichment, oxycline, core of the OMZ, etc. Selected samples will be analyzed and the choice of the samples will be determined once rate measurements have been finalized.

During the EXPERIMENTS large amounts of samples were generated, which will be analyzed in the home laboratory, such as for nitrogen fixation rate measurements. As a first result it can be deduced from chlorophyll data that at 18°S, the site of the last bioassay experiment, the phytoplankton community is limited by the availability of fixed inorganic nitrogen compounds (Fig. 3.11).

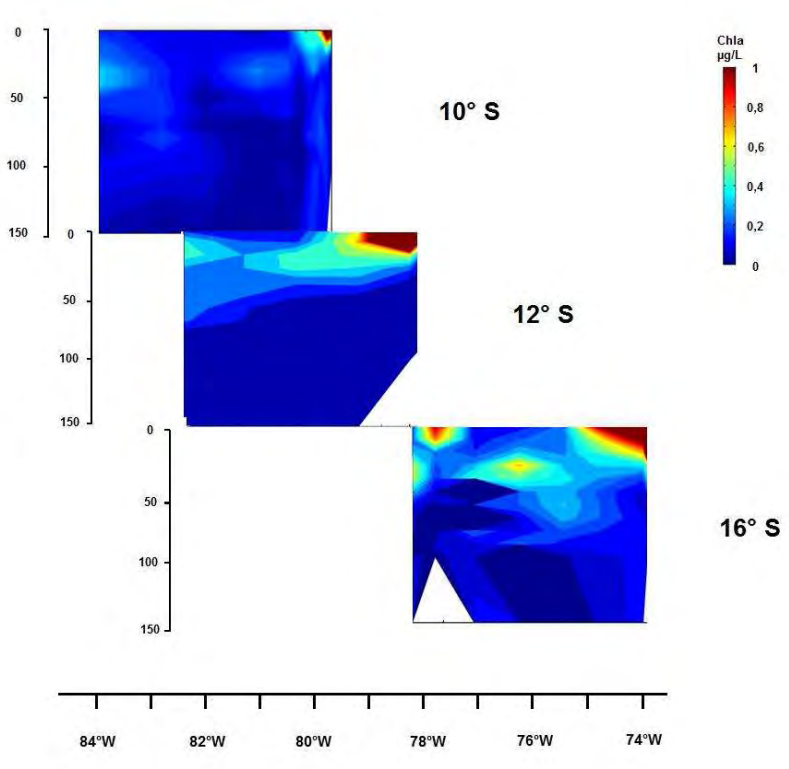

Fig. 3.10: Chlorophyll-a concentration transects in µg/L against water depth along the three transects at 10°, 12° and 16° south.

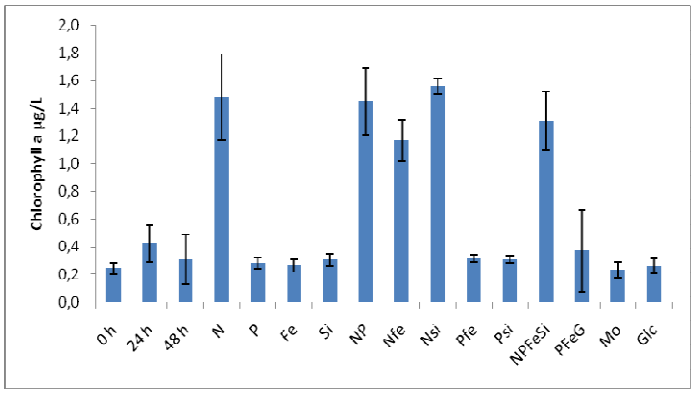

Fig. 3.11: Bioassay SFB 3; Chlorophyll-a concentration in µg/L versus amended nutrients. Each bar represents the mean of three bottle incubations. Error bar = 1 standard deviation in each direction. In all experiments, in which compounds containing N were added, an increase in productivity is clearly seen.

3.4.4. Pelagic Community Response to Changes in Nutrient Stoichiometry

(U. Sommer,H. Hauss,J. Franz,P. Fritsche)

Inorganic macronutrient inventories in tropical upwelling areas are increasingly influenced by growing oxygen minimum zones, since inorganic nitrogen loss occurs due to biological processes under sub-/anoxic conditions (denitrification, anammox). In addition, metal-bound phosphate is released from the shelf sediments under reducing conditions. Nutrient levels (Si, N, P) and their ratios determine the functional type, size structure, and species composition of the phytoplankton community, as well as its elemental composition. This, in turn, may affect the nutritional value of phytoplankton for primary consumers and higher trophic levels, as well as the efficiency of the biological pump.

3.4.4.1 Objectives

The goal of the goal of the cruise was to experimentally test the influence of N:P ratios on phytoplankton dynamics in on-board mesocosm trials. In addition, station work along transects was conducted to be able to describe the reservoirs and fluxes of macronutrients associated with the oxygen minimum zone, as well as the horizontal distribution of zooplankton.

3.4.4.2 Methods

We conducted three short-term (~7d) growth trials during the cruise. Furthermore, field sampling on 24 CTD stations along the four transects was conducted for POC, PON, POP, DOC, DON, DOP, phytoplankton pigments (HPLC), biogenic silicate (BSi) and transparent exopolymer particles (TEP), while samples for dissolved nutrients were taken by the MPI Bremen group to be measured in the home laboratory. The experimental setup comprised twelve 70L mesocosm bags that floated in four flow-through water baths for cooling. For the first time, gimbal-mounted water baths to prevent spilling were used on this cruise. Temperatures within the mesocoms were generally less than 2°C warmer than the SST. Surface water for the initial filling was obtained from the Niskin bottles (5m depth). As an experimental treatment, N and P levels were manipulated by initial fertilization, while the Si concentration was adjusted to the same replete level in all mesocosms. The phytoplankton response was monitored on a daily basis in terms of community structure, production, fatty acid composition, and distribution of dissolved and particulate carbon, nitrogen and phosphorus. Specifically, samples were taken for nutrient concentrations (N, P, Si, performed on board), POC, PON, POP, DOC, DON, DOP, HPLC, BSi, TEP, fatty acid methyl ester analysis (FAME), cell counts of microplankon (inverted microscope method, performed on board) and flow cytometry for the assessment of nanoplankton abundance and bacterial biomass.

From the mesocosm experiments and from the CTD-casts, samples for the determination of particulate organic carbon and nitrogen (POC/PON) and particulate organic phosphorus (POP) were filtered (200 mbar) onto precombusted (450°C for 5 h) GF/F filters (ø 25 mm) with a vacuum pump. Samples for biogenic silicate measurements were filtered onto cellulose acetate filters (pore size=0.65 µm; ø 25 mm) and samples to perform high performance liquid chromatography (HPLC) and fatty acid methyl ether (FAME) analysis were filtered onto GF/F filters (ø 25 mm). FAME samples were only taken initially and at termination of the trials.

In order to determine the content of transparent exopolymer particles (TEP) within the mesocosm experiments, samples were filtered at low vacuum pressure (< 150 mbar) onto

polycarbonate filters (pore size=0.45µm; ø 25 mm) and stained with a calibrated and filtered (0.2 µm) alcian blue solution. All sample filters were stored at -20°C.

Water samples from the CTD-casts for the analysis of dissolved organic carbon (DOC) were immediately filled from the Niskin bottles into precombusted glass vials and stored at -20°C. DOC samples from the mesocosms were filtered through combusted (450°C for 5 h) GF/F filters (ø 25 mm) prior to frozen storage due to the high density of organic matter in the mesocosms.

Analysis of dissolved organic nitrogen and phosphorus (DON/DOP) from the mesocosms and the CTD-casts was performed onboard following the method of Koroleff (1977). Inorganic nutrient samples obtained from the daily mesocosm sampling were filtered through 5 µm cellulose acetate filters (ø 25 mm) and analyzed following Grasshoff *et al*. (2002).

Corresponding to the mesocosm experiments, satellite trials were run using the copepod *Oncaea sp.* fed with phytoplankton originating from the mesocosms after these had reached the limited phase. Copepods were separated alive from net samples and were distributed into groups of 50 individuals in twelve 2.5 L bottles containing water from the mesocosms (plus an initial sample of 50), in which they were incubated for four days. Upon termination of the trials, copepods were counted, photographed for prosome length measurements and frozen at -80°C for dry weight and RNA/DNA ratio determination.

Zooplankton net hauls were conducted on 25 stations subsequent to completion of the CTD casts using two WP2 nets with a mesh size of 320 and 150µm, respectively. The 320µm net was hauled vertically from 40m to the surface and the catch was fixed in 4% formaldehyde for later analysis of biomass and community structure. The 150µm net, combined with a closing mechanism, allowed gentle capture from 40-30m water depth. The catch of the latter was sorted alive for experiments or photographed for length measurements and transferred in groups into pre-weighed tin boats and dried over night at 60°C for determination of dry weight, C and N.

3.4.4.3 Results (Shipboard)

Phytoplankton counts revealed that there was a considerable effect of nutrient availability on the community structure of the primary producers. Generally, the addition of NO_3^- significantly increased the total biomass of protists (Fig. 3.12A), indicating that the system was N-limited. Also, it was evident that there was a differential response of the various types of algae, e.g. in the third mesocosm trial, the species clearly favored by N-addition were the dinoflagellate *Prorocentrum triestinum* (Fig. 3.12B) and the diatom *Pseudonitzschia* sp. (Fig 3.12C), while *Heterosigma* sp. (Fig. 3.12D) and *Phaeocystis globosa* (Fig. 3.12D) were favored by increased P levels.

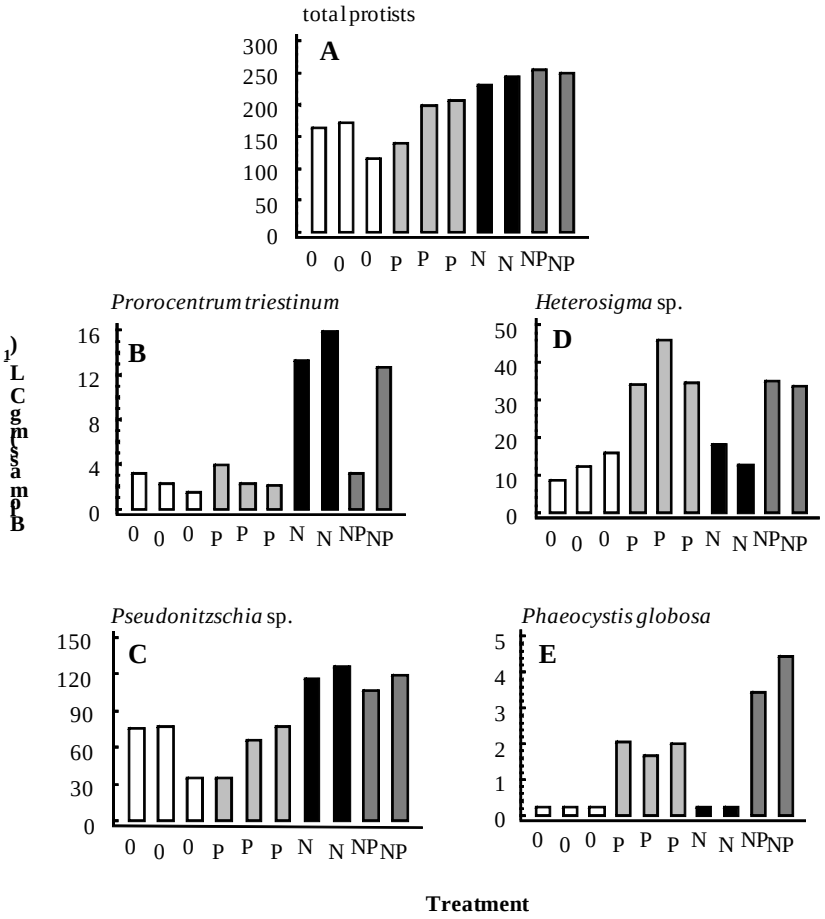

Fig. 3.12: Shipboard results from the third mesocosm experiment: Biomass (mg C L^{-1}) of species in the different nutrient supply treatments. 0 = ambient, P = PO_4 addition, N = NO_3 addition, NP = both added. Note different scaling on y-axis.

3.4.5. Trace Metal Mobilization in the Peruvian OMZ

(C. Schlosser,A. Dammshäuser,O. Baars)

3.4.5.1 Objectives

While it is now established that iron (Fe) and other trace metals (zinc, cadmium, etc.) can be (co)limiting nutrients for phytoplankton growth, we still know little about the processes, and fluxes, by which these trace metals are supplied to the ocean (rivers, atmospheric dust, resuspension and/or diffusion/remobilisation from shelf sediments). Additionally there is a lack of basic information regarding processes in the water column and the sediments, such as particle scavenging/biotic uptake, solubility and particle remineralization, which affect trace metal distribution and transport. A detailed study of trace metal speciation in the Peruvian upwelling zone allows an investigation of the key processes controlling biogeochemistry and remobilization of trace metals from sediments to seawater in OMZ regions. This work is part of a key project within SFB754, which aims to combine WATER COLUMN and POREWATER work in the OMZ of the Eastern Tropical Pacific in order to improve our understanding of benthic-pelagic coupling in the present day ocean. The water column work performed during this cruise was focused on the investigation of the chemical speciation of iron and related metals (Cd, Zn, Co, Cu and Mn), whose chemical behaviour and distribution are altered by oxygen-mediated redox changes, both in the water column and underlying sediment porewaters.

3.4.5.2 Methods

At 18 stations (red dots in Fig. 1; GO-FLO #1-19), seawater for trace metal analysis was sampled by trace metal clean GO-FLO samplers (8 L), at five stations multiple casts were performed for diel cycle studies (GO-FLO #1-5). The samplers were deployed from the ship's own Kevlar wire (Seriendraht) with seawater samples obtained from the surface until 800 m water depth (euphotic zone, OMZ, and underlying water masses). All shipboard handling, sampling and analysis were performed in a Class-5 clean room container (IFM-GEOMAR). The collected seawater was filtered through a 0.2 μm Sartorius cartridge filter. A limited dataset using cross-flow filtration (10 kDa membrane filter) was also obtained on seawater from two stations (GO-FLO #11 and #17) at 4 different depths to separate the colloidal and soluble size fractions. Filtered seawater samples were also collected for later analysis (dissolved Zn, Cd, Co, Pb, Mn, Cu, Fe, Ni) in the laboratory in Kiel. Trace metal speciation measurements (Fe, Zn, Cd) were performed onboard using voltammetric methods or otherwise stored frozen for later analysis in Kiel. At 18 locations (black dots in Fig. 1.4.1.3), seawater from the CTD rosette was used for H_2O_2/Fe(II) measurements using a new dual analysis method (Croot, 2008) which allows the simultaneous measurement of these two short-lived redox species.

3.4.5.3 Results (Shipboard)

Total dissolved Fe concentrations measured onboard by a DPD based spectrophotometric FIA method suggested that iron levels were relatively high (5 – 10 nmol L^{-1}) but uniform in the water column (Fig. 3.13a). However, the lack of agreement with Fe(II) measurements suggested baseline problems of the shipboard DPD method and the shipboard results will have to be checked against measurements of total dissolved Fe concentrations by conventional methods in the laboratory in Kiel. Onboard Fe^{2+} and H_2O_2 measurements showed higher concentrations of these photochemically produced species in surface seawater (Figs. 3.13c,d). Higher dissolved

Fe^{2+} concentrations were also measured throughout the OMZ in close proximity to the sea floor (Fig. 3.13b), indicating diffusion from the anoxic sediments.

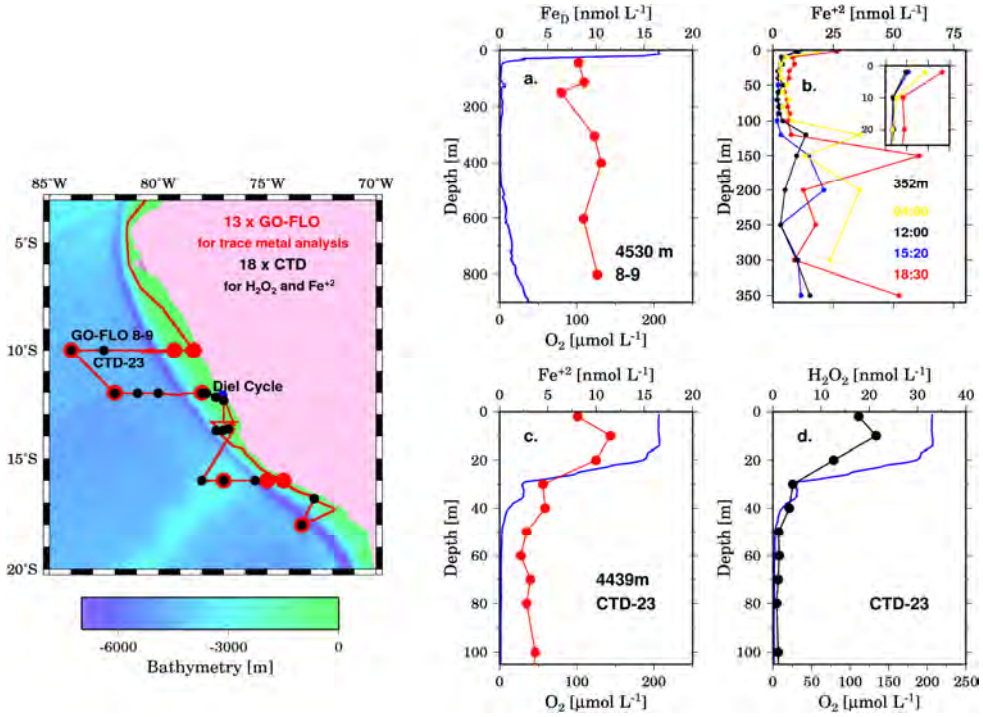

Fig. 3.13: (left) Bathymetry of the surveyed area, overlain by the cruise track (red line) and sampling locations (red spots: GO-FLO; black spots: CTD/RO). Preliminary results for CTD O_2 (blue line in diagrams a, c, and d), total dissolved Fe (a), Fe^{2+} (b,c), and H_2O_2 (d) concentration versus depth (m) are shown in the diagrams. The diel cycle data (b.) shows the highest surface Fe^{2+} concentration in the late afternoon and in the early morning. H_2O_2 showed a strong decrease with depth (d.) mirroring the O_2 concentration in seawater.

The speciation of Zn and Cd in the water column was examined in the coastal upwelling zone off Peru. A total of 43 samples from 7 stations and depths of up to 800 m were collected along transects at 10°S, 12°S, 16°S and 18°S from the open ocean to the coastal zone. Speciation was performed shipboard by metal titration using Anodic Stripping Voltammetry (ASV). For stations north of 16°S a significant amount of labile Zinc (> 0.1 nM) was found in the upper water column. Further south concentrations decreased and low pM values were reached at stations 028 and 047 at depths of up to 200m, which may be related to the reduced influence of upwelling. In stations north of 16°S a pronounced sub-surface maximum of Zn ligands was visible but only in samples from the upper water column at 16°S and 18°S organic complexation dominated the speciation of Zn. For Cd, labile concentrations were always in the low pM range in the top sample but increased quickly with depths to values of up to 0.65 nM. High Cd values found in the upwelling region are in agreement with the usually prevailing high PO_4^{3-} concentrations. In samples from depths <50 m complexation with organic ligands was strong and ligand concentrations were highest. No significant difference in labile Cd was found between 0.2 µm and 10 kDa filtered samples suggesting the absence of Cd associated with colloids.

3.4.6. Neodymium and Silicon Isotope Distribution

(P. Grasse, R. Stumpf,)

Large volume water samples were collected for the isotopic characterization of neodymium ($^{143}Nd/^{144}Nd$) and Silicon isotopes ($^{28}Si/^{30}Si$). Silicate is an important nutrient for diatoms, one of the most abundant primary producers in the upwelling region. Because diatoms prefer light over heavy isotopes during biomineralization of biogenic silicate, the enrichment of heavy isotopes in seawater is an indicator for silicate utilization and the productivity of diatoms (e.g. Reynolds et al., 2005). In the upwelling area off the Peruvian Coast, the isotopic signature of Si in water will also be influenced by new supply of silicate with different isotopic values, which requires independent information about water mass mixing. Due to the fact that Nd isotopes acquire their isotopic signatures through weathering of rocks with particular isotopic compositions, i.e. continental rocks have a lower $^{143}Nd/^{144}Nd$ compared with mantle rocks and young volcanic rocks, the Nd isotope signature fingerprints the origin of water masses (cf. Frank, 2002). The information obtained from the combination of the biologically influenced Si isotope signatures and the quasi-conservative Nd isotopes will, together with the detailed investigations of the nitrogen cycle and the local physical oceanography, lead to a better understanding of water mass mixing and upwelling intensity and at the same time will improve the applicability of Nd and Si isotopes as tracers for paleo-oceanographic processes.

All water samples were taken from the CDT/Rosette. In total 108 samples for Nd isotope were taken at 38 stations. For each sample, 20 l of seawater were collected in cubitainers from discrete depths, which resulted in a total of 2160 litres of seawater. Samples were filtered through a 0.45µm Polycarbonate Filter and acidified with distilled 12M HCl. To precipitate the Neodymium a Fe(III)-Chloride Solution was added and brought to pH 7-8 using ammonia.

A total of 80 samples were obtained for silicon isotope analysis were from 18 stations. For each sample 500 ml of seawater were collected. The samples were immediately filtered through a 0.45µm polycarbonate filter, acidified with distilled 12M HCl and then stored for transport to Kiel.

The samples will be analyzed for Nd and Si concentrations and isotope compositions at IFM-GEOMAR in Kiel using an MC-ICP-MS (Multi-Collector Inductively Coupled Plasma-Mass Spectrometer)

3.4.7. Natural Radioisotopes

(J. Scholten)

The Peru ocean margin is characterized by high particle flux and a well-defined oxygen minimum zone. The main objective of the radionuclide investigations was to study a boundary scavenging effect, i.e. the preferential removal of particle reactive radionuclides (^{230}Th, ^{231}Pa) from the water column in areas of high particle flux in relation to their reduced removal in open ocean waters. The second objective was to investigate to what extent oxygen minimum zones are sources for radium. The behaviour of radium is expected to be closely related to that of manganese. Thus the release of radium from suboxic and anoxic sediments to seawater is expected. The gradients of radium (^{228}Ra, ^{226}Ra) in the water column may be used to estimate the flux of other elements released from the sediments.

Water samples were collected using Niskin water bottles attached to the CTDT-Rosette. Water obtained from selected depths was filled into 20l cubitainers, acidified with distilled 12M HCl, and stored for transport to the home laboratory. At five locations water profiles were obtained resulting in a total of 57 water samples (Table 3.2). These profiles were located at near-shore sites (Station No. 012-1, 032-1, 033-1) as well as in the open ocean (Stations No. 010-2/5, 030-2).

Tab. 3.2: List of locations for Radium isotope samples

Station No.	Gear No.	Date 2008/09	Position Lat. [°S]	Position Long. [°W]	Time [UTC]	Depth [m]
010-2	CTD/RO-32	07.01.	12°07,00'	78°54,00'	12:00	60 38
010-5	CTD/RO-33	07.01.	12°07,00'	78°54,00'	13:51	60 35
012-1	CTD/RO-36	08.01.	12°02,04'	77°51,00'	07:14	73 4
013-3	CTD/RO-38	08.01.	12°02,05'	77°47,33'	16:58	35 3
030-2	CTD/RO-64	13.01.	16°00,00'	75°33,00'	15:13	61 65
032-1	CTD/RO-68	14.01.	16°00,00'	74°20,00'	06:51	70 6
033-1	CTD/RO-69	14.01.	16°00,00'	74°14,70'	08:54	25 0

3.4.8. Inorganic Carbon in the Peru Coastal Upwelling Zone

(G. Friederich)

The Peruvian upwelling system and the associated offshore waters are a source of carbon dioxide (CO_2) to the atmosphere. The elevated partial pressure of carbon dioxide (pCO_2) at the sea surface in this region can be attributed to a combination of upwelling, surface heating and influences of the underlying oxygen minimum zone on upwelling source waters. In recent years a considerable amount of sea surface pCO_2 data has been collected in this region (Friederich et al. 2008) and this cruise provided the opportunity to collect a comprehensive suite of subsurface measurements of dissolved inorganic carbon (DIC).

3.4.8.1 Objectives

Sea surface measurements of pCO_2 were made at all times during the cruise. The sea surface data will be used in combination with meteorological information to estimate air-sea fluxes of CO_2. Samples for DIC analysis were collected throughout the water column at most hydrographic stations and discrete pCO_2 measurements were made from water column samples at selected stations. These data may be utilized to estimate re-mineralization and community production in the upwelling source waters and the oxygen minimum zone.

3.4.8.2 Methods

Sea surface pCO_2 was determined with a showerhead equilibrator supplied by a continuous stream of seawater from the ship's clean seawater system. A non-dispersive infrared gas analyzer (LI-COR 6262) was used to measure the mixing ratio of CO_2 in the headspace gas. All results are reported as the mixing ratio of CO_2 in dry air at one atmosphere corrected to the temperature recorded at the ship's water intake. Atmospheric CO_2 measurements could not be made since the required calibration gases did not clear customs in Guayaquil prior to departure.

Total dissolved inorganic carbon was measured immediately after collection of samples from the CTD rosette. CO_2 was stripped from acidified samples and measured with a non-dispersive infrared gas analyzer (LI-COR 7000). Samples were run in triplicate and reference materials supplied by Dr. Andrew Dickson at Scripps Institute of Oceanography were used for calibration at each station. The precision of this method is estimated to be 0.05% or better.

Discrete water column pCO_2 measurements were made immediately after sample collection from the CTD rosette. Samples were equilibrated in a miniature dynamic headspace equilibrator at a constant temperature. A non-dispersive infrared gas analyzer (LI-COR 7000) was used to measure the mixing ratio of CO_2 in the headspace gas.

3.4.8.3 Results (Shipboard)

The sea surface pCO_2 measurements indicate that the majority of the study region was a source of CO_2 to the atmosphere during this survey (Fig. 3.14). The range of pCO_2 was from a low of about 250 ppm to a maximum of about 1400 ppm. High and low extremes were found near the coast and the highest pCO_2 was observed in a region of strong upwelling near 14°S. Some of the lowest pCO_2 value appeared to be associated with “Red Tide”-like algal blooms. The spatially averaged pCO_2 in the coastal zone south of 5°S was about 540 ppm while the offshore spatial average was near 450 ppm. Atmospheric pCO_2 was estimated to be approximately 384.5 ppm during the time of this survey.

DIC distributions near the shelf provided indications of considerable local re-mineralization within the low oxygen upwelling waters (Fig. 3.15). Hydrogen sulphide was observed in waters over the shelf south of 12°S. Preliminary estimates indicate that there may have been DIC enrichment up to 30 µmol kg^{-1} in the sulphide bearing waters compared to offshore low oxygen waters with similar physical characteristics.

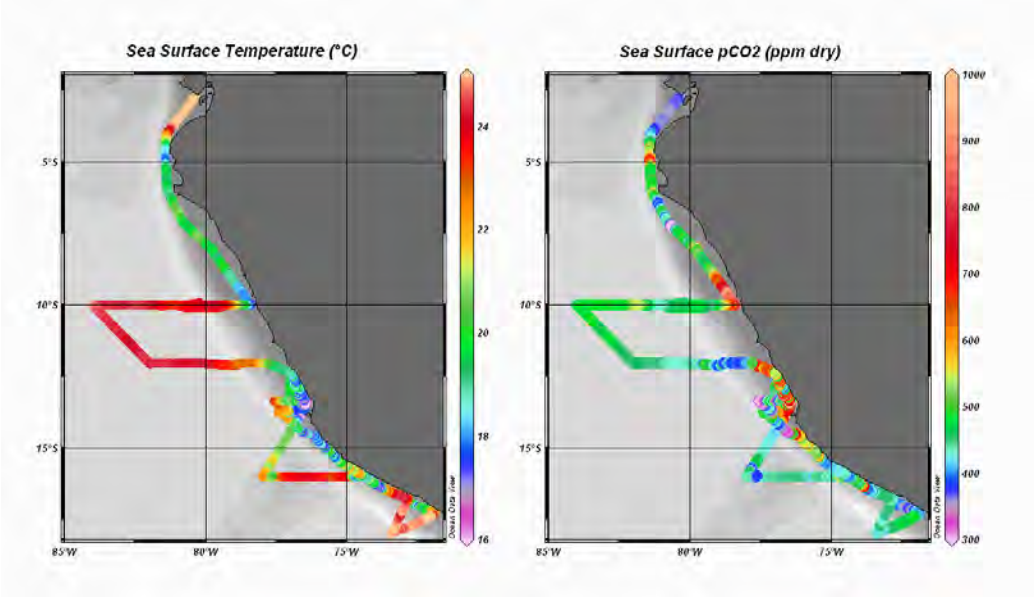

Fig. 3.14: Sea surface temperature and pCO_2 distribution along the cruise track.

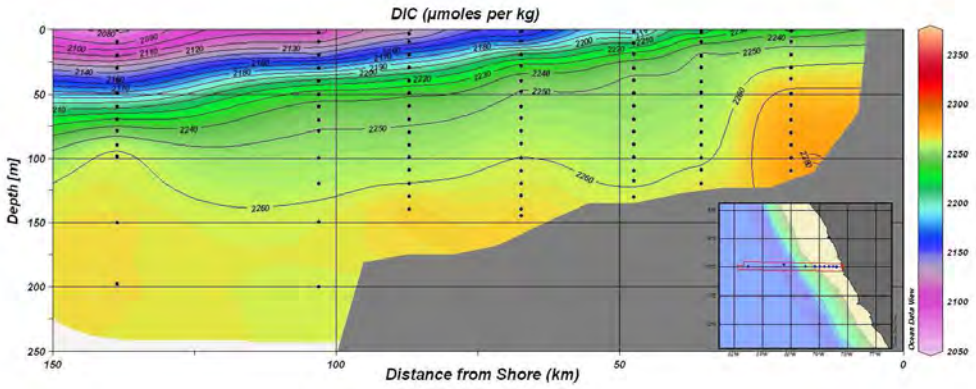

Fig. 3.15: Detail of the DIC section sampled near 10°S.

3.5 Ship's Meteorological Station

(H. Sonnabend, W.-T. Ochsenhirt)

RV METEOR left the harbour of Guayaquil in the morning of 27.12.2008 to drop anchor quite nearby in a bay of river Guaye. Having finished final scientific preparations at this place, Meteor headed at air temperatures of around 29 degrees Celsius and sunshine directly for the first working area near the coast of Peru at the latitude of 10 degrees south, only interrupted by some CTD-Stations on the way.

In the meantime a ridge of high pressure extended from Northern Chile as a small belt towards the northern parts of Peru, while a nearly stationary flat trough ran right in front along the coasts of Ecuador and Peru. This trough was flanked in the southwest by another ridge extending from the large Southeast Pacific Subtropical high towards the sea areas around 18°S, 90°W.

Soon after having entered the Gulf of Guayaquil the south hemispheric trade wind set in, shifting gradually from southwesterly directions in the beginning to southerly or southeasterly directions lateron along the coasts of Peru. Apart from the morning of 28.12., when wind speed temporarily exceeded 20 knots, the trade wind remained light to moderate throughout the transit time towards the first working area essentially.

Entering the sphere of influence of the Humboldt Current off the coasts of Northern Peru, air temperatures dropped down quickly to values around 20 degrees Celsius, while the water temperatures found their level between 17 and 19 degrees Celsius. It became misty at times and during 29.12. low stratus clouds and local fog patches drifted from the sphere of upwelling water across the cruise line of RV Meteor.

During the following night the start point for the first zonal section along 10°S only a few miles off the coast of Peru was reached by partly dense fog. The water temperatures at the coastal upwelling centre dropped down to a minimum of 15.7°C while the air temperatures didn't exceed 16 – 17°C. At soft southeasterly winds the visibility began to improve in the course of the morning when the fog lifted to low stratus gradually. Having finished station works RV Meteor continued its section westward. Soon after leaving the coastal cold water sphere the visibility improved rapidly while the southeastlery trade wind became moderate again. Around turn of the year and throughout the following days the weather was mainly fair with good visibilities and a gentle to moderate breeze from the southeast. The temperatures of air and water

reached values of about 23 degrees Celsius. However, a long termed swell from southsouthwest arrived at the working area New Year's Day reaching it's maximum height of about 3 meters on 3.1.09 before levelling down again to 1,5 – 2 meters within the next days.

Having finished station work at 10°S, 84°W in the evening of 4.1., RV Meteor headed for 82°W, the start point of the second section along 12°S towards the coast. At almost unchanged wind- and sea state conditions the following stations up to the coast south of Lima were carried out unhindered and apart from an interruption on 6.1., the series of mainly sunny days was continued. Visibilities however deteriorated significantly when reaching the sphere of upwelling water and especially in the morning low stratus clouds drifted over the working area. The temperatures of the air didn't exceed 20°C while the water temperatures moved between 16 and 19°C.

The trade wind took a comparatively lively interlude on 10./11.01., when the wedge of the Southeast Pacific Subtropical high extended a little bit northeastward intensifying the gradient of air pressure to the nearly stationary trough along the coast of Peru. As a result of this development the wind increased to 5 – 6 Beaufort associated with wave heights of 2 – 2.5 meters in the morning of 10.1. and up to nearly 7 Beaufort in the evening of the same day, when Meteor carried out a station in the vicinity of some isles in the northern part of the bay of Pisco. The water temperatures dropped down to an intermediate minimum value of 14.0°C.

In the morning of 11.1., RV Meteor arrived at the western most corner of the section along 16°S with continued fresh to strong southeasterly breeze and a corresponding sea state of 2 – 2.5 meters. While wave heights levelled down to 1.5 – 2 meters soon, the fresh trade wind consisted during the next days short before RV Meteor arrived near the coast in the morning of 14.1. There the wind decreased to a soft breeze temporarily. Having finished some offshore stations, Meteor returned to the seaward position from the day before, where the southeast trade wind became moderate to fresh again. As a result of seasonal shower- and thunderstorm activity over the Andes of Peru and Bolivia, large fields of high and medium high cloudiness drifted over the working areas at times. Until the afternoon of 15.1., the remaining offshore stations around the final point were carried out at a soft to moderate breeze from southeast. Afterwards RV Meteor headed along the coast towards an additional section along ~18°S.

During 16.1., the flat coastal trough weakened in its southern part making room for the ridge of high pressure which took over its place for the next few days. Consequently the air pressure gradient weakened and the trade wind calmed down to a soft breeze. In the morning of the following day a long termed southsouthwesterly swell of about 2 – 2.5 Meters arrived at 18°S, 73.4°W where Meteor carried out another station. Next day the ship steamed again parallel to the coast towards northwest to extensive station work at 13,8°'S,77,0°'W with a soft to moderate breeze from southeast to east shifting southeast to south later on.

From 19.01., partially dense patches of fog drifted over the cruise line and working areas from always second part of the night until early noon.

To sum up it can be said that the cruise M77/3 was favoured by predominantly moderate trade winds associated with the corresponding sea state. It was mainly sunny and apart from occasionally some drizzle in patches of fog no precipitation was measured throughout the whole cruise.

3.6 Station List M77/3

Tab. 3.3:

Station No.	Gear No.	Date 2008/09	Position start Lat. [°S]	Long. [°W]	Time [UTC]	Depth [m]	Position end Lat. [°S]	Long. [°W]	Time [UTC]	Depth [m]
ME773/804-1	CTD/RO-1	28.12.	3°59,98'	81°23,52'	09:0 5	1079	4°00,02'	81°23,48'	10:07	1081
ME773/804-2	CTD/RO-2	28.12.	4°00,00'	81°23,48'	11:0 0	1082	4°00,02'	81°23,48'	11:26	1085
ME773/805-1	CTD/RO-3	28.12.	6°00,01'	81°21,70'	22: 35	1001	6°00,02'	81°21,67'	22:41	998
ME773/805-2	CTD/RO-4	28.12.	6°00,01'	81°21,67'	23:0 9	999	6°00,01'	81°21,67'	23:58	999
ME773/805-3	CTD/RO-5	29.12.	6°00,01'	81°21,67'	00:5 7	995	6°00,01'	81°21,67'	01:52	989
ME773/805-4	GO-FLO-0	29.12.	6°00,01'	81°21,67'	02:1 3	992	6°00,01'	81°21,67'	03:08	991
ME773/806-1	CTD/RO-6	29.12.	8°00,02'	79°50,70'	17:0 6	138	8°00,03'	79°50,69'	17:23	137
ME773/806-2	IFISH-1	29.12.	8°00,07'	79°50,67'	17:32	138	8°00,25'	79°46,68'	18:04	130
ME773/807-1	CTD/RO-7	30.12.	10°00,00'	78°22,89'	07: 02	110	10°00,01'	78°22,85'	07:16	113
ME773/807-2	GO-FLO-1	30.12.	10°00,01'	78°22,82'	08: 04	111	10°00,01'	78°22,82'	08:36	112
ME773/807-3	PCTD/RO-1	30.12.	10°00,01'	78°22,82'	09 :24	111	10°00,01'	78°22,82'	17:01	111
ME773/807-4	GO-FLO-2	30.12.	10°00,05'	78°22,82'	17: 16	111	10°00,06'	78°22,82'	17:40	110
ME773/807-5	CTD/RO-8	30.12.	10°00,06'	78°22,82'	17: 51	111	10°00,05'	78°22,82'	18:07	111
ME773/807-6	CTD/RO-9	30.12.	10°00,05'	78°22,82'	18: 22	111	10°00,05'	78°22,82'	18:27	111
ME773/807-7	CTD/RO-10	30.12.	10°00,06'	78°22,82'	18 :42	111	10°00,05'	78°22,82'	18:47	111
ME773/807-8	CTD/RO-11	30.12.	10°00,05'	78°22,82'	18 :58	112	10°00,05'	78°22,82'	19:03	111
ME773/807-9	CTD/RO-12	30.12.	10°00,05'	78°22,82'	19 :15	111	10°00,05'	78°22,82'	19:19	111
ME773/807-10	WP2-1	30.12.	10°00,05'	78°22,82'	19:48	111	10°00,05'	78°22,82'	19:58	111
ME773/807-11	GO-FLO-3	30.12.	10°00,05'	78°22,82'	20 :08	111	10°00,05'	78°22,82'	20:36	112
ME773/807-12	ISP-1	30.12.	10°00,05'	78°22,82'	20:52	111	10°00,05'	78°22,82'	23:37	112
ME773/807-13	GO-FLO-4	30.12.	10°00,05'	78°22,82'	23 :45	112	10°00,05'	78°22,82'	00:10	111
ME773/807-14	ISP-2	31.12.	10°00,05'	78°22,82'	00:55	112	10°00,05'	78°22,82'	03:40	112
ME773/807-15	GO-FLO-5	31.12.	10°00,05'	78°22,82'	03 :44	112	10°00,05'	78°22,82'	04:13	112
ME773/807-16	WP2-2	31.12.	10°00,05'	78°22,82'	04:20	111	10°00,07'	78°22,81'	04:39	111
ME773/808-1	CTD/RO-13	31.12.	10°00,00'	78°29,94'	05 :33	147	10°00,0'	78°29,90'	05:51	148
ME773/809-1	CTD/RO-14	31.12.	10°00,01'	78°37,98'	06 :45	149	10°00,00'	78°37,98'	08:19	149
ME773/810-1	CTD/RO-15	31.12.	9°59,98'	78°48,03'	09: 36	151	9°59,97'	78°48,02'	09:52	147
ME773/811-1	CTD/RO-16	31.12.	9°59,99'	78°58,01'	11: 56	138	10°00,01'	78°58,00'	12:14	139
ME773/811-2	PCTD/RO-2	31.12.	10°00,01'	78°58,00'	13 :30	138	10°00,01'	78°58,00'	19:08	138
ME773/811-3	CTD/RO-17	31.12.	10°00,02'	78°58,00'	19 :23	138	10°00,01'	78°57,98'	19:37	137
ME773/812-1	CTD/RO-18	31.12.	9°59,98'	79°08,00'	20: 40	331	9°59,98'	79°08,00'	21:13	333
ME773/001-1	GO-FLO-6	01.01.	9°59,99'	79°28,01'	13:4 0	1659	10°00,01'	79°28,00'	14:21	1657
ME773/001-2	CTD/RO-19	01.01.	10°00,01'	79°28,00'	14 :27	1662	10°00,01'	79°28,00'	16:23	1657
ME773/001-3	GO-FLO-7	01.01.	10°00,01'	79°28,00'	16: 31	1668	10°00,01'	79°28,00'	17:36	1661
ME773/001-4	WP2-3	01.01.	10°00,01'	79°28,00'	17:42	1655	10°00,01'	79°28,00'	17:50	1669
ME773/001-5	WP2-4	01.01.	10°00,01'	79°28,00'	18:00	1658	10°00,01'	79°28,01'	18:10	1662
ME773/002-1	CTD/RO-20	02.01.	9°55,31'	80°13,44'	01: 44	6296	9°55,31'	80°13,44'	03:08	6317
ME773/002-2	CTD/RO-21	02.01.	9°55,31'	80°13,44'	03: 30	6296	9°55,31'	80°13,44'	03:44	6303

Station No.	Gear No.	Date 2009	Position start		Time [UTC]	Depth [m]	Position end		Time [UTC]	Depth [m]
			Lat. [°S]	Long. [°W]			Lat. [°S]	Long. [°W]		
ME773/003-1	CTD/RO-22	02.01.	10°00,03'	81°30,10'	10 :53	4713	10°00,03'	81°30,10'	12:02	4708
ME773/003-2	ISP-3	02.01.	10°00,02'	81°30,01'	13:18	4714	10°00,00'	81°30,00'	18:04	4695
ME773/003-3	WP2-5	02.01.	10°00,00'	81°30,00'	18:10	4695	10°00,00'	81°30,00'	18:16	4695
ME773/003-4	WP2-6	02.01.	10°00,00'	81°30,00'	18:22	4695	10°00,07'	81°30,06'	18:32	4713
ME773/003-5	PCTD/RO-3	02.01.	10°00,10'	81°30,12'	18 :50	4695	10°00,13'	81°30,14'	01:57	4698
ME773/003-6	ISP-4	03.01.	10°00,13'	81°30,14'	05:42	4697	10°00,13'	81°30,14'	10:11	4697
ME773/003-7	ISP-5	03.01.	10°00,06'	81°30,50'	13:14	4716	10°00,06'	81°30,50'	16:45	4697
ME773/003-8	ISP-6	03.01.	10°00,06'	81°30,50'	17:14	4696	10°00,06'	81°30,51'	21:00	4699
ME773/004-1	CTD/RO-23	04.01.	9°59,99'	82°29,99'	02: 27	4444	10°00,00'	82°30,00'	04:19	4438
ME773/004-2	CTD/RO-24	04.01.	10°00,00'	82°30,00'	04 :49	4453	10°00,00'	82°30,01'	05:08	4451
ME773/005-1	GO-FLO-8	04.01.	10°00,01'	84°00,01'	13: 00	4523	10°00,01'	84°00,01'	14:08	4534
ME773/005-2	CTD/RO-25	04.01.	10°00,01'	84°00,01'	14 :11	4537	10°00,01'	84°00,01'	15:36	4537
ME773/005-3	GO-FLO-9	04.01.	10°00,01'	84°00,01'	15: 53	4532	10°00,01'	84°00,01'	16:33	4538
ME773/005-4	WP2-7	04.01.	10°00,01'	84°00,01'	16:43	4530	10°00,03'	83°59,99'	16:50	4527
ME773/005-5	WP2-8	04.01.	10°00,02'	84°00,00'	16:55	4531	10°00,05'	83°59,99'	17:03	4528
ME773/005-6	PCTD/RO-4	04.01.	10°00,03'	84°00,01'	17 :22	4521	10°00,03'	84°00,01'	22:38	4529
ME773/006-1	CTD/RO-26	05.01.	10°07,53	83°52,83	00:0 0	4550	10°07,53	83°52,83	03:40	4550
ME773/007-1	WP2-9	05.01.	12°01,95'	82°00,01'	19:32	4744	12°01,94'	82°00,01'	19:38	4752
ME773/007-2	GO-FLO-10	05.01.	12°01,98'	81°59,97'	19 :48	4751	12°01,98'	81°59,99'	21:10	4760
ME773/007-3	CTD/RO-27	05.01.	12°01,98'	81°59,99'	21 :15	4749	12°01,98'	81°59,99'	22:36	4749
ME773/007-4	GO-FLO-11	05.01.	12°01,98'	81°59,99'	23 :30	4748	12°01,98'	81°59,99'	00:15	4746
ME773/007-5	IFISH-2	06.01.	12°02,67'	81°59,98'	00:3 5	4750	12°01,97'	80°56,80'	08:56	4687
ME773/008-1	CTD/RO-28	06.01.	12°01,97'	80°56,80'	09 :00	4683	12°02,00'	80°56,79'	10:29	4683
ME773/008-2	CTD/RO-29	06.01.	12°02,00'	80°56,79'	10 :55	4677	12°02,00'	80°56,80'	11:15	4685
ME773/008-3	ISP-7	06.01.	12°02,00'	80°56,80'	11:51	4679	12°02,00'	80°56,80'	14:02	4684
ME773/008-4	WP2-10	06.01.	12°02,00'	80°56,80'	14:13	4679	12°02,00'	80°56,80'	14:22	4679
ME773/008-5	WP2-11	06.01.	12°02,00'	80°56,79'	14:25	4687	12°02,00'	80°56,80'	14:33	4678
ME773/008-6	PCTD/RO-5	06.01.	12°02,00'	80°56,80'	15 :10	4677	12°02,00'	80°56,80'	20:52	4679
ME773/009-1	CTD/RO-30	07.01.	12°02,00'	80°00,00'	02 :00	4765	12°02,00'	80°00,00'	03:40	4756
ME773/010-1	CTD/RO-31	07.01.	12°07,02'	78°54,02'	10 :00	6030	12°07,00'	78°54,00'	11:22	6029
ME773/010-2	CTD/RO-32	07.01.	12°07,00'	78°54,00'	12 :00	6038	12°07,00'	78°54,00'	13:12	6029
ME773/010-3	WP2-12	07.01.	12°07,00'	78°54,00'	13:17	6033	12°07,00'	78°54,01'	13:23	6033
ME773/010-4	WP2-13	07.01.	12°07,00'	78°54,01'	13:30	6037	12°07,00'	78°54,02'	13:36	6026
ME773/010-5	CTD/RO-33	07.01.	12°07,00'	78°54,01'	13 :51	6035	12°07,00'	78°54,00'	18:08	6032
ME773/011-1	GO-FLO-12	08.01.	12°02,00'	78°00,00'	00 :55	1768	12°02,00'	78°00,00'	02:11	1766
ME773/011-2	CTD/RO-34	08.01.	12°02,00'	78°00,00'	02 :18	1766	12°02,00'	78°00,01'	03:39	1768
ME773/011-3	GO-FLO-13	08.01.	12°02,00'	78°00,01'	03 :46	1767	12°02,00'	78°00,00'	04:24	1765
ME773/011-4	CTD/RO-35	08.01.	12°02,00'	78°00,01'	04 :28	1764	12°02,01'	78°00,00'	05:47	1761
ME773/012-1	CTD/RO-36	08.01.	12°02,04'	77°48,91'	07 :14	734	12°02,02'	77°48,93'	08:00	724
ME773/013-1	CTD/RO-37	08.01.	12°02,03'	77°47,34'	08 :34	355	12°02,03'	77°47,34'	09:11	352
ME773/013-2	PCTD/RO-6	08.01.	12°02,03'	77°47,34'	10 :25	354	12°02,05'	77°47,34'	16:40	352

Station No.	Gear No.	Date 2009	Position start Lat. [°S]	Long. [°W]	Time [UTC]	Depth [m]	Position end Lat. [°S]	Long. [°W]	Time [UTC]	Depth [m]
ME773/013-3	CTD/RO-38	08.01.	12°02,05'	77°47,33'	16 :58	350	12°02,06'	77°47,34'	17:32	353
ME773/013-4	WP2-14	08.01.	12°02,06'	77°47,34'	17:40	353	12°02,06'	77°47,34'	17:48	354
ME773/013-5	WP2-15	08.01.	12°02,06'	77°47,34'	17:52	354	12°02,06'	77°47,33'	17:58	352
ME773/013-6	CTD/RO-39	08.01.	12°02,06'	77°47,33'	18 :06	351	12°02,05'	77°47,33'	18:12	351
ME773/013-7	CTD/RO-40	08.01.	12°02,05'	77°47,33'	18 :26	351	12°02,05'	77°47,33'	18:30	349
ME773/013-8	CTD/RO-41	08.01.	12°02,06'	77°47,33'	18 :42	351	12°02,06'	77°47,33'	18:48	352
ME773/013-9	CTD/RO-42	08.01.	12°02,06'	77°47,33'	18 :58	350	12°02,06'	77°47,33'	19:03	350
ME773/013-10	CTD/RO-43	08.01.	12°02,06'	77°47,33'	2 0:13	352	12°02,06'	77°47,33'	20:38	352
ME773/013-11	CTD/RO-44	08.01.	12°02,05'	77°47,33'	2 3:22	353	12°02,06'	77°47,33'	00:00	351
ME773/013-12	PCTD/RO-7	09.01.	12°02,06'	77°47,32'	0 0:29	350	12°02,05'	77°47,32'	02:15	351
ME773/013-13	ISP-8	09.01.	12°02,06'	77°47,33'	03:00	350	12°02,09'	77°47,32'	05:15	354
ME773/013-14	ISP-9	09.01.	12°02,09'	77°47,32'	06:26	354	12°02,14'	77°47,32'	10:00	355
ME773/014-1	CTD/RO-45	09.01.	12°05,28'	77°40,22'	11 :00	424	12°05,27'	77°40,23'	11:15	417
ME773/015-1	CTD/RO-46	09.01.	12°07,82'	77°33,93'	12 :16	166	12°07,84'	77°33,92'	12:35	165
ME773/016-1	CTD/RO-47	09.01.	12°10,40'	77°27,68'	13 :28	152	12°10,40'	77°27,66'	13:47	151
ME773/017-1	CTD/RO-48	09.01.	12°12,93'	77°21,35'	14 :43	132	12°12,94'	77°21,34'	15:03	132
ME773/018-1	CTD/RO-49	09.01.	12°18,16'	77°08,75'	16 :30	100	12°18,16'	77°08,75'	16:51	100
ME773/019-1	CTD/RO-50	09.01.	12°21,76'	77°00,09'	18 :02	100	12°21,79'	77°00,05'	18:20	101
ME773/019-2	WP2-16	09.01.	12°21,80'	77°00,06'	18:30	99	12°21,80'	77°00,05'	18:38	100
ME773/019-3	PCTD/RO-8	09.01.	12°21,81'	77°00,01'	21 :05	100	12°21,81'	77°00,01'	02:53	100
ME773/019-4	CTD/RO-51	10.01.	12°21,81'	77°00,01'	03 :02	101	12°21,81'	77°00,01'	03:17	100
ME773/020-1	GLIDER-1	10.01.	13°39,95'	77°00,04'	13: 34	879	13°41,02'	77°01,14'	18:30	1294
ME773/020-2	CTD/RO-52	10.01.	13°40,50'	77°00,91'	15 :50	1008	13°40,50'	77°00,91'	16:30	1008
ME773/021-1	CTD/RO-53	10.01.	13°39,97'	76°47,09'	20 :06	337	13°40,00'	76°47,10'	20:38	337
ME773/021-2	WP2-17	10.01.	13°40,00'	76°47,10'	20:42	338	13°40,00'	76°47,10'	20:50	339
ME773/021-3	WP2-18	10.01.	13°40,00'	76°47,10'	21:00	339	13°40,00'	76°47,10'	21:08	339
ME773/022-1	CTD/RO-54	10.01.	13°39,99'	76°30,81'	22 :58	128	13°40,00'	76°30,80'	23:27	131
ME773/023-1	WP2-19	11.01.	15°59,98'	78°00,00'	15:30	3425	15°59,90'	78°00,04'	15:48	3437
ME773/023-2	CTD/RO-55	11.01.	16°00,00'	78°00,04'	16 :20	3420	15°59,90'	78°00,04'	17:43	3445
ME773/024-1	CTD/RO-56	11.01.	16°00,28'	77°39,85'	19 :47	2868	16°00,27'	77°39,84'	19:52	2868
ME773/025-1	CTD/RO-57	11.01.	16°00,04'	77°40,16'	20 :35	2907	15°59,98'	77°40,15'	20:54	2905
ME773/025-2	WP2-20	11.01.	16°00,14'	77°40,16'	21:14	2893	16°00,12'	77°40,17'	21:17	2908
ME773/026-1	CTD/RO-58	11.01.	16°01,14'	77°42,60'	21 :47	2822	16°01,17'	77°42,57'	22:06	2832
ME773/027-1	CTD/RO-59	11.01.	15°59,00'	77°38,23'	22 :57	2628	15°59,00'	77°38,23'	23:17	2612
ME773/028-1	GO-FLO-14	12.01.	15°59,99'	77°00,02'	02 :47	2362	16°00,09'	76°59,72'	04:03	2349
ME773/028-2	CTD/RO-60	12.01.	15°59,96'	76°59,95'	04 :16	2354	15°59,96'	76°59,93'	05:42	2357
ME773/028-3	GO-FLO-15	12.01.	15°59,96'	76°59,93'	05 :48	2353	16°00,00'	76°59,84'	06:58	2348
ME773/028-4	PCTD/RO-9	12.01.	16°00,00'	76°59,84'	07 :30	2352	16°00,00'	76°59,84'	13:55	2351
ME773/028-5	CTD/RO-61	12.01.	16°00,00'	76°59,84'	14 :06	2353	16°00,00'	77°00,00'	16:05	2359
ME773/028-6	ISP-10	12.01.	16°00,00'	77°00,00'	16:13	2359	16°00,00'	77°00,00'	20:16	2365
ME773/028-7	WP2-21	12.01.	16°00,00'	77°00,00'	20:19	2361	16°00,00'	77°00,00'	20:25	2360

Station No.	Gear No.	Date 2009	Position start		Time [UTC]	Depth [m]	Position end		Time [UTC]	Depth [m]
			Lat. [°S]	Long. [°W]			Lat. [°S]	Long. [°W]		
ME773/028-8	WP2-22	12.01.	16°00,00'	77°00,00'	20:27	2357	16°00,00'	77°00,00'	20:34	2359
ME773/028-9	ISP-11	12.01.	16°00,00'	77°00,00'	20:44	2357	16°00,00'	77°00,00'	00:37	2359
ME773/029-1	CTD/RO-62	13.01.	15°59,95'	76°16,05'	07 :32	3315	15°59,96'	76°16,08'	08:57	3313
ME773/030-1	CTD/RO-63	13.01.	16°00,00'	75°33,00'	13 :01	6164	16°00,00'	75°33,00'	14:26	6169
ME773/030-2	CTD/RO-64	13.01.	16°00,00'	75°33,00'	15 :13	6165	16°00,00'	75°33,00'	16:45	6164
ME773/030-3	CTD/RO-65	13.01.	16°00,00'	75°33,00'	17 :18	6166	16°00,00'	75°33,00'	21:13	6166
ME773/030-4	WP2-23	13.01.	16°00,00'	75°33,00'	21:19	6161	16°00,00'	75°32,99'	21:27	6159
ME773/030-5	WP2-24	13.01.	16°00,00'	75°32,99'	21:30	6167	15°59,99'	75°32,96'	21:35	6168
ME773/030-6	CTD/RO-66	13.01.	15°59,98'	75°32,93'	21 :52	6166	15°59,95'	75°32,93'	22:15	6162
ME773/031-1	CTD/RO-67	14.01.	16°00,00'	74°36,64'	04 :07	1501	16°00,06'	74°36,55'	05:19	1462
ME773/032-1	CTD/RO-68	14.01.	15°59,96'	74°20,92'	06 :51	706	15°59,98'	74°20,93'	07:53	706
ME773/033-1	CTD/RO-69	14.01.	15°59,92'	74°14,69'	08 :54	250	15°59,92'	74°14,69'	09:22	250
ME773/033-2	CTD/RO-70	14.01.	15°59,92'	74°14,69'	09 :43	253	15°59,92'	74°14,69'	10:10	249
ME773/033-3	GO-FLO-16	14.01.	15°59,92'	74°14,69'	10 :30	250	15°59,92'	74°14,69'	11:13	249
ME773/034-1	CTD/RO-71	14.01.	16°00,01'	74°10,97'	11 :49	116	16°00,01'	74°10,97'	12:03	116
ME773/034-2	WP2-25	14.01.	16°00,01'	74°10,97'	12:08	116	16°00,01'	74°10,97'	12:14	116
ME773/034-3	WP2-26	14.01.	16°00,01'	74°10,97'	12:19	116	16°00,01'	74°10,97'	12:26	116
ME773/035-1	RO-1	14.01.	16°00,01'	74°37,04'	14:45	1 622	16°00,01'	74°37,04'	14:49	1624
ME773/035-2	RO-2	14.01.	16°00,01'	74°37,04'	15:01	1 622	16°00,01'	74°37,04'	15:05	1624
ME773/035-3	RO-3	14.01.	16°00,01'	74°37,04'	15:14	1 622	16°00,01'	74°37,04'	15:18	1624
ME773/035-4	RO-4	14.01.	16°00,01'	74°37,04'	15:28	1 622	16°00,01'	74°37,04'	15:32	1624
ME773/036-1	CTD/RO-72	14.01.	16°00,02'	74°59,95'	18 :40	2801	16°00,03'	74°59,98'	19:40	2856
ME773/036-2	PCTD/RO-10	14.01.	16°00,01'	75°00,00'	2 0:10	2835	16°00,01'	75°00,00'	02:04	2845
ME773/036-3	GO-FLO-17	15.01.	16°00,01'	75°00,00'	02 :24	2854	16°00,05'	74°59,83'	03:08	2780
ME773/037-1	ISP-12	15.01.	16°00,02'	74°11,00'	08:01	116	16°00,02'	74°10,99'	11:11	115
ME773/037-2	CTD/RO-73	15.01.	16°00,02'	74°11,00'	11 :27	115	16°00,01'	74°11,00'	11:41	118
ME773/038-1	PCTD/RO-11	15.01.	16°00,00'	74°14,70'	1 3:01	252	16°00,00'	74°14,70'	16:17	252
ME773/038-2	WP2-27	15.01.	16°00,00'	74°14,70'	16:30	254	16°00,00'	74°14,69'	16:37	250
ME773/038-3	WP2-28	15.01.	16°00,00'	74°14,69'	16:38	250	16°00,00'	74°14,67'	16:46	246
ME773/039-1	CTD/RO-74	16.01.	16°43,58'	72°47,53'	10 :37	135	16°43,59'	72°47,50'	10:47	127
ME773/040-1	CTD/RO-75	16.01.	16°46,30'	72°49,17'	11 :24	121	16°46,38'	72°49,14'	11:38	122
ME773/041-1	CTD/RO-76	16.01.	16°49,14'	72°50,49'	12 :13	255	16°49,21'	72°50,34'	12:40	251
ME773/041-2	WP2-29	16.01.	16°49,21'	72°50,34'	12:49	251	16°49,21'	72°50,34'	12:56	254
ME773/041-3	WP2-30	16.01.	16°49,21'	72°50,34'	12:58	253	16°49,21'	72°50,34'	13:03	248
ME773/042-1	CTD/RO-77	16.01.	17°13,36'	72°00,08'	18 :02	163	17°13,36'	72°00,10'	18:20	165
ME773/043-1	CTD/RO-78	16.01.	17°17,71'	71°54,21'	19 :30	121	17°17,71'	71°54,21'	19:44	121
ME773/044-1	CTD/RO-79	16.01.	17°20,69'	71°56,39'	20 :24	277	17°20,71'	71°56,42'	20:50	284
ME773/044-2	WP2-31	16.01.	17°20,71'	71°56,42'	20:54	280	17°20,71'	71°56,42'	21:00	281
ME773/044-3	PCTD/RO-12	16.01.	17°20,71'	71°56,42'	2 2:05	284	17°20,71'	71°56,39'	02:05	256
ME773/045-1	CTD/RO-80	17.01.	17°31,51'	72°19,15'	05 :10	1546	17°31,52'	72°19,15'	06:21	1548
ME773/046-1	CTD/RO-81	17.01.	17°41,98'	72°41,98'	08 :48	3231	17°41,98'	72°41,99'	10:13	3240

Station No.	Gear No.	Date 2009	Position start Lat. [°S]	Position start Long. [°W]	Time [UTC]	Depth [m]	Position end Lat. [°S]	Position end Long. [°W]	Time [UTC]	Depth [m]
ME773/046-2	IFISH-3	17.01.	17°42,61'	72°42,35'	10:3 0	3790	17°59,94'	73°24,89'	15:05	4850
ME773/047-1	GO-FLO-18	17.01.	18°00,00'	73°25,01'	15 :16	4841	18°00,00'	73°25,01'	16:32	4841
ME773/047-2	CTD/RO-82	17.01.	18°00,00'	73°25,01'	16 :34	4836	18°00,00'	73°25,01'	17:58	4842
ME773/047-3	GO-FLO-19	17.01.	18°00,00'	73°25,01'	18 :08	4851	18°00,00'	73°25,01'	18:44	4841
ME773/047-4	WP2-32	17.01.	18°00,00'	73°25,01'	18:50	4839	18°00,00'	73°25,01'	18:56	4837
ME773/047-5	WP2-33	17.01.	18°00,00'	73°25,01'	18:58	4841	18°00,00'	73°25,01'	19:05	4840
ME773/048-1	CTD/RO-83	18.01.	16°49,04'	72°50,55'	10 :00	257	16°49,03'	72°50,55'	10:18	254
ME773/049-1	CTD/RO-84	18.01.	16°46,30'	72°49,00'	11 :26	119	16°46,30'	72°48,98'	11:39	119
ME773/050-1	WP2-34	18.01.	16°09,32'	74°08,04'	19:08	766	16°09,31'	74°08,04'	19:13	765
ME773/051-1	CTD/RO-85	19.01.	14°34,97'	76°06,04'	07 :39	137	14°34,95'	76°06,01'	07:54	129.0
ME773/052-1	CTD/RO-86	19.01.	14°29,26'	76°20,58'	09 :30	247	14°29,26'	76°20,59'	09:56	248
ME773/053-1	CTD/RO-87	19.01.	13°45,01'	77°20,04'	17 :20	3389	13°45,02'	77°20,05'	17:45	3390
ME773/053-2	WP2-35	19.01.	13°45,01'	77°20,03'	17:52	3399	13°45,02'	77°20,06'	18:00	3390
ME773/053-3	WP2-36	19.01.	13°45,02'	77°20,05'	18:08	3387	13°45,02'	77°20,07'	18:14	3390
ME773/054-1	CTD/RO-88	19.01.	13°45,10'	77°02,05'	20 :03	1890	13°45,11'	77°02,05'	20:30	1896
ME773/054-2	PCTD/RO-13	19.01.	13°45,10'	77°02,05'	2 1:18	1892	13°45,10'	77°02,05'	02:25	####
ME773/054-3	CTD/RO-89	20.01.	13°45,10'	77°02,05'	02 :32	1888	13°45,10'	77°02,05'	02:54	1889
ME773/055-1	CTD/RO-90	20.01.	13°45,00'	77°25,34'	05 :15	3967	13°45,01'	77°25,35'	07:46	3966
ME773/056-1	CTD/RO-91	20.01.	13°45,03'	77°02,02'	10 :06	1886	13°45,00'	77°02,00'	10:19	1887
ME773/056-2	ISP-13	20.01.	13°45,00'	77°02,00'	10:43	1894	13°44,99'	77°01,97'	14:17	1878
ME773/056-3	CTD/RO-92	20.01.	13°44,99'	77°01,96'	14 :22	1884	13°44,99'	77°01,97'	14:44	1877
ME773/056-4	CTD/RO-93	20.01.	13°44,99'	77°01,97'	15 :04	1877	13°44,99'	77°01,97'	16:07	1879
ME773/056-5	PCTD/RO-14	20.01.	13°44,99'	77°01,97'	1 6:28	1877	13°44,99'	77°01,97'	18:46	1877
ME773/056-6	CTD/RO-94	20.01.	13°44,99'	77°01,97'	19 :02	1881	13°44,99'	77°01,97'	19:20	1878
ME773/056-7	WP2-37	20.01.	13°44,99'	77°01,96'	19:26	1876	13°44,99'	77°01,96'	19:34	1877
ME773/056-8	WP2-38	20.01.	13°44,99'	77°01,95'	19:38	1876	13°44,99'	77°01,94'	19:46	1877
ME773/056-9	ISP-14	20.01.	13°45,00'	77°01,95'	20:30	1874	13°45,01'	77°01,95'	23:40	1878
ME773/057-1	CTD/RO-95	21.01.	13°20,99'	77°35,02'	03 :25	3071	13°20,99'	77°35,02'	04:47	3070
ME773/058-1	CTD/RO-96	21.01.	13°20,97'	77°00,05'	07 :52	1165	13°21,00'	77°00,02'	08:50	1175
ME773/059-1	CTD/RO-97	21.01.	13°20,77'	76°48,36'	10 :29	250	13°20,77'	76°48,37'	10:54	250
ME773/060-1	CTD/RO-98	21.01.	13°20,99'	76°34,00'	12 :24	121	13°20,99'	76°34,00'	12:38	121
ME773/061-1	CTD/RO-99	21.01.	13°21,01'	76°23,38'	13 :59	164	13°21,01'	76°23,38'	14:12	154
ME773/061-2	WP2-39	21.01.	13°21,01'	76°23,38'	14:14	159	13°21,01'	76°23,37'	14:20	162
ME773/061-3	WP2-40	21.01.	13°21,01'	76°23,37'	14:24	162	13°21,01'	76°23,37'	14:30	161
ME773/062-1	PCTD/RO-15	21.01.	13°21,00'	76°44,89'	1 7:04	160	13°21,00'	76°44,90'	21:28	160
ME773/063-1	CTD/RO-100	21.01.	13°29,98'	76°34,01'	2 3:16	127	13°29,98'	76°34,01'	23:31	127
ME773/064-1	CTD/RO-101	22.01.	13°29,98'	76°27,51'	0 0:21	107	13°29,98'	76°27,50'	00:34	108
ME773/065-1	PCTD/RO-16	22.01.	13°20,99'	76°30,00'	0 1:43	108	13°21,00'	76°30,00'	04:43	110
ME773/066-1	CTD/RO-102	22.01.	13°09,96'	76°31,03'	0 6:03	96	13°09,98'	76°31,00'	06:16	93
ME773/067-1	CTD/RO-103	22.01.	13°09,99'	76°35,99'	0 6:51	114	13°10,00'	76°36,00'	07:04	115
ME773/068-1	CTD/RO-104	22.01.	13°09,99'	76°42,02'	0 7:46	129	13°09,98'	76°42,00'	07:58	130

Station No.	Gear No.	Date 2009	Position start Lat. [°S]	Position start Long. [°W]	Time [UTC]	Depth [m]	Position end Lat. [°S]	Position end Long. [°W]	Time [UTC]	Depth [m]
ME773/069-1	CTD/RO-105	22.01.	13°00,04'	76°44,02'	0 9:11	130	13°00,04'	76°44,02'	09:25	130
ME773/070-1	CTD/RO-106	22.01.	13°00,08'	76°36,54'	1 0:19	105	13°00,08'	76°36,54'	10:31	104
ME773/071-1	CTD/RO-107	22.01.	12°49,98'	76°43,00'	1 1:47	113	12°49,97'	76°43,00'	12:00	115
ME773/072-1	CTD/RO-108	22.01.	12°49,99'	76°50,01'	1 2:45	142	12°49,99'	76°50,01'	13:00	141
ME773/073-1	CTD/RO-109	22.01.	12°40,00'	76°46,01'	1 4:20	102	12°39,99'	76°46,01'	14:34	104
ME773/073-2	WP2-41	22.01.	12°39,99'	76°46,01'	14:41	106	12°39,99'	76°46,01'	14:49	103
ME773/073-3	WP2-42	22.01.	12°39,99'	76°46,01'	14:50	100	12°39,99'	76°46,01'	14:55	104
ME773/074-1	CTD/RO-110	22.01.	12°30,01'	76°55,02'	1 6:27	120	12°30,01'	76°55,01'	16:42	115
ME773/075-1	CTD/RO-111	22.01.	12°21,77'	77°00,00'	1 7:48	100	12°21,78'	76°59,97'	18:00	100

List of abbreviations:

CTD/RO	CTD and Rosette with 24 Niskin bottles
RO	Rosette with 24 Niskin bottles for surface water sampling
PCTD/RO	Pump CTD and Rosette with 8 Niskin bottles
ISP	WTS-LV Sampler (WTS 6-1-142LV) in-situ-pumps
GO-FLO	4 Go-Flo bottles on a Kevlaer Line
WP2	Plankton Net
IFISH	Towed fish for trace metal clean surface water sampling
GLIDER	Autonomous glider with O_2 sensor

3.7 Concluding Remarks

Almost all planned sampling and measurements could be carried out during the cruise. Of Meteor's vessel-mounted RDI Ocean Surveyor ADCP, the deeper-reaching 38 kHz ADCP was broken, which resulted in reliable velocity measurements for or only the upper 700 m depth. In addition, one of the newer cables was damaged and as a result only combined continuous water sampling and CTD monitoring were possible with an older cable up to a water depth of 1800 m. The damaged cable was exchanged immediately after the end of the leg in Callao. These technical problems did, however, not result in any major restrictions of the scientific program which was focussed on the uppermost 1800 m of the water column and did thus not lead to major problems for carrying out the scientific program of the cruise.

The only major deviations from the planned activities were enabled by more efficient than anticipated sampling and measurements during the three sections at 10°S, 12°S, and 16°S. This made some additional shiptime available, which was used for sampling and measurements along a 4th section between 17°S and 18°S and also enabled detailed sampling of the extreme oxygen minimum and associated H_2S occurrences on the shelf south of Callao on the way back to port towards the end of Leg M77/3.

We would like to thank to Captain Niels Jakobi and his crew for the friendly cooperative atmosphere and their competent technical assistance which helped to largly maintain the narrow time schedule. The Leitstelle METEOR and Mrs. Weigert (Contiways Travel) provided

perfect logistical and administrative support. This work was funded by the Deutsche Forschungsgemeinschaft within the Collaborative Research Centre 754 “Climate – Biochemistry Interactions in the Tropical Ocean”.

Data and Sample Storage and Availability

Most of the data were collected within the Kiel Sonderforschungsbereich (SFB) 754. In Kiel a joint data management team is active, which stores the data from the Kiel SFB-574, the Kiel SFB 754 and the Kiel Excellence Cluster in a web-based multi-user-system. In a first phase the data are only available to the user groups. After a limited time of protection these data will be made public by distributing them to national and international data archives through the IFM-GEOMAR data management team. Data obtained during cruise M77/3 and thereafter in home laboratories are stored on the data management server in Kiel are the CTD-profiles, the chemical parameters from the bottle casts, the GO-FLOs, and the Pump-CTD, including all dissolved element and isotopic data obtained, the shipboard ADCP data and the Glider data.

3.8 References

Croot, P.L., Bluhm, C., Schlosser, C., Streu, P., Breitbarth, E., Frew, R., Van Ardelan, M., 2008, Regeneration of Fe(II) during EIFeX and SOFeX. Geophys. Res. Lett., 35, L19606, 10.1029/2008GL035063.

Frank, M., 2002, Radiogenic isotopes: Tracers of past ocean circulation and erosional input. Rev. Geophys., 40, 1001, 10.1029/2000RG000094.

Friederich, G.E., Ledesma, J., Ulloa, O., Chavez, F.P., 2008, Air-sea carbon dioxide fluxes in the coastal southeastern tropical Pacific. Progress In Oceanography, 79, 156-166.

Grasshoff, K., Kremling, K., Ehrhardt. M., 2002 ,Methods of Seawater Analysis. Wiley-VCH.

Karstensen, J., Ulloa, O., 2009, Peru–Chile Current System. In: John H. Steele, Karl K. Turekian, and Steve A. Thorpe, Editor(s)-in-Chief, Encyclopedia of Ocean Sciences, Academic Press, Oxford, Pages 4240-4248, ISBN 978-0-12-374473-9.

Koroleff, F., 1977, Simultaneous persulfate oxidation of phosphorus and nitrogen compounds in water. In: K. Grasshoff (Ed.), Report of the Baltic Intercalibration Workshop, Annex Interim Commission for the Protection of the Environment of the Baltic Sea.

Reynolds, B.C., Frank, M., Halliday, A.N., 2006, Silicon isotope fractionation during nutrient utilization in the North Pacific. Earth Planet. Sci. Lett., 244, 431-443.

METEOR-Berichte 11-2

Climate-biogeochemistry interactions in the tropical ocean of the SE-American oxygen minimum zone

PART 4

Cruise No. 77, Leg 4

January 27, 2009 – February 18, 2009
Callao (Peru) – Colon (Panama)

L. Stramma, P. Ayon, K. Barz, P. Croot, M. Dunker, A. Funk, P. Grasse, I. Grefe,C. Helguero, H.-J. Hirche, T. Kalvelage, J. Karstensen, A. Kock, S. Komander-Hoepner, J. Ledesma, F. Malien, E. Montes-Herrera, M. Müller, G. Niehus, M. Nielsen, W.-T. Ochsenhirt, L. Patara, E. Ryabenko, J. Scholten, R. Stumpf, L. Vasquez, K. Wuttig, Z. Xue, J. Zocher

Table of Contents Part 4 (M77/4)

METEOR-Berichte 11-2

Climate-biogeochemistry interactions in the tropical ocean of the SE-American oxygen minimum zone

PART 4

Cruise No. 77, Leg 4

January 27, 2009 – February 18, 2009
Callao (Peru) – Colon (Panama)

L. Stramma, P. Ayon, K. Barz, P. Croot, M. Dunker, A. Funk, P. Grasse, I. Grefe, C. Helguero, H.-J. Hirche, T. Kalvelage, J. Karstensen, A. Kock, S. Komander-Hoepner, J. Ledesma, F. Malien, E. Montes-Herrera, M. Müller, G. Niehus, M. Nielsen, W.-T. Ochsenhirt, L. Patara, E. Ryabenko, J. Scholten, R. Stumpf, L. Vasquez, K. Wuttig, Z. Xue, J. Zocher

Table of Contents Part 4 (M77/4)

4.1. Participants

Name	Discipline	Institution
Stramma, Lothar, Dr.	Fahrtleiter / Chief Scientist	IFM-GEOMAR
Ayon, Patricia	zooplankton	IMARPE
Barz, Kristina, Dr.	zooplankton	AWI
Croot, Peter, Dr.	trace elements	IFM-GEOMAR
Dunker, Mirja	oxygen, nutrients	IFM-GEOMAR
Funk, Andreas, Dr.	ADCP	IFM-GEOMAR
Grasse, Patricia	silicon, neodymium	IFM-GEOMAR
Grefe, Imke	biology	IFM-GEOMAR
Helguero, Carlos, Dr.	chemistry, observer	Ecuador
Hirche, Hans-Jürgen, Dr.	zooplankton	AWI
Kalvelage, Tim	biology	MPI
Karstensen, Johannes, Dr.	CTD-processing	IFM-GEOMAR
Kock, Annette	nitrous oxide	IFM-GEOMAR
Komander-Hoepner, Sigrun	CTD-watch	IFM-GEOMAR
Ledesma, Jesus	oxygen	IMARPE
Malien, Frank	oxygen, nutrients	IFM-GEOMAR
Montes-Herrera, Enrique	nitrogen isotopes	UMASS
Müller, Mario	CTD-watch, computer	IFM-GEOMAR
Niehus, Gerd	CTD-watch, container	IFM-GEOMAR
Nielsen, Martina	CTD-watch, customs	IFM-GEOMAR
Ochsenhirt, Wolf-Thilo	meteorology	DWD
Patara, Lavinia	salinometry, CTD-watch	CMCC
Ryabenko, Evgenia	nitrogen isotopes	IFM-GEOMAR
Scholten, Jan, Dr.	GEOTRACES	IAEA-MEL
Stumpf, Roland	silicon, neodymium	IFM-GEOMAR
Vasquez, Luis	oceanography	IMARPE
Wuttig, Kathrin	trace elements	IFM-GEOMAR
Xue, Zichen	cadmium	ICL
Zocher, Johanna	CTD-watch	IFM-GEOMAR

DWD	Deutscher Wetterdienst
IFM-GEOMAR	Leibniz-Institut für Meereswissenschaften an der Universität Kiel
AWI	Alfred Wegener Institut für Polar- und Meeresforschung
IMARPE	Instituto del Mar del Peru
ICL	Imperial College London
IAEA-MEL	International Atomic Energy Agency Marine Environmental Laboratories
UMASS	University of Massachusetts School for Marine Science and Technology
CMCC	Euro-Mediterranean Center for Climate Change

4.2 Research Program

In the eastern tropical Pacific and Atlantic extended horizontal oxygen minimum zones (OMZs) exists in the depth range 100 to 900 m. Oxygen minimum values in the eastern Pacific become suboxic with dissolved oxygen of less than 1 μmol kg^{-1}. The OMZs are a consequence of a combination of sluggish ocean ventilation, which supplies oxygen, and enhanced respiration, which consumes oxygen (e.g. Karstensen et al. 2008). Model runs predict a dissolved oxygen decline in the ocean for climate change projections under global warming. Observations in some selected areas of the tropical oceans showed expanding oxygen minimum zones over the last 50 years (Stramma et al. 2008). Oxygen is a key parameter in the marine biogeochemical system, as well as in the ecosystem. As a consequence, oxygen is also a key parameter for better understanding the ocean's role in climate.

The research cruise METEOR M77/4 was carried out in the context of the Sonderforschungsbereich (SFB-754, 'Climate – Biogeochemistry Interactions in the Tropical Ocean') which investigates changes in the oxygen minimum zones of the tropical oceans. Leg M77/4 had two main subjects. One main subject was to conduct a detailed survey of the present day distribution of the water masses and the strength of the oxygen minimum zone in the southeastern Pacific. This was mainly carried out to detect changes in comparison to earlier surveys. A further main subject of the work was the investigation of geochemical components in the water column. For the investigation of circulation, water mass mixing and the influence of biological productivity, samples for the analysis of neodymium, silicon and nitrogen isotopes, as well as a number of natural radionuclides were sampled. Their distribution in the water column can be seen as 'stock-taking' under today's circulation and ventilation conditions and can be used in paleo-oceanographic investigations. The cruise M77/4 focused on the open ocean area where oxygen richer water is supplied to the OMZ and is closely linked to the third leg, where these investigations were made on the near-shelf areas and was complemented by additional biogeochemical measurements.

The goal of the hydrographic measurements was to derive the present day distribution of the water mass and oxygen distribution in the oxygen minimum zone (OMZ) of the southeastern Pacific and resolve the oxygen differences in comparison with older data sets in the supply paths to the OMZ. On the leg M77/4 a meridional section at 85°50'W as well as 3 zonal sections at 3°35'S, 6°S and 14°S were measured. Together with the measurements of the other 3 cruise legs this will lead to a well resolved distribution of the water masses and the oxygen status near and within the upwelling areas in the eastern equatorial Pacific at the time of the cruise.

Water sampling for chemical parameters focused on the isotopic characterization of neodymium (Nd) and silicon (Si) in water masses of Southern Ocean and central Pacific origin and their mixtures in the upwelling region of the Tropical Eastern Pacific. Based on these results, the extent of dissolved Si isotope fractionation induced by diatom productivity during active upwelling will be compared with the nitrogen (N) isotope distribution of dissolved nitrate, in order to assess the effects of mixing of water masses with a preformed Si and N isotope composition and to assess the effects of denitrification on the N isotopes. The information obtained from the unique combination of the biologically influenced Si isotopes and the quasi-conservative Nd isotopes will lead to a better understanding of water mass

mixing and upwelling intensity and at the same time will improve the applicability of Nd and Si isotopes as tracers for paleo-oceanographic processes within the SFB-754. Further sampling was made for excess N_2 (or N_2/Ar) and N_2O in the water column as an indicator for subsurface fixed nitrogen removal.

The overall aim of the trace metal work was to improve our understanding of the processes controlling the iron (Fe) and phosphate supply from sediments under low oxygen conditions. Fe is an essential element for many biochemical processes in phytoplankton in the ocean and is the limiting element in many parts of the global ocean and thus there are strong interactions between Fe and phytoplankton productivity. While Fe^{2+} is the thermodynamically less favored redox state of iron under oxic conditions it is however an important intermediate species in seawater systems for the transformation of iron from one species to another.

Within the GEOTRACES program (An international study of the marine biogeochemical cycles of trace elements and their isotopes) the relationship between boundary scavenging, particle type and the distribution of dissolved and particulate ^{230}Th and ^{231}Pa in the water column was investigated.

Some biological sampling within the context of the SFB-754 was carried out. The goal was to collect biological information on the major microbial types present along the transects and to see how they vary with depth and oxygen concentration. This will be particularly interesting in order to compare the results and diversity from the Pacific Ocean with the data to be collected along similar north-south transects in the Atlantic Ocean.

High resolution studies of the vertical and horizontal distribution of zooplankton and its relation to environmental factors was studied using LOKI, a newly developed optical plankton detection system. Of special interest is the role of physical (T, S) and chemical (oxygen) gradients in structuring the plankton communities in the water column.

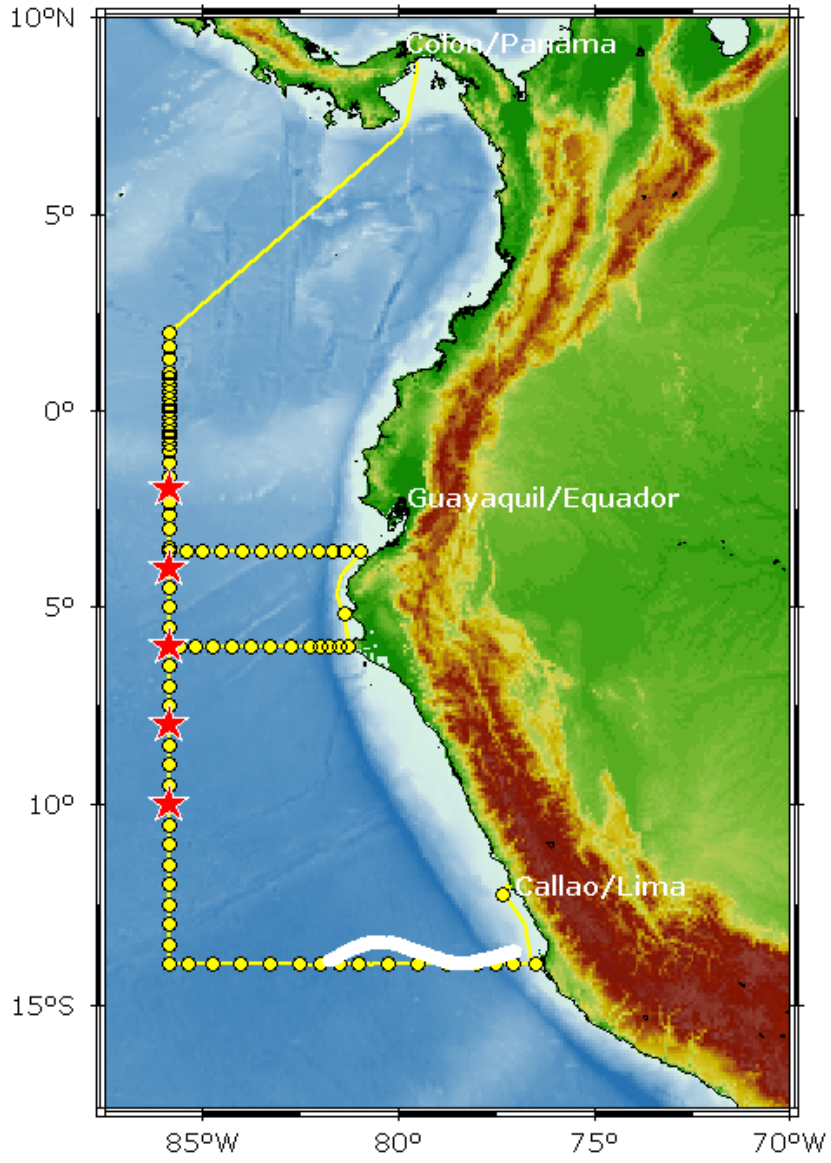

Fig. 4.1: Cruise track of METEOR cruise M77/4, dots indicate the locations of the CTD-stations, red stars locations of float deployment and the white line the Glider path.

4.3 Narrative of the Cruise

On 26 January the scientific crew except the 3 Peruvian scientists boarded RV METEOR. After lunch Peter Croot, Hans Jürgen Hirche und Lothar Stramma drove to the Instituto del Mar del Peru (IMARPE) and together with the chief scientist of the previous leg M77/3, Martin Frank, held a seminar series at IMARPE. The three Peruvian scientists tried to bring their scientific equipment on the ship, and part of the equipment was already on board, but customs officer came on board and after longer discussion the equipment had to be removed again.

On 27 January the 3 Peruvian cruise participants boarded METEOR early in the morning. At 9:30 local time METEOR left the port of Callao to drop anchor off the port of Callao and bunker. At 18:30 local time METEOR could finally start the research cruise. Little later on 28 January at 01:06 UTC a first successful test CTD station was carried out at 12°13.9’S,

77°19.0'W. At 14 UTC the first station of the section at 14°S (Figure 4.1) was done at the shelf at 200 m water depth with a GO-FLOW cast for the trace metal work and a CTD cast. The measurements were continued eastward including a station to 3000 m for GEOTRACES water sampling. On 29 January the section along 14°S was continued. A first test with the LOKI, a newly developed optical plankton detection system, was made and the first zooplankton samples were received, however the optical plankton detection procedure still failed.

The Glider, which was deployed on leg M77/3 on 11 January, was successfully recovered on 30 January at 14°02'S, 82°10'W. A second profile with LOKI was completely successful, providing a large amount of electronic zooplankton counts during the cast. On 31 January the CTD-section along 14°S was terminated with a deep CTD-station at 85°50'W. As most groups had large water requirements from the rosette the 24 bottles could not provide all water needed and another shallow CTD/rosette station had to be made to sample more water. In-between the 2 CTD-casts 2 GO-FLOW profiles and a LOKI profile were taken.

On February 1 a section northward along 85°50'W was started with 30 miles station spacing. This section reoccupies a section made in 1993 and the aim was to investigate water mass and oxygen changes 16 years later. On February 2 a first pair of 2 profiling floats with oxygen sensors was deployed at 10°S, 85°50'W. The section northward along 85°50'W was continued. On February 3 a second pair of 2 floats with oxygen sensors was deployed at 8°S, 85°50'W, while we received the information that the first profiles from the two floats deployed at 10°S were already transmitted. The section northward along 85°50'W was continued to 6°30'S, where it was interrupted to first do a section along 3°35'S towards the Peruvian shelf and continue the northward section along 85°50'w after returning on a 6°S section. The transit to 3°35'S was used to do a barbeque on the deck. In the morning of February 4 the first station of the 3°35'S section was made. The eastern part of the 3°35'S section was done including a deep station to the bottom off the shelf break and a final station at the 200 m depth contour with the Peruvian coast in sight on 6 February. In the evening the section was finished and METEOR steamed south off the Peruvian coast.

The 6°S section began on 7 February at the 200 m depth contour. From this location the 6°S section was carried out westward with CTD/rosette, LOKI and GO-FLOW measurements. In the evening of 9 February the 6°S section was terminated at 85°50'W with a deep station. Two floats were deployed at 6°S and afterwards the interrupted 85°50'W section was continued northward, first still with 30 sm station spacing. As there is a complicated equatorial system of zonal currents and countercurrents the station spacing was reduced to 20 sm between 2°S and 2°N and even 10 sm between 1°S and 1°N. The last GO-FLOW samples were taken at 0°20'N, the last LOKI station at 1°40'N and the CTD/rosette work was terminated at 2°N in the evening of 13 February local time (14 February UTC time). After terminating the station work RV METEOR made the transit towards the entrance of the Panama Canal. In the morning of 16 February METEOR reached the anchorage off Panama City. As a lot of ships were waiting at the entrance of the Panama Canal, the time for the Panama Canal Passage was shifted from 17 February to the evening of 18 February. As most of the scientific crew had to reach a flight back to Europe in the evening of 18 February, the scientific crew left METEOR at the anchorage and did not stay on board for the Panama

Canal Passage. METEOR entered the Panama Canal in the evening of 18 February 2009 and reached Colon in the early morning of 19 February 2009.

4.4 Preliminary Results

4.4.1 CTD program in the tropical Pacific

(J. Karstensen, A. Funk)

During M77/4 a total of 91 CTD profiles have been acquired (see station map figure 4.1 and table 4.5) using one CTD system configuration (see table 4.1 for details). The system was equipped with double sensors for temperature, conductivity, and oxygen and comparison of the pair data showed that the sensors were very stable. We tried to mount for some coastal stations a PAR sensor but unfortunately the port on the SBE did not work properly.

Tab. 4.1: Details of CTD system configuration during M77/4

Profile	1 to 91
Sea-Bird 9	IFM-GEOMAR CTD#5, serial# 09p10108-0410
Primary Conductivity	Serial #2537
Secondary Temperature	Serial #1494
Primary Temperature	Serial #4867
Secondary Conductivity	Serial #2120
Primary Oxygen (SBE-43)	Serial #215
Secondary Oxygen (SBE-43)	Serial #1302
Pressure	Serial #61184
Fluorometer	Dr. Haardt, IFM-GEOMAR #1, *Mode: None*
Altimeter	Installed (0-300m above bottom)
Transmissiometer	Not installed

The raw data was first processed with SBE software to filter outliers, align sensors response times, etc. In a second step a calibration of the pressure (decks offset), temperature (lab calibration), conductivity (bottle samples) and oxygen (bottle samples) sensors followed. The CTD data processing was done on daily basis to monitor the stability of the system. In total 232 salinity and 1197 oxygen bottle samples have been analysed and used for the calibration. The data was sorted by deviation between lab analysed and CTD observed values and only the 66% of lowest deviation are used for the calibration. This method excludes samples which might be either bad or sampled in high gradient regions, where a comparison with the CTD data is not useful. The Winkler titration method for oxygen was based on one single Thiosulfid solution that resolved the full range of expected oxygen concentrations (approx. 300µmol/kg to ~0µmol/kg). Consequently the values reported here have a resolution of 0.5µmol/kg which is near the concentrations in the oxygen minimum zone itself. At the rosette, oxygen samples were taken immediately after the system came on board and always first of all samples to be taken.

The final calibration is likely to be done with the primary sensors. Preliminary calibration showed a marginally lower RMS misfit between calibrated sensor data and bottle data, for salinity we obtained an RMS better than 0.001 PSS-78 (secondary sensor: <0.001 PSS-78) and for oxygen 0.74µmol/kg (secondary sensor: 1.16µmol/kg).

Fluorometer voltage was calibrated based on CTD and chlorophyll-a filtration data collected during leg M77/3. It resulted in the following conversion equation:

Chl-a (microgr/l) =1.46*Fluorometer-Voltage – 0.05, this calibration considered the use of night data only (minimizing quenching effects etc.).

Overall three zonal sections at approximately 3°35'S, 6°00'S and 14°00'S and one meridional section along 85°50'W from 14°00'S to 2°00'N have been occupied. One test station (#1) was done in shelf waters on our way from Callao/Peru to the first zonal section at 14°S. Not many stations have been occupied in water shallower than 1000m as the former legs concentrated it activities more on the shelf and near-shelf region.

The upper layer hydrography shows the transition from the more subtropical waters in the south to the tropical waters in the north. Along the density range 26.0-26.4 kg/m^3 fading influence of so called 'Shallow Salinity Minimum Water' (SSMW) is visible. This water mass originates from an outcrop between 20 to 30°S off Chile and carries higher oxygenated waters northward into the upwelling regions off Peru. With decreasing contributions from the SSMW to the north the depth of the upper boundary of the oxycline rises toward the mixed layer base in a region between 4°S to 8°S. The ventilation through SSMW appears to feedback on biological primary productivity as well as its densest boundary (26.4 kg/m^3) aligns with the secondary chlorophyll-a maximum, which again slowly rises towards the surface on the more northern sections and merges with the primary chlorophyll-a maximum.

The meridional section along 85°50'W was a re-occupation of a section occupied in March/April 1993 with RV KNORR during the WOCE program. The high quality data will allow comparison and detecting even small changes over the last 15 years. A preliminary analysis (Fig. 4.2) revealed a freshening trend of most of the upper 1500m with a parallel cooling of the upper 500m and more of a warming below but only to the north of 8°S. This might be a signature of reduced equatorial upwelling. In oxygen there is a decrease in the equatorial upper ocean north of 3°S however an increase around 500 m depth south of 3°S. Changes in the oxygen content may appear not as coherent but further analysis is required here.

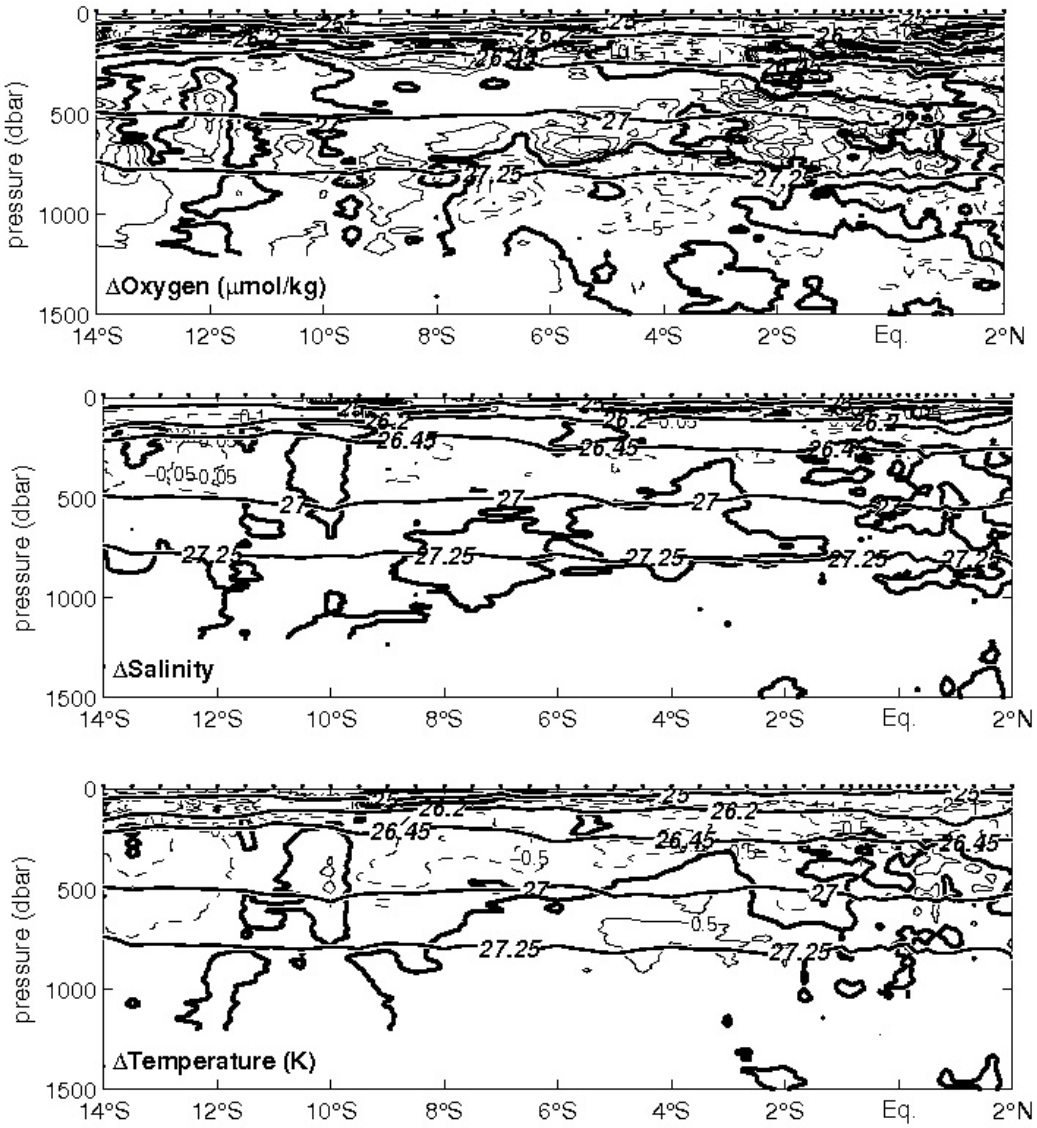

Fig. 4.2: Differences in oxygen, salinity and temperature between 2009 and 1993 for the 85°50'W section (solid lines for positive; dashed lines for negative values). For reference the potential density 25.0, 26.2, 26.45, 27.0 and 27.25 kg/m³ are included.

4.4.2 Current Observation

(A. Funk)

4.4.2.1 Ocean surveyor: Technical aspects

It was planned to use two vessel-mounted RDI Ocean Surveyor ADCPs during the cruise from January 27th to February 13th. One unit (75 kHz, OS75) is permanently fixed to the ship's hull, the second unit (38 kHz, OS38) was lowered into the well located in mid-ship and fixed hydraulically. However, this second unit (OS38) had severe errors already during the previous leg M77/3. A replacement of the cable connecting the board unit (chassis) located in Rechnerraum 723 to the transducer in the well omitting any further junction box did not solve the issue. A resistance check on the cable as well as on the transducer showed a low resistance connection between pins A and W or 1 and 2 that should show high resistance. For a future

harbor stop an inspection of this instrument by a technician from RDI to solve this issue was proposed.

The OS75 was used in narrow-band mode with 50 bins of 16m length. During the previous leg a configuration with a higher resolution of 100 bins of 8m length did not reach sufficiently high echo amplitudes due to the lack of scatter particles in the OMZ. A change to larger 16m bins solved this problem and this configuration was kept for this leg. An acoustic interference with the ship's Doppler log (78 kHz) is a known problem of the OS75 onboard METEOR, so that the use of the Doppler Log was restricted to the CTD stations, except for two cases when the mate forgot to switch it off. During some of the last stations the Doppler Log has not been used at all.

Data was recorded by RDI VMDAS 1.40 software using a MS Windows 2000 PC.
Navigation data was available from several sources:

1. Heading from FibreOpticGyro (FOG) via synchro interface, binarily recorded with pings;
2. Position from ASHTECH GPS via synchro interface, binarily recorded with pings;
3. Position from ASHTECH GPS and heading, pitch and roll from ASHTECH array, separately recorded as NMEA text strings via serial interface.
4. Heading from FibreOpticGyro (FOG), separately recorded as NMEA text strings via serial interface.

For unknown reasons #1 the binarily recorded heading from FOG showed a constant value during the whole cruise. However, the separately recorded FOG heading worked reliably during the whole cruise. The preferred source of heading used for data processing is the long-term stable GPS-ASHTECH heading. As already known from previous cruises the ASHTECH has several data gaps of typically 5-10 minutes durations and also sometimes shows implausible values. During these periods time, position or heading have been replaced by PC time, position from C-NAV GPS or FOG heading. C-NAV position and FOG heading have been extracted from the ship's database system DSHIP. For all these replacements an offset that changes linearly in time has been applied.

Water track calibration of the misalignment angle was improved by applying a time offset of 9 seconds to the heading and -1 second to the navigation data. The final calibration yields a misalignment angle of -1.38° and an amplitude factor of 1.0055. Standard deviations are 0.30° for the misalignment angle and 0.0059 for the amplitude factor.

4.4.2.2 Current sections

The ADCP measured continuously during the cruise. The data was mapped onto a regular grid using a Gaussian-weight interpolation scheme. Three zonal sections along 14°S, 6°S and 3°35'S and one meridional section along 85°50'W were produced.

a) Zonal sections

The three zonal sections reach from 85°50'W eastwards to the Peruvian shelf. In the 14°S section (Fig. 4.3), the equatorward Peru Coastal Current is found at about 76.5°W reaching from the surface to 270 m depth with maximum velocities of 15cm/s. Farther west between 77°W and 79°W the poleward Peru Chile Counter Current is found with maximum velocities

of up to 15 cm/s. The Peru Chile Current is centered at 79°30'W with a shallow core and a core velocity of more than 40 cm/s. West of the Peru-Chile current an anticyclonic eddy is seen. The two sections farther north at 6°S and at 3°35'S show a mainly northward flow west of 84°W and a southward flow east of 84°W in the upper 200 m.

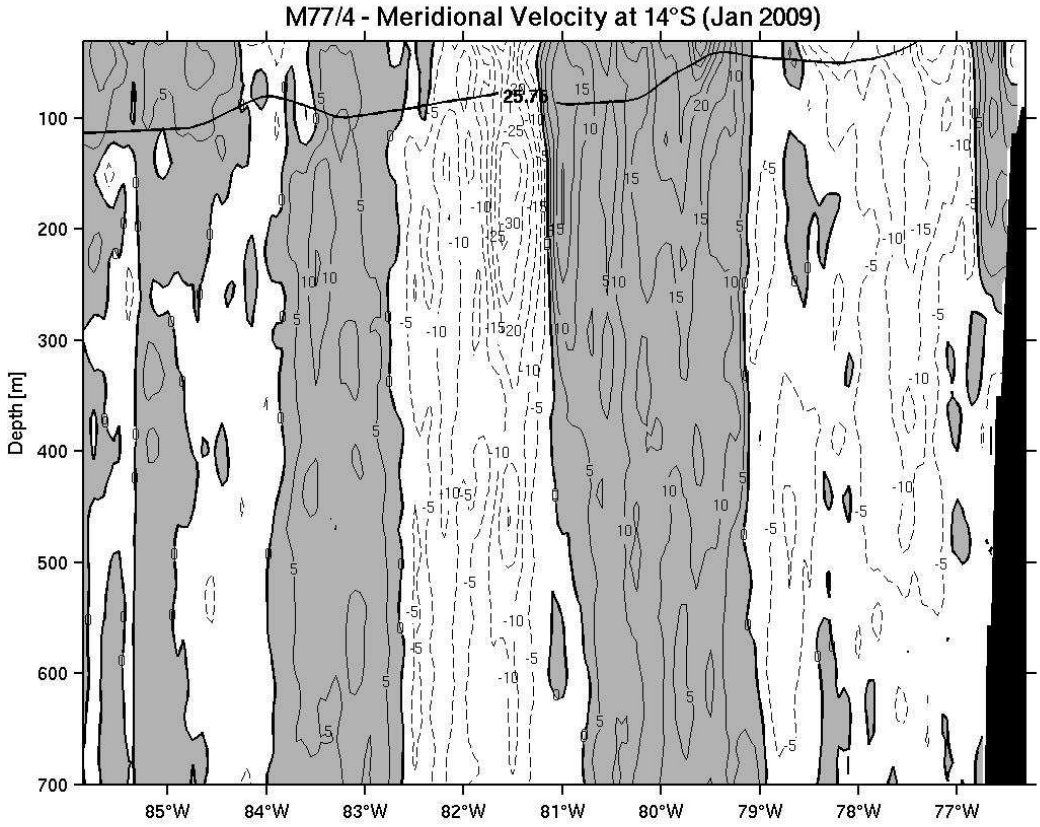

Fig. 4.3: Meridional velocity in cm/s along 14°S measured by the 75 kHz Ocean Surveyor. The thick contour line denotes the σ_θ = 25.75 kg/m³ isopycnal.

b) Meridional section along 85°50'W

The meridional section along 85°50'W was split in two parts, one extending from 14°S to 3°35'S and one from 6°S to 2°N. For composing a continuous section from 14°S to 2°N, the first realization has been used for producing the final section (Fig. 4.4). A weak Equatorial Undercurrent with maximum velocities of about 15 cm/s is found between 1°30'S and 1°30'N with a core depth of about 100m, however the core is deeper in the south and shallower in the north. South of the equatorial region an alternating zonal current structure is found. The near surface currents in this structure show mainly eastward currents in the region of the Southern Subsurface Countercurrent between 7°S and 5°S and between 13°S and 9°S as a strong South Equatorial Countercurrent and mainly westward currents south of 13°S and between 9°S and 7°S. The westward flowing South Equatorial Current between 4 to 5°S and 2 to 3°S reaches to depths of at least 700 m. The Eastward flow at 250 to 550 m centered at 1°S is the Southern Intermediate Countercurrent.

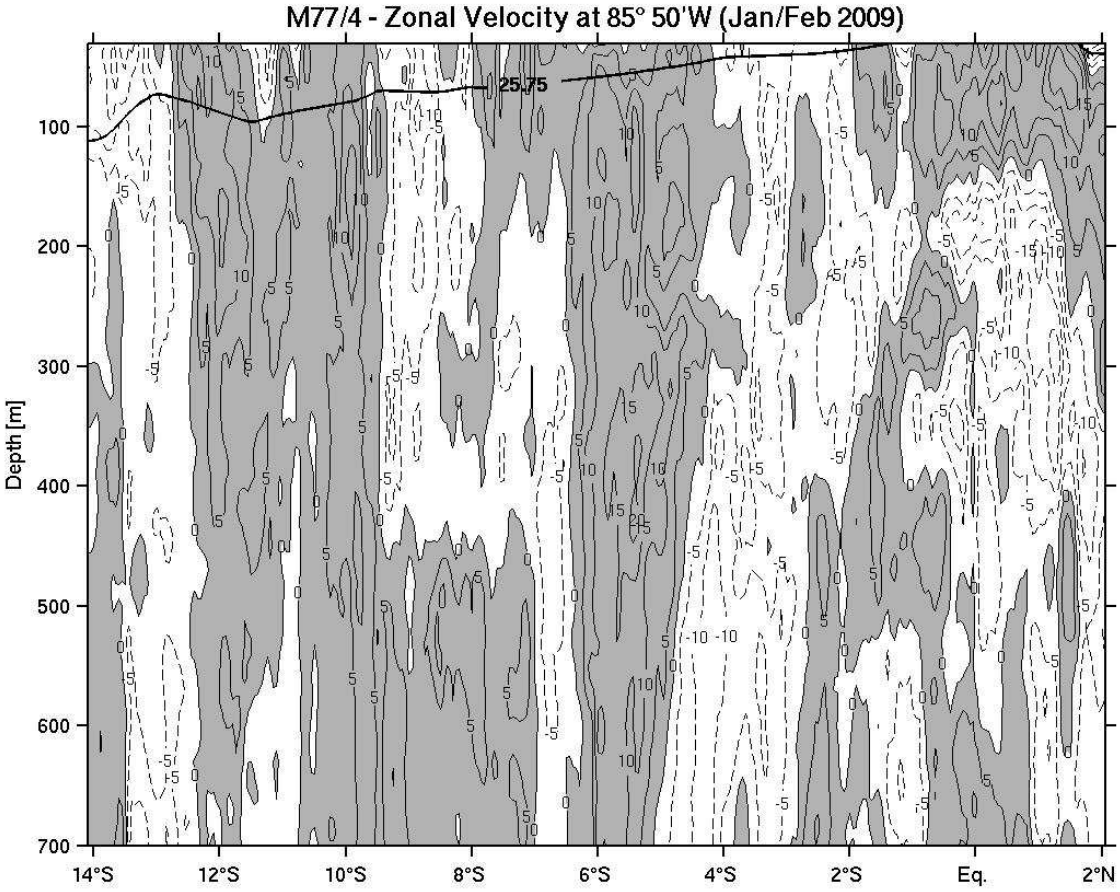

Fig. 4.4: Zonal velocity in cm/s along 85°50'W measured by the 75 kHz Ocean Surveyor. The thick contour line denotes the σ_θ = 25.75 kg/m³ isopycnal.

4.4.3 Glider Operations

(J. Karstensen)

During M77/3 the IFM05 Glider (Serial number 87) has been deployed on January, 10th 2009 at 13°40’S, 77°W and was recovered during M77/4 in the morning of January, 30th 2009 at 14°02.22'S, 82°10.12'W. Both, deployment and recovery have been done using the METEOR Zodiac. Two persons from the crew and one from the scientific party have been straight lowered from/to the ship’s deck using a crane. We were informed from colleagues in Kiel about the last surfacing of the glider and spotted it right away without getting another position via the local Freewave HF radio station. The recovery in calm seas went quick. During recovery a damage of the fin of the glider was discovered, it is unclear if this happened during the recovery or if the vehicle suffered an animal attack confirmed by deep scratches at GPS antenna. The glider was equipped with a newly calibrated CTD, an oxygen optode (serial #691), a Wetlabs FLNTUSL. Originally it was planned to have a second glider (IFM02) running in parallel but this failed through technical reasons (CTD not functioning, oil leak at fin).

The glider was programmed to head for a way point at 85°W/14°S and to not correct for drift by steering against it. The resulting track (Fig. 4.5) looks like a sine as the vehicle has been deflected first to south and then to the north by currents. Although consistent with a deflection first by the southward flowing Peru/Chile Counter Current and than by the northward flowing Peru/Chile Current an intense eddy may also be the reason for this flow pattern.

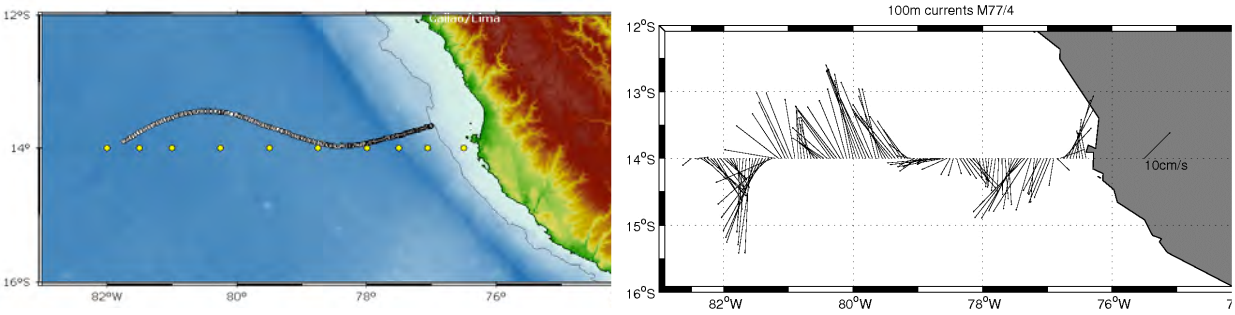

Fig. 4.5: (left) Glider track (white dots), deployment took place during M77/3 off Peru at 1000m depth line. The dots along 14°S show the CTD cast positions. (right) Ocean current data at 100m depth from M77/4 shipboard ADCP.

In comparison to the 10 CTD cast of a 30' to 45' horizontal resolution the glider provides about 18 times more profiles for this section with a much higher resolution of the parameter distribution in the upper 500 to 1000m of the water column (Fig. 4.6).

It is mandatory to carefully calibrate the un-pumped glider CTD SBE47 with typical problems in C/T response time differences. The oxygen optode data also requires calibration for saturation as well as temperature, pressure and salinity. The calibrated CTD data near to the glider track will serve as base data set for comparison. For the oxygen optode a direct comparison with CTD data is available from M77/3. It should be mentioned that the observational data itself can also be used for calibration as the whole spectrum of oxygen values, from saturated at the surface to nearly zero in the oxygen minimum zone, is covered.

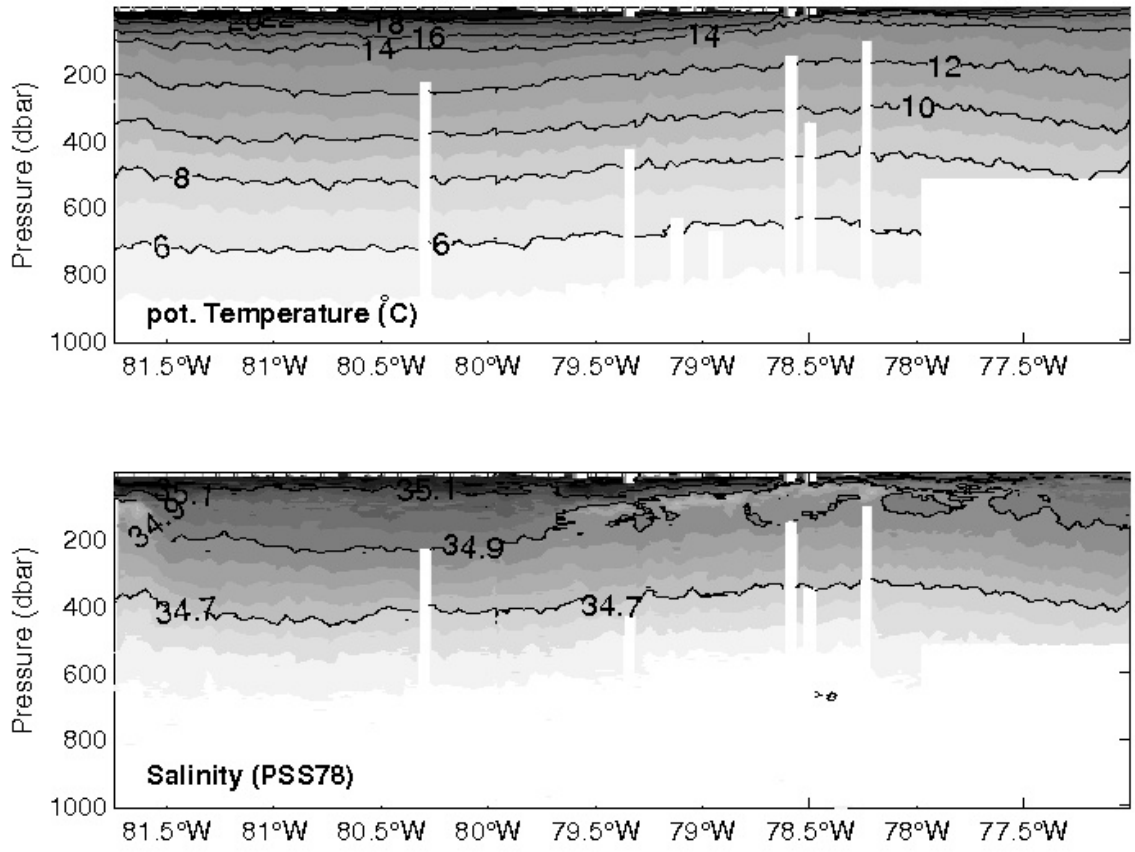

Fig. 4.6: Section of potential temperature (upper frame) and salinity (lower frame) along the zonal Glider section at about 14°S.

4.4.4 APEX float deployment

(L. Stramma, M. Müller)

During the cruise M77/4 10 profiling ARGO floats with oxygen sensor were deployed. Five of them were ballasted to drift at 400 m depth and five at 1000 m depth. The floats drift at that depth for 10 days and then sink to 1500 m to start a profile with pressure, temperature, conductivity and oxygen measurements and send the data via satellite to the ARGOS network. Then they sink to their mission depth to start a new cycle.

A pair of a 400 m and a 1000 m float were deployed at 10°S, 8°S, 6°S, 4°S and 2°S (Fig. 4.1), all at 85°50'W. For better in-situ calibration the floats started in a deep profile first modus and were deployed right after a CTD-profile, and they transmitted the first profile in less than a day. The spreading paths of the Apex floats (Fig. 4.7a) from the deployment time between 2 February 2009 at 10°S and 11 February 2009 at 2°S (see Tab. 4.5) and 11 May 2009 shows an westward spreading for the floats at 2°S to 6°S for the 400 m as well as the 1000 m floats. The float pairs at 8°S and 10°S were moving southeastwards. Looking up the float deployment sites on the ADCP section at 85°50'W (Fig. 4.4) shows that at 400 m the 2°S float followed the eastward flowing Southern Intermediate Countercurrent only for 10 days and then turned south and was carried westward like the 4°S float by the deeper part of the South Equatorial Current. Although the 6°S float was deployed in the eastward flowing Southern Subsurface Countercurrent, it was carried southward and then was captured by the

westward flow south of 6°S The float at 8°S was deployed just at a transition between east- and westward flow and the float at 10°S entered the deeper part of the South Equatorial Countercurrent.

The oxygen profiles from the floats resolve well the oxygen minimum layer. Near the equator at 2°S (black lines) show the restricted vertical extent of the low oxygen layer in comparison to the profiles further south to 10°S (light grey). The final calibration is expected for the near future and the changes in oxygen along the flow path are expected to provide additional new information on the structure of the oxygen minimum zone in the tropical eastern South Pacific.

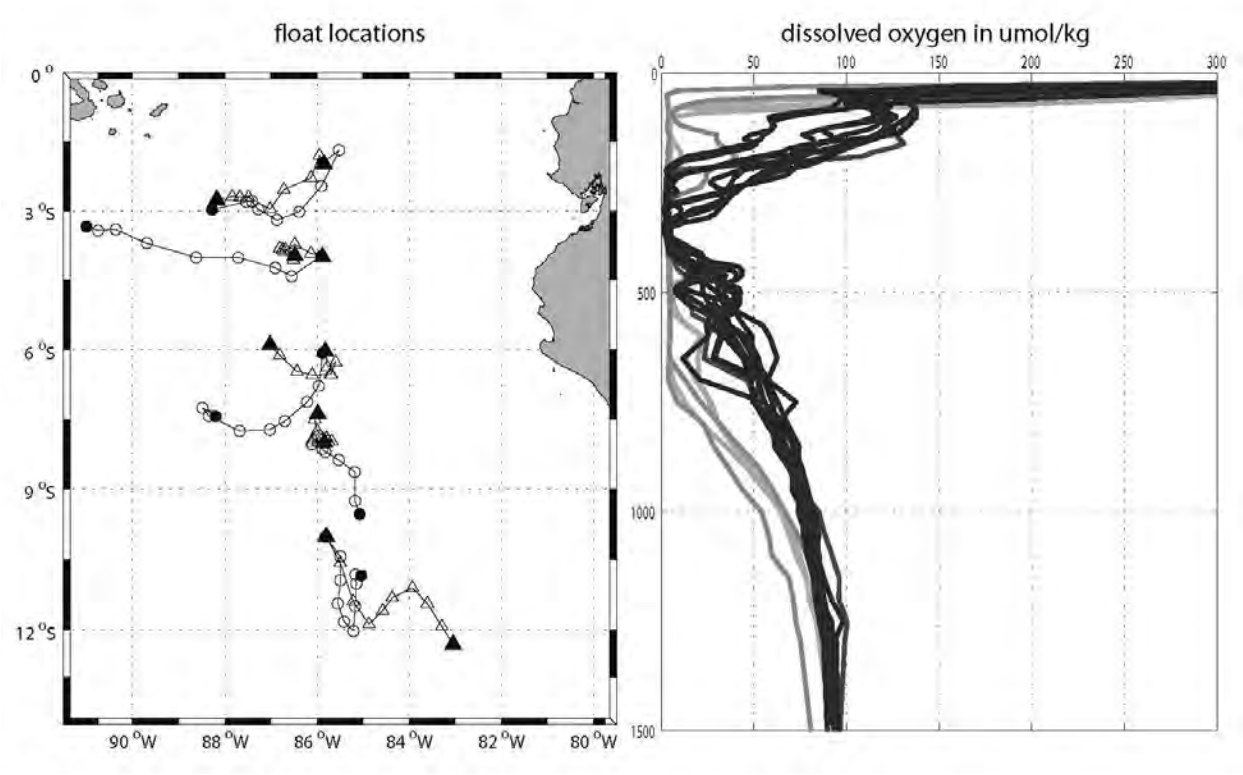

Fig. 4.7: Apex float spreading paths at 400 m depth (circles) and 1000 m (triangles) in 10 day steps (status 11 May 2009, left) and the two most recent oxygen profiles recorded and transmitted by the floats (right) with gray scale for the distance to the equator (black nearest to the equator, light grey most distant profiles.

4.4.5 Redox Sensitive Chemical Species in the Tropical Eastern Pacific and in Peruvian shelf waters

(P. Croot, K. Wuttig)

Objectives/Introduction:

This work was a key part of project B5 in SFB754 which aims to combine *water column* and *porewater sampling* in the Oxygen Minimum Zone (OMZ) of the Eastern Tropical Pacific (Peru Upwelling) in order to improve our understanding of benthic-pelagic coupling in the present day ocean. This work examines key *chemical species*, most notably the key nutrients

iron and phosphate, whose chemical behaviour and distribution are altered via oxygen mediated redox changes, in both the water column and sediment porewaters. During the earlier cruises M77/1 and M77/3 the focus was on the Peruvian shelf and the direct benthic-water column interaction. For M77/4 the focus shifted to examining the extent that the sediment sources of reduced metals from the shelf influenced open ocean trace metal biogeochemistry.

Previous work along the Peruvian shelf (Hong and Kester 1986) has identified the presence of high concentrations of Fe(II) originating from the sediments in contact with OMZ waters. However it is currently unknown how far this signal persists out into the open ocean and this is important for understanding the supply of iron from the Peruvian shelf to the open ocean waters of the Tropical South Eastern Pacific and its potential role in controlling primary productivity (Bruland et al. 2005). An important consideration here also in assessing this iron supply is the lifetime of the Fe (II) in the OMZ waters and in the absence of O_2 the most important oxidant is H_2O_2. Currently there has only been a single published report on H_2O_2 in Peruvian waters (Zika et al. 1985) and the present work was designed to improve our knowledge and understanding or processes influencing the distribution of H_2O_2 and Fe(II) in the Eastern Tropical Pacific and Peruvian shelf waters.

Iodine is potentially a key element for climate change as iodine emissions from the ocean strongly influence the formation of new aerosol particles with impacts on cloud formation and radiative balances. The source and mechanism of iodine emissions from the ocean is poorly understood, as are other more fundamental aspects of iodine biogeochemistry in seawater such as the cycling between the major iodine species; Iodate and iodide. We investigated the biogeochemistry of iodine in the poorly studied waters of the Peruvian Oxygen Minimum Zone (OMZ). Central to this work are investigations into the threshold level for dissolved O_2 at which iodate was reduced to iodide in waters below the euphotic zone.

Work at Sea:

During M77/4 we undertook 15 stations and a total of 26 GO-FLO casts at which 111 samples were taken for later analysis in Kiel. Samples for trace metals will be analyzed upon return to Kiel for the following metals: Fe, Cd, Zn, Cu, Co, Ni and Mn. Short lived redox species were measured directly at sea: H_2O_2 and Fe(II) profiles were measured at 36 stations (23 CTD, 13 GO-FLO) during the course of M77/4 from a wide range of ocean environments Iodide profiles were measured at 7 stations during the course of M77/4. Ancillary measurements for CDOM measurements (10 stations) and colloidal sized particles (all 15 GO-FLO stations) were also made. Additionally over 500 individual Microtops measurements for AOT (Atmospheric Optical Thickness) were collected during the course of M77/4.

Preliminary Results:

High concentrations of Fe(II) were encountered in the bottom waters of all of the shelf stations occupied indicating the strong flux of Fe(II) originating from the sediments. A more reduced Fe (II) signal was also seen in the OMZ waters of the open ocean. H_2O_2 concentrations were relatively low throughout the surveyed region despite the strong sunlight and this is believed to be due to a combination of slow production and fast decay.

Apparent high H_2O_2 concentrations were detected in the presence of high Fe(II) levels but this appears to be more an analytical interference in the H_2O_2 assay from the oxidation of the

Fe(II) in the detector leading to the formation of H_2O_2 *in situ.* Further work was carried out at sea to ascertain if this effect was able to be corrected for and the results adjusted accordingly to determine the true H_2O_2 concentration in the presence of significant Fe(II).

Iodide concentrations were high along the productive shelf regions with a distinct difference seen between the north and south of the Peruvian shelf with overall lower iodide levels in the slightly more oxygenated northern waters. In all regions sampled, the OMZ was clearly demarcated as a zone of high iodide (see an example in figure 4.8) with an inverse relationship between O_2 and I^-. The threshold O_2 level for iodate reduction was apparently around 10 µM with lower levels of O_2 seeing sharp increases in the iodide concentrations. Interestingly there was some indication that close to the sediments total iodine may be enriched in the water column and this signal transported offshore in the core of the OMZ, suggesting a possible sedimentary source for iodide.

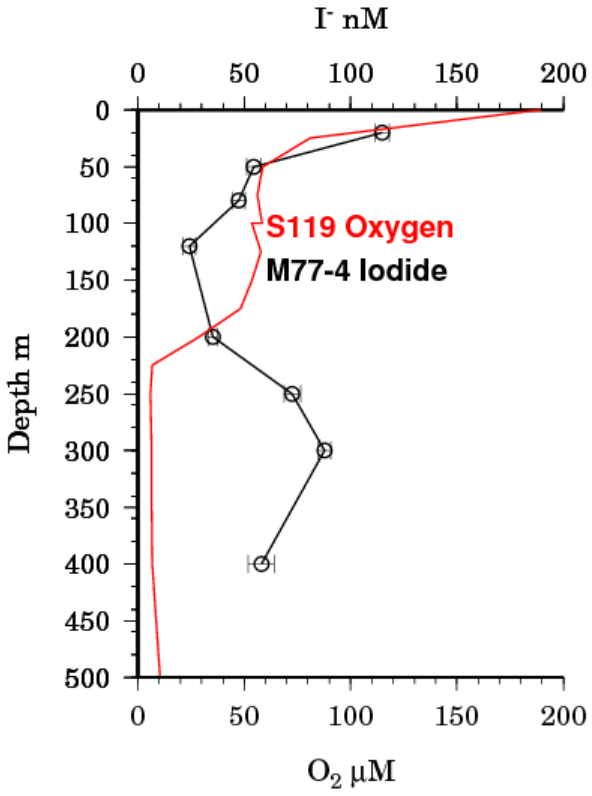

Fig. 4.8: Vertical distribution of Iodide and Oxygen (data courtesy of Frank Malien, IFM-GEOMAR) in the transition between the Open Ocean and the Peruvian shelf at 3°35'S.

Preliminary investigation of the CDOM data shows that typically in the OMZ waters 4 distinct regions could be seen in the vertical data. (i) Bleached surface waters with low absorbance coefficients at 355 nm. (ii) A region around 50-100 m with high absorption at 355 nm presumably related to production of new organic material by phytoplankton. (iii) A deeper high absorbance (355 nm) region consistent with the OMZ which may be related to decomposition of sinking organic material. (iv) Uniform absorption coefficient (355 nm) values in the deep ocean.

4.4.6 Microbiological sampling

4.4.6.1 Reaction pathways for the conversion of inorganic N-species

(T. Kalvelage)

The Peruvian upwelling area is one of the most productive areas of the world's oceans due to the transport of nutrient-rich water from greater depths to the sunlit surface. At the same time an extensive oxygen minimum zone (OMZ), caused by the advection of oxygen-depleted water masses and the remineralisation of organic matter sinking out of the euphotic zone, is found

in this region leading to massive N-nutrient loss by anaerobic processes, such as denitrification and anaerobic ammonium oxidation (anammox). Little is known about how these microbially-mediated processes are controlled by the presence/absence of oxygen and how they are linked to other reactions in the marine N-cycle like nitrification or dissimilatory nitrate reduction to ammonium (DNRA).

To investigate reaction pathways for the conversion of inorganic N-species (nitrate, nitrite and ammonium) and determine rates of N-loss incubation experiments were performed at 7 stations (84, 93, 101, 109, 119, 123, 134; Figure 4.9) during M77/4 using the ^{15}N-tracer technique. Water from the oxycline,

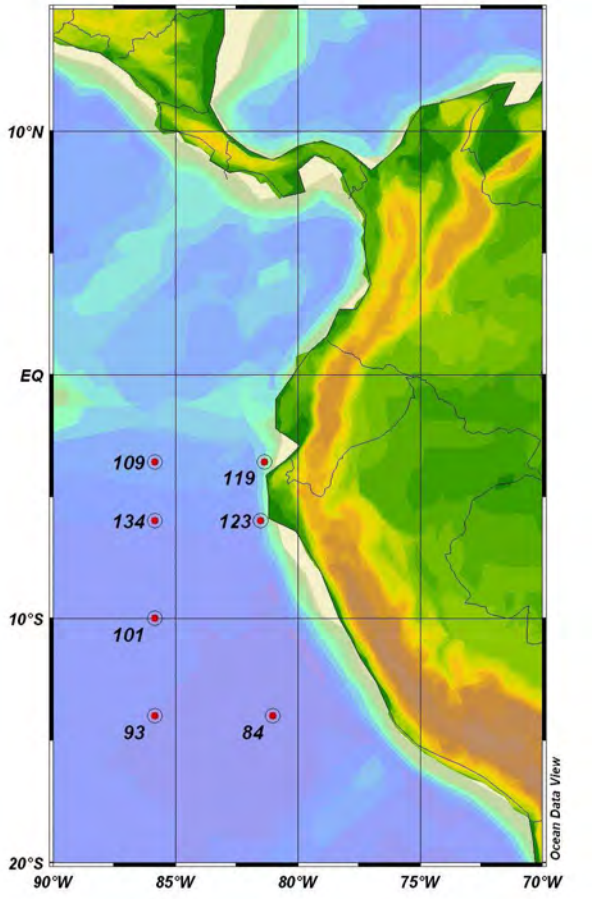

Fig. 4.9: Locations of the incubation experiments.

the upper OMZ, the core of the OMZ and the lower OMZ, was amended with different combinations of labeled (^{15}N) and unlabelled (^{14}N) N-species at different oxygen concentrations and incubated at in-situ temperature. Incubations were terminated after 0, 6, 12, 24 and 48 hours. The time series will be analyzed isotope-ratio mass spectrometry (IRMS) for labeled products ($^{29}N_2$, $^{30}N_2$, $^{15}NO_3^-$, $^{15}NO_2^-$, $^{15}NH_4^+$) of the various reactions catalyzed by microbes. Furthermore, incubation experiments were performed to quantify respiration rates and the remineralisation of particulate and dissolved organic matter (POM/DOM), using oxygen-microsensors as well as $^{18}O_2$ as a tracer. Microbes responsible for the above-mentioned reactions will be identified and quantified by 16S-rRNA gene sequencing of DNA samples collected on filters combined with fluorescent in-situ hybridization (FISH) applied on fixed seawater samples.

4.4.6.2 Microbial impact on the nitrogen cycle

(I. Grefe)

Bioavailable nitrogen is a potentially limiting nutrient, especially in the open ocean and in tropical surface waters. During M77/4 different samples were taken to investigate parts of the microbial impact on the nitrogen cycle in the tropical Pacific, including the OMZ off Peru.

A possible input for bioavailable nitrogen is nitrogen fixation, mediated by the enzyme nitrogenase. One of its subunit is encoded by the *nifH* gene. The enzyme is inhibited by oxygen and it was only found in prokaryotes so far.

Depth profiles were taken at 15 stations. 1 to 2 liters of seawater were filtered on membrane filters with 0.2 µm pore size. The samples were taken from up to 12 different depths between the surface and 2800 m. They will be screened for *nifH* copies at the IFM-GEOMAR in Kiel.

Incubation experiments were run at 6 stations along the 85° W transect. Water samples from the surface and two to three other depths from the core of the OMZ and the oxyclines were labeled with ^{13}C Bicarbonate and $^{15}N_2$ gas. The bottles were incubated for 24 hours in incubators on the working deck or in the 14°C room to simulate *in situ* light and temperature. After one day the incubation was broken down by filtration on precombusted GF/F-filters. Several filter samples for DNA, POC/PON and Chlorophyll were taken at the beginning and the end of the experiment. Furthermore, water samples for DIC, nutrients and AFC were collected at initial and breakdown conditions, as well as FISH and NanoSIMS samples.

All filter and water samples will be analyzed at IFM-GEOMAR, Kiel and MPI, Bremen.

4.4.7 Vertical and horizontal distribution of zooplankton in relation to environmental parameters as assessed with LOKI

(Hans-Jürgen Hirche, Dr. Kristina Barz, Patricia Ayon, Luis Vasquez)

LOKI:

The LOKI system (Lightframe On-sight Keyspecies Investigation) is an optical gear recently developed by AWI and ISITEC. It is used to study the vertical and horizontal variability of mesoplankton distribution on small scales down to the decimeter level. An adopted setup of camera and an especially designed illumination unit allows LOKI to take up to 14 frames per second with shutter times below 50 µs at good signal to noise ratios. From the underwater unit, objects are cut out in real time from the frames taken and stored with a time-stamp. For each object this time-stamp is coupled to the environmental parameters and metadata during the data processing procedure. Thus each image of an organism has the complete information on environmental parameters (temperature, salinity, depth, fluorescence, oxygen, position). The data processing setup is done in a browser frontend, connected with a SQL based database. LOKI can be towed vertically and horizontally with up to 2 knots.

Preliminary results:

The goal during cruise M77/4 was to study the vertical distribution of zooplankton in the south-eastern Pacific in relation to environmental parameters and especially the oxygen minimum zone. Another goal was to study diel vertical migration.

During M 77/4, the LOKI system was deployed vertically on 26 stations (Tab. 4.2, Fig. 4.10) to its temporary maximum operation depth of 500 m whenever bottom depths allowed. Four additional hauls were taken to test camera settings and sampling efficiency of LOKI. During the hauls LOKI produced between 3500 and 12.000 images. In order to assign these images to taxonomic groups, a plankton net (0.2 mm) was attached which collected all organisms that passed the optical system. With the knowledge of the taxonomic composition of the sample obtained by microscopic analysis, six representative hauls were analyzed image by image onboard. Images of each taxon, that could be identified, were stored to produce a reference catalogue. The generally good image quality allowed distinguishing a total of 74 taxa, in several cases to the species level. Later in the laboratory the plankton samples will be completely analyzed and counted and finally compared with the images. Furthermore the images will serve to feed an automatic image analysis system. The tropical Pacific with its high diversity is a challenge for optical plankton identification. While some taxa allow easy determination like the euphausiids, which are distinguished by the shape of the eyes, other groups like the copepods, the most abundant group in the zooplankton, impose severe problems to optical species identification, as their specific characteristics like the spines on the fifth swimming leg cannot be captured in photographic images. Also, the specimens are photographed in all possible positions, which puts another constraint on identification. Nevertheless, knowledge of the community composition and a trained eye can achieve a taxonomic resolution in this small size class (0.3 to 10 mm), which is sufficient to answer many scientific questions.

Fig. 4.10: Plankton species recorded with LOKI during M 77/4. Images are not the same scale.

Our sampling scheme will allow to study diel vertical migration (2 noon and 2 midnight samples), and the zooplankton distribution along 2 transects perpendicular to the Peruvian coast (13 stations), and on a meridional transect along 85°50´W (11 samples). A preliminary view on the data shows a high spatial variability of zooplankton community composition. While a surprisingly high number of taxa is inhabiting the OMZ, their abundance there is relatively low. The overwhelming part of the zooplankton is only found above the oxycline.

Further data analysis will enable us to correlate species distribution with their physico-biological environment on a small scale and to understand their physiological requirements. Especially the change of the thickness of the OMZ and the depth of the oxycline encountered during this cruise will provide new insight into the role of the OMZ in structuring the pelagic system.

Tab. 4.2: LOKI stations during M 77/4

Station	Date	Haul No.	Station	Date	Haul No.
M 77/88	30.01.2009	1	M 77/123	7.2.2009	17
M 77/91	31.01.2009	2	M 77/124	7.2.2009	18
M 77/93	31.01.2009	3	M 77/125	7.2.2009	19
M 77/95	1.2.2009	4	M 77/128	8.2.2009	20
M 77/98	1.2.2009	5	M 77/129	8.2.2009	21
M 77/106	3.2.2009	6, 7,8	M 77/130	8.2.2009	22, 23
M 77/109	4.2.2009	9	M 77/135	9.2.2009	24
M 77/115	5.2.2009	10	M 77/143	11.2.2009	25
M 77/117	5.2.2009	11,12	M 77/145	11.2.2009	26
M 77/118	6.2.2009	13	M 77/149	12.2.2009	27
M 77/119	6.2.2009	14	M 77/152	12.2.2009	28
M 77/120	6.2.2009	15	M 77/157	13.2.2009	29
M 77/122	7.2.2009	16	M 77/160	13.2.2009	30

4.4.8 Water sampling

4.4.8.1 Oxygen and nutrients sampling

(F. Malien, M. Dunker)

Oxygen samples were taken in 100 mL glass bottles with glass stoppers. After the bottles were carefully rinsed they were filled to the top and 1 mL $MgCl_2$ and 1 mL NaI/NaOH solution were added. The bottles were closed and then shaken for approximately one minute and immediately measured once all the samples were taken. Oxygen was analyzed on 1350 Niskin bottles from 64 CTD casts according to a standard titration after Winkler (Grashoff, 1999). 116 duplicate oxygen samples were taken and analyzed at 51 stations, and the precision of the measurement was 0,246 (SD 0,319) µmol/L. The own potassium iodate standard was compared with a CSK 0,01 N potassium iodate standard solution (Wako).

The water for the nutrient analyses was sampled in 60 mL PP bottles with screw caps. The bottles were rinsed twice and then filled. Nutrients (nitrite, nitrate, phosphate, silicate) were determined in 1314 samples from 61 CTD casts.

The nutrient analysis was made with a Continuous-Flow-Autoanalyzer-(CFA) System developed and built at IFM-GEOMAR according to Grashoff et al. (1999). For the determination of phosphate, the method by Bran and Luebbe (Method No. G-175-96 Rev 8) was used.

110 duplicate nutrient samples were taken and analyzed at 50 of the stations, and the precision of the measurement was for nitrite 0,007 (SD 0,011) µmol/L, nitrate 0,278 (SD 0,277) µmol/L, phosphate 0,009 (SD 0,011) µmol/L, silicate 0,180 (SD 0,283) µmol/L.

The own mixed standard was compared with reference material of nutrient (The General Environmental Technos Co, Ltd., Osaka, Japan).

4.4.8.2 Determination of N_2O, NH_2OH and N_2H_4

(A. Kock)

Nitrous oxide (N_2O) acts as an atmospheric greenhouse gas with significant contribution of the oceans to the annual emissions to the atmosphere. It is produced during nitrification and denitrification. Both processes show a high sensitivity to oxygen concentrations in the water column. Enhanced production of N_2O is found in suboxic environments due to nitrification as well as denitrification. Consumption of N_2O takes place as soon as the oxygen level falls at very low levels as further reduction to N_2 takes place. In these areas N_2O profiles show a characteristic double peak structure framing the OMZ whereas in areas with higher oxygen concentrations N_2O profiles have only one peak at the depth of the minimum oxygen level. While in the majority of the surface ocean N_2O concentrations are close to equilibrium with the atmosphere, highly supersaturated waters are brought to the surface in upwelling areas. Thus, these areas act as hot-spots of N_2O emissions to the atmosphere.

Hydroxylamine (NH_2OH) and hydrazine (N_2H_4) are intermediate products in different microbial processes in the N-cycle. Hydroxylamine is produced in the first reaction step of nitrification while hydrazine evolves as characteristic intermediate in the ANAMMOX process. Detecting these substances in the water column can help tracking down key processes in the N-cycle and the contribution of the different processes to the N_2O formation. While hydroxylamine measurements have been carried out in several marine environments, the detection of hydrazine in seawater by conversion to N_2O is a novel method that was applied for the first time during M77/4.

Objective of the sampling program was to examine the water column distribution of N_2O with emphasis on the coastal stations and the export of N_2O to the atmosphere due to coastal upwelling. Furthermore, the vertical distribution of NH_2OH should be investigated at selected stations and the new method of N_2H_4 detection should be applied to seawater samples for the first time. An overview of the sampled stations is given in table 4.3.

N_2O was measured on board with a GC/ECD system. Triplicate samples (duplicates at stations #120-128) of 25 mL volume were drawn from the rosette without bubbles and treated with mercuric chloride (sat., 0.05 mL/vial) within four hours after sampling. For analysis, a 10 mL helium (5.0, AirLiquide, Germany) headspace was added to the sample. After a minimum equilibration time of 2 h a subsample from the headspace was injected manually into the GC using a gas tight syringe. The measurements were calibrated against two certified standard gas mixtures of N_2O in synthetic air.

For NH_2OH and N_2H_4 analysis, additional duplicate samples (triplicates at stations #88 and #109) were taken at selected depths. Another eight (twelve at stations #88 and #109) samples were taken for standard addition.

Hydroxylamine samples were acidified directly after sampling with 0.2 mL acetic acid (glacial). 0.5 mL of different hydroxylamine standards were added to the twelve (eight) extra samples. The samples were shaken manually. Afterwards, 0.2 mL of iron-(III)-solution were added to convert NH_2OH to N_2O. The reaction was stopped after 3 h by addition of mercuric chloride (sat, 0.05 mL/vial). The converted samples were analyzed according to the same method as N_2O samples.

Tab. 4.3: Overview of N_2O, NH_2OH and N_2H_2 sampling during M77/4

Station #	Amount of Samples		
	N_2O	NH_2OH	N_2H_2
77	32	-	-
78	45	-	-
80	54	-	-
82	51	-	-
84	63	-	-
88	69	33	-
93	81	-	-
99	54	-	-
103	36	-	-
107	69	-	30
109	60	39	24
115	42	-	-
117	69	28	24
119	51	-	12
120	48	-	-
121	20	-	-
122	20	-	-
123	36	26	24
125	36	-	-
128	34	-	-
134	78	30	26
152	36	-	-
Total Number of Samples	~1000	~150	~120

Hydrazine samples were acidified directly after sampling with 0.4 mL hydrochloric acid (2M). 0.5 (0.3) mL of different hydrazine standards were added to the extra samples. The samples were shaken manually. Afterwards, 0.2 mL of nitrite solution were added to each sample to convert N_2H_4 to N_2O. The converted samples were analyzed according to the same method as N_2O samples within 48 h after sampling.

4.4.8.3 Determination of ^{230}Th, ^{231}Pa and radium isotopes (^{223}Ra, ^{224}Ra, ^{226}Ra, ^{228}Ra)

(J. Scholten)

During M77/4 sampling of seawater for the determination of ^{230}Th, ^{231}Pa and radium isotopes was conducted. These investigations intend to contribute to the international GEOTRACES program which aims at a better understanding of the processes controlling the distribution of isotopes in the marine environment. Our objective during M77/4 was to investigate if the different particle flux between the upwelling off Peru and the open ocean leads to a boundary scavenging effect, i.e. the preferential removal of particle reactive elements at ocean margins. Furthermore we want to study how the oxygen minimum zone influences the release of radium from the sediments. Radium is released from the sediments to the water column via advection and diffusion. By comparing the radium isotope ratios (i.e. ^{224}Ra/^{223}Ra: for time scale days to weeks; ^{228}Ra/^{226}Ra time scale of years) in the source and in the parcel of water of interest the time can be estimated since the water mass was last in contact with the sediments. In combination with trace element measurements (e.g. Fe and Mn) fluxes of these elements from the sediments can be estimated. So far such studies have not been undertaken in oxygen minimum zones.

At selected stations 200 -400 L of surface seawater was pumped in plastic containers. Radium was extracted by pouring the water over Mn-impregnated acrylic fibers. First measurements of the short-lived radium isotopes ^{223}Ra and ^{224}Ra were performed on-board the ship by means of the delayed coincidence counter (RaDDeC). The long-lived ^{228}Ra and ^{226}Ra will be measured in the home lab. Additional 1 L – 20 L samples for radium measurements were obtained from selected CTD casts. For ^{230}Th and ^{231}Pa 20 L determinations 20 L of seawater was sampled from CTD casts. About 10 L were filtered, and all samples were stored in cubitainers for later transport to the home lab. Additional particulate surface samples were collected using the clean seawater inlet of the ship.

The samples obtained will allow us to obtain new information on the behavior of the radionuclides ^{230}Th, ^{231}Pa and radium isotopes in the East Pacific.

4.4.8.4 δ15N measurements from particulate organic nitrogen (PON), dissolved inorganic nitrogen (DIN) species and N2 gas in seawater

(E. Ryabenko, E. Montes-Herrera)

The nitrogen and oxygen isotope ratios of nitrate and nitrite, as well as the δ^{15}N of PON, ammonium and N_2, provide powerful tools for investigating the nitrogen cycle in the ocean. A number of important biogeochemical processes result in isotopic fractionation and alteration of the δ^{15}N budget that can be measured using isotope ratio mass spectrometry (IRMS). This allows for studies of DIN cycling (e.g. assimilation, remineralization and nitrification) as well as identification of sinks and sources of nitrogen in the ocean (e.g. nitrogen fixation and denitrification).

Our objectives during M77/4 cruise were to investigate the isotopic signals of different members of the nitrogen cycle under OMZ conditions.

770 water samples from 59 CTD stations were collected for DIN (nitrate, nitrite and ammonium) and N_2 $\delta^{15}N$ analysis. Samples which had nitrite over 0.1µM were frozen, and those with no nitrite were acidified with 0.5 mL of 25% HCl and stored at room temperature.

PON samples were taken from surface waters with GFF and nitex filters for isotopic analysis as well.

727 water samples from CTD stations were collected for N_2/Ar analysis. These were poisoned with saturated $HgCl_2$.

Water samples for N_2/Ar and $\delta^{15}N$ analysis and half of the samples for DIN $\delta^{15}N$ analysis will be analyzed at the School of Marine Sciences and Technology (SMAST) of the University of Massachusetts Dartmouth (USA). The other half will be analyzed at IFM-GEOMAR.

Tab. 4.4: Number of 15N-DIN and N_2/Ar taken during M77/4

						# of samples taken	
Station	**Date**	**Time**	**Latitude**	**Longitude**	**Depth [m]**	**15N-DIN**	**N2/Ar**
ME774/077-2	28.01.09	13:29	13°59.98' S	76°30.60' W	198,9	20	10
ME774/078-1	28.01.09	17:35	13°59.91' S	77°3.49' W	3020,5	10	5
ME774/078-2	28.01.09	20:36	13°59.91' S	77°3.49' W	3025,7	20	10
ME774/080-1	29.01.09	3:58	13°59.95' S	77°59.97' W	4635,6	24	12
ME774/082-2	29.01.09	14:00	14°0.00' S	79°30.01' W	4516,6	24	12
ME774/083-2	29.01.09	19:40	14°0.00' S	80°15.01' W	4649,6	19	19
ME774/084-1	30.01.09	0:35	13°59.99' S	80°59.93' W	4806,4	14	14
ME774/088-2	30.01.09	14:00	14°0.00' S	82°30.00' W	4930,6	15	15
ME774/089-1	30.01.09	21:15	13°59.99' S	83°15.02' W	4857,1	16	16
ME774/090-1	31.01.09	2:00	13°59.98' S	84°0.01' W	5 035	16	16
ME774/093-3	31.01.09	19:18	14°0.00' S	85°50.00' W	4579,4	9	9
ME774/093-5	31.01.09	23:37	14°0.00' S	85°50.00' W	4592,2	11	11
ME774/096-1	01.02.09	11:43	12°29.98' S	85°50.01' W	4354,9	12	12
ME774/097-1	01.02.09	15:34	11°59.97' S	85°50.04' W	4389,1	12	12
ME774/099-1	01.02.09	23:40	11°0.00' S	85°50.02' W	4415,2	12	12
ME774/102-2	02.02.09	13:00	9°30.00' S	85°50.00' W	4376,5	13	13
ME774/103-1	02.02.09	18:18	9°0.02' S	85°50.02' W	4 251	11	11
ME774/104-1	03.02.09	0:24	8°30.00' S	85°50.00' W	4 231,3	15	15
ME774/105-1	03.02.09	4:10	8°0.02' S	85°49.97' W	42 05,6	11	11
ME774/107-2	03.02.09	14:04	7°0.00' S	85°50.00' W	3 971,4	12	12
ME774/108-1	03.02.09	18:56	6°29.98' S	85°50.00' W	4111	13	13
ME774/109-1	04.02.09	11:28	3°35.01' S	85°50.03' W	3260,8	9	9
ME774/109-3	04.02.09	15:10	3°35.00' S	85°50.00' W	3262,8	9	9
ME774/110-1	04.02.09	18:13	3°35.05' S	85°24.98' W	3423	15	15
ME774/111-1	04.02.09	21:47	3°35.00' S	85°0.05' W	3 389	13	13
ME774/112-1	05.02.09	1:46	3°35.08' S	84°30.03' W	3 308,6	15	15
ME774/115-3	05.02.09	15:04	3°35.00' S	83°0.00' W	2 722,3	15	15
ME774/116-1	05.02.09	21:24	3°35.00' S	82°30.00' W	3599,4	15	15
ME774/117-1	06.02.09	1:12	3°35.00' S	82°0.97' W	40 84,4	8	8
ME774/117-3	06.02.09	5:20	3°35.01' S	82°0.97' W	40 78,6	9	9
ME774/119-3	06.02.09	16:00	3°35.00' S	81°20.64' W	1047,6	12	12

ME774/120-2	06.02.09	21:14	3°35.53' S	80°56.89' W	219,1	10	10
ME774/121-1	07.02.09	7:20	5°10.01' S	81°21.02' W	1 52	10	10
ME774/122-2	07.02.09	13:34	6°0.00' S	81°15.45' W	1 98,7	10	10
ME774/123-3	07.02.09	17:13	6°0.00' S	81°30.03' W	2 423,2	12	12
ME774/124-1	07.02.09	21:00	6°0.00' S	81°45.01' W	4 789,1	6	6
ME774/124-3	08.02.09	1:42	6°0.00' S	81°45.00' W	47 84,8	9	9
ME774/125-2	08.02.09	4:46	6°0.00' S	82°0.00' W	517 3,3	14	14
ME774/128-2	08.02.09	15:42	6°0.00' S	83°15.00' W	3 773,4	11	11
ME774/129-2	08.02.09	20:28	6°0.00' S	83°45.00' W	4 073,7	16	16
ME774/130-3	09.02.09	0:56	6°0.00' S	84°15.00' W	31 56,3	14	14
ME774/133-1	09.02.09	12:56	6°0.00' S	85°35.06' W	3 991,6	10	10
ME774/134-1	09.02.09	16:02	6°0.03' S	85°50.05' W	4 102,9	9	9
ME774/134-2	09.02.09	20:03	6°0.00' S	85°50.00' W	4 113,4	16	16
ME774/135-2	10.02.09	1:34	5°30.00' S	85°50.00' W	3 891,4	13	13
ME774/137-2	10.02.09	11:44	4°29.94' S	85°50.06' W	3565,4	13	13
ME774/138-1	10.02.09	17:00	4°0.05' S	85°49.95' W	3 445,5	16	16
ME774/139-1	10.02.09	22:45	3°30.03' S	85°50.01' W	3390,5	13	13
ME774/140-1	11.02.09	3:00	3°0.08' S	85°49.98' W	32 10,7	12	12
ME774/143-2	11.02.09	13:28	2°0.01' S	85°50.01' W	2 750,7	14	14
ME774/144-2	11.02.09	17:37	1°40.00' S	85°50.00' W	2518	16	16
ME774/145-2	11.02.09	23:51	1°20.06' S	85°50.07' W	2449,9	14	14
ME774/146-1	12.02.09	3:00	0°59.96' S	85°50.04' W	2 240,9	11	11
ME774/151-2	12.02.09	16:44	0°10.00' S	85°50.05' W	2718,3	12	12
ME774/152-3	12.02.09	20:40	0°0.02' S	85°50.01' W	2 907,8	12	12
ME774/155-1	13.02.09	6:40	0°30.03' N	85°50.01' W	2 812,5	13	13
ME774/158-1	13.02.09	14:28	1°0.09' N	85°50.02' W	2 769,8	16	16
ME774/160-2	13.02.09	21:37	1°39.99' N	85°49.99' W	2607	15	15
ME774/161-1	14.02.09	1:26	2°0.01'N	85°50.06'W	2584	13	10

DOAS:

Additionally measurements were carried out for iodine oxides determinations in the atmosphere. A MiniDOAS from the Institut für Umweltphysik Heidelberg (Jens Tschritter) was installed on the pile deck in the beginning of the cruise (on 26 January 2009) and uninstalled on 14 February in the end of the cruise. The DOAS measured continuously absorption spectra of the atmosphere in different angles to the horizon. Calibration of the system against the Hg spectrum was performed in the beginning and in the middle of the cruise.

4.4.8.5 Silicon and Neodymium

(P. Grasse, R. Stumpf)

During M77/4 we sampled seawater for the determination of the isotopic ratios of neodymium ($^{143}Nd/^{144}Nd$) and silicon ($^{28}Si/^{30}Si$). Because diatoms prefer light over heavy isotopes during biomineralization of silicate the enrichment of heavy isotopes in seawater is an indicator for silicate utilization and the productivity of diatoms. In the upwelling area off the Peruvian Coast, the isotopic signature of Si in water is also influenced by new supply of silicate with different isotopic values, which makes it important to understand the water mass contribution. Due to the fact that Nd isotopes acquire their isotopic signatures through weathering of rocks

with particular isotopic compositions, i.e. continental rocks have a lower $^{143}Nd/^{144}Nd$ compared with mantle rocks and young volcanic rocks, the Nd signature can show the origin of water masses. The information obtained from the combination of the biologically influenced Si isotopes and the quasi-conservative Nd isotopes will lead to better understanding of water mass mixing and upwelling intensity in this region.

All water samples were taken from the CDT/Rosette. In total 97 neodymium samples were taken at 69 stations. For each sample we collected 20 L in cubitainers from different depth, which was in total 1940 liters of seawater. Samples were filtered through a 0.45µm Polycarbonate Filter and acidified with distilled 12M HCl. To precipitate the neodymium we used a Fe(III)-chloride solution.

Silicon was sampled on 15 stations. In total 70 samples were taken. For each silicon sample we collected 500 mL of seawater. The samples were immediately filtered through a 0.45µm polycarbonate filter, acidified with distilled 12M HCl and than stored for the transport to Kiel.

During the cruise it was not possible to analyze the samples. At the IFM-GEOMAR in Kiel the samples will be analyzed with an MC-ICP-MS (Multi-Collector Inductively Coupled Plasma-Mass Spectrometer) to determine the isotopic compositions of neodymium and silicon.

4.4.8.6 Cadmium

(X. Xue)

It has long been know that the biological activity of the oceans is regulated by the availability of the major nutrients phosphate, nitrate, and silicate. More recently, however, it has also been recognized that micronutrient trace elements, such as Cadmium (Cd), also play an important role in limiting marine productivity. However, the oceanic cycle of cadmium is still poorly understood, despite its importance for phytoplankton growth and paleoceanographic applications. Further insight into the processes that govern the marine distribution of Cd may therefore be provided by Cd isotope measurements.

Therefore, we investigate Cd stable isotope fractionation in the oceans to further enhance our understanding of the marine cycling and role of bioactive Cd. In addition, this research will also help to assess whether Cd isotopes may be employed as a proxy of nutrient utilization.

During the cruise M77/4, we collected 8 water profiles in the eastern South Pacific Ocean in total, which are from the stations 78, 86, 93, 97, 109, 117, 124 and 134, respectively. The water samples were transported from CTD/rosette to the lab with 10 L plastic cubic container, where they were filtered through 0.45 um Millipore cellulose filters into cleaned 2 L, 5 L and 10 L PE containers and subsequently acidified with distilled 12M HCl. All the other pre-treatment (double spiking, Cd isolating and column chromatography) and sample analysis will be finished in Earth Science and Engineering department, Royal School of Mine, Imperial College London.

4.4.9 DVS Meteorological and Surface Underway Data

(Lavinia Patara, Johannes Karstensen)

Different types of meteorological and ocean surface data have been recorded during M77/4. Meteorological data include air temperature at 20 m height, air pressure, and precipitation, wind speed at 40 m height, relative humidity, incoming shortwave and long-wave radiation and UVA radiation. Ocean surface data include temperature (SST) and salinity (SSS). Processing of the data involved: averaging starboard and port sensors, except for air temperature, where the minimum temperature was used to avoid overestimation related to strong insolation, and wind speed, where the maximum wind speed was used in order to avoid underestimation related to the ship shielding effect. The sea surface data SSS and SST were compared with the upper 3 m average of the calibrated CTD data. The comparison indicates that the original SST and SSS data are on average too low of 0.64 ± 0.24 °C and 0.15 ± 0.06 respectively. New time series of calibrated values are then produced which are used to derive, by means of bulk formulas, other variables such as seawater density, wind stress, outgoing long-wave radiation, sensible heat flux and latent heat flux.

Along the cruise track (Figure 4.1) varying ocean and atmospheric conditions are encountered. Lower SSTs (< 20°C) are found in the Peru upwelling region, whereas relatively higher SSTs (around 25°C) are found in offshore areas (Fig. 4.11). Air temperature (not shown) and SST exhibit similar trends and average values are 24.1°C for the former and 24.5°C for the latter. SSS is highest (~35.5) in the offshore subtropical domain south of 8°S, whereas it decreases approaching the equator, where values may be as low as 32.5. Low SSS and high SST values are also locally found off the coast of Peru at 3°S. Surface seawater density (not shown) exhibits highest values in the Peru upwelling region (>25 kg m^{-3}) and is overall lower in the subtropical gyre domain and approaching the equator (<23 kg m^{-3}). Sea level pressure (not shown) oscillates with a tide-related semi-diurnal cycle around its average value of 1012 dbar, except when passing through the subtropical gyre domain south of 12°S where it attains 1015 dbar. Wind speed is on average 5 m sec^{-1} and has a dominant south-easterly component along the covered track; wind stress (not shown) remains in general below 0.15 N m^{-2}.

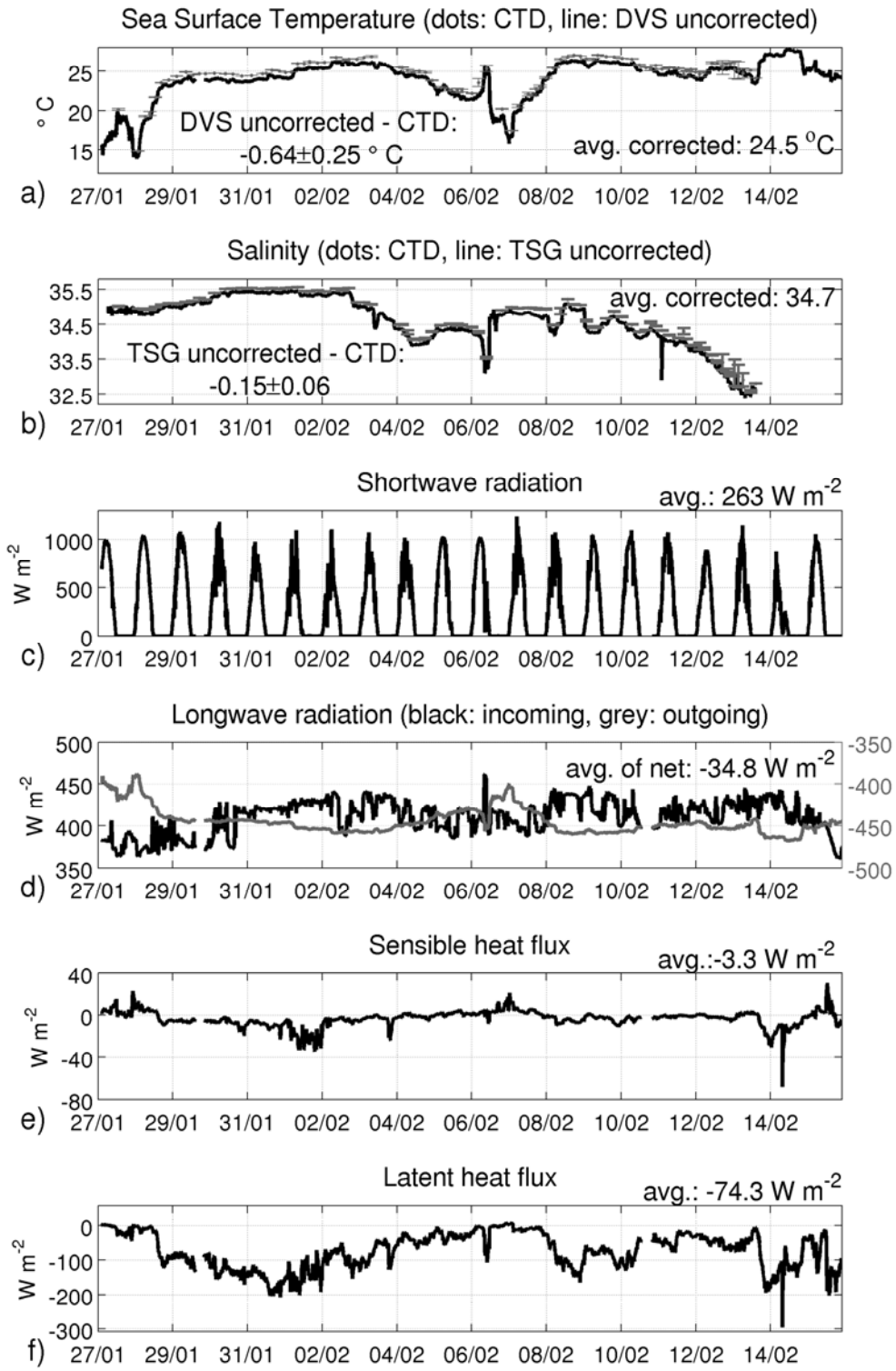

Fig. 4.11: Meteorological and ocean surface data recorded during M77/4: a) SST in ℃ (black line) and comparison with CTD measurements (grey dots and error bars: average over the first 3 m depth and associated standard deviation), b) SSS (black line) and comparison with CTD measurements (grey dots and error bars: same as for SST), c) shortwave radiation in W m^{-2}, d) long wave radiation in W m^{-2} (black line: incoming, grey line: outgoing), e) sensible heat flux in W m^{-2}, f) latent heat flux in W m^{-2}.

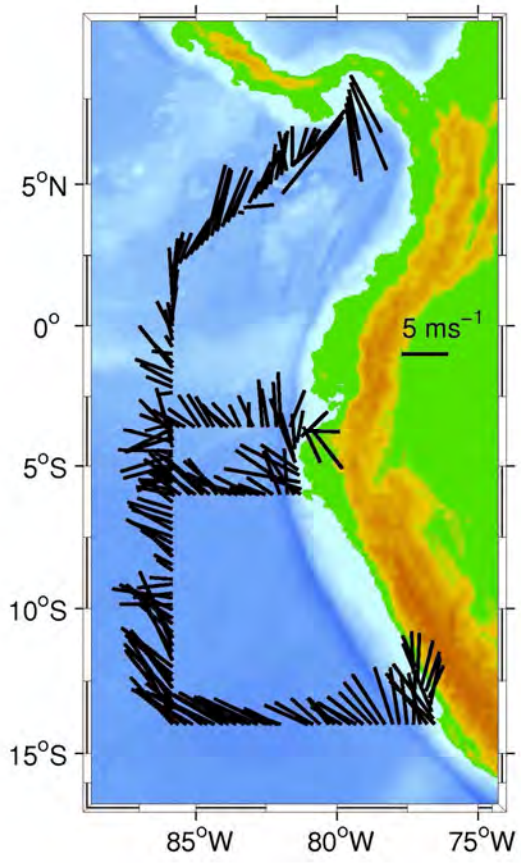

Fig. 4.12: Wind field recorded during M77/4

Relative humidity (not shown) is on average 78% with higher values near the Peru coast and lower values in the subtropical offshore region south of 12°S. Shortwave radiation and net long-wave radiation are on average 262 W m^{-2} and -35 W m^{-2} respectively, with long-wave heat gains being somewhat higher in offshore regions, and long-wave heat losses decreasing in the Peru upwelling domain where SST is lower. Sensible heat flux is on average -3 W m^{-2} and it is generally positive in the Peru upwelling region and negative or close to zero in offshore areas, in agreement with air-sea temperature differences (not shown). Latent heat flux is on average of -74 W m^{-2} and tends to be more negative when relative humidity is lower and wind speed and SST higher. Precipitation (not shown) is not occurring throughout most of the time series except for a few short events, the most intense of which (>80 mm day^{-1}) is encountered at 4°N. The wind field (Fig. 4.12) is dominated by the trade winds with winds from the southeast.

4.5 Ship's Meteorological Station

(W.-T. Ochsenhirt)

Cruise and weather conditions during leg M77 / 4:
METEOR left the port of Callao on 27 January 2009 in the evening, heading south. During the outward voyage to 14°S the weather situation was dominated by a subtropical high with a centre near 31°S 88°W. The corresponding winds came from southerly directions with Bft 3-4. Arriving at 14°S METEOR headed westerly and the southerly swell was increasing to 2-2,5 metre with constant winds from south to southeast 3 to 4 Bft, sometimes 2 Bft, since the pressure gradient was low. On 31 January METEOR arrived at the most westerly point near 14°S 85.8°W and encountered southerly winds of Bft 4.

Since the afternoon of the day before the clouds had increased and some light showers were observed without significant gusts.

The further cruise from there headed northerly along 85.8W until 3.6°N. The wind did not change significantly and remained southeast to east with 2-4 Bft.

Some convective cloud areas drifted from Peru to the working area of RV METEOR.

The vessel arrived at the latitude 03.6° S in the morning of 2 February with a southeasterly wind of about 3 Bft and frequent but weak showers during the night before. The ship was north of a ridge from a high near 38°S 110°W.

On 06 February METEOR arrived at 03.6°S 81°W with light and variable winds. On the same day a transit to 06°S, 81.3°W began. METEOR arrived at that waypoint in the morning of the following day. Accompanied by mainly light southwesterly winds the cruise went along the latitude of 06°S until 85,8°W. Then METEOR sailed northerly. The wind was nearly constant with southwest of about 3 Bft, interrupted by some periods of light and variable winds.

On 12 February METEOR passed the equator. On the next day the investigations were finished and the vessel headed for Panama. The area of the intertropical convergence zone (ITCZ) was weak and the corresponding winds encountered were light and variable.

During the night from 18 to19 February the passage via the Panama Canal followed and the leg of the voyage M77/4 ended in the morning of 19 February 2009 in the harbour of Colon.

4.6 Station List M77/4

Tab. 4.5: The general M77/4 station list, measured parameters are defined at the end of the table.

Station	P#	Date	Time	Latitude	Longitude	Depth [m]	Gear	Comment/parameter measured
ME774/076-1	1	28.01.09	01:05	12°13.97' S	77°19.03' W	127,9	CTD/RO	Test station
ME774/077-1		28.01.09	12:55	13°59.98' S	76°30.60' W	199,4	GO-FLO	1, 2, 12,
ME774/077-2	2	28.01.09	13:29	13°59.98' S	76°30.60' W	198,9	CTD/RO	2, 3, 4, 5, 7, 10, 11,15
ME774/078-1	3	28.01.09	17:35	13°59.91' S	77°3.49' W	3020,5	CTD/RO	1, 2, 3, 4, 5, 7, 9,12,13, 11, 15
ME774/078-2	4	28.01.09	20:36	13°59.91' S	77°3.49' W	3025,7	CTD/RO	1, 2, 3, 4, 5, 7, 9,12, 13, 11, 15
ME774/079-1	5	29.01.09	00:07	13°59.99' S	77°30.05' W	5160,3	CTD/RO	12, 15
ME774/080-1	6	29.01.09	03:58	13°59.95' S	77°59.97' W	4635,6	CTD/RO	2, 3, 7,
ME774/081-1	7	29.01.09	08:43	13°59.99' S	78°45.05' W	4438,6	CTD/RO	14
ME774/082-1		29.01.09	13:30	13°59.95' S	79°30.02' W	4508,7	GO-FLO	
ME774/082-2	8	29.01.09	14:00	14°0.00' S	79°30.01' W	4516,6	CTD/RO	1, 2, 3, 7, 8, 12, 11, 15
ME774/082-3		29.01.09	14:55	14°0.00' S	79°30.01' W	4513,5	GO-FLO	
ME774/083-1		29.01.09	19:12	13°59.99' S	80°15.00' W	4659	LOKI	
ME774/083-2	9	29.01.09	19:40	14°0.00' S	80°15.01' W	4649,6	CTD/RO	1, 3, 4, 5, 7, 8, 14
ME774/084-1	10	30.01.09	00:35	13°59.99' S	80°59.93' W	4806,4	CTD/RO	1, 2, 3,6, 7, 8, 14
ME774/085-1	11	30.01.09	04:22	14°0.02' S	81°30.03' W	4972,7	CTD/RO	
ME774/086-1	12	30.01.09	08:14	14°0.01' S	81°59.98' W	4897	CTD/RO	13, 11, 15
ME774/087-1		30.01.09	11:10	14°2.22' S	82°10.12' W	4768,2	GLIDER	
ME774/088-1		30.01.09	13:25	14°0.00' S	82°30.00' W	4930,2	GO-FLO	4, 5, 9, 10
ME774/088-2	13	30.01.09	14:00	14°0.00' S	82°30.00' W	4930,6	CTD/RO	1, 2, 3, 7, 8,12
ME774/088-3		30.01.09	15:08	14°0.00' S	82°30.00' W	4942,2	GO-FLO	4, 5, 9, 10
ME774/088-4		30.01.09	16:20	14°0.00' S	82°30.00' W	4925,8	LOKI	
ME774/089-1	14	30.01.09	21:15	13°59.99' S	83°15.02' W	4857,1	CTD/RO	1, 3, 4, 5, 7, 8, 14
ME774/090-1	15	31.01.09	02:00	13°59.98' S	84°0.01' W	5035	CTD/RO	3, 7,
ME774/091-1		31.01.09	06:45	13°59.97' S	84°45.05' W	4862,4	LOKI	
ME774/091-2	16	31.01.09	07:56	13°59.99' S	84°45.02' W	5097,6	CTD/RO	
ME774/092-1	17	31.01.09	11:58	13°59.96' S	85°20.00' W	4759,1	CTD/RO	1, 4, 5, 8,12
ME774/093-1		31.01.09	17:25	13°59.99' S	85°50.01' W	4573,8	GO-FLO	4, 5, 9
ME774/093-2		31.01.09	18:10	14°0.00' S	85°50.00' W	4592,6	LOKI	
ME774/093-3	18	31.01.09	19:18	14°0.00' S	85°50.00' W	4579,4	CTD/RO	1, 2, 3, 4, 5,6,7, 8,12,13, 11, 14, 15
ME774/093-4		31.01.09	22:37	14°0.00' S	85°50.00' W	4591,4	GO-FLO	9
ME774/093-5	19	31.01.09	23:37	14°0.00' S	85°50.00' W	4592,2	CTD/RO	1, 2, 3, 7, 8,13, 11, 15, 14
ME774/094-1	20	01.02.09	03:00	13°30.02' S	85°50.05' W	4679,4	CTD/RO	
ME774/095-1		01.02.09	06:45	12°59.99' S	85°50.01' W	4037,3	LOKI	
ME774/095-2	21	01.02.09	07:50	13°0.00' S	85°50.00' W	4056,3	CTD/RO	15
ME774/096-1	22	01.02.09	11:43	12°29.98' S	85°50.01' W	4354,9	CTD/RO	1, 3, 7, 8
ME774/097-1	23	01.02.09	15:34	11°59.97' S	85°50.04' W	4389,1	CTD/RO	1, 3, 4, 5, 7, 8,13, 15, 14
ME774/098-1		01.02.09	19:23	11°29.99' S	85°50.01' W	4432,1	LOKI	
ME774/098-2	24	01.02.09	19:40	11°30.00' S	85°50.00' W	4424,8	CTD/RO	1, 4, 5, 8,12, 14
ME774/099-1	25	01.02.09	23:40	11°0.00' S	85°50.02' W	4415,2	CTD/RO	1, 2, 3, 4, 5, 7, 8,15
ME774/100-1	26	02.02.09	03:38	10°30.02' S	85°50.01' W	4321,1	CTD/RO	
ME774/101-1	27	02.02.09	08:00	10°0.00' S	85°50.00' W	4420,2	CTD/RO	1,6,8, 11, 14, 15
ME774/101-2		02.02.09	09:23	9°59.99' S	85°50.00' W	4411,4	FLOAT	
ME774/101-3		02.02.09	09:27	10°0.05' S	85°49.94' W	4401,7	FLOAT	
ME774/102-1		02.02.09	12:27	9°30.01' S	85°50.01' W	4373,7	GO-FLO	4, 5,
ME774/102-2	28	02.02.09	13:00	9°30.00' S	85°50.00' W	4376,5	CTD/RO	1, 3, 7, 8,12
ME774/102-3		02.02.09	14:20	9°30.00' S	85°50.00' W	4366,2	GO-FLO	4, 5
ME774/103-1	29	02.02.09	18:18	9°0.02' S	85°50.02' W	4251	CTD/RO	1, 2, 3, 4, 5, 7, 8, 15, 14
ME774/104-1	30	03.02.09	00:24	8°30.00' S	85°50.00' W	4231,3	CTD/RO	1, 3, 4, 5, 7, 8
ME774/105-1	31	03.02.09	04:10	8°0.02' S	85°49.97' W	4205,6	CTD/RO	1, 3, 7, 8, 15
ME774/105-2		03.02.09	05:31	8°0.01' S	85°49.99' W	4206,5	FLOAT	
ME774/105-3		03.02.09	05:36	8°0.09' S	85°49.96' W	4202,2	FLOAT	
ME774/106-1		03.02.09	08:36	7°29.99' S	85°50.00' W	4136,1	LOKI	
ME774/106-2	32	03.02.09	09:34	7°30.00' S	85°50.00' W	4137,8	CTD/RO	

Station	P#	Date	Time	Latitude	Longitude	Depth [m]	Gear	Comment/parameter measured
ME774/107-1		03.02.09	13:24	7°0.02' S	85°50.01' W	3970,5	GO-FLO	
ME774/107-1		03.02.09	13:26	7°0.02' S	85°50.02' W	3975,4	GO-FLO	4, 5
ME774/107-2	33	03.02.09	14:04	7°0.00' S	85°50.00' W	3971,4	CTD/RO	1, 2, 3, 7, 8,12
ME774/107-3		03.02.09	15:06	7°0.00' S	85°50.00' W	3972,5	GO-FLO	4, 5
ME774/108-1	34	03.02.09	18:56	6°29.98' S	85°50.00' W	4111	CTD/RO	1, 3, 4, 5, 7, 8, 14
ME774/109-1	35	04.02.09	11:28	3°35.01' S	85°50.03' W	3260,8	CTD/RO	1, 2, 3,6, 7, 8,12,13, 11, 14, 15
ME774/109-2		04.02.09	13:56	3°35.00' S	85°50.00' W	3262,6	LOKI	
ME774/109-3	36	04.02.09	15:10	3°35.00' S	85°50.00' W	3262,8	CTD/RO	1, 2, 3, 7, 8,13, 11, 14, 15
ME774/110-1	37	04.02.09	18:13	3°35.05' S	85°24.98' W	3423	CTD/RO	1, 3, 7, 8
ME774/111-1	38	04.02.09	21:47	3°35.00' S	85°0.05' W	3389	CTD/RO	1, 3, 4, 5, 7, 8, 14
ME774/112-1	39	05.02.09	01:46	3°35.08' S	84°30.03' W	3308,6	CTD/RO	1, 3, 7, 8,12, 15
ME774/113-1	40	05.02.09	05:40	3°35.00' S	83°59.99' W	3198,7	CTD/RO	1,8, 14
ME774/114-1	41	05.02.09	09:40	3°35.00' S	83°30.00' W	3019,3	CTD/RO	
ME774/115-1		05.02.09	13:26	3°35.08' S	83°0.01' W	2714,9	GO-FLO	4, 5
ME774/115-2		05.02.09	13:58	3°35.00' S	83°0.00' W	2723,4	LOKI	
ME774/115-3	42	05.02.09	15:04	3°35.00' S	83°0.00' W	2722,3	CTD/RO	1, 2, 3, 7, 8,12, 11, 15
ME774/115-4		05.02.09	17:15	3°35.00' S	83°0.00' W	2721,8	GO-FLO	4, 5
ME774/116-1	43	05.02.09	21:24	3°35.00' S	82°30.00' W	3599,4	CTD/RO	1, 3, 4, 5, 7, 8
ME774/117-1	44	06.02.09	01:12	3°35.00' S	82°0.97' W	4084,4	CTD/RO	1, 2, 3, 7, 8,12,13, 11, 15
ME774/117-2		06.02.09	04:08	3°35.01' S	82°0.97' W	4061,2	LOKI	
ME774/117-3	45	06.02.09	05:20	3°35.01' S	82°0.97' W	4078,6	CTD/RO	1, 2, 8,12,13, 11, 15
ME774/118-1		06.02.09	08:29	3°35.00' S	81°40.00' W	3935,3	LOKI	
ME774/118-2	46	06.02.09	09:42	3°34.99' S	81°40.00' W	3935,6	CTD/RO	1,8
ME774/119-1		06.02.09	14:24	3°35.00' S	81°20.65' W	1181,6	GO-FLO	4, 5, 9
ME774/119-2		06.02.09	14:58	3°35.00' S	81°20.64' W	1019	LOKI	
ME774/119-3	47	06.02.09	16:00	3°35.00' S	81°20.64' W	1047,6	CTD/RO	1, 2, 3,6, 7, 8,12, 14, 15
ME774/119-4		06.02.09	16:56	3°35.00' S	81°20.64' W	1047,7	GO-FLO	4, 5
ME774/120-1		06.02.09	20:34	3°35.53' S	80°56.89' W	219,9	LOKI	
ME774/120-2	48	06.02.09	21:14	3°35.53' S	80°56.89' W	219,1	CTD/RO	1, 2, 4, 5, 8,12,13, 11, 15
ME774/121-1	49	07.02.09	07:20	5°10.01' S	81°21.02' W	152	CTD/RO	1, 2, 3, 4, 5, 7, 8, 10, 12
ME774/122-1		07.02.09	13:00	6°0.01' S	81°15.44' W	198	LOKI	
ME774/122-2	50	07.02.09	13:34	6°0.00' S	81°15.45' W	198,7	CTD/RO	1, 2, 3, 4, 5, 7, 8, 9, 10, 12,13, 11
ME774/123-1		07.02.09	15:28	5°59.99' S	81°30.09' W	7,7	GO-FLO	4, 5, 9,10
ME774/123-2		07.02.09	16:00	6°0.00' S	81°30.06' W	2419,4	LOKI	
ME774/123-3	51	07.02.09	17:13	6°0.00' S	81°30.03' W	2423,2	CTD/RO	1, 2, 3, 7, 8, 12, 14
ME774/123-4		07.02.09	18:23	6°0.00' S	81°30.03' W	2421	GO-FLO	4, 5,6, 10
ME774/124-1	52	07.02.09	21:00	6°0.00' S	81°45.01' W	4789,1	CTD/RO	1, 3, 4, 5, 7, 8,12,13
ME774/124-2		08.02.09	00:38	6°0.00' S	81°45.00' W	4765,1	LOKI	
ME774/124-3	53	08.02.09	01:42	6°0.00' S	81°45.00' W	4784,8	CTD/RO	1, 3, 7, 8,12,13
ME774/125-1		08.02.09	03:46	5°59.97' S	82°0.02' W	5170,9	LOKI	
ME774/125-2	54	08.02.09	04:46	6°0.00' S	82°0.00' W	5173,3	CTD/RO	1, 2, 3, 7, 8,12, 15
ME774/126-1	55	08.02.09	07:12	6°0.00' S	82°15.04' W	4440,1	CTD/RO	
ME774/127-1	56	08.02.09	10:58	5°59.99' S	82°45.00' W	4166,7	CTD/RO	15
ME774/128-1		08.02.09	14:40	5°59.99' S	83°14.99' W	3749,2	LOKI	
ME774/128-2	57	08.02.09	15:42	6°0.00' S	83°15.00' W	3773,4	CTD/RO	1, 2, 3, 7, 8,12,
ME774/129-1		08.02.09	19:22	6°0.00' S	83°45.01' W	4075,2	LOKI	
ME774/129-2	58	08.02.09	20:28	6°0.00' S	83°45.00' W	4073,7	CTD/RO	1, 3, 7, 8, 14
ME774/130-1		09.02.09	00:15	5°59.97' S	84°15.00' W	3164	LOKI	
ME774/130-2		09.02.09	00:35	6°0.00' S	84°15.00' W	3157,1	LOKI	
ME774/130-3	59	09.02.09	00:56	6°0.00' S	84°15.00' W	3156,3	CTD/RO	1, 3, 7, 8,12, 15
ME774/131-1	60	09.02.09	05:05	5°59.99' S	84°45.00' W	4045,8	CTD/RO	
ME774/132-1	61	09.02.09	09:00	6°0.00' S	85°10.04' W	3964,2	CTD/RO	14
ME774/133-1	62	09.02.09	12:56	6°0.00' S	85°35.06' W	3991,6	CTD/RO	1, 3, 7, 8
ME774/134-1	63	09.02.09	16:02	6°0.03' S	85°50.05' W	4102,9	CTD/RO	1, 2, 3, 7, 8,12,13, 11, 14, 15
ME774/134-2	64	09.02.09	20:03	6°0.00' S	85°50.00' W	4113,4	CTD/RO	1, 2, 3, 4, 5,6, 7, 8,12,13, 11, 14, 15
ME774/134-3		09.02.09	21:25	6°0.01' S	85°50.00' W	4106,7	FLOAT	
ME774/134-4		09.02.09	21:26	6°0.03' S	85°49.98' W	4126,7	FLOAT	
ME774/135-1		10.02.09	00:32	5°30.01' S	85°50.07' W	3883,9	LOKI	

Station	P#	Date	Time	Latitude	Longitude	Depth [m]	Gear	Comment/parameter measured
ME774/135-2	65	10.02.09	01:34	5°30.00' S	85°50.00' W	3891,4	CTD/RO	1, 3, 7, 8, 15
ME774/136-1	66	10.02.09	05:36	4°59.98' S	85°50.01' W	3816,1	CTD/RO	15
ME774/137-1		10.02.09	11:10	4°29.97' S	85°50.04' W	3554,7	GO-FLO	4, 5, 9
ME774/137-2	67	10.02.09	11:44	4°29.94' S	85°50.06' W	3565,4	CTD/RO	1, 3, 7, 8,12
ME774/137-3		10.02.09	12:58	4°29.99' S	85°50.03' W	3553	GO-FLO	4, 5
ME774/138-1	68	10.02.09	17:00	4°0.05' S	85°49.95' W	3445,5	CTD/RO	1, 3, 4, 5, 7, 8, 14
ME774/138-2		10.02.09	19:35	4°0.10' S	85°50.03' W	3441,2	FLOAT	
ME774/138-3		10.02.09	19:35	4°0.10' S	85°50.03' W	3441,2	FLOAT	
ME774/139-1	69	10.02.09	22:45	3°30.03' S	85°50.01' W	3390,5	CTD/RO	1, 3, 7, 8
ME774/140-1	70	11.02.09	03:00	3°0.08' S	85°49.98' W	3210,7	CTD/RO	1, 3, 7, 8, 15
ME774/141-1	71	11.02.09	06:06	2°39.93' S	85°49.99' W	3148,4	CTD/RO	14
ME774/142-1	72	11.02.09	09:20	2°20.01' S	85°49.98' W	3118,8	CTD/RO	
ME774/143-1		11.02.09	12:25	2°0.01' S	85°50.02' W	2734,6	LOKI	
ME774/143-2	73	11.02.09	13:28	2°0.01' S	85°50.01' W	2750,7	CTD/RO	1, 3, 4, 5, 7, 8, 11, 15, 14
ME774/143-3		11.02.09	14:44	2°0.16' S	85°50.02' W	2805	FLOAT	
ME774/143-4		11.02.09	14:46	2°0.21' S	85°50.03' W	2844,9	FLOAT	
ME774/144-1		11.02.09	17:00	1°39.99' S	85°50.05' W	2523,1	GO-FLO	4, 5, 10
ME774/144-2	74	11.02.09	17:37	1°40.00' S	85°50.00' W	2518	CTD/RO	1, 3, 7, 8,12
ME774/144-3		11.02.09	19:40	1°40.00' S	85°50.00' W	2518,6	GO-FLO	4, 5, 10
ME774/145-1		11.02.09	22:49	1°20.03' S	85°50.03' W	2449,4	LOKI	
ME774/145-2	75	11.02.09	23:51	1°20.06' S	85°50.07' W	2449,9	CTD/RO	1, 3, 4, 5, 7, 8, 14
ME774/146-1	76	12.02.09	03:00	0°59.96' S	85°50.04' W	2240,9	CTD/RO	1, 3, 7, 8, 15
ME774/147-1	77	12.02.09	05:58	0°49.95' S	85°50.06' W	2403,6	CTD/RO	
ME774/148-1	78	12.02.09	07:56	0°40.04' S	85°50.07' W	2560,7	CTD/RO	
ME774/149-1		12.02.09	10:12	0°30.01' S	85°50.01' W	2774	LOKI	
ME774/149-2	79	12.02.09	11:15	0°30.01' S	85°50.01' W	2768,7	CTD/RO	1,8
ME774/150-1	80	12.02.09	13:34	0°20.09' S	85°50.02' W	3013,8	CTD/RO	14
ME774/151-1		12.02.09	15:50	0°10.00' S	85°50.13' W	2724,2	GO-FLO	4, 5
ME774/151-2	81	12.02.09	16:44	0°10.00' S	85°50.05' W	2718,3	CTD/RO	1, 3, 7, 8, 14
ME774/152-1		12.02.09	19:00	0°0.03' S	85°50.00' W	2905,7	GO-FLO	4, 5
ME774/152-2		12.02.09	19:37	0°0.02' S	85°50.00' W	2906,5	LOKI	
ME774/152-3	82	12.02.09	20:40	0°0.02' S	85°50.01' W	2907,8	CTD/RO	1, 2, 3, 7, 8,12, 11, 15, 14
ME774/152-4		12.02.09	22:58	0°0.02' S	85°50.00' W	2908,8	GO-FLO	4, 5
ME774/153-1	83	13.02.09	00:50	0°9.98' N	85°50.06' W	2892,6	CTD/RO	1,8
ME774/153-2		13.02.09	02:02	0°9.99' N	85°50.04' W	2883	GO-FLO	4, 5
ME774/154-1		13.02.09	03:46	0°20.04' N	85°50.06' W	3033,2	GO-FLO	4, 5, 10
ME774/154-2	84	13.02.09	04:30	0°20.01' N	85°50.00' W	3024,2	CTD/RO	
ME774/155-1	85	13.02.09	06:40	0°30.03' N	85°50.01' W	2812,5	CTD/RO	1, 3, 7, 8
ME774/156-1	86	13.02.09	08:55	0°40.06' N	85°49.99' W	2744,2	CTD/RO	
ME774/157-1		13.02.09	11:14	0°50.06' N	85°49.94' W	2704,6	LOKI	
ME774/157-2	87	13.02.09	12:17	0°50.00' N	85°50.00' W	2685,4	CTD/RO	
ME774/158-1	88	13.02.09	14:28	1°0.09' N	85°50.02' W	2769,8	CTD/RO	1, 3, 4, 5, 7, 8,12
ME774/159-1	89	13.02.09	17:30	1°20.06' N	85°49.98' W	2943	CTD/RO	11, 15, 14
ME774/160-1		13.02.09	20:36	1°39.98' N	85°49.96' W	2612,4	LOKI	
ME774/160-2	90	13.02.09	21:37	1°39.99' N	85°49.99' W	2607	CTD/RO	1, 3, 7, 8, 15, 14
ME774/161-1	91	14.02.09	01:26	2°0.01'N	85°50.06'W	2584	CTD/RO	1, 3, 4, 5, 7, 8

O_2 = 1	N_2O = 2	N_2/AR = 3	Fe(II) = 4	H_2O_2 = 5
Bio-Bremen = 6	^{15}N = 7	Nutrients = 8	Iodide = 9	FE iso = 10
Si iso = 11	Geotraces = 12	Cd iso = 13	Bio-Kiel = 14	Nd = 15

4.7 Concluding remarks

Most of the planned measurements for this cruise leg could be carried out during the cruise. The major limitation had been that both of Meteor's vessel-mounted RDI Ocean Surveyor ADCP were requested to be used to measure the velocity distribution covering the entire low oxygen zone down to about 1200 m depth. However, the deeper-reaching 38 kHz ADCP was broken and could not be fixed during the cruise and needed a repair by the manufacturer. In consequence reliable velocity measurements could be done only to about 700 m depth.

This report represents the status shortly after the cruise M77/4. Since then the different groups worked with the collected data sets and reported on the results either on scientific meetings or used the data for publications (e.g. Czeschel et al. 2011) or manuscripts in preparation.

We very much appreciated the professionalism and seamanship of crew, officers and Captain of F.S. METEOR which made this work a success. Financial support came from the Deutsche Forschungsgemeinschaft for the Sonderforschungsbereich 754 "Climate-Biogeochemistry Interactions in the tropical Ocean".

Data and Sample Storage and Availability

Most of the data were collected within the Kiel Sonderforschungsbereich (SFB) 754. In Kiel a joint Datamanagement-Team is active, which stores the data from the Kiel SFB-574, the Kiel SFB 754 and the Kiel Excellenzcluster in a webbased multi-user-system. In a first phase the data are only available to the user groups. After a limited time of protection these data will be made public by distributing them to national and international data archives through the IFM-GEOMAR data management team. Data from cruise M77/4 stored on the datamanagement server in Kiel are the CTD-profiles, the chemical parameters from the bottle casts including delta-^{15}N, the dissolved metal data from the GO-FLO, the shipboard ADCP data and the Glider data. The 10 floats deployed on M77/4 are made continuously available online on the public Coriolis server. All 10 floats were transmitting data in mid-January 2011, almost 2 years after the deployment.

4.8 References

Bruland, K. W., Rue, E.L., Smith, G.J., Ditullio, G.R., 2005, Iron, macronutrients and diatom blooms in the Peru upwelling regime: brown and blue waters of Peru. Marine Chemistry, 93, 81-103.

Czeschel, R., Stramma, L., Schwarzkopf, F.U., Giese, B.S., Funk, A., Karstensen, J., 2011, Middepth circulation of the eastern tropical South Pacific and its link to the oxygen minimum zone. Journal of Geophysical Research, 116, C011015, doi:10.1029/2010JC006565..

Grasshoff, K., Kremling, K., Ehrhardt, M., 1999, Methods of seawater analysis. Wiley-VCH, Weinheim, 600 pp.

Hong, H., Kester, D.R., 1986, Redox state of iron in offshore waters of Peru. Limnology and Oceanography, 31, 512-524.

Karstensen, J., Stramma, L., Visbeck, M., 2008,. Oxygen minimum zones in the eastern tropical Atlantic and Pacific Oceans. Progress in Oceanography, 77, 331-350.

Stramma, L., Johnson, G.C., Sprintall, J., Mohrholz, V., 2008, Expanding oxygen-minimum zones in the tropical oceans. Science, 320, 655-658.

Zika, R. G., Saltzman, E.S., Cooper, W.J., 1985, Hydrogen Peroxide concentrations in the Peru Upwelling area. Marine Chemistry, 17, 265-275.